

**“SYNTHESIS OF ZINC OXIDE NANOPARTICLES AND
THEIR APPLICATIONS FOR INHIBITION OF BIOFILM
FORMATION IN DRUG RESISTANT
MICROORGANISMS”**

A THESIS SUBMITTED TO

D.Y.PATIL EDUCATION SOCIETY (DEEMED TO BE UNIVERSITY), KOLHAPUR

(Declared u/s 3 of the UGC Act 1956)

FOR THE DEGREE OF DOCTOR OF PHILOSOPHY

IN MICROBIOLOGY

UNDER THE FACULTY OF INTERDISCIPLINARY STUDIES

BY

MISS.PRANJALI PRABHAKAR MAHAMUNI

M. Sc. (Microbiology)

UNDER THE GUIDANCE OF

DR. (Prof.) P. G. SHADIJA.

M.D. (Microbiology), (DCP)

AND

CO-GUIDANCE OF

DR. R. A. BOHARA.

D. Pharm, M. Sc, Ph.D

CENTRE FOR INTERDISCIPLINARY RESEARCH

D.Y.PATIL EDUCATION SOCIETY

DEEMED TO BE UNIVERSITY, KOLHAPUR-416006 (M.S), INDIA

July 2020

DECLARATION

I hereby declare that the work presented in this thesis entitled **“Synthesis of Zinc oxide Nanoparticles and Their Application For Inhibition of Biofilm Formation in Drug Resistant Microorganisms”** is entirely original and was carried out by me independently in the D.Y. Patil Education Society (Institution Deemed to be University), Kolhapur under the supervision of Dr. (Prof.) P. G. Shadija, and Dr. R. A. Bohara, I further declare that it has not formed the basis for the award of any degree, diploma, fellowship or associate ship or similar title of any University or institution. The extent of information derived from the existing literature has been indicated in the body of the thesis at appropriate places giving the references.

Place: Kolhapur

Date:

Research Student,

Miss. Pranjali Prabhakar Mahamuni.

Centre for Interdisciplinary Research

D. Y. Patil Education Society,

(Deemed to be University),

Kolhapur- 416 006, (M.S) India

CERTIFICATE

This is to certify that the thesis entitled **“Synthesis of Zinc oxide Nanoparticles and Their Applications for Inhibition of Biofilm Formation in Drug Resistant Microorganisms”** is submitted herewith for the degree of Doctor of Philosophy in Microbiology to D.Y. Patil Education Society, Kolhapur by **Miss. Pranjali Prabhakar Mahamuni** is absolutely based upon her own work under my supervision. Neither this thesis nor any part of it has been submitted elsewhere for any degree/diploma or any other academic award anywhere before.

Place:

Date:

Research Guides

Prof.(Dr.) P. G. Shadija.

D.Y. Patil Medical College,
Kolhapur-416 006 (M.S.) India.

Co-Guide



06/09/2020

Dr. R.A. Bohara.

D. Pharm, M. Sc, Ph.D

Research Director and Dean

Prof. (Dr.) C. D. Lokhande.

Center for Interdisciplinary Research

D.Y. Patil Education Society, Kolhapur-416 006 (M.S.) India.

Acknowledgement

I feel short of words but filled with heartfelt emotions to bow down to the Ganapati bappa and H.H. Shrimataji Nirmala Devi, my father Mr. Prabhakar R. Mahamuni, my mother Mrs. Shashikala P. Mahamuni and my in-laws family, who provide me the strength to take every small and big step and instilled the ambition to do my best in every aspect of my life and also in accomplishment of this thesis. I must acknowledge the great support of my husband Mr. Rahul U. Badiger who shouldered equally with me towards the completion of this thesis.

I wish to express my deep sense of gratitude and profound thanks to my supervisor Dr. (Prof.) P. G. Shadija and Dr. R. A. Bohara Government of Ireland., Irish Research council Postdoctoral Fellow, CÚRAM, Centre for Research in Medical Devices, National University of Ireland, Galway, Ireland, for their invaluable guidance, constant encouragement, inspiring and thought provoking discussions throughout my Ph.D. program. I would like to acknowledge my well-wisher Dr. Manohar V. Badiger, Emeritus Scientists, Polymer Science and Engineering Division, CSIR-National Chemical Laboratory, Dr. Homi Bhabha Road, Pune, for being supportive at every stage of my doctoral work. I have been able to learn a great deal from them and consider my association with them as a rewarding experience.

I also express my gratitude to Prof. (Dr.) C. D. Lokhande, Research Director and Dean, D. Y. Patil Education Society, Kolhapur for his great support and encouragement.

My deep appreciation to Dr. V.V. Bhosale, and Mr. S.P. Kole, the Registrar and finance officer of D.Y. Patil Education Society, Kolhapur who provided constant support and encouragement throughout my

research work. I would like to address sincere thanks to Mrs. Pooja and Mr. Ramdas for helping in all ways possible. I am also thankful to all the teaching and non-teaching staff members for their support during my doctoral work. I am thankful to my friends in Centre for Interdisciplinary Research, D.Y. Patil University, Kolhapur, Shivaji University, Kolhapur and National Chemical Laboratory, Pune who have contributed to the successful completion of this work one way or other.

A Special thanks to all the group members without their unconditional help and support, this study would not have been successful. I am lucky to have had the opportunity to meet all of you. I wish to thank to all my friends for being there for me always. It is their constant support; unconditional infinite love and belief in my capabilities which has made me to achieve my goals. I sincerely apologize for any omissions and sincerely thanks all concert.

Ms. Pranjali Prabhakar Mahamuni.



CONTENT

Chapter 1

Introduction

1.1 Introduction	1
1.2 Bacterial biofilm: Mechanism of formation and risk dissemination	2
1.3 Drug- resistance	3
1.4 Different approaches to control biofilm and planktonic cells Of bacteria	5
1.4.1 Plant-derived antimicrobial compounds	5
1.4.2 Polymers	6
1.4.3 Enzymes	6
1.4.4 Antimicrobial peptides	6
1.4.5 Polysaccharides	7
1.4.6 Ionic fluids	7
1.4.7 Bio-surfactants	7
1.4.8 Nano-materials	8
1.5 Properties of ideal antibacterial and antibiofilm agents	10
1.5.1 Biocompatibility	10
1.5.2 Antimicrobial peptides	10
1.5.3 Surfaces	10
1.5.4 Size and shape	11
1.5.5 Stability at different temperature and pH	11
1.5.6 Other properties	11
1.6 Zinc oxide nanoparticles: Properties and biomedical	

applications	11
1.6.1 Anticancer activity	13
1.6.2 Bio-imaging	13
1.6.3 Anti-diabetic activity	14
1.6.4 Anti-inflammatory activity	14
1.6.5 Anti-fungal activity	14
1.6.6 Antibacterial and antibiofilm activity	14
1.6.7 Wound healing ability	15
1.6.7.1 Wound	15
1.6.7.2 Wound-healing process	15
1.6.7.3 Wound dressing	17
1.6.7.4 Properties of ideal wound dressing material	19
1.6.7.5 Biomaterial used for wound dressing	20
1.6.7.5.1 Biopolymers	21
1.6.7.5.1.1 PHBV	22
1.6.7.5.1.2 Sources of PHBV	22
1.6.7.5.1.3 Properties of PHBV	23
1.6.7.5.1.4 Structure of PHBV	23
1.6.7.5.1.5 Molecular weight	24
1.6.7.5.1.6 Composite electrospun fibers of PHBV and PEO	24
1.7 Statement of problem	25
References	28

Chapter 2

ZnO nanoparticles as an antibacterial and antibiofilm agent: Survey of development

2.1 Introduction	37
2.2 Properties of bulk ZnO and nano ZnO	38
2.3 Synthesis approaches	39
2.3.1 Importance of polyols in chemical synthesis of ZnO	
Nanoparticles	42
2.4 Factors affecting antimicrobial and antibiofilm activity of ZnO	
NPs	43
2.4.1 Solubility and concentration	43
2.4.2 Shape	44
2.4.3 Shape	44
2.4.4 UV illumination effect	45
2.4.5 Surface defects	45
2.5 Nanomaterials and wound dressing materials	46
2.5.1 ZnO embedded biomaterials for wound dressing applications	48
2.5.1.1 Electrospinning technique	48
2.6 Mechanism of antibacterial and antibiofilm activity of ZnO NPs	49
2.6.1 Liberation of reactive oxygen species	51
2.6.2 Release of Zn^{+2} ions	53
2.6.3 Other possible mechanism	54
References	56

Chapter 3

Characterization techniques

3.1 Introduction	64
3.2 Synthesis approaches	64
3.2.1 Electrospinning technique	65

3.3 Characterization techniques	66
3.3.1 Structural and phase analysis	66
3.3.1.1 X-ray diffraction	66
3.3.1.2 Fourier Transform Infrared Spectroscopy (FTIR)	69
3.3.1.3. Thermogravimetric Analysis (TGA)	71
3.3.1.4. Differential Scanning Calorimetry (DSC)	73
3.3.1.5. Ultra violet- Visible (UV-Vis) spectroscopy	74
3.3.2 Elemental analysis	76
3.3.2.1 Energy Dispersive X-ray spectroscopy (EDX)	76
3.3.3 Morphological analysis	77
3.3.3.1 Scanning Electron Microscopy (SEM)	77
3.3.3.2. Transmission Electron Microscopy (TEM)	78
3.3.4 Mechanical Properties	79
3.3.5. Biological Characterization	80
3.3.5.1. Biocompatibility	80
3.3.5.1.1. Cytocompatibility study	81
3.3.5.1.2. Hemocompatibility	82
3.3.5.2. Swelling behavior	82
3.3.6.2 Antibacterial activity	83
3.3.6.2.1. Agar well diffusion method	83
3.3.6.2.2. Agar disc diffusion method	84
3.3.6.2.3. Minimum Inhibitory Concentration	85
3.3.6.3. Antibiofilm activity	85
References	87

Chapter 4

Synthesis and characterization of zinc oxide nanoparticles by using polyol chemistry

4.1 Introduction	90
4.2 Experimental	90
4.2.1. Synthesis of ZnO NPs by using diethylene glycol and triethylene glycol	90
4.2.2. Characterization Studies	93
4.2.2.1. Structural analysis	93
4.2.2.2. Spectroscopic analysis	93
4.2.2.3. Morphological analysis	93
4.2.2.4. Elemental analysis	93
4.2.2.5. Thermal analysis	93
4.3. Results and Discussion	93
4.3.1. Structural analysis	93
4.3.1.1. X-ray diffraction	93
4.3.2. Spectroscopic analysis	95
4.3.2.1. UV-visible spectroscopy	95
4.3.2.2. Fourier Transform Infrared Spectroscopy	96
4.3.3. Morphological analysis	98
4.3.3.1. Field Emission Scanning Microscopy (FESEM) And Transmission Electron Microscopy (TEM)	98
4.3.4. Elemental analysis	102
4.3.4.1. Energy Dispersive X-ray	102
4.3.5. Thermal analysis	104
4.3.5.1. Thermogravimetric analysis	104
4.4. Conclusion	105

References	107
------------	-----

Chapter 5

Comparative study of antibacterial and antibiofilm activity of ZnO NPs synthesized by using polyols

5.1. Introduction	109
5.2. Experimental	109
5.2.2. Reagent and Material	110
5.2.3. Bacterial sample preparation	110
5.2.4. Determination of Antibacterial activity by Agar Well Diffusion assay	110
5.2.5. Determination of Minimum Inhibitory Concentration (MIC)	111
5.2.6. Determination of Growth curves of bacteria	111
5.2.7. Antibiofilm activity	111
5.2.8. Hemocompatibility	112
5.2.9. Cell viability study of ZnO NPs	113
5.3 Results and discussion	114
5.3.1 Antimicrobial activity of ZnO NPs	114
5.3.1.1 Determination of the antibacterial activity of all synthesized ZnO NPs	114
5.3.1.2 Determination of minimum inhibitory concentration of all synthesized ZnO NPs	116
5.3.1.3 Determination of growth curve of bacterial cells	117
5.3.1.4 Determination of antibiofilm activity	118
5.3.2 Biocompatibility study of ZnO NPs	121
5.3.2.1 Hemocompatibility of all synthesized ZnO NPs	121
5.3.6 Cell viability study of all synthesized ZnO NPs	122

5.4 Conclusions	123
References	125

Chapter 6

Synthesis and characterization of hybrid PHBV-PEO-ZnO microfibers prepared by using the electrospinning technique

6.1 Introduction	126
6.2 Experimental	127
6.2.1 Electrospinning technique	127
6.2.2 Importance of incorporation of ZnO NPs in polymers	127
6.2.3 Synthesis procedure	128
6.2.3.1 Preparation of PHBV-PEO-ZnO electrospinning solution	128
6.2.3.2 Electrospinning process	128
6.2.3.3 Characterization of prepared microfibers	129
6.2.3.3.1 Spectroscopic analysis	129
6.2.3.3.2 Morphological analysis	129
6.2.3.3.3 Elemental analysis	129
6.2.3.3.4 Thermal analysis	130
6.2.3.3.5 Mechanical Properties	130
6.2.3.3.6 Swelling studies	130
6.3 Results and discussion	130
6.3.1 Spectroscopic analysis	130
6.3.2 Morphological analysis	132
6.3.3 Elemental analysis	133
6.3.4 Thermal analysis	134

6.3.5 Mechanical properties	137
6.3.6 Swelling behavior	139
6.4 Effect of reinforcement of ZnO NPs in PHBV-PEO	139
Microfibers	
6.5 Conclusions	140
References	142

Chapter 7

Antibacterial, antibiofilm and biocompatibility studies of ZnO-PHBV-PEO microfibers

7.1 Introduction	144
7.2 Experimental	144
7.2.1 Reagents and materials	144
7.2.2 Determination of Antibacterial activity	145
7.2.3 Determination of antibiofilm activity	145
7.2.4 Biocompatibility	146
7.2.4.1 Hemocompatibility study of synthesized microfibers	146
7.2.4.2 Cell viability study of Microfibers	146
7.3 Results and Discussion	147
7.3.1 Determination of the antibacterial activity of synthesized PHBV-PEO-ZnO microfibers	147
7.3.2 Determination of antibiofilm activity	149
7.3.3 Mechanism of antibacterial and antibiofilm activity of PHBV-PEO-ZnO microfibers	151
7.3.4 Biocompatibility	151
7.3.4.1 Determination of hemocompatibility	151

7.3.4.2 Cell viability study	152
7.3.4.2.1 Selection of cell line	152
7.3.4.2.2 Selection of Cytotoxicity assay	153
7.3.4.2.3 MTT assay of synthesized PHBV-PEO-ZnO	154
Microfibers	
7.3.4.2.4 Mechanism of cytotoxicity of synthesized	155
Microfibers	
7.4 Conclusions	156
References	158

Chapter 8

Summary and conclusion

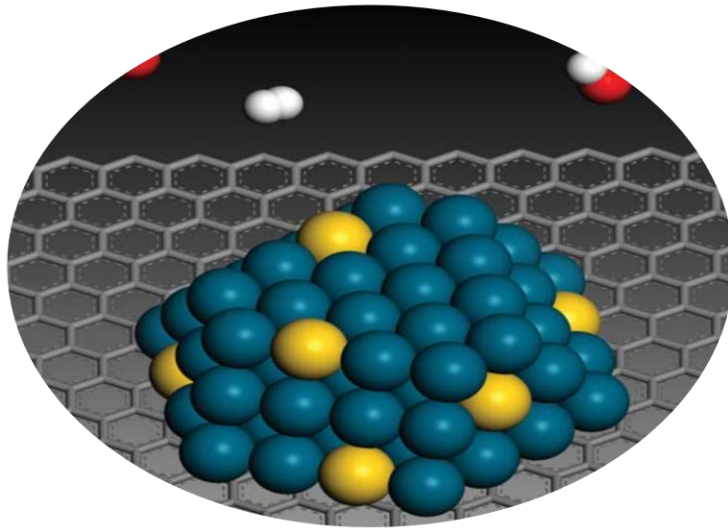
8.1 Introduction	161
8.2 Competent component of the thesis	162
8.3 Summary of thesis	167
8.4 Major conclusions	168
8.5 Future scope of the thesis	172

List of publications

Curriculum vitae

CHAPTER 1

Introduction



Scientific discovery and scientific knowledge have been achieved only by those who have gone in pursuit of it without any practical purpose whatsoever in view."

-Louise Pasture

Chapter 1: Introduction

1.1 Introduction

Since the origin of human existence, bacterial infections have become a challenge to human life. Historically bacteria have been recognized to be planktonic (freely swimming) cells, but recent studies have been evaluated that microorganisms remain aggregated into the complex extracellular polymeric substance (EPS) known as a biofilm, in which cells adhered to each other and the surface.¹ The microorganisms in biofilm experience cell to cell contact in a multicellular structure.^{2,3} The broad range of bacteria can form biofilm include Gram-positive *Staphylococcus aureus* to Gram-negative *Pseudomonas aeruginosa*. Biofilm grows on natural surfaces like teeth and wounds and/or artificial surfaces like medical implants, medical devices, catheters, lab equipment, and industrial setups.⁴ Biofilm-related infections account for over 65% of human microbial infections. Biofilm formed on the medical implants causes several infections and expend a high amount for treating and diagnosing biofilm-related infections. Biofilm-associated infections have affected millions of people and caused death worldwide.⁵

Micro-organisms that form biofilm are less sensitive to antibiotics and are highly resistant to the host-immune system than their planktonic form. Resistance developed by micro-organisms is due to frequent changes in surface antigens by the alteration in the gene expressions.⁶ Antibiotic resistance increases as the biofilm mature.⁷ There are three hypotheses for the development of antibiotic resistance. The first hypothesis suggests the lack of penetration into the biofilm matrix which is due to the presence of many water-filled channels that causes failure of the action. Second is the change in microenvironment of biofilm and the last one is that subpopulation of bacteria in biofilm may differentiate into protective phenotypes.⁸

The development of antibiotic resistance is the most difficult to treat and to eradicate. Human skin is one of the important, largest, and protective organs in the body. Each year several people get affected by skin injury of both acute and chronic nature. Initially, micro-organisms of a preparative stage of the infected process include Gram-positive bacteria like *Staphylococcus aureus* (*S. aureus*) and *Streptococcus pyogenes* (*S. pyogenes*). Gram-negative bacteria such as *Pseudomonas aeruginosa* (*P. aeruginosa*) and *Escherichia coli* (*E. coli*) are involved in the later stages of infection.⁹ The symptoms of wound infections are pus formation, spreading redness, increased pain or swelling, and fever. Wound infections occur due to the growth and development of micro-organisms within the wound area.¹⁰ The existence of drug-resistant

Chapter 1: Introduction

bacteria in the wound infections cause delayed wound healing process when treated with conventional antibiotics. The emergence of biofilm-associated wound infections can be partly treated by different approaches like the use of antibacterial wound dressing materials, local antimicrobial delivery, use of antimicrobial natural or synthetic peptides or use of phase therapy.^{11,12} However, these strategies have limitations like most of wound dressing materials present in the market possess low mechanical properties, inadequate blood clotting ability, and insufficient antibacterial activities. The use of local antimicrobial delivery system may show initially high-burst release and low-tail release that create a danger of antibiotic resistance. Use of antimicrobial natural or synthetic peptides is limited for large scale use. In phase therapy, the detailed interaction mechanism with bacteria and human host is still unclear, which make its use on large-scale. So there is an urgent need to develop an alternative strategy to treat drug-resistant bacterial infections.¹²

1.2 Bacterial biofilm: Mechanism of formation and risk dissemination

Biofilm is the community of micro-organisms that remain enclosed in the self-generated extracellular polymeric matrix (EPS).¹³ Along with EPS biofilm also contain carbohydrate-binding protein, pili, flagella, extracellular deoxyribonucleic acid (DNA), and fibers. Steps involved in the formation of biofilm are, (i) initial attachment (reversible stage), (ii) irreversible attachment, (iii) micro-colonies formation, (iv) maturation, (v) dissemination or detachment from the matrix.¹⁴ In the first step for biofilm formation bacteria get attached to any surface. Before adhering, pre-conditioning of the surface occurs by organic or inorganic macromolecules. Different factors such as roughness, hydrophobicity or hydrophilicity, porosity and pore topology of the surface are responsible for the attachment of bacterial cells to surface.¹⁴ The presence of flagella, pili, fimbriae and glycocalyx influences the degree of attachment. During the second stage bacteria form micro-colonies.^{15,16} These micro-colonies produce an extracellular polymeric substance by quorum sensing. It is cell-to-cell signaling that expresses the biofilm specific genes that result in the formation of EPS matrix and maturation. In the final stage, bacteria disperse from the matured biofilm and start a new cycle.¹⁷ The schematic representation of biofilm development is given in figure 1.1

Chapter 1: Introduction

During the biofilm formation, the initial phase of attachment of micro-organisms to the surface can be targeted to prevent biofilm development. The inhibition of early stages of development includes targeting EPS production, and cell division.¹⁸

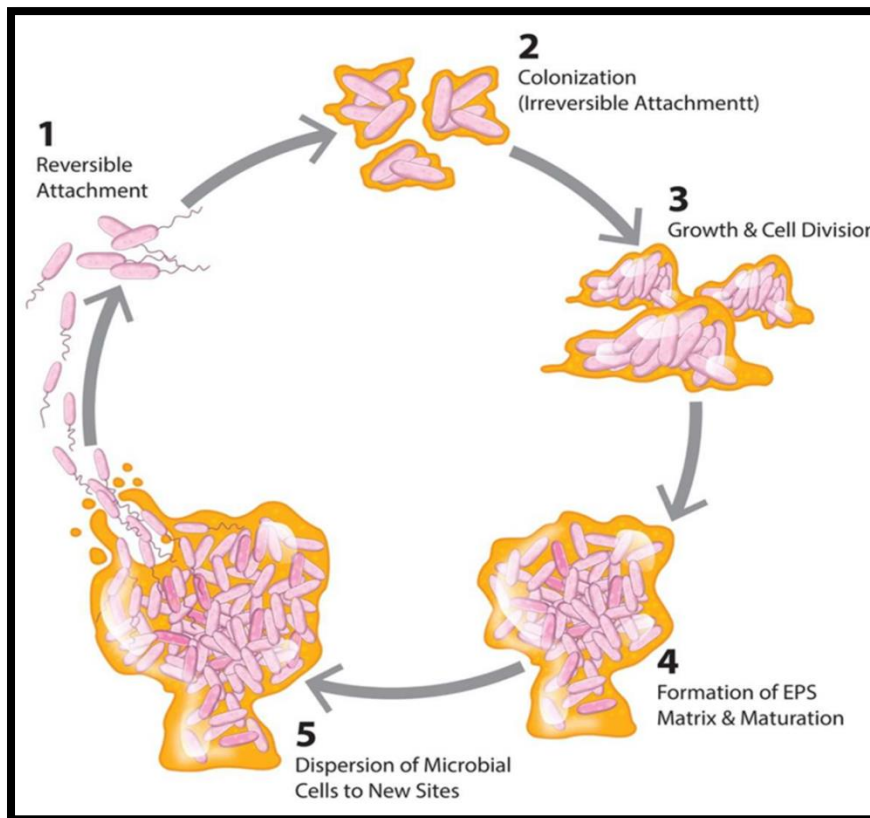


Figure1.1: Steps involved in biofilm formation. (1) Planktonic cells adhere to the surface reversibly through their surface appendages like pili, flagella (2) Motility is inhibited and develop irreversible attachment to form microcolonies (3) Cells grow and divide (4) Bacteria secrete slimy extracellular polymeric matrix of protein and polysaccharides. At this stage maturation of biofilm take place (5) Detachment and reversion to planktonic form.¹⁹

1.3 Drug-resistance

Specific strains of bacteria have started to develop antibiotic resistance. They were slowing down the action of antibiotics led to the release of new antibacterial drugs. The introduction of the new molecule takes at least a decade, whereas microbes take only one or two years to develop resistance and this highlights the urgent requirement of use of the other antimicrobial therapies.^{20,21} A possible mechanism of antibiotic resistance in a biofilm can be explained by three hypotheses. The first hypothesis suggests that lack of penetration inside the

Chapter 1: Introduction

matrix leads to the failure of antibiotic action. Some antibiotics with positive charge get bound to a negatively charged biofilm matrix, and this interferes with the antibiotic's entry to the biofilm depth.⁷ The second hypothesis suggests that the changes in the micro-environment of the biofilm result in the failure in the action of antibiotics. Cells near the biofilm surface efficiently utilize available nutrients and oxygen before they penetrate inside the deeper layers of the biofilm that lead to the development of anaerobic conditions.^{22,23} Some antibiotics like aminoglycosides, fluroquinolones and β -lactamases unable to show antibacterial action effectively in anaerobic conditions.^{24,25} Also, the change in the osmotic environment induces the osmotic stress response responsible for antibiotic resistance followed by reducing the number of entry channels like porins in the cell that limit the permeability of cell membrane to antibiotics.²⁶⁻³⁰ The third hypothesis suggests that the subpopulation of bacteria within a biofilm may differentiate into a protective phenotype similar to that of spore formation. This results in drug-resistance in this population.^{31,32} Different hypotheses for the development of antibiotic resistance are given in figure 1.2.

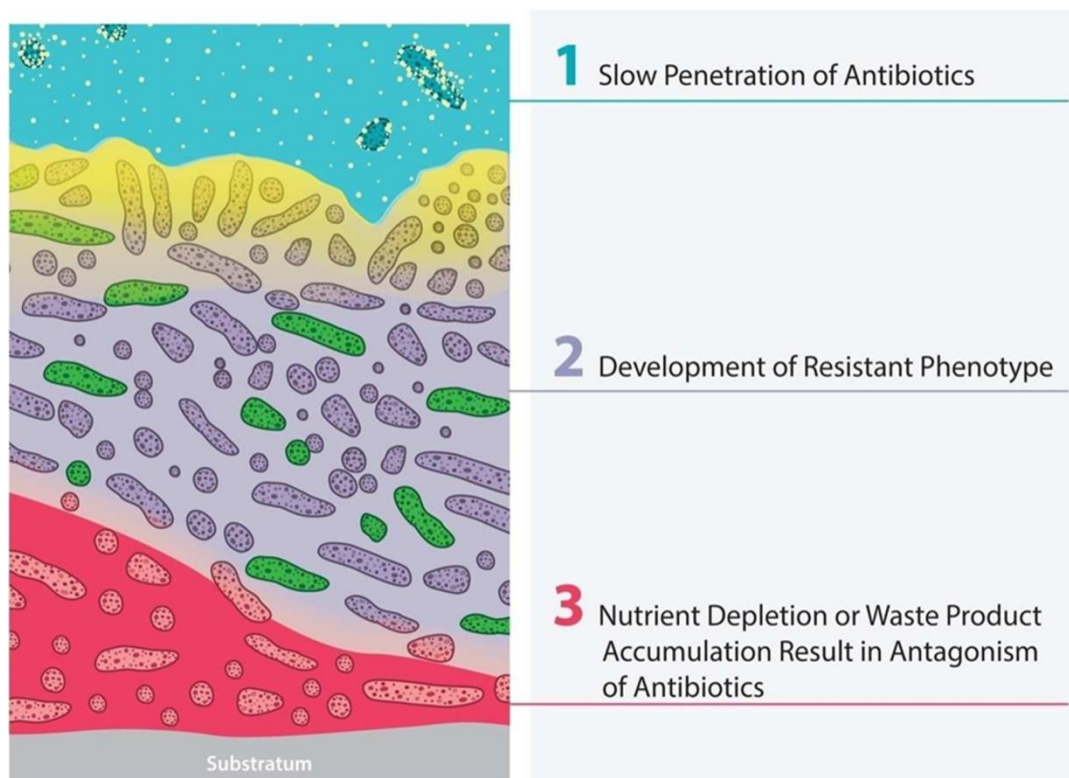


Figure 1.2: Different hypotheses of antibiotic resistance in biofilm (The surface to which biofilm is attached shown at the bottom and antibiotics at the top) (1) Poor penetration of antibiotics in

Chapter 1: Introduction

the surface layer of biofilm due to extracellular polymeric matrix (2) Development of persisters (3) In the zone of nutrient depletion or waste product accumulation the action of antibiotics may fail.³³

1.4 Different approaches to control biofilm and planktonic cells of bacteria

Different antibacterial agents show variable efficiency towards the biofilm that can be improved by enhancing the antibacterial activity of materials. Different materials can be used to control biofilm in any infections including wound infections. These materials can inhibit biofilm in different ways including preventing initial attachment of bacteria to a surface or by disrupting biofilm during the maturation step or by destroying bacterial cells in wound infections.^{34–38} The different antibacterial and antibiofilm agents are discussed below.³⁷

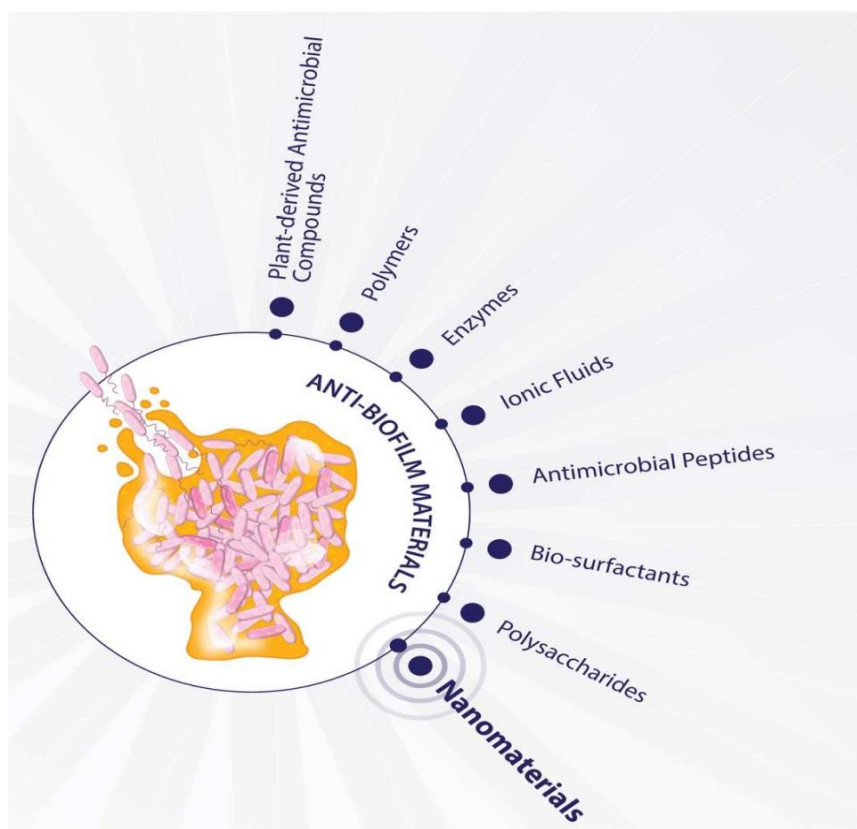


Figure1.3: Schematic representation of different materials like plant-derived antimicrobial compounds, polymers, enzymes, ionic fluids, antimicrobial peptides, biosurfactants, polysaccharides and nanomaterials used to control biofilm by inhibiting different steps in biofilm formation.^{38,39}

Chapter 1: Introduction

1.4.1 Plant-derived antimicrobial compounds

Different plant extracts can be used to treat a variety of diseases. Compounds extracted from plants are mostly the plant's secondary metabolites which may contain different categories of active ingredients. These materials are safe, cost-effective and exhibit activity without any side effects.⁴⁰⁻⁴²

1.4.2 Polymers

The use of antimicrobial polymers has gained much more attention. A polymeric hydrophilic coating with the use of polyethylene glycol (PEG), for the development of antifouling surfaces, reduces or blocks the adhesion of the cells. However, the use of PEG is restricted due to its tendency of auto-oxidation that forms aldehyde and lowers the protein resistant ability in an alkaline condition.⁴¹⁻⁴³ Polymer films also can be used as drapes for the surgical incision. Many studies suggested the use of polymers in dressing or as medical devices for the improvement in the wound healing process.^{44,45} Polyurethane (PU) is used in many semi-permeable dressings because of its ability to act as a good barrier, oxygen permeability, and impermeability to bacteria and liquid. A drawback of such material is that these dressings are non-absorbent that may cause the accumulation of exudates underneath such dressing films. Natural polymers like alginate, fucoidan, silk sericin, keratin, collagen, chitosan, pectin, pullulan, cellulose, and chitin are used for the preparation of wound dressing materials.⁴⁶

1.4.3 Enzymes

Deoxyribonuclease I (DNases I), lysostaphin, α -amylase, lyase, and lactonase are some examples of matrix-degrading enzymes of one more emerging group of antimicrobial enzymes is that of anti-quorum sensing enzymes. Acyl homoserine lactones (AHL) are the best-known quorum sensing molecules. Quorum sensing enzymes like lactonases prevent AHL from binding to the target regulators.⁴⁷ However, costly enzyme production limits the use of enzymes in the biomedical applications.⁴⁷⁻⁴⁹

1.4.4 Antimicrobial peptides

Antimicrobial peptides (ABPs) target biofilm disruption via different mechanisms that are degradation of signals in the biofilm, an increase in permeability, reduced activity of biofilm-associated genes, preventing adhesion and, decreases motility. ABPs interfere with quorum sensing (QS) system and degrade signal producing molecules or secondary messengers (ppGpp)

Chapter 1: Introduction

for example, DJK5, DJK6.⁵⁰ Genes responsible for the biofilm regulation are also targeted by some ABPs like ZAP1, ALS3.⁵¹ They target metabolically active cells within the biofilm as they are of cationic nature. Motility of microbes affects the biofilm function as it is a pre-adhesive stage when bacteria move to the surface. This action can be hampered by some ABPs like LL-37, modified 1037.⁵² Anti-biofilm peptides show exciting broad-spectrum activity and are less sensitive towards the development of resistance. They can also be used in combination with conventional sensitivity towards the development of resistance. However, high production cost, laborious synthesis procedures and potential toxicity limit their use. It has been reported that no peptides have received approval for clinical applications by the United States, Food and Drug Administration (FDA).⁵³

1.4.5 Polysaccharides

Recent studies reported the ability of polysaccharides to inhibit biofilm formation. None of the antibiofilm polysaccharides exhibited bacteriostatic or bactericidal activity. It acts as a surfactant molecule and changes the physical properties of the cells and surfaces or by modulating gene expression affecting biofilm formation or competitive inhibition of multi-valent carbohydrate-protein interaction. However, no significant effect was observed on thoroughly developed biofilm. The use of the antibiofilm polysaccharides in the medical and industrial fields is favorable as they possess properties like broad-spectrum activity, biocompatibility, and biodegradability.^{54, 55} However, much more research is required into their biological role to validate their use as an alternative antibiofilm agent.^{54–57}

1.4.6 Ionic fluids

Ionic fluids are the liquid salts that consist of cations and anions which can be modified independently. The activity of ionic fluid mainly depends upon their alkyl chain length. For example, 1-alkyl-3-methylimidazolium, 1-alkylquinolium bromide are ionic fluids. These are non-flammable, non-volatile fluids with thermal stability, chemical stability, density, solubility, viscosity, melting point <100, good conductivity, solvating ability, and recyclability. These are also termed as green solvents. But, their toxic nature limits their use in the medical fields.⁵⁸

1.4.7 Bio-surfactants

Chapter 1: Introduction

Bio-surfactants possess surface tension reducing properties, detergency, low-toxicity, biodegradability, effectiveness in various conditions, and foaming. However, their large scale production costs are expensive and limit their use in different fields.^{59,60}

1.4.8 Nano-materials

Nanotechnology has attracted significant attention worldwide in the research field of modern material science. Nanotechnology is currently developing fields that have extensive applications in the scientific research area. The Greek word “nano” is derived from the word “dwarf” and denotes a deduction in size, time, of 10^{-9} , which is billionth of a meter or three to five atoms in width equivalent to 10^0\AA . The science and engineering used in the design, synthesis, characterization, and applications of materials that contain the smallest particles of 1-100 nm is “Nanotechnology”. The concept of nanotechnology has roots in the idea of last century’s some scientists.⁶¹ On December 29, 1959, the American physicist Richard Feynman had given a talk under the title “There’s Plenty of Room at the Bottom” at an American Physical Society meeting. In this talk, he described the importance “of manipulating and controlling things on a small scale” and how they could “tell us much of great interest about the strange phenomena that occur in complex situations”.⁶² The term “nano-technology” was first coined by the Japanese scientist Norio Taniguchi of Tokyo University of Science, in 1974.⁶³ However, this term was not used until 1981, when Eric Drexler, who was completely unaware of Taniguchi’s prior use of the term, published his first paper on nanotechnology. The American engineer K. Eric Drexler developed molecular nanotechnology that leads to nanosystem machinery manufacturing. He developed the principle of manipulation of an atom by atom, by the control of the structure of matter at the molecular level, that can build molecular system with atom-by-atom precision, yielding a variety of nanomachines.⁶⁴ Nanotechnology has potential applications in different fields like water decontamination, electronic devices, information technologies, drug delivery, and production of lighter materials. The study of nanotechnology deals with the material that possesses the following properties,

- Possess minimum of one dimension less than 10nm.
- Physical and chemical properties can be controlled through the synthesis approaches.
- Allows the manufacture of larger structures.

Chapter 1: Introduction

In nature, nanotechnology is present for the synthesis of bioentities in the body, such as proteins, enzymes, carbohydrates, DNA, RNA and, viruses, which form the components of the cell. The size of many biological molecules possesses the size in the nanoscale range of 1-100 nm.

For the synthesis of nano-engineered materials and devices, precursors from solid, liquid or gas phases with a different set of experimental techniques are used. In general, most of the synthetic methods can be divided into two approaches: “top down” and “bottom up” approaches or their combinations. In “bottom up” approach macroscale materials are broken down into nanoscale materials physically or chemically and in “top down” approach nanoscale materials are arranged atom-by-atom or molecule-by-molecule. Nanotechnology is an interdisciplinary research field in which many physicists, chemists, biologists, material scientists and other specialists are involved. It includes the production and applications of manipulated materials at nanoscale in a variety of fields.^{65,66} The amalgamation of nanoscience with technology provides newly developed techniques, replacing older techniques. It is today’s most advanced technology and also called as “extreme technology”, as it gives excellent accuracy to the molecule or atoms size. The increasing scope of this new technology provides the size-dependent unique and previously unnoticed properties and much more. These nanoscale materials are effective in treating infectious diseases even in antibiotic-resistant strains, in vitro and, in-vivo models. This phenomenon is due to large surface area to volume ratio that gives unique mechanical, chemical, electrical, optical, magnetic and electro-optical properties that differ from bulk counterpart.⁶⁷

Nanomaterials have attracted greater attention than other antimicrobial agents. Silver nanoparticles show antibacterial activity because of their dissolution and generation of Ag^+ ions. These ions get internalized and liberate reactive oxygen species. In the case of biofilm inhibition, Ag^+ ions prevent the penetration of amine, thiols or carboxylates. Ag NPs tend to agglomerate that can adversely affect their antimicrobial activity and therefore their surface functionalisation is necessary before application.⁶⁸ Gold NPs also exhibit antimicrobial activity by the additional mechanism like inhibiting intra-cellular ATP synthesis and t-RNA binding. However, their use is restricted by their killing ability of limited strains, poor storage stability, and high cost.^{69,70} Graphene-based NPs show size and shape dependent antimicrobial activity. They are less water-soluble due to their hydrophobic nature and mainly possess contact killing ability but prevention of biofilm is only minimal.⁷¹

Chapter 1: Introduction

Recently zinc oxide NPs have gained even more attention as they possess the highest toxicity against drug resistant micro-organisms. ZnO NPs exhibit a way of antimicrobial action as that compared to other nanoparticles. They initially destroy the bacterial cell wall, then enter the cell, and finally deposited in the cell membrane leading to death.⁷² The toxicity of ZnO NPs does not always depend upon the internalization in bacteria; these NPs can alter the microenvironment near the bacterial cell and liberates reactive oxygen species and induce their solubility.⁷³ Among the nanoparticles these are highly preferred as ZnO is recognized as a safe material by the US food and Drug Administration (21 CFR 182.899).⁷⁴ ZnO fulfills the requirements of ideal antibacterial and antibiofilm agent.⁷⁵

1.5 Properties of ideal antibacterial and antibiofilm agent:

Two approaches that can be considered to treat biofilm to prevent its formation or to remove already formed biofilm. Biofilm formation can be hampered by avoiding the initial attachment of cells to surface by surface modification or treating cells in such a way that it will block the cell attachment. Physical activities like sloughing, erosion and dispersion can remove preformed biofilm.^{76,77} To act as ideal antibacterial and antibiofilm agent, the material should possess following properties:

1.5.1 Biocompatibility

The materials to be used as an antibacterial and antibiofilm agent in the bio-medical field, their toxicity towards mammalian cells should be evaluated. The materials which are used in wound dressing applications are capable of being in contact with bodily fluids and tissues for prolonged periods, so their adverse reactions should be studied before application.^{78,79}

1.5.2 Antimicrobial properties

The material should possess good antibacterial activity. Antimicrobial activity of material mostly depends upon pH, type of micro-organism, population size, structural conditions such as molecular weight, concentration, derivative form, source, morphology, temperature and, duration of exposure, etc.^{80,81} Some of the factors that affect antimicrobial activity are explained here. Guo et al.⁸² synthesized imidazolium (Im), quaternary ammonium and 1, 4-diazabicyclo [2.2.2] octane-1, 4-dium (DABCO-dium) cation-based small molecule cationic compounds, and their corresponding side/main chain cationic polymers >small molecule cationic compound. Devlieghere et al.⁸³ studied the effect of pH on the antimicrobial activity of chitosan. He observed

Chapter 1: Introduction

that chitosan showed higher antimicrobial activity at low pH, as the amino group of the chitosan gets ionized at pH <6.⁸³

1.5.3 Surface

To prevent biofilm-related infections the material to be used should be biocompatible. The material should be flexible so that the surfaces modifications that will target it towards biofilm and can get interact with the biofilm structure.⁸⁴

1.5.4 Size and shape

Bacterial biofilm get protected in an EPS matrix. This matrix blocks the penetration of the anti-biofilm agent from reaching the inside by the diffusion. The size and shape of an antibacterial and antibiofilm agent are very significant factors that significantly influence the degree of antibacterial and antibiofilm activity.⁸⁵ As the bacterial cell ranges from 0.2-10 micron, the smaller material can get readily penetrate the biofilm matrix and then into the bacterial cell. For example, spherical carbon dots less than 10nm composed of sp³ hybridized carbon exhibited good antibacterial activity. The shape of the material has tremendous significant influence on the intensity of antibacterial and antibiofilm activity during morphological interaction. Sharp edges, spikes, pillars or protrusions on the surface of the antibacterial agent pierce and rupture the bacterial cell due to high local stress.⁸⁶ Hicky et al.⁸⁷ observed the degree of antibacterial activity of gold nanoparticles having sphere, star and, flower-shape against *Staphylococcus aureus* and concluded that flower-shaped gold nanoparticles comparatively showed more shape-dependent activity.

1.5.5 Stability at different temperature and pH

Pourali et al.⁸⁸ evaluated the effect of two different temperatures on the antibacterial activity of the biosynthesized silver NPs and showed that the biological silver NPs before heat treatment were more bactericidal than heat treated silver NPs (100 and 300°C). TEM images showed that the average size of the heated silver NPs was >100 nm and <100nm of non-heated NPs. So, the temperature affects the size of NPs and the penetration inside the cell.

1.5.6 Other properties

Chapter 1: Introduction

The antibacterial and antibiofilm agent should possess unique structure, be easy and cost-effective to produce, attach firmly to the surface which is to be developed as an antibiofilm surface and will not be able to develop the resistance.⁸⁹

1.6 Zinc oxide nanoparticles: Properties and biomedical applications

Zinc oxide NPs fulfill the requirement of the ideal antibacterial and antibiofilm agent. Among all NPs, ZnO NPs have gained greater attention because of its unique properties such as the high surface area to volume ratio, cost-effective material, and prolonged environment stability.^{90,91} ZnO NPs are II-IV semiconductors with wide bandgap energy, which is, 3.3eV and high excitation energy, 60eV. Therefore it can sustain too large electric fields, high temperatures, and high power operations.⁹² It is highly applicable in solar cells, photocatalysis, and chemical sensors.^{93,94} ZnO occurs in wurtzite, zinc blend and rock salt structures. The wurtzite phase is more stable thermodynamically at ambient conditions (figure 1.3). In a wurtzite structure Zn^{2+} and O^{2-} are alternatively stacked along the C axis.⁹⁵

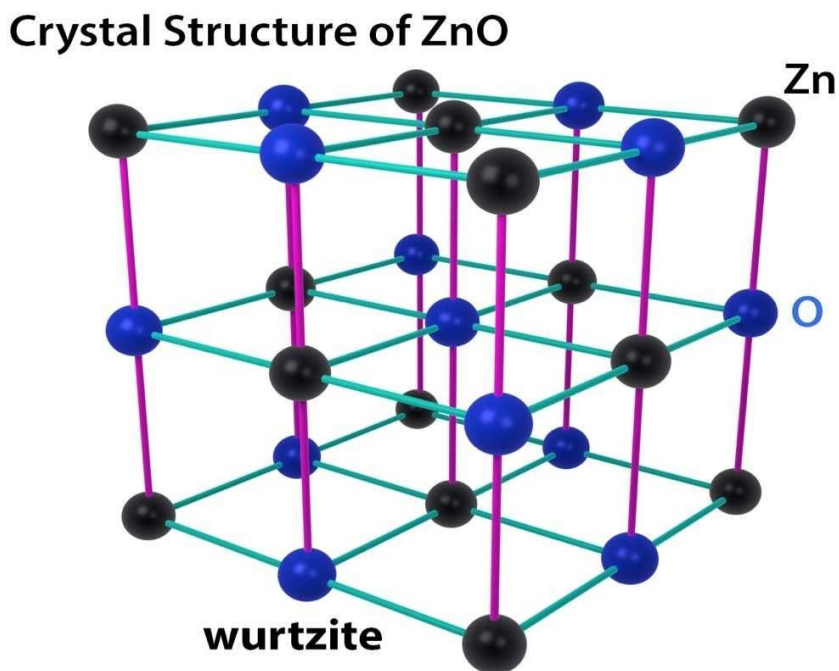


Figure 1.4: Crystal structure of ZnO in wurtzite phase which is most stable in ambient condition and so most common.⁹⁵

Chapter 1: Introduction

ZnO NPs has been reported widely for their anti-microbial, anti-diabetic, anti-fungal, anti-tumor and variety of other properties (figure 1.4). It is also commonly used in the cosmetic lotions as it is also known to maintain UV blocking and has absorbing capabilities as well as being an astringent in wound healing, anti-hemorrhoids, eczema, and excoriation in human medicine.⁹⁶

ZnO shows a high range of optical absorption in UVA (400 nm-315 nm) and UVB (315 nm-280 nm) region which enhances its antibacterial property. ZnO also possess strong ionic bonding in Zn-O.^{97,98}

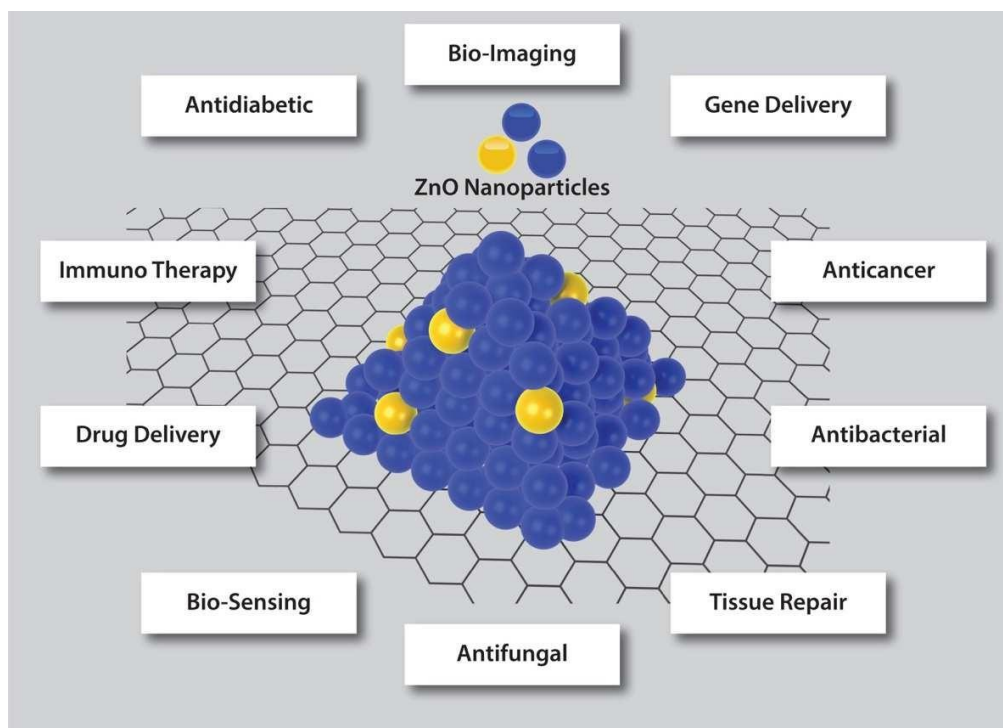


Figure1.5:Different bio-medical applications of ZnO NPs.³⁹

1.6.1 Anti-cancer activity

Among the other biomedical applications, the anticancer activity of ZnO NPs has been well reported. It exhibits the anticancer property by the generation of reactive oxygen species (ROS) and by inducing apoptosis. It possesses the good electrostatic properties that enhance its use for anticancer activity.⁹⁹ The isoelectric point of ZnO NPs is 9-10, so these NPs possess a strong positive charge on their surface under the physiological conditions. In contrast, cancer cells possess a high concentration of anionic phospholipids on the surface; so, they have large considerable negative membrane potential. Thus, the strong electrostatic interaction takes place

Chapter 1: Introduction

in between positively charged ZnO and negatively charged cancer cells, enhancing the cellular uptake, phagocytosis, and cytotoxicity of ZnO NPs.^{100,101}

1.6.2 Bio-imaging

The inherent photo-luminescence properties are useful in biosensing applications.¹⁰² Kang et al.¹⁰³ prepared a ZnO-gated nanoplatform for multimodality bio-imaging. ZnO NPs also can act as a contrast agent for trimodal imaging in-vitro and in-vivo tumor diagnosis. ZnO NPs can be used in the imaging of cultured cells.¹⁰⁴

1.6.3 Anti-diabetic activity

The zinc ions have an essential role in the synthesis of insulin, their storage, and secretion.¹⁰⁵ In some studies, ZnO NPs were proved as an anti-diabetic agent as compared with ZnSO₄, which was proved by the improved glucose disposal, insulin levels, and zinc status. ZnO Ps also can be tested in combination with the anti-diabetic drug, red sandalwood, and vildagliptin.^{106,107}

1.6.4 Anti-inflammatory activity

Nano-ZnO can enter the deep layers of allergic skin as compared with bulk-ZnO. Nano-ZnO can suppress local skin inflammation and induces IgE antibody production. According to the authors, this action is the result of non-specific reactions caused by the release of Zn²⁺ ions affecting the IgE antibody production by B cells.¹⁰⁸

1.6.5 Anti-fungal activity

Surendra et al.¹⁰⁹ synthesized ZnO NPs from *M. oleifera* which showed toxicity against plant pathogens, namely *Alternaria saloni* and *Sclerotium rolfsii* strains. Jain et al.¹¹⁰ studied the effect of ZnO NPs on the viability of *Candida albicans* in which they observed the concentration-dependent effect of ZnO NPs.

1.6.6 Antibacterial and antibiofilm activity

The antibacterial and antibiofilm activity of ZnO NPs is mainly due to their ability to generate oxidative stress. ZnO NPs release Zn⁺ ions, that interact with the thiol group of respiratory enzymes and inhibit their action.¹¹⁰ When ZnO NPs interacts with cell membrane it generates reactive oxygen species (ROS) that include O[•], HO[•]₂, H₂O₂, and HO[•] that damages cell by inducing oxidative stress response. The imbalance between generated ROS and their

Chapter 1: Introduction

reducing equivalents is termed as oxidative stress. ROS irreversibly damages bacterial cell membranes, DNA, and mitochondria, resulting in the death of bacterial cells.¹¹¹ Another important mechanisms for antibacterial and antibiofilm activity of ZnO NPs is the release of zinc ions in an aqueous media that contain ZnO and bacteria. Other mechanisms include the interaction of positively charged H_2O_2 that can easily interact with the bacterial cell. It is reported that, after membrane disruption by H_2O_2 or HO^\bullet , negatively charged ROS can easily penetrate the cytoplasmic region, which enhances antibacterial and antibiofilm activity.^{112,113}

1.6.7 Wound-healing ability

ZnO NPs have been reported for their use in the wound-dressing applications due to their strong antimicrobial properties and epithelialization stimulating the effect of zinc.¹¹⁴

1.6.7.1 Wound

The wound is the damage of underlying tissue with disruption in anatomical structure and function due to accidents, surgery, burns etc. The wounds can be classified into several types based on wound depth, tissue loss, and type of injury, location or clinical appearance. In general, they are classified into two types based on wounds with tissue loss and without tissue loss. Wounds by tissue loss include second and third-stage burn wounds, diabetic foot ulcers etc. and wounds without tissue loss include first stage burn wounds and other wounds. Based on the period of the healing process, wounds are divided as acute and chronic wounds. The acute wound takes about 8-12 weeks for healing, and chronic wound takes about 12 weeks for the healing process. Wounds that involve the only epidermis are called as a superficial wound while wound that includes the epidermis, deep dermal layer, and blood vessels is considered as partial-thickness wounds. When wound consists of epidermis, dermis and sub-cutaneous tissue is referred as full-thickness wounds.¹⁰

1.6.7.2 Wound-healing process

The wound healing process is a multistep process that consists of cell growth and tissue regeneration. This process mainly includes coagulation or hemostasis, inflammation, proliferation, and remodeling or maturation phase (figure 1.6).

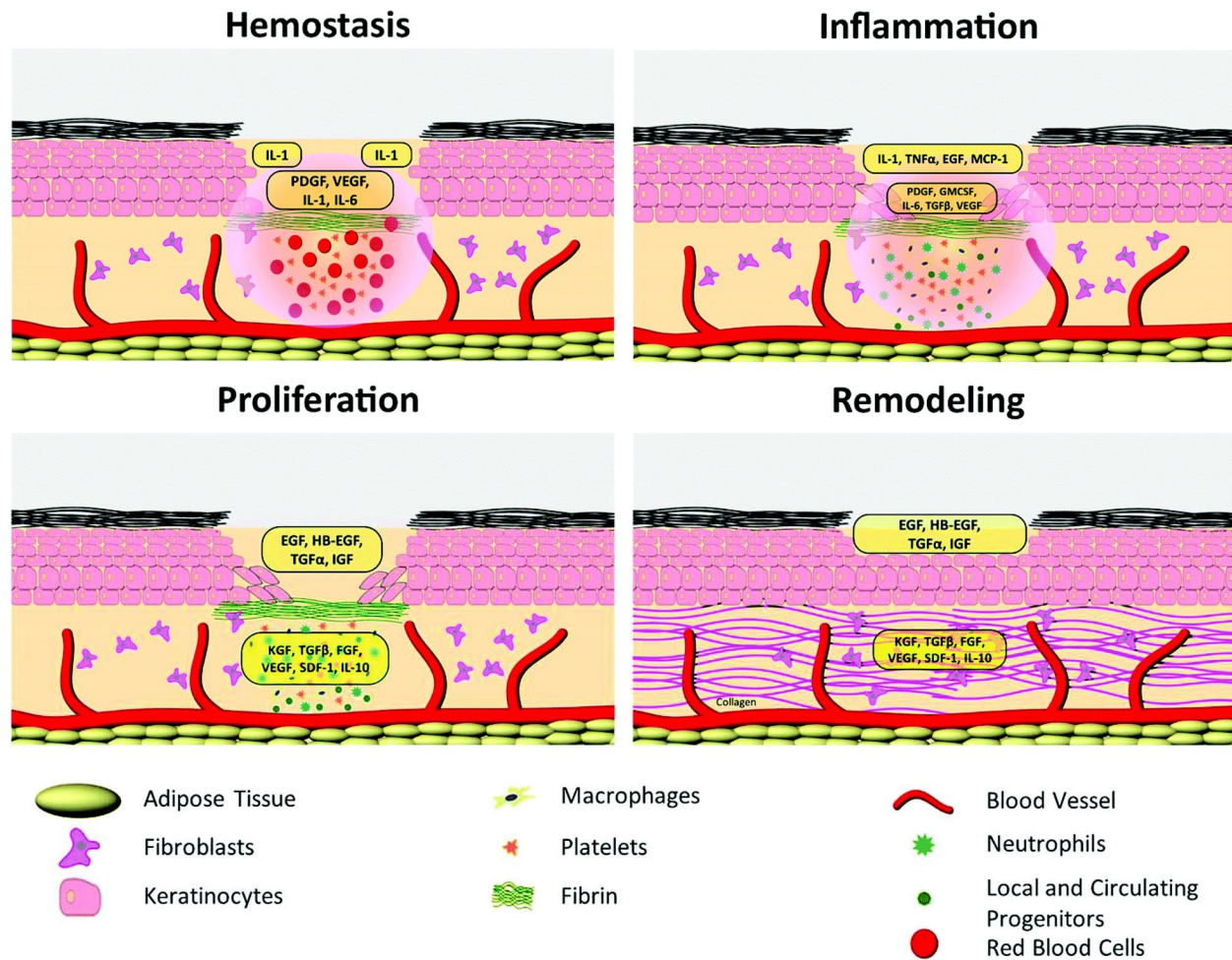


Figure 1.6: Schematic representation of wound-healing process, (i) Hemostasis, (ii) Inflammation, (iii) Proliferation, and (iv) Remodeling.¹¹⁵

The first phase in the wound healing process takes place in the first few minutes after injury. In this phase, the body activates its emergency repair system, the blood clotting system, and forms a mesh to block the drainage. The blood clot releases cytokines and growth factors such as interleukin-1 (IL-1) β , transforming growth factor (TGF), tumor necrosis factor (TNF), platelet-derived growth factor (PDGF), basic fibroblast growth factor (bFGF), epidermal growth factor (EGF), migration of neutrophils (after 6 h), and formation of initial matrix for early wound healing by fibrins, lymphocytes and histocytes (after 12 h).

The second phase is called the defensive/inflammatory phase that includes the destruction of bacteria and removal of debris. In this phase, dead and damaged cells are cleared. White blood cells, neutrophils, monocytes, and lymphocytes get differentiated into macrophages, for the

Chapter 1: Introduction

destruction of bacteria. Neutrophils also release substances like proteases and reactive oxygen species (ROS) that causes damage.

The proliferative phase starts from 3rd day after wounding and lasts for about two weeks. In this phase, fibroblast migration, deposition, collagen synthesis, angiogenesis and granulation tissue formation takes place in the wounded area. Fibroblasts generate glycosaminoglycans and proteoglycans that are major significant factors of the extracellular matrix (ECM).

In the last remodeling phase, the new tissue slowly gains strength and flexibility. Therefore, vascular densities of the wound return to normal. Scar maturation is another significant step in this phase of healing. Collagen remodeling may last for two years.¹¹⁶

1.6.7.3 Wound dressings

The wound dressing materials are mainly used for healing the wound. These materials are designed based on the type of wound, severity, and position of the wound. The process of wound healing gets affected by a variety of factors like insufficient blood supply, foreign bodies, infection types, topical steroids, and antiseptics. Any wound that is unable to heal within a few weeks is expected by a healthcare professional. The type of micro-organisms infecting the wound is an essential factor in patients with a skin wound. The risk associated with wound infection is increased by the increased concentration of pathogens and the presence of vascular disease, edema, malnutrition, diabetes, and corticosteroids. The important signs of soft tissue infections are pus formation, swelling of the wound site, increased erythema, pain, odor and fever in patients.¹⁰

The use of suitable dressing materials is an important factor for proper care of the wound and a faster wound healing process. Previously, the wound dressing materials used for healing are of bandages and gauze, with different degree of absorption. Nowadays, researchers have focused on the newer type of dressings with quick healing capability, maintain a moist environment, control of infection, control of wound exudates etc.¹¹⁷

Wound dressing materials can be classified into two types, traditional dressings, and modern wound dressings. The traditional dressings include natural or synthetic bandages, cotton wool, and gauze, while foam, hydrocolloids, alginates, hydrogel, composites, and antimicrobial dressings are modern wound dressing materials.

Chapter 1: Introduction

Gauze is the most commonly used traditional wound dressing made from woven or non-woven gauze. Gauze can absorb exudates and act as a non-barrier material that promotes dryness in wounds. But gauze dressing requires frequent changing to save healthy tissues from maceration. These materials are cost-effective and easy to produce. Nevertheless, because of excess wound drainage, dressings become moistened and get adhered to the wound that makes painful during removal. Bandages are made up of cotton wool and cellulose. Synthetic bandages are made up of polyamide materials.¹¹⁸

Modern wound dressings are designed to maintain and enhance wound-healing. These are categorized as film, foam, gel, and hydrocolloids. Film dressings are useful for primary and secondary wound dressings, made up of the sterile plastic sheets of polyurethane and coated with adhesive. Films have capacity of autolytic debridement and impermeable to bacteria and liquid. They are flexible and do not require additional taping. These are majorly used in the epithelializing wound, superficial wound and wound with less exudate.^{119,120}

Foam dressings made up of porous polyurethane foam which is hydrophilic or hydrophobic with or without adhesive borders. Generally, the outer layer is impermeable to liquid due to its hydrophobic properties. It is permeable to water, oxygen, carbon dioxide and water vapor. It is protective, thermally stable, and highly absorbent. They are applicable in case of granulating wounds and lower leg ulcers.¹²¹

Hydrocolloid dressings consist of two layers an inner colloidal layer and outer water-impermeable layer. An inner layer possesses properties like self-adhesive, gel forming, and composed of hydrophilic colloid particles like pectin, gelatin, and elastomer. It can absorb exudates and swells in a gel like mass over the wound. It also provides a moistened environment and thermal insulation to the wound. The outer layer prevents the entry of bacteria and protects from foreign substances, shearing, and contamination. Hydrocolloid dressings are available in a variety of size/shapes and in powder, paste or granular form. They are applicable in case of partial and full-thickness wounds with low-moderate exudates, necrotic wounds, minor burns and ulcers. They are not applicable in case of clinically contaminated wounds.¹²²

Hydrogel-based dressings are of natural or synthetic polymers. It is made up of a network of water-soluble, hydrophilic, and polymer chains. Hydrogels dressings are highly flexible similar to natural tissues as they contain high water content (70-90%). Hydrogels can be used as

Chapter 1: Introduction

scaffolds in tissue engineering, drug delivery, and wound dressings etc. These dressings can maintain a moist environment, cooling sensation, swelling ability and healing ability without scar.¹²³

Alginate dressing is prepared from the sodium and calcium salts in foam or fibrous sheets form. Alginate can control wound exudates and bacterial infection. These types of dressings are preferred in case of diabetic wounds, venous wounds, full-thickness burns, split-thickness graft donor sites, ulcer, and cavity wounds. It also activates macrophages for the production of TNF- α which starts inflammatory signals.¹²⁴

Bioactive wound dressings are biocompatible, non-toxic and biodegradable. These can be derived from natural or artificial sources like collagen, hyaluronic acid, chitosan, alginate and elastin. Growth factors or antimicrobial agents can be incorporated in these types of dressings to enhance wound healing process.¹²⁵

The composite dressings are composed of multiple layers that give more than one function for wound healing. It is made up of an adhesive border of transparent materials or nonwoven fabric tape which helps in preventing sticking to granulating tissues, and middle layer is made up of absorptive material that maintain moist environment. The outer layer protects the wound from bacterial infections. These are preferred as primary or secondary dressings.¹²⁶

Antimicrobial wound dressing reduces the risk of infection used in partial and full-thickness wounds. These types of dressings are available in the market in the form of film, sponge, impregnate, woven absorptive products, non-adherent barrier or combination of materials.¹²⁷

1.6.7.4 Properties of ideal wound dressings

The wound dressing material should be non-toxic, biocompatible, able to prevent dehydration, maintain moist environment within wound area, allow the gas transfer, and prevent the wound from bacteria and dust. Besides, it should be non-adhesive that can remove easily.¹²⁸



Figure 1.7: Properties of ideal wound dressing materials.

The properties of ideal wound dressing materials are given in figure 1.7, which are listed below,

- ✚ It should maintain high humidity condition within wound area.
- ✚ It should possess high transport rate of gaseous and water vapor.
- ✚ It should control the amount of exudates.
- ✚ It should be non-toxic and biocompatible.
- ✚ It should possess blood-clotting ability
- ✚ It should be biodegradable.
- ✚ It should have oxygen barrier capacity.
- ✚ It should have enough mechanical strength.

1.6.7.4 Bio-materials used for wound dressing

Natural biomaterials have been used from long time in biomedical applications. These are not only obtained from the biological source but materials are used in biomedical applications. The natural biomaterials used for wound dressing applications are classified as polymers and nanobiomaterials. In nanobiomaterials, ceramics and metals are included. Ceramic materials are polycrystalline materials which are non-metallic in nature with good mechanical strength, hardness, stiffness, low density, and corrosion resistance. However, due to sensitivity to cracks

Chapter 1: Introduction

and other defects ceramic materials are used in limited amount as compared with metallic and polymer materials. The metals have properties like electrical and thermal conductivity, mechanical strength, corrosion resistance, and cheap. Therefore, these materials can be widely used in biomedical fields and in wound dressing applications.¹²⁹

Polymers are biocompatible, flexible, easily available materials with good mechanical strength. So they are widely used in biomedical applications like tissue engineering, drug-delivery, wound healing and wound dressing applications.

On the basis of their origin polymers can be classified into natural (biopolymers) or synthetic polymers. Natural polymers are obtained from renewable sources like animals or plants and synthetic polymers are obtained from non-renewable sources. Natural polymers are biocompatible, biodegradable and easy to produce as compared with synthetic polymers.¹³⁰

1.6.7.4.1 Biopolymers

Biopolymers are biological macromolecules that are classified into two types, polysaccharides and proteins on the basis of sources from they obtained. The polymers obtained from plant and animal resources, are polysaccharides (cellulose, chitosan, pectin), and protein are obtained from collagen, α -keratin, etc. In addition, the polymers those are obtained from microbes occur abundantly. Also they are fast and easy to grow from microbes than plants or animal sources.¹³¹

Chitosan is abundantly used polymer produced by the deacetylation of chitin which is other type of polymeric polysaccharide. Chitosan is mainly composed of D-glucosamine and N-acetyl-D-glucosamine joined by glycosidic bonds. It is bioactive polymer with a wide range of applications because of its properties like antibacterial activity, non-toxicity, easy modification, and biodegradability. It is widely used in biomedical applications like controlled drug delivery, tissue engineering, wound-healing, and gene delivery. It is also used in waste water treatment for the removal of dyes, odor, organic pollutants, and inorganic heavy metal ions from industrial waste water; also the hydrogels of chitosan can be used to carry dyes uptake and release studies. In agriculture fields, chitosan are used as an excellent alternative to synthetic pesticides to lower the harmful effect to the human and environment. It can be also used in the field of food packaging, cosmetics, and paper making industries.¹²⁴

Cellulose is one of the most abundantly occurring organic polymers on the planet. It is polysaccharide that contains a linear chain of several hundred to thousands of β (1 \rightarrow 4) linkages

Chapter 1: Introduction

of d-glucose. It is insoluble in organic solvents. It is non-toxic, biodegradable polymer due to which it is used in various fields like nanotechnology, pharmaceutical industries, food industries, cosmetics, and textiles.¹³²

Collagen is obtained from fibroblasts and most abundant protein in the human body. It enhances the wound healing process. Type I collagen can be obtained from animal sources. It is degraded to produce gelatin.¹³³

1.6.7.4.2 Poly (3-hydroxybutyrate-co-3-hydroxyvalerate) (PHBV)

1.6.7.4.2.1 Sources of PHBV

PHBV is a biopolymer produced by microorganisms with excellent biocompatibility and biodegradability. The polymers obtained from bacteria are exo-polysaccharide, proteins, lipids, and polyesters like polyhydroxyalkanoates (PHAs). These were observed by the Beijerinck in 1988 as inclusion bodies in bacteria. Later, in 1927 Lemoigne extracted and identified these granular inclusions as poly (3-hydroxybutyrate) (PHB). These inclusion bodies are enclosed in the cytoplasm of wide varieties of both Gram-positive and Gram-negative microorganisms when they face nutrition deficiency in elements such as nitrogen, phosphorus, magnesium, and sulphur, and in presence of excess carbon. It is widely reported that PHAs produced by Gram-negative bacteria contain high levels of endotoxins, which can show inflammatory, pyrogenic, and other reactions that restrict their application if not removed during purification. Therefore, PHB with less endotoxin can be used for biomedical applications. This can be achieved by recombinant *Escherichia coli* by NaOH digestion or by treating with hydrogen peroxide.¹³⁴

The structure and molecular weight of PHAs can be modified by altering the growth conditions. Varieties of PHAs and their co-polymers can be isolated from different types of bacterial species. There are above 150 possible monomers which are divided on the basis of a number of carbons in monomer via short chain length (scl) PHAs (example, PHB, poly (3-hydroxyvalerate) (PHV), poly (example, PHB, poly (3-hydroxyvalerate-co-valerate) (PHBV), medium chain length (mcl) PHAs (example, polyhydroxyoctanoate (PHO), polyhydroxynanoate (PHN), polyhydroxyhexanoate (PHHx), polyhydroxyheptanoate (PHHp) and long chain length (lcl) PHAs.¹³⁵

1.6.7.4.2.2 Properties of PHBV

Chapter 1: Introduction

Poly (3-hydroxybutyrate-co-3-hydroxyvalerate) (PHBV) is biocompatible, thermoplastic, biodegradable and non-toxic polyester produced by bacteria that make it promising agent in the biomedical field. The degradation product of PHBV, (R)-3-hydroxybutyric acid is a component of blood that promotes its use in the different biomedical fields such as sutures, prosthetic devices, drug delivery system and surgical clips. Many studies suggested that PHBV can enhance cell proliferation, such as fibroblasts, keratinocytes, and neural cells. However, due to its poor mechanical performance, high crystallinity, inherent rigidity, and hydrophobicity this material is not explored much explored. PHBV biopolymer can be widely used in different fields, but its applications have been restricted because of its poor mechanical properties, mainly due to its fragility. Their defects can be overcome by the addition of various monomers in the polymer chain to form copolymers.¹³⁶ The biocompatible and biodegradable properties of PHBV made it an excellent material for broad applications. In addition, its absorption ability, biological origin, non-toxicity, piezoelectricity, and thermoplasticity make it a very outstanding material for biomedical applications like drug release, absorbable surgical sutures, wound dressing material, and medical packing.¹³⁷

1.6.7.4.2.3 Structure of PHBV

PHBV is aliphatic polyester having the chemical structure as shown in the figure 1.8. It is less toxic, biodegradable, and biocompatible to different types of cells having high degree of crystallinity and resistance to ultraviolet radiation. However, it is rigid, with low melting temperature than PHB, and soluble in chlorinated solvents. It possesses good oxygen barrier capacity, chemical inactivity, viscosity, and good mechanical properties, like high surface tension and high flexibility than PHB. The physical and mechanical properties of PHBV mainly relay on the amount of 3HV present in the copolymer. For example, the PHBV with the increased amount of 3HV degrades at a high rate as the crystallinity of PHBV increases with an increase in 3HV content. The melting point of PHBV also decreases with an increase in the 3HV content. So, the selection of PHBV with proper 3HV content is an important factor that depends upon the type of application.

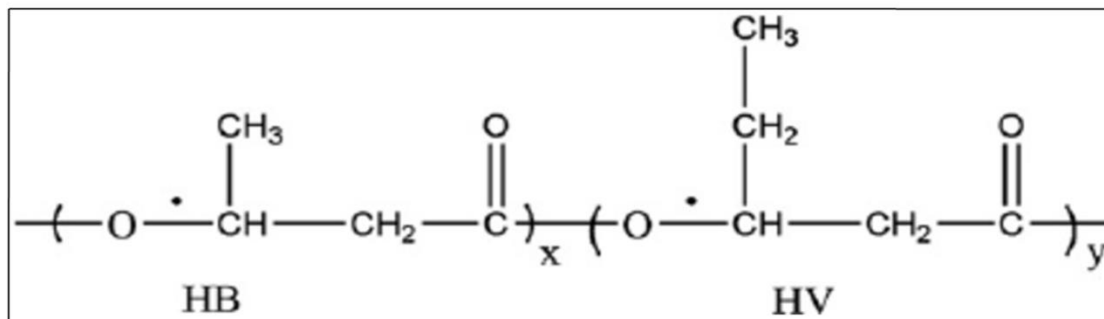


Figure1.8: Chemical structure of poly(3-hydroxybutyrate-co-3-hydroxyvalerate)PHBV.¹³⁴

1.6.7.4.2.4 Molecular weight

The molecular weight of polymer gives the information of the polymer chain and degree of polymerization that can affect mechanical and biodegradability properties, so it is an important factor for the determination of polymer properties. The molecular weight of the polyhydroxyalkanoates relies upon the type of microorganisms and the type of extraction method employed.¹³⁸

1.6.7.4.2.5 Composite electrospun PHBV-PEO fibers

The applications of pure PHBV are limited due to their poor mechanical strength, and fragility. To overcome this problem it should be blended with other polymers. The reinforcement approaches used for the preparation of PHBV composites are the combination of PHBV and other materials, like polymers, natural fibers, and different types of nanomaterials for expanding their applications.¹³⁹

Poly (ethylene) oxide (PEO) is one of the most biocompatible hydrophilic synthetic polymers. It is approved by the Food and Drug Administration for use in biomedical applications.

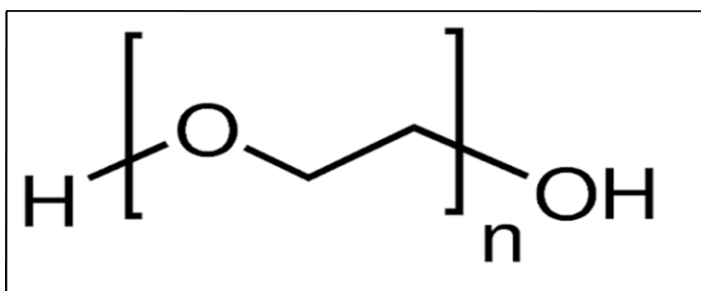


Figure1.9: Structure of Poly (ethylene) oxide (PEO).¹³⁴

Chapter 1: Introduction

It possesses excellent properties like maximum solubility in water and organic solvents, non-toxicity, non-immunogenicity, non-antigenicity, and low absorption of surface properties. This polymer is easy to blend with PHBV by electrospinning technique. It is well reported that the blending of PHBV with PEO improves mechanical, thermal, and physical properties. Bianco et al¹³⁴ investigated the improved properties of PHBV/PEO blends as compared with neat PHBV, mainly influencing the addition of PEO in different amounts in morphology, thermal, and mechanical properties. Structure of PEO is given in the figure 1.9.

The incorporation of ZnO NPs into PHBV polymer has gained much more attention in the nanocomposite field as ZnO is widely reported for its strong antibacterial activity against a broad spectrum of microorganisms.¹⁴⁰

1.7 Statement of the problem

Bio-contamination allows microbes to settle down at the infection site, where they withstand antibiotic treatment, so reducing antibiotic sensitivity. It is well reported that specific strains of microbes started to develop antibiotic resistance. Bacteria in a biofilm are more effectively protected from the host immune system than from planktonic bacteria. Multidrug resistance patterns in Gram-positive and Gram-negative bacteria are difficult to treat and indeed untreatable with conventional antibiotics. Drug resistance in infectious wound bacteria is difficult to treat with conventional antibiotics that delay the wound-healing process. Fast wound closure is an important factor in the care of acute or chronic wound infections. Wound infection mostly due to indigenous microflora or environments in the wound area. This can be cured by protecting the wound with antibacterial dressing materials. Antibacterial agents control the infections within the area of the wound. However, to treat infection by drug-resistant bacteria there is an urgent need to use a new antibacterial agent rather than conventional antibiotics.

Among different metal oxide nanoparticles, ZnO NPs are widely reported for their antibacterial and antibiofilm activities against a broad spectrum of Gram-positive and Gram-negative bacteria with low toxicity to human cells at the appropriate concentration. Also, these NPs reduce microbial adhesion, proliferation and biofilm growth due to their strong antibacterial activity. ZnO NPs damage bacterial cells by formation of ROS including $O^{\bullet-}$, HO^{\bullet}_2 , H_2O_2 and Zn^{+2} ions. They can also promote keratinocyte migration towards the wound site and improve the healing process. However, the intensity of antibacterial and antibiofilm activity of ZnO NPs

Chapter 1: Introduction

mainly depends upon the size of NPs. It is inversely proportional to the size of the nanoparticles. ZnO NPs are widely reported for their antibacterial and antibiofilm activities against a broad spectrum of micro-organisms. These nanoparticles can reduce microbial adhesion, proliferation, and biofilm growth. ZnO NPs destroy bacterial cells by the formation of reactive oxygen species including $O^{\bullet-}$, HO^{\bullet}_2 , H_2O_2 , HO^{\bullet} , and Zn^{2+} ions. To make their potential use in antibacterial wound dressing material their addition to polymers is important.

These nanoparticles should be blend into electrospun fibers for their wound dressing applications. The large surface area and porosity of electrospun nanofibers make them good agents for wound dressing applications that can protect the wound from bacterial penetration and dehydration. These properties make them suitable for wound dressing material, for chronic wounds.

Poly (3-hydroxybutyrate-co-3-hydroxyvalerate) (PHBV) is a natural biopolymer that possesses good properties like biocompatibility, biodegradability, non-toxicity and thermo plasticity. However, due to its poor mechanical performance, high crystallinity, inherent rigidity, and hydrophobicity this material is not explored much. To overcome this problem PHBV can blend with other hydrophilic polymers. Among those polymers, polyethylene oxide (PEO) which is certified by the FDA is highly preferred because of its excellent properties like biocompatibility, hydrophilicity, and malleability. It is non-immunogenic, non-antigenic, non-toxic and low adsorption capacity of surface proteins. Furthermore, from PEO it is easy to obtain nanofibers by electrospinning technique than other polymers because of its high solubility in water as well as in different types of organic solvents. The blends of PHBV-PEO has been prepared earlier, but not used for the further antibacterial applications.

Based upon the above consideration this thesis highlights the synthesis and characterization of ZnO NPs, ZnO incorporation in PHBV-PEO microfibers for antibacterial and antibiofilm activities. In light of this problem we carried out the work in this thesis with the following objectives:

- To synthesize the pure ZnO NPs by using different approaches like; (i) regular synthesis in polyols, (ii) in the presence of sodium acetate, and (iii) increasing reaction time, polyols used are diethylene glycol and triethylene glycols, by using the reflux method and to study their morphological, thermal, spectroscopic and elemental properties.

Chapter 1: Introduction

- To investigate their antibacterial, antibiofilm activities, hemocompatibility, and cell viability properties of all synthesized ZnO NPs.
- To incorporate ZnO NPs with maximum antibacterial activity into the matrix of PHBV-PEO and to investigate their morphology, thermal, mechanical, spectroscopic, and swelling behavior.
- To evaluate their antibacterial, antibiofilm efficacy and to determine their biocompatibility, cell viability ability.

Chapter 1: Introduction

References

- 1 V. Van Giau, S. S. A. An and J. Hulme, *Drug Des. Devel. Ther.*, 2019, **13**, 327–343.
- 2 M. R. Parsek and P. K. Singh, *Annu. Rev. Microbiol.*, 2003, **57**, 677–701.
- 3 R. Vasudevan, *J. Microbiol. Exp.*, 2014, **1**, 1–16.
- 4 L. J. Bessa, P. Fazii, M. Di Giulio and L. Cellini, *Int. Wound J.*, 2013, 1–6.
- 5 H. Joo and M. Otto, *Chem. Biol.*, 2012, **19**, 1503–1513.
- 6 B. S. Tseng, W. Zhang, J. J. Harrison, T. P. Quach, J. L. Song, J. Penterman, P. K. Singh, D. L. Chopp, A. I. Packman and M. R. Parsek, *Environ. Microbiol.*, 2013, **15**, 2865–2878.
- 7 W. N. Wright, M. D. Susan, P. E. S. Mary and L. W. Harold, *Antimicrob. Agents Chemother.*, 1988, **32**, 518–523.
- 8 M. Sugano, H. Morisaki, Y. Negishi, Y. Endo-Takahashi, H. Kuwata, T. Miyazaki and M. Yamamoto, *J. Liposome Res.*, 2016, **26**, 156–162.
- 9 D. R. Harper, H. M. R. T. Parracho, J. Walker, R. Sharp, G. Hughes and M. Werthé, *Antibiotics*, 2014, **3**, 270–284.
- 10 S. Guo and L. A. Dipietro, *Crit. Rev. Oral Biol. Med.*, 2010, **89**, 219–229.
- 11 H. J. Busscher, H. C. Van Der Mei, G. Subbiahdoss, P. C. Jutte, J. J. A. M. Van Den Dungen, S. A. J. Zaat, M. J. Schultz and D. W. Grainger, *Sci. Transl. Med.*, 2012, **4**, 1–10.
- 12 A. M. Carmona-ribeiro, *Int. J. Environ. Res. Public Health*, 2018, **15**, 1–29.
- 13 M. Chen, Q. Yu and H. Sun, *Int. J. Mol. Sci.*, 2013, **14**, 18488–18501.
- 14 M. Kostakioti, M. Hadjifrangiskou and S. J. Hultgren, *Cold Spring Harb. Perspect. Med.*, 2013, **3**, 1–23.
- 15 M. C. M. van Loosdrecht, B. E. Rittmann, J. P. Boltz, G. T. Daigger, B. F. Smets and E. Morgenroth, *Water Sci. Technol.*, 2017, **75**, 1753–1760.
- 16 J. Mystkowska, K. Niemirowicz-Laskowska, D. Łysik, G. Tokajuk, J. R. Dąbrowski and R. Bucki, *Int. J. Mol. Sci.*, 2018, **19**, 1–18.
- 17 M. Fletcher and G. I. Loeb, *Appl. Environ. Microbiol.*, 1979, **37**, 67–72.
- 18 B. Vu, M. Chen, R. J. Crawford and E. P. Ivanova, *Molecules*, 2009, **14**, 2535–2554.

Chapter 1: Introduction

- 19 T. S. Tshikantwa, M. W. Ullah, F. He and G. Yang, *Front. Microbiol.*, 2018, **9**, 1–19.
- 20 C. A. Arias and B. E. Murray, *N. Engl. J. Med.*, 2015, **372**, 1168–1170.
- 21 S. B. Levy and M. Bonnie, *Nat. Med.*, 2004, **10**, S122–S129.
- 22 P. S. Stewart, T. Zhang, R. Xu, B. Pitts, M. C. Walters, F. Roe, J. Kikhney and A. Moter, *npj Biofilms Microbiomes*, 2016, **2**, 1–8.
- 23 E. Werner, F. Roe, A. Bugnicourt, M. J. Franklin, A. Heydorn, B. Pitts and P. S. Stewart, *Applied Environ. Microbiol.*, 2004, **70**, 6188–6196.
- 24 B. Alberts, A. Johnson, J. Lewis, M. Raff, K. Roberts and P. Walter, *Antimicrob. Agents Chemother.*, 2004, **48**, 2659–2664.
- 25 O. Ljmmjoh, P. G. Nvdpe, S. S. Yoon, R. Coakley, G. W. Lau, S. V Lymar, B. Gaston, A. C. Karabulut, R. F. Hennigan, S. Hwang, G. Buettner, M. J. Schurr, J. E. Mortensen, J. L. Burns, D. Speert, R. C. Boucher and D. J. Hassett, *J. Clin. Invest.*, 2006, **116**, 436–446.
- 26 J. N. Anderl, M. J. Franklin and P. S. Stewart, *Antimicrob. Agents Chemother.*, 2000, **44**, 1818–1824.
- 27 I. Olsen, *Eur. J. Clin. Microbiol. Infect. Dis.*, 2015, **34**, 877–886.
- 28 B. Sharma, A. V. Brown, N. E. Matluck, L. T. Hu and K. Lewis, *Antimicrob. Agents Chemother.*, 2015, **59**, 4616–4624.
- 29 S. Hansen, K. Lewis, M. Vulić, M. R. Parsek, T. Tolker-Nielsen, I. Keren, D. Shah, A. Spoering, N. Kaldalu and K. Lewis, *Antimicrob. Agents Chemother.*, 2008, **11**, 560–566.
- 30 K. Lewis, *Annu. Rev. Microbiol.*, 2010, **64**, 357–372.
- 31 M. Greenspan and C. E. Tschiegg, *Nucl. Instruments Methods*, 1970, **82**, 310–312.
- 32 C. L W., M. A G. and S. S P., *J. Appl. Microbiol.*, 2000, **88**, 22–30.
- 33 S. L. Percival, L. Suleman, C. Vuotto and G. Donelli, *J. Med. Microbiol.*, 2015, **64**, 323–34.
- 34 B. Pritt, L. O’Brien and W. Winn, *Am. J. Clin. Pathol.*, 2007, **128**, 32–34.
- 35 Y. Evliyaoğlu, M. Kobaner, H. Çelebi, K. Yelsel and A. Doğan, *Urol. Res.*, 2011, **39**, 443–449.

Chapter 1: Introduction

- 36 X. Li, P. Li, R. Saravanan, A. Basu, B. Mishra, S. H. Lim, X. Su, P. A. Tambyah and S. S. J. Leong, *Acta Biomater.*, 2014, **10**, 258–266.
- 37 Y. Dong, X. Li, T. Bell, R. Sammons and H. Dong, *Biomed. Mater.*, 2010, **5**, 1–8.
- 38 E. Fadeeva, V. K. Truong, M. S. B. N. Chichkov, R. J. Crawford, J. Wang and E. P. Ivanova, *Langmuir*, 2011, **27**, 3012–3019.
- 39 P. P. Mahamuni-Badiger, P. M. Patil, M. V. Badiger, P. R. Patel, B. S. Thorat-Gadgil, A. Pandit and R. A. Bohara, *Mater. Sci. Eng. C*, 2020, **108**, 1–74.
- 40 E. Sánchez, C. Rivas Morales, S. Castillo, C. Leos-Rivas, L. García-Becerra and D. M. Ortiz Martínez, *Evidence-based Complement. Altern. Med.*, 2016, **2016**, 1–8.
- 41 F. Siedenbiedel and J. C. Tiller, *Polymers (Basel)*, 2012, **4**, 46–71.
- 42 M. Kang, S. Kim, H. Kim, Y. Song, D. Jung, S. Kang, J.-H. Seo, S. Nam and Y. Lee, *ACS Appl. Mater. Interfaces*, 2019, acsami.8b18301.
- 43 N. V. Efremova, S. R. Sheth and D. E. Leckband, *Langmuir*, 2001, **17**, 7628–7636.
- 44 A. Hucknall, S. Rangarajan and A. Chilkoti, *Adv. Mater.*, 2009, **21**, 2441–2446.
- 45 F. Khan, P. Manivasagan, D. T. N. Pham, J. Oh, S. K. Kim and Y. M. Kim, *Microb. Pathog.*, 2019, **128**, 363–373.
- 46 M. Mir, M. Najabat, A. Afifa, B. Ayesha, G. Munam and A. Shizza, *Prog. Biomater.*, 2018, **7(1)**, ., 1–21.
- 47 L. Dong, A. Henderson and C. Field, *J. Nanotechnol.*, 2012, **2012**, 1–8.
- 48 G. Ferreres, A. Bassegoda, J. Hoyo, J. Torrent-Burgués and T. Tzanov, *ACS Appl. Mater. Interfaces*, 2018, **10**, 40434–40442.
- 49 B. Thallinger, E. N. Prasetyo, G. S. Nyanhongo and G. M. Guebitz, *Biotechnol. J.*, 2013, **8**, 97–109.
- 50 C. De La Fuente-Núñez, F. Reffuveille, S. C. Mansour, S. L. Reckseidler-Zenteno, D. Hernández, G. Brackman, T. Coenye and R. E. W. Hancock, *Chem. Biol.*, 2015, **22**, 196–205.
- 51 P. Morici, R. Fais, C. Rizzato, A. Tavanti and A. Lupetti, *PLoS One*, 2016, **11**, 1–15.

Chapter 1: Introduction

- 52 H. Hirt and S.-U. Gorr, *Antimicrob. Agents Chemother.*, 2013, **57**, 4903–4910.
- 53 I. A. Khmel and A. Z. Metlitskaya, *Mol. Biol.*, 2006, **40**, 169–182.
- 54 M. Li, J. Ding, Y. Tao, B. Shi and J. H. Chen, *Int. J. Polym. Sci.*, 2019, **2019**, 1–2.
- 55 J. Y. Jun, M. J. Jung, I. H. Jeong, K. Yamazaki, Y. Kawai and B. M. Kim, *Mar. Drugs*, 2018, **16**, 1–13.
- 56 N. Wittschier, C. Lengsfeld, S. Vortheims, U. Stratmann, J. F. Ernst, E. J. Verspohl and A. Hensel, *J. Pharm. Pharmacol.*, 2007, **59**, 777–786.
- 57 J. Valle, S. Da Re, N. Henry, T. Fontaine, D. Balestrino, P. Latour-Lambert and J.-M. Ghigo, *Proc. Natl. Acad. Sci.*, 2006, **103**, 12558–12563.
- 58 L. Carson, P. K. W. Chau, M. J. Earle, M. A. Gilea, B. F. Gilmore, S. P. Gorman, M. T. McCann and K. R. Seddon, *Green Chem.*, 2009, **11**, 492–497.
- 59 K. Sambanthamoorthy, X. Feng, R. Patel, S. Patel and C. Parnavitana, *BMC Microbiol.*, 2014, **14**, 1–9.
- 60 D. K. F. Santos, R. D. Rufino, J. M. Luna, V. A. Santos and L. A. Sarubbo, *Int. J. Mol. Sci.*, 2016, **17**, 1–31.
- 61 G. A. Silva, M. Sc and D. Ph, *Surg. Neurol.*, 2004, **61(3)**, 216–220.
- 62 M. G. “Richard Feynman: A Life in Science”, J. Gribbin, 2001, 1–207.
- 63 " Proc. N. Taniguchi., "On the Basic Concept of ‘Nano-Technology’, J. S. of P. Intl. Conf. Prod. Eng. Tokyo, Part II and (1974). Engineering, .
- 64 R. T. Koodali, K. J. Klabunde and W. I. Nano, *Nanotechnology: Fundamental Principles and Applications*, 2012.
- 65 "Tracing and disputing G. A. Hodge, D. M. Bowman, A. D. Maynard and the story of nanotechnology" (2010)., .
- 66 . C. P. Poole, F. Owens, “*Introduction to nanotechnology*”, 2004, **43(17)**, 2196–2197.
- 67 C. N. R. R. J. Jortner, *Pure Appl. Chem.*, 2011, **74**, 1491–1506.
- 68 J. Fei, J. Zhao, C. Du, A. Wang, H. Zhang, L. Dai and J. Li, *ACS Nano*, 2014, **8**, 8529–8536.

Chapter 1: Introduction

- 69 S. M. Dizaj, F. Lotfipour, M. Barzegar-Jalali, M. H. Zarrintan and K. Adibkia, *Mater. Sci. Eng. C*, 2014, **44**, 278–284.
- 70 Z. Jiang, A. Sahar, X. Li, S. M. Robinson, V. M. Rotello, K. Saha, M. A. Riley, D. F. Moyano and A. Gupta, *ACS Nano*, 2014, **8**, 10682–10686.
- 71 X. Zou, L. Zhang, Z. Wang and Y. Luo, *J. Am. Chem. Soc.*, 2016, **138**, 2064–2077.
- 72 C. H. Li, C. C. Shen, Y. W. Cheng, S. H. Huang, C. C. Wu, C. C. Kao, J. W. Liao and J. J. Kang, *Nanotoxicology*, 2012, **6**, 746–756.
- 73 I. Sondi and B. Salopek-Sondi, *J. Colloid Interface Sci.*, 2004, **275**, 177–182.
- 74 D. L. Romana, K. H. Brown and J.-X. Guinard, *J. Food Sci.*, 2006, **67**, 461–465.
- 75 J. Hou, Y. Wu, X. Li, B. Wei, S. Li and X. Wang, *Chemosphere*, 2018, **193**, 852–860.
- 76 Q. Wu, Y. Wang and G. Q. Chen, *Artif. Cells, Blood Substitutes, Biotechnol.*, 2009, **37**, 1–12.
- 77 F. Hizal, I. Zhuk, S. Sukhishvili, H. J. Busscher, H. C. Van Der Mei and C. H. Choi, *ACS Appl. Mater. Interfaces*, 2015, **7**, 20304–20313.
- 78 E. Jäger, R. K. Donato, M. Perchacz, A. Jäger, F. Surman, A. Höcherl, R. Konefał, K. Z. Donato, C. G. Venturini, V. Z. Bergamo, H. S. Schrekker, A. M. Fuentefria, M. G. Raucci, L. Ambrosio and P. Štěpánek, *RSC Adv.*, 2015, **5**, 85756–85766.
- 79 S. Goswami, D. Thiagarajan, G. Das and A. Ramesh, *ACS Appl. Mater. Interfaces*, 2014, **6**, 16384–16394.
- 80 G. Wei, A. N. Campagna and L. A. Bobek, *Ann. clinical Microbiol. Antimicrob.*, 2007, **10**, 1–10.
- 81 M. J. Hajipour, K. M. Fromm, A. Akbar Ashkarran, D. Jimenez de Aberasturi, I. R. de Larramendi, T. Rojo, V. Serpooshan, W. J. Parak and M. Mahmoudi, *Trends Biotechnol.*, 2012, **30**, 499–511.
- 82 F. Y. Jiangna Guo, Jing Qin, Yongyuan Ren, Bin Wang, Hengqing Cui, Yingying Ding, Hailei Mao, *Polym. Chem.*, 2018, **00**, 1–3.
- 83 F. Devlieghere, A. Vermeulen and J. Debevere, *Food Microbiol.*, 2004, **21**, 703–714.
- 84 V. Carniello, B. W. Peterson, H. C. van der Mei and H. J. Busscher, *Adv. Colloid*

Chapter 1: Introduction

- Interface Sci.*, 2018, **261**, 1–14.
- 85 K. E. Jones, N. G. Patel, M. A. Levy, A. Storeygard, D. Balk, J. L. Gittleman and P. Daszak, *Nature*, 2008, **451**, 990–993.
- 86 S. Lim and S. M. Hudson, *Carbohydr. Res.*, 2004, **339**, 313–319.
- 87 D. J. Hickey, M. Andersson, M. Stolzoff, T. J. Webster and J. Penders, *Int. J. Nanomedicine*, 2017, **12**, 2457–2468.
- 88 P. Pourali, M. Baserisalehi, S. Afsharnezhad, J. Behravan, R. Ganjali, N. Bahador and S. Arabzadeh, *BioMetals*, 2013, **26**, 189–196.
- 89 H. Choi, S. Y. Ham, E. Cha, Y. Shin, H. S. Kim, J. K. Bang, S. H. Son, H. D. Park and Y. Byun, *J. Med. Chem.*, 2017, **60**, 9821–9837.
- 90 G. S. Dhillon, S. Kaur and S. K. Brar, *Int. Nano Lett.*, 2014, **4**, 1–11.
- 91 N. A. Salahuddin, M. El-kemary and E. M. Ibrahim, *Nanosci. Nanotechnol.*, 2015, **5**, 82–88.
- 92 H. Mirzaei and M. Darroudi, *Ceram. Int.*, 2017, **43**, 907–914.
- 93 X. Bai, L. Li, H. Liu, L. Tan, T. Liu and X. Meng, *ACS Appl. Mater. Interfaces*, 2015, **7**, 1308–1317.
- 94 A. A. Reinert, C. Payne, L. Wang, J. Ciston, Y. Zhu and P. G. Khalifah, *Inorg. Chem.*, 2013, **52**, 8389–8398.
- 95 G. Modi, *Adv. Nat. Sci. Nanosci. Nanotechnol.*, 2015, **6**, 1–8.
- 96 P. Uikey and K. Vishwakarma, *Int. J. Emerg. Technol. Comput. Sci. Electron.*, 2016, **21**, 239–242.
- 97 Z. Song, T. A. Kelf, W. H. Sanchez, M. S. Roberts, J. Rička, M. Frenz and A. V. Zvyagin, *Biomed. Opt. Express*, 2011, **2**, 3321–3333.
- 98 N. Padmavathy and R. Vijayaraghavan, *Sci. Technol. Adv. Mater.*, 2008, **9**, 035004.
- 99 P. K. Mishra, H. Mishra and A. Ekielski, *Drug Discov. Today*, 2017, **6446**, 1–15.
- 100 M. Li, L. Zhu and D. Lin, *Environ. Sci. Technol. 2011*, 2011, 1977–1983.
- 101 S. D. Vallabhapurapu, V. M. Blanco and M. K. Sulaiman, *Oncotarget*, 2015, **6**, 34375–

Chapter 1: Introduction

- 34388.
- 102 H. Jiang, H. Wang and X. Wang, *Appl. Surf. Sci.*, 2011, **257**, 6991–6995.
- 103 Y. Kang, Y. Z. Wu, X. Hu, X. Xu, J. Sun, R. Geng, T. Huang, X. Liu, Y. Ma, Y. Chen, Q. Wan, X. Qi, G. Zhang, X. Zhao and X. Zeng, *Sci. Rep.*, 2017, **7**, 1–11.
- 104 H. M. Xiong, *Adv. Mater.*, 2013, **25**, 5329–5335.
- 105 N. S. Wahba, S. F. Shaban, A. A. A. Kattaia and S. A. Kandeel, *Ultrastruct. Pathol.*, 2016, **40**, 358–373.
- 106 A. Nazarizadeh and S. Asri-rezaie, *AAPS PharmSciTech*, 2016, **17**, 834–843.
- 107 R. M. El-gharbawy, A. Mahmoud and S. E. Abu-risha, *Biomed. Pharmacother.*, 2016, **84**, 810–820.
- 108 M. Ilves, J. Palomäki, M. Vippola, M. Lehto, K. Savolainen, T. Savinko and H. Alenius, *Part. Fibre Toxicol.*, 2014, **11**, 1–12.
- 109 T. V Surendra, S. M. Roopan, N. A. Al-dhabi, M. V. Arasu and G. Sarkar, *Nanoscale Res. Lett.*, 2016, **11**(1), 1–10.
- 110 A. Jain, R. Bhargava and P. Poddar, *Mater. Sci. Eng. C*, 2013, **33**, 1247–1253.
- 111 L. Hanley, *J. Biomed. Mater. Res. B Appl. Biomater.*, 2010, **94B**, 22–31.
- 112 L. S. Reddy, M. M. Nisha, M. Joice and P. N. Shilpa, *Pharm. Biol.*, 2014, **52**, 1388–1397.
- 113 K. R. Raghupathi, R. T. Koodali and A. C. Manna, *Langmuir*, 2011, **27**, 4020–4028.
- 114 A. B. G. Lansdown, F. R. C. Path, U. Mirastschijski and N. Stubbs, *Wound repair Regen.*, 2007, **15**, 2–16.
- 115 S. K. Nethi, S. Das, C. R. Patra and S. Mukherjee, *Biomater. Sci.*, 2019, **7**, 2652–2674.
- 116 H. Sinno and S. Prakash, *Plast. Surg. Int.*, 2013, **2013**, 1–7.
- 117 I. Unalan, S. J. Endlein, B. Slavik, A. Buettner, W. H. Goldmann, R. Detsch and A. R. Boccaccini, *Pharmaceutics*, 2019, **11**, 1–16.
- 118 P. Basu, U. Narendrakumar, R. Arunachalam, S. Devi and I. Manjubala, *ACS Omega*, 2018, **3**, 12622–12632.
- 119 V. Leung, R. Hartwell, H. Yang, A. Ghahary and F. Ko, *Tech. Proc. 2012 NSTI*

Chapter 1: Introduction

- Nanotechnol. Conf. Expo, NSTI-Nanotech 2012*, 2012, **3**, 166–169.
- 120 N. Devi and J. Dutta, *Int. J. Biol. Macromol.*, 2017, **104**, 1897–1904.
- 121 E. P. S. Tan and C. T. Lim, *Compos. Sci. Technol.* **66**, 2006, **66**, 1102–1111.
- 122 H. C. Williams, L. Naldi, C. Paul, A. Vahlquist, S. Schroter and R. Jobling, *Acta Derm. Venereol.*, 2006, **86**, 485–497.
- 123 H. Chen, X. Xing, H. Tan, Y. Jia, T. Zhou, Y. Chen, Z. Ling and X. Hu, *Mater. Sci. Eng. C*, 2017, **70**, 287–295.
- 124 W. Paul and C. P. Sharma, *Trends Biomaterials Artif. Organs*, 2004, **18**, 18–23.
- 125 S. Mandla, D. Huyer and M. Radisic, *APL Bioeng.*, 2018, **2**, 1–13.
- 126 C. Liu, J. Guo, X. Yan, Y. Tang, A. Mazumder, S. Wu and Y. Liang, *Environ. Rev.*, 2017, **25**, 225–244.
- 127 M. Abhilash and R. Augustine, *Diabetes Healthc. an Overv.*, 2014, **2014**, 273–314.
- 128 A. M. Abdelgawad, S. M. Hudson and O. J. Rojas, *Carbohydr. Polym.*, 2014, **100**, 166–178.
- 129 R. Z. Murray, Z. E. West, A. J. Cowin and B. L. Farrugia, *Burn. Trauma*, 2019, 1–9.
- 130 E. A. Kamoun, E. S. Kenawy and X. Chen, *J. Adv. Res.*, 2017, **8**, 217–233.
- 131 N. K. and G. V. R. Bhagyashri S Thorat Gadgil, *Medchemcomm*, 2017, **8**, 1774–1787.
- 132 J. Shokri and K. Adibkia, in *Application of cellulose and cellulose Derivatives in Pharmaceuticals*, 2013, pp. 47–66.
- 133 K. H. Huong, M. J. Azuraini, N. A. Aziz and A. A. A. Amirul, *J. Biosci. Bioeng.*, 2017, **124**, 76–83.
- 134 A. L. Rivera-Briso and Á. Serrano-Aroca, *Polymers (Basel)*, 2018, **10**, 1–28.
- 135 S. H. Diermann, M. Lu, Y. Zhao, L. J. Vandi, M. Dargusch and H. Huang, *J. Mech. Behav. Biomed. Mater.*, 2018, **84**, 151–160.
- 136 S. Y. H. Abdalkarim, H. Y. Yu, D. Wang and J. Yao, *Cellulose*, 2017, **24**, 2925–2938.
- 137 S. Modi, K. Koelling and Y. Vodovotz, *Eur. Polym. J.*, 2015, **47**, 179–186.
- 138 L. Hsiao, J. Lin, P. Sankatumvong, T. Wu and S. Li, *Appl Biochem Biotechnol*, 2016,

Chapter 1: Introduction

180(5), 852–871.

139 M. Koller, L. Maršálek, M. M. de Sousa Dias and G. Braunegg, *N. Biotechnol.*, 2017, **37**, 24–38.

140 A. Bianco, M. Calderone and I. Cacciotti, *Mater. Sci. Eng. C*, 2013, **33**, 1067–1077.

CHAPTER 2

Zinc oxide nanoparticles as an antibacterial and antibiofilm agent: Survey of development

IF 5.8

Journal Pre-proof

Biofilm formation to inhibition: Role of zinc oxide-based nanoparticles

Pranjali P. Mahamuni-Badiger, Pooja M. Patil, Manohar V. Badiger, Pratiksh R Patel, Bhagyashi S. Thorat- Gadgil, Abhay Pandit, Raghvendra A. Bohara

PII: S0928-4931(19)32379-3

DOI: <https://doi.org/10.1016/j.msec.2019.110319>

Reference: MSC 110319

To appear in: *Materials Science & Engineering C*



“Prepare for the unknown by studying how others in the past have coped with the unforeseeable and the unpredictable.”

-George S. Patton

Chapter 2: ZnO nanoparticles as an antibacterial and antibiofilm agent: Survey of development

2.1 Introduction

Nanotechnology is related to the manufacture and applications of materials of size up to 100 nm. They are extensively used in different fields such as material science, agriculture, food industry, cosmetic, medical and diagnostic applications.¹ At the nanometer size, the characteristics of materials become different than those at the macro size. Nanosized inorganic materials have exhibited remarkable antibacterial activity because of their unique properties like a high surface area to volume ratio, varieties in morphology, stability at high temperature, pressure, and unique chemical and physical properties.² Most of the inorganic nanoparticles with antibacterial properties are metallic and metal oxide nanoparticles that include silver, copper, gold, titanium oxide, and zinc oxide.^{3,4} Recently, among all inorganic nanoparticles zinc oxide nanoparticles have gained much more attention as they possess the highest toxicity against microorganisms. The advantage of the use of ZnO nanoparticles as an antimicrobial agent is that they contain mineral elements are essential to human and show vigorous activity when administered in a small amount. Zinc is organically known as helper molecule without which about 300 enzymes for example, carbonic anhydrase, carboxypeptidase, and alcohol dehydrogenase become non-functional. After iron, zinc is the essential trace element in the human body.⁵

ZnO-NPs are also used in several industrial areas like UV-light-emitting devices, photocatalysts, pharmaceuticals and cosmetics. Desirable properties like non-toxicity, self-cleansing property, biocompatibility and antimicrobial activity of ZnO nanoparticles make them convenient for the use in sunscreens as a UV-blocker and lots of other medical applications. ZnO is categorized as a “GRAS” (generally recognized as safe) substance by the US Food and Drug Administration (FDA).⁶ Also as compared with other metal oxide nanoparticles ZnO NPs are cheap and relatively less toxic to a human being with excellent antibacterial, anti-cancer, wound healing, anti-inflammation, anti-diabetic and bio-imaging applications.^{7,8}

Chapter 2: ZnO nanoparticles as an antibacterial and antibiofilm agent: Survey of development

The antibacterial and antibiofilm activities of ZnO Nps mainly depend upon their morphology. ZnO NPs exhibit varieties of morphology like nanocombs, nanorings, nanohelices, nanobelts, nanowires, and nanocages. Their morphology mainly depends upon the type of synthesis used. Different synthesis methods like chemical, physical, and biological methods are employed for synthesis. For their application in wound dressing materials ZnO NPs should be embedded in suitable materials that form nanocomposites.^{9,10}

Nanocomposites (NCs) are the second generation in nanotechnology that deals with the combination of homo or hetero nanoparticles for different applications. There is also a current trend in which the combination of metal or metal oxide with natural polymers is performed for their application in wound dressings. These materials require minimum processing, possess antibacterial activity and enhance the wound healing process. ZnO NPs are one of the promising materials that can be incorporated in polymers. The development of novel wound dressing materials is an important task to treat wounds infected by drug-resistant bacteria. Micro-organisms that form biofilm are less sensitive to antibiotics and are highly resistant to the host-immune system than their planktonic form. Resistance developed by micro-organisms is due to frequent changes in surface antigens by the alteration in the gene expressions. The continuous development of antimicrobial resistance of specific strains toward antibiotics highlights the importance of the use of innovative wound dressing materials.^{11,12}

2.2 Properties of bulk ZnO and nano ZnO

Zinc oxide (ZnO) occurs within the earth's crust as a mineral zincite, synthesis methods prepare most of it which is used commercially. ZnO is less toxic and biocompatible with human skin. As compared with bulk ZnO, the nanoscale ZnO has the potential to enhance the fabric operation. Nanotechnology includes the synthesis, characterization, and exploration of materials in the nanometer range (1-100nm). In nanotechnology, the materials show unique and advanced properties of physicochemical and biological properties and functionalities due to the nanoscale

Chapter 2: ZnO nanoparticles as an antibacterial and antibiofilm agent: Survey of development

range. These nano-materials confer larger surface area to volume ratio as compared with bulk ZnO. Nano ZnO shows size-related properties significantly different from bulk ZnO. Nanoparticles show more significant variation in their structures as compared with bulk. Therefore, nano ZnO is applicable in varieties of fields.¹³ General properties of zinc oxide compound are given in table 2.1,

Table 2.1: General properties of ZnO compound ¹⁴

Molecular formula	ZnO
Molecular weight	81.406g/mol
Band gap energy	3.3 eV
Density	5.606g/cm ⁻¹
Melting point	1975°C (decomposes)
Boiling point	2360°C
Solubility in water	0.16 mg/100ml (30°C)
Odor	Odorless
Color	White
Stable phase at 30K	Wurtzite

2.3 Synthesis approaches

Zinc oxide can be obtained in a variety of structures that depend upon the synthesis methods used. Among the ways of synthesizing nanoparticles, there are chemical, physical, and biological methods.

Chapter 2: ZnO nanoparticles as an antibacterial and antibiofilm agent: Survey of development

Chemical methods consist of a liquid phase synthesis and a gas phase synthesis. The liquid phase synthesis includes hydrothermal synthesis, precipitation, a polyol method, a sol-gel method, colloidal methods, precipitation from microemulsion, and mechano-chemical processes, while vapor-phase synthesis includes pyrolysis gas condensation method. The precipitation method is a widely used method to produce ZnO, in which the reduction of zinc salt solution by a reducing agent occurs that, restricts the particle growth to a specific dimension. The process of co-precipitation can be controlled by adjusting parameters like pH, temperature, and reaction time.¹⁵ The sol-gel method is yet another simple means of synthesis. An advantage of this method is the gain of the highly pure and uniform structure of ZnO.¹⁶ Solvothermal and hydrothermal processes gives a variety of zinc nanostructures like thin films, bulk powders as well as one dimensional (1D), 2D, and 3D forms. Shahid et al.¹⁷ have synthesized ZnO NPs by using the solvothermal method, and they studied the effect of size of nanoparticles on the inhibition of bacterial growth and the mechanism of antibacterial activity of zinc oxide nanoparticles against methicillin-sensitive and methicillin-resistant *Staphylococcus aureus*. The use of solvents for such processes as or calcination is not restricted in these synthesis methods and this makes them an easy and convenient means of synthesis.¹⁷ The use of polyols in the synthesis process allows nanoparticles to be produced with high crystallinity by avoiding agglomeration and controlled morphology as they possess unique properties such as high boiling point, a high dielectric constant and solubility of metal salt precursors.¹⁸ Pranjali et al.¹⁹ synthesized ZnO NPs by using different conditions such as regular synthesis in polyols like diethylene glycol and triethylene glycol, in the presence of sodium acetate and by extending the reaction time. They observed size dependent antibacterial and antibiofilm activity against *Staphylococcus aureus* and *E.coli*, from which it was, concluded that with decrease in particle size, antimicrobial activity increases. The gas phase method of synthesis mostly uses the technique of spray pyrolysis. Another method utilizes inert gas condensation which is further divided into physical vapor deposition and chemical vapor deposition.²⁰

Chapter 2: ZnO nanoparticles as an antibacterial and antibiofilm agent: Survey of development

Table 2.2: Advantages and disadvantages of different synthesis approaches

Sr. No	Synthesis method	Advantage	Disadvantage
1.	Mechano-chemical process	Simple, can be used on a large scale, low production cost, small particle size, high crystallinity.	A large amount of impurities. ²¹
2.	Co-precipitation method	Simple, cheap, the reaction can be controlled by controlling reaction parameters	Agglomerated particles. ²²
3.	Sol-gel method	Simple, cheap, reliable, Repeatable	Agglomerated particles, large production is difficult. ²³
4.	Solvothermal-hydrothermal Method	The high degree of crystallinity, high purity.	High pressure and high temperature are required. ²⁴
5.	Microemulsion method	Easy, reversible, thermodynamically stable	Require surfactants for stability, limited solubilizing capacity for substance having high melting point. ²⁵
6.	Biological method	Cost effective, Eco friendly	Lack of uniform size distribution. ²⁶

Physical or mechanical methods of synthesis consist of high energy ball milling, physical vapor deposition, sputter deposition, laser ablation melt mixing, and ion implantation. These

Chapter 2: ZnO nanoparticles as an antibacterial and antibiofilm agent: Survey of development

methods are widely used for industrial processes that yield ZnO with high production rates.²⁷ For ZnO synthesis the biological approach or green synthesis that uses green routes. These include the use of micro-organisms such as bacteria, fungi, algae, and plants for the synthesis of nanoparticles. Plants from the *Lamiaceae* family are widely used for synthesis as *Anisochilus carnosus*, *Plectranthus amboinicus* and *Azadirachta indica* from the *meliaceae* family which allows the formation of ZnO of various size, and shape with agglomeration. The size of nanoparticles reduced with the increase in the amount of plant extract.²⁸

By using microbes, ZnO can be synthesized either extracellularly or intracellularly. Jehad et al.²⁹ synthesized spherical shaped ZnO NPs from *Aspergillus niger* with an average diameter between 39.4-114.6nm. Bacterium such as *Aeromonas hydrophila* was used to produce spherical and oval ZnO nanoparticles with an average size of 57.72nm that showed antibacterial activity against *Pseudomonas aeruginosa* and *Aspergillus flavus*.³⁰ The advantages and disadvantages of the different synthesis methods are given in table 2.2.

2.3.1 Importance of polyols in chemical synthesis of ZnO nanoparticles

In most of the other synthesis approaches, nanoparticles get agglomerated because of the large specific area and high surface energy. Also, the bond formation of Zn-O-Zn among nanoparticles due to the presence of water molecules in the synthesis process results in high agglomerates, that limits the application of ZnO nanoparticles. So, the absence of water in synthesis process is an essential criterion to prevent hard agglomeration of ZnO NPs.³¹

Polyalcohols or polyols are the class of compounds with reducing properties used for the preparation of metal nanoparticles, known as a “polyol process”. The term polyol was first used by the Fievet, Lagier and Figlarzin 1989 to designate liquid-phase synthesis route to get metals from their oxides, hydroxides or salts in polyols. The use of polyols offer several advantages, (i) The presence of several –OH groups in polyols causes high boiling point, that permits synthesis at relatively high temperature yielding highly crystalline materials, (ii) the reducing medium

Chapter 2: ZnO nanoparticles as an antibacterial and antibiofilm agent: Survey of development

protects the prepared metal particles from oxidation, (iii) it co-ordinates metal precursors and particle surface that minimizes agglomeration, (iv) their high viscosity favors diffusion control that helps for particle growth for controlled structures and morphologies. Polyols themselves act as a solvent and stabilizing agent that control the particle growth and reduces particles agglomeration. Also the synthesis is easy to carry out and doesn't require multiple steps or advanced experimental condition or types of equipments.³²

Chemically, the polyol family starts with ethylene glycol (EG). Based on the EG, the polyols consist of two main series of molecules: i) diethylene glycol (DEG), triethylene glycol (TEG), tetra ethylene glycol (TrEG), and so on upto polyethylene glycol (PEG). The use of proper precursor is an essential step for the successful formation of nanomaterials. At a particular temperature, sudden precipitation of ZnO takes place. As polyols act as chelating agents, the surface of growing particles gets complexed by the polyols. Because of this chelation, the grain growth is restricted and agglomeration of particle doesn't occur. The particle size of ZnO NPs mainly depends upon glycol chain length. With increasing glycol chain length, the particle size of ZnO NPs also gets increased.³³

2.4 Factors affecting antibacterial and antibiofilm activity of ZnO NPs

ZnO NPs destroy the integrity of bacterial cell membrane, minimize cell surface hydrophobicity, and lowers the expression of oxidative stress-resistant genes in bacteria. ZnO NPs also can destroy biofilm formation and inhibit hemolysis by hemolysin toxin produced by pathogens. However, their antibacterial and antibiofilm activity get affected by different factors described below,

2.4.1 Solubility and concentration

The toxicity of ZnO NPs is due to Zn^{2+} ions released in the aqueous medium. The antibacterial and antibiofilm activity is mainly due to the interaction of ZnO NPs with microbial cells. Zn^{2+} ions are released by the extracellular dissolution of zinc oxide nanoparticles.³⁴ At low

Chapter 2: ZnO nanoparticles as an antibacterial and antibiofilm agent: Survey of development

concentration of ZnO NPs, the antibacterial and antibiofilm activity is relatively less, but at higher concentrations (100µg/ml), they show toxicity against different pathogens. The concentration of generated ROS is directly proportional to the concentration of ZnO NPs.³⁵ ROS induces the decrease in mitochondrial membrane potential leading to apoptosis. It was also suggested that increasing concentration and solubility could stimulate the leakage of lactate dehydrogenase and alters the morphology of the cell at a concentration of about 50-100 mg/L.³⁶

2.4.2 Shape

Many studies reported that the intensity of antibacterial and antibiofilm activities gets affected by the morphology of ZnO NPs. The morphology depends upon the type of synthesis process used. Therefore, according to the type of application the synthesis parameters such as type of precursor, solvents, and physicochemical parameters like temperature, pH is controlled.³⁷ The shape-dependent activity of ZnO NPs can be correlated with the number of active facets present in the NPs. Synthesis and growth methods determine the holding of numerous active facets in NPs. Rod structure of ZnO has (111) and (100) facets in nanoparticles; while spherical nanostructures mainly include (100) facets. High atom density facets with (111) facets show higher antibacterial activity.³⁸ The shape of ZnO NPs can affect their mechanism of internalization like rod and wire shaped NPs can get easily penetrated the cell wall of bacteria than spherical ZnO NPs.³⁹ Also the larger number of polar surfaces that possess a higher number of oxygen vacancies enhances the antibacterial activity, as higher number of the oxygen vacancies increases the generation of ROS species.⁴⁰

2.4.3 Size

The size of ZnO NPs plays the leading role in the intensity of antibacterial and antibiofilm activity. It is inversely proportional to the size of the nanoparticle. ZnO NPs with the smaller size can easily get internalized into the bacterial membrane because of their large surface area, therefore increasing their antibacterial activity.⁴¹ Large numbers of studies reported the

Chapter 2: ZnO nanoparticles as an antibacterial and antibiofilm agent: Survey of development

effect of particle size on the antibacterial activity, and it is crucial to control the small particle size (high specific surface area) to obtain the best antibacterial activity. The amount of release of H_2O_2 mainly depends upon the surface area of ZnO.⁴² The larger surface area and the high number of oxygen species on the surface of ZnO NPs show more significant antibacterial activity by smaller particles.^{43,44} Mahamuni et al¹⁹ reported that among all synthesized ZnO NPs, a particle of least size ~15 nm in size exhibited maximum antibacterial and antibiofilm activity against Gram-positive *Staphylococcus aureus* and Gram-negative *Proteus vulgaris*. It was concluded that the size of the ZnO NPs is inversely proportional to the size and directly proportional to the concentration. The size-dependent bactericidal activity of ZnO NPs is due to penetration and deposition of NPs inside the cells until the NPs reached the cytoplasmic region.¹²

2.4.4 UV illumination effect

ZnO shows higher photocatalytic activity among all inorganic photocatalytic materials. ZnO NPs can absorb UV light that enhances its conductivity. The increased conductivity mainly enhances the interaction of ZnO NPs with bacteria. The photoconductivity can be related to the surface electron depletion region that deals with negative oxygen species (O^{2-} , O_2^{2-}) that remain adsorbed on the surface.⁴⁵ ZnO NPs in an aqueous solution under the influence of UV radiation show phototoxic effect that can generate ROS such as hydrogen peroxide, and superoxide ions. These generated ROS can get penetrated inside the cells and kill bacteria.⁴⁶ This property makes the use of ZnO NPs in medical fields for antibacterial applications. It is reported that the antibacterial activity of ZnO NPs gets changed under UV light and in the dark to kill the bacteria.⁴⁷ The photo-excitation of ZnO NPs results in the removal of the oxygen molecules from the surface that leads to decreased surface potential and photoconductivity of ZnO NPs. Generation of oxygen species such as H_2O_2 , O^{2-} and OH^- by the UV light is harmful to bacteria and destroy active enzymes, DNA, and protein.⁴⁸

2.4.5 Surface defects

Chapter 2: ZnO nanoparticles as an antibacterial and antibiofilm agent: Survey of development

The surface defect is one of the factors that affect the mechanism of antibacterial and antibiofilm activity. This is because the surface of ZnO NPs contains numerous edges and corners, and so possess potential reactive sites. Surface defects strongly affect the toxicity of ZnO NPs. Some reports suggested that the antibacterial activity of ZnO NPs is because of membrane injury by the surface defects like edges, and corners on the surface of ZnO. For the use of ZnO NPs in the desired applications, the surface defects, impurities, and associated charge carriers can be controlled.^{49,50}

The material to be used as an antibacterial agent should possess properties like biocompatibility, antimicrobial properties, surface activity, appropriate size and shape, and stability at different pH and temperature. ZnO NPs possess all these properties for their use in wound dressing applications as an antibacterial and antibiofilm agent.

2.5 Nanomaterials and wound dressing materials

Wound dressings have been traditionally used to protect the wound from external contamination. The wound dressing materials like cotton and wool that behave as a passive barrier and replaced by many advanced dressings to create a protective barrier. Variety of combinations of both synthetic and natural materials have been adapted as sponges, hydrogels, films, hydrocolloids, and nanofibrous mats etc.⁵¹

Nanotechnology studies the synthesis, structure, and dynamic of atomic and molecular nanomaterials. Due to the antibacterial properties of metal oxide nanoparticles, they act as an ideal candidate for the integration in wound dressing materials. The different types of nanomaterials used for wound treatment are shown in figure 2.1.

Chapter 2: ZnO nanoparticles as an antibacterial and antibiofilm agent: Survey of development

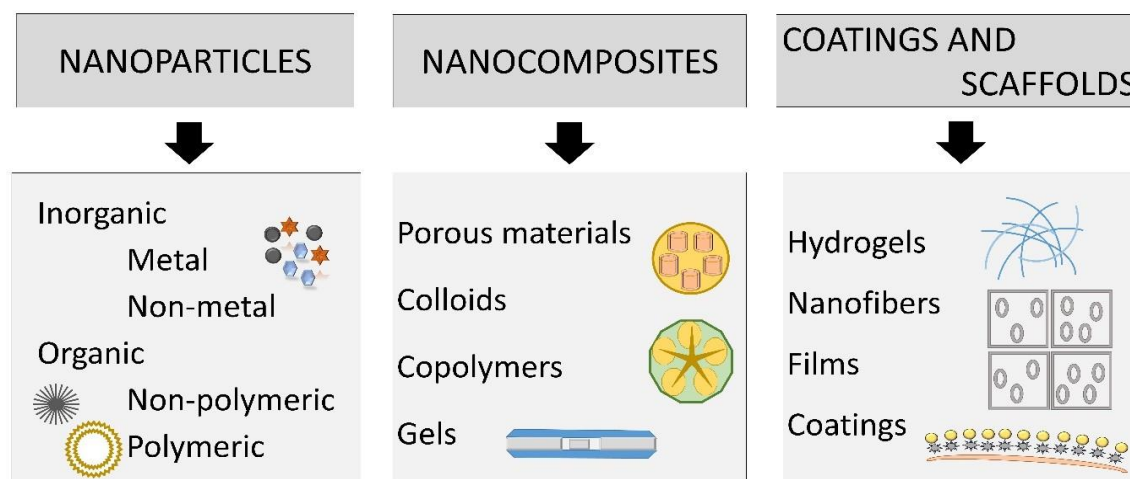


Figure: 2.1 Different types of nanomaterials used in wound treatment

Nanomaterials can be designed in varieties of structures. Nanoparticles can be used in two approaches: (i) NPs that possess properties for wound closure, (ii) NPs can be used as a carrier for therapeutic agents. In metal or metal oxide nanoparticles silver, gold, and zinc compounds because of their unique properties, antibacterial activity, and biocompatibility. Their toxicity depends upon morphology, surface fictionalization, surface charge and polydispersity index.⁵²

Nanocapsule encloses an active agent within it and shows controlled releases at a specific time interval. They enhance the penetration of active ingredients into deep layers of the dermis. The disadvantage is that the activity of the substances may get reduced.⁵³ Nanospheres are composed of a porous polymer matrix on which active substances like amino acids, minerals, or organic substances can bind. Therefore, active compounds get stable and show increased biocompatibility.⁵¹ Nanocarriers are synthetic, non-ionic surfactants. Also, they represent surface receptors for binding to specific loci that enhanced the activity of active agent by reducing adverse reactions.⁵⁴ Nanoemulsions are homogenous, thermally stable oil-in-water emulsion. Their droplet size is of 100nm that also include a surfactant and active substances. Their

Chapter 2: ZnO nanoparticles as an antibacterial and antibiofilm agent: Survey of development

drawback is the uncontrolled deposition of active substances in the reticular dermis.⁵⁵ Nanocolloids consist of non-ionic metal nanoparticles (1.5-5nm) highly dispersed in demineralized water because of Brownian movement that permits them to internalize in prokaryotic and eukaryotic cells and to show antimicrobial activity.⁵¹

The nanomaterials have a large number of fascinating materials with unique physical and chemical properties. These consist of nanoparticles or quantum dots, nanowires, nanorods, nanofibers, nanotubes, and nanosheets. Among these nanomaterials, nanofibers possess great potential for various applications. The nanofibers possess unique properties like a high surface area to volume ratio and high porosity, make them promising agents in many advanced applications.⁵²

2.5.1 Zinc oxide embedded biomaterials for wound dressing applications

Zinc oxide NPs is promises stable antibacterial agent by interacting with the bacterial cell membrane. Zinc is an essential element for living cells, and essential in the wound healing process particularly in delayed wound healing and burns. The topical application of zinc reduces inflammation, enhances re-epithelialization, and inhibits the growth in chronic wounds.⁵⁶ Zinc element is co-factor in enzyme metalloproteinase, and also crucial in the enhancement of regeneration of ECM. ZnO NPs possess antibacterial, anti-inflammatory, and antiseptic properties and also widely used in the production of cosmetics, skin creams, ointments.⁵⁷ The intensity of wound healing depends upon the size and concentration of the nanoparticles. ZnO shows high antibacterial activity because of small size and high surface area to volume ratio. ZnO NPs promotes keratinocytes migration and re-epithelialization when added in hydrogel wound dressings.⁵⁸ The microporous chitosan hydrogel-ZnO NPs dressing shows the high capacity of absorbing wound exudates and forms hemostatic blood clots with antibacterial properties. The nano-formulation of ZnO with the biocompatible polymer can promote the

Chapter 2: ZnO nanoparticles as an antibacterial and antibiofilm agent: Survey of development

activity at minimum doses. ZnO NPs acts in a biphasic manner that releases Zn ions. Its rapid hydration occurs to form hydrated ZnO that act as an antibacterial agent.⁵⁹

Shalumon et al.⁶⁰ prepared sodium alginate/poly(vinyl alcohol)/ZnO NPs (with a concentration of 0.5, 1,2 and 5%) nanofibrous mats by the electrospinning technique. They observed antibacterial activity against bacterial strains *Staphylococcus aureus* and *Escherichia coli*. The zones of inhibition in both strains were increased with increased concentration of ZnO NPs, while cytotoxicity results showed the decreased cell viability with increased concentration of ZnO NPs.

Chen et al.⁶¹ prepared gelatin-ZnO fibers by side-by-side electrospinning for wound dressing application. They exhibited better antibacterial activity against *Staphylococcus aureus* and *Escherichia coli* with more than 90% reduction in bacteria and showed no cytotoxicity. These biodegradable, nontoxic and antibacterial fibers can be used as a potential candidate in wound dressing materials.

Poly (3-hydroxybutyrate-co-3-hydroxyvalerate) (PHBV) is biocompatible, thermoplastic, biodegradable, and non-toxic polyester produced by bacteria that make it promising a agent in the biomedical field.⁶² The degradation product of PHBV, (R)-3-hydroxybutyric acid is a blood component that promotes its use in the different biomedical fields. Many studies suggested that PHBV can enhance cell proliferation, such as fibroblasts, keratinocytes, and neural cells.^{63,64} However, due to its poor mechanical performance, high crystallinity, inherent rigidity, and hydrophobicity this material is not explored much.⁶⁵ Therefore, defects of PHBV can be overcome by blending them with hydrophilic polymers such as gelatin,⁶⁶ chitosan,⁶⁷ PLA,^{68,69} and poly(ethylene oxide) (PEO).⁶⁵ Among these polymers, polyethylene oxide (PEO) which is certified by the FDA is highly preferred because of its properties like biocompatibility, hydrophilicity, and malleability. It is mainly used in biomedical fields, mostly in blood-contacting devices because of its non-immunogenicity, non-antigenicity, non-toxicity and low

Chapter 2: ZnO nanoparticles as an antibacterial and antibiofilm agent: Survey of development

adsorption of surface proteins. Furthermore, from PEO it is easy to obtain nanofibers by electrospinning technique than other polymers because of its high solubility in water as well as in different types of organic solvents.⁷⁰ The incorporation of ZnO NPs into PHBV polymer has gained much more attention in the nanocomposite field as ZnO is widely reported for its vigorous antibacterial activity against a broad spectrum of microorganisms. ZnO nanofibers have been synthesized by using materials like natural polymers, synthetic polymers, carbon based nano-materials, semiconducting nanomaterials and composite nanomaterials. Out of all current methods used to synthesize nanofibers, electrospinning is the most reliable and widely used technique.

2.5.1.1 Electrospinning technique

It is composed of a syringe with a nozzle, an electric field source, a counter electrode, and a pump. It's principle is based upon the concept of electrostatics in which for the synthesis, the electrostatic repulsion forces under high electrical field are used.⁷¹ The solution to be electrospun is filled in a syringe nozzle and a large electric field is applied across them. When the solution is released, their droplets at the tip forms a cone shaped deformation as there is potential difference between the nozzle and the grounded target. As the charged jet promotes, the solvent in the solution evaporates and forms stable continuous nanofibers on the grounded target. The properties of nanofibers get affected by parameters used, such as solution properties, temperature, humidity, tip-counter distance, applied electric voltage, and flow rate.⁷²

Other than the conventional electrospinning technique, several modifications in this method have been reported later. This includes the multineedle, needleless, and co-electrospinning technique. In recent years the increasing emergence of novel strategies for the generation of nanofibers in a larger scale is used like CO₂ laser supersonic drawing, solution blow spinning, centrifugal jet spinning, and electrohydrodynamic direct writing.⁷³

2.6 Mechanism of antibacterial and antibiofilm activity of ZnO NPs

Chapter 2: ZnO nanoparticles as an antibacterial and antibiofilm agent: Survey of development

Cells in biofilm develop more resistance than planktonic bacterial cells towards antimicrobial agents. In this regard, the functions of ZnO nanocomposites are very important, as they possess more properties of multiple materials than the pure form of ZnO. Thaya et al.⁷⁴ synthesized chitosan coated silver-zinc oxide nanocomposite (Cs/Ag/ZnO) and performed antibiofilm activity against Gram-positive bacteria like *Bacillus licheniformis* and *Bacillus cereus* and Gram-negative bacteria like *Vibrio parahaemolyticus* and *Proteus vulgaris* where they saw a more efficient inhibition of biofilm in Gram positive bacteria than that of Gram negative bacteria at 30 µg/ml concentration. Also, they showed that the hydrophobicity index and extracellular polymeric substance (EPS) production in both Gram-positive and Gram-negative bacteria decreased after treatment with Cs/Ag/ZnO nanocomposite. The antimicrobial effect of ZnO is considerably more with polymer chitosan and Ag nanoparticles, and these provide a development of biomaterials and an effective agent in controlling microbial infections.⁷⁴ Zinc oxide nanoparticles show a great antibacterial ability that can limit the growth of microorganisms. Different properties of ZnO that enhance their potential use as an antibacterial and antibiofilm agents are shown in figure 2.2. Researchers proposed multiple mechanisms for the damage of cells induced by ZnO nanoparticles. However, the actual mechanism is not fully understood and is still controversial. Nevertheless, distinctive mechanisms have been proposed that include direct interaction with a bacterial cell, damage to cell integrity, the liberation of ROS species and antimicrobial Zn²⁺ ions, damage of lipids, proteins, carbohydrates, and DNA by oxidative stress, lipid peroxidation that disrupts vital cell functions.⁷⁵ Many studies suggested that the intensity of antibacterial activity was significantly affected by morphology.⁷⁶ The shape of nanoparticles affects their mechanism of internalization so that rod and wire shaped nanoparticles are penetrated more easily than spherical shaped nanoparticles. Mahamuni et al.¹⁹ found that among all synthesized ZnO nanoparticles, a particle of at least with ~ 15 nm in size exhibited maximum antibacterial and antibiofilm activity against Gram-positive *Staphylococcus aureus* (NCIM2654) and Gram-negative *Proteus vulgaris* (NCIM2613). It is widely reported that the antibacterial activity of ZnO nanoparticles is inversely proportional to the size and

Chapter 2: ZnO nanoparticles as an antibacterial and antibiofilm agent: Survey of development

directly proportional to concentration.¹⁹ Commonly studied mechanisms are explained as follows.

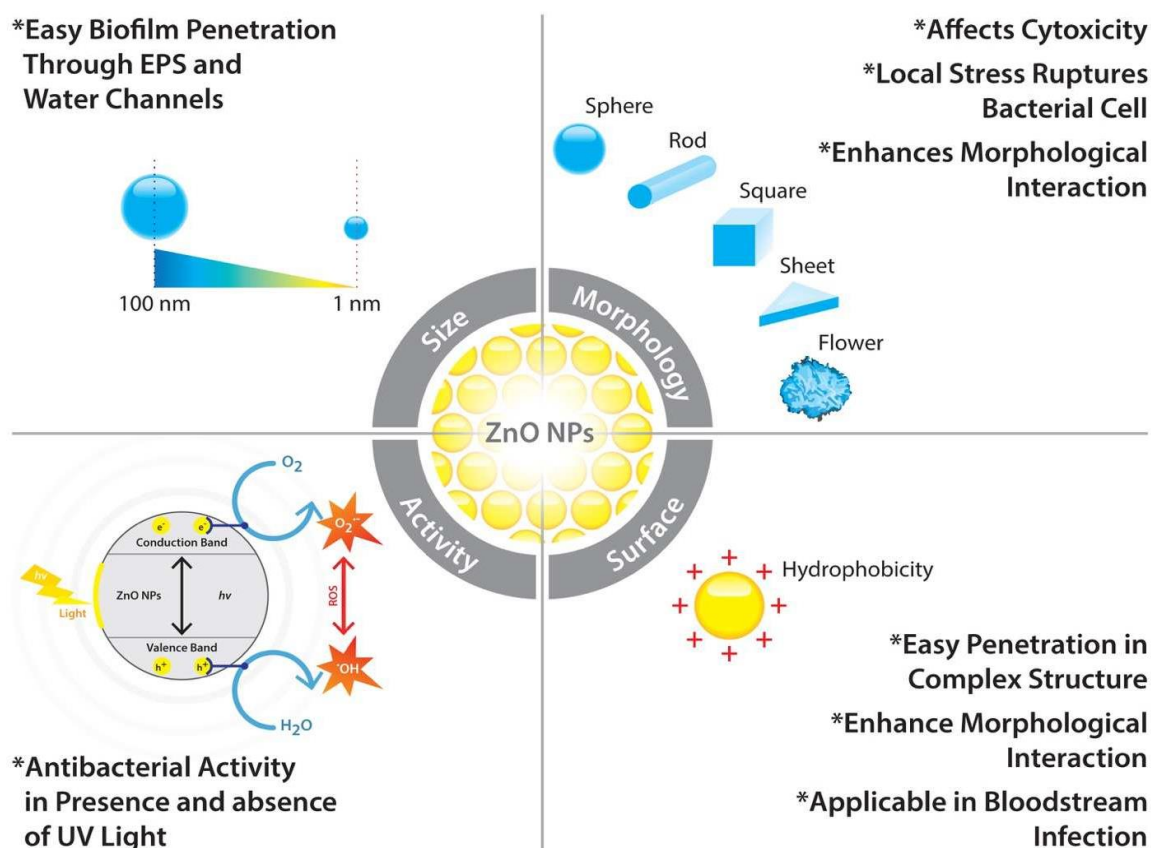


Figure 2.2: Size and shape, surface and interior properties of ZnO NPs that enhance their use in biofilm related infections.⁷⁵

Size of pores generally ranges from 10nm up to few micrometers, with nanometer size ZnO NPs can easily get penetrated through EPS and water channels. Variations in shape enhance the morphological interactions. Hydrophobicity enhances their penetration in complex

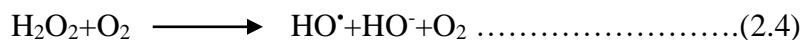
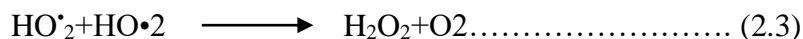
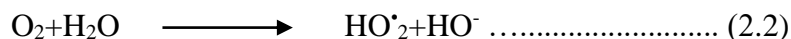
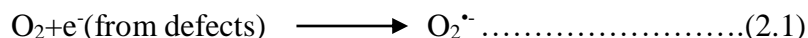
Chapter 2: ZnO nanoparticles as an antibacterial and antibiofilm agent: Survey of development

structure and makes them applicable in bloodstream infections. Interior properties promote their antibacterial activity in the presence and absence of UV light.

2.6.1 Liberation of reactive oxygen species (ROS):

This is the most widely reported and accepted mechanism for the antibacterial activity of ZnO. Reactive oxygen species include highly reactive ionic species, free radicals such as $O^{\bullet-}$, $HO\bullet_2$, H_2O_2 and $HO\bullet$ that damage cells by inducing an oxidative stress response.^{77,78} Disturbance of the balance between generated ROS and their reducing equivalents is termed as oxidative stress.⁷⁹ As ZnO possesses enormous considerable exciton binding energy (60 meV), they generate bound electron-hole pairs when exposed to photons with $\lambda < 390\text{ nm}$.⁸⁰ When ZnO is under UV or visible light, it liberates electron or whole pairs with free electrons in the conduction band (e^-_{CB}) and valence band (h^+_{VB}). These pairs produce OH^{\bullet} and H^+ by interaction with water, then the conduction band electron with oxygen undergoes several of reactions and produces intermediates like $O^{\bullet-}$, $HO\bullet_2$, H_2O_2 , and $HO\bullet$ on ZnO surface.⁸¹ Negatively charged anions cannot enter the cytoplasmic membrane, only H_2O_2 can be internalized and damage the cell.⁸² The concentration of ROS species increases as the concentration of ZnO NPs increases. Raghupathi et al.⁸³ studied the effect of UV irradiated ZnO on bacteria. He observed complete removal of viable cells of *S. aureus* after 30 minutes of exposure to UV. This activity under the presence of UV highlights the critical role of ROS in biocidal activity. Ionization of carboxylic, phosphate and amino groups on the cell surface gives a negative charge to the cell that significantly affects the accumulation of ZnO NPs on the cell surface. Because of the negative charge on the cell surface, ZnO NPs are internalized in a thick peptidoglycan layer of Gram-positive bacteria readily than thin layer of Gram-negative bacteria.⁸⁴ Generation of ROS is contradictory. Several studies reported this mechanism under light while some reported it in a dark condition.^{85,86} Surface defects in ZnO crystals are mainly responsible for the liberation of ROS in dark conditions. ROS generation is followed by the release of electrons under dark condition through the following steps,

Chapter 2: ZnO nanoparticles as an antibacterial and antibiofilm agent: Survey of development



2.6.2 Release of Zn^{2+} ions:

One of the essential mechanisms for the antibacterial activity of ZnO is the generation of zinc ions in an aqueous media containing ZnO and bacteria. The mechanism of attachment of ZnO to the cell surface and its transport inside the cell is different for that of Gram-positive and Gram-negative bacteria because of the differences in cell wall composition. Gram-positive bacterial cell contains a thick layer of peptidoglycan along with teichoic acid and lipoteichoic acid. These acids act as chelating agents for Zn^{2+} ions and transport inside the cell.⁸⁷ However, Gram -positive bacteria are less sensitive to the damage due to Zn^{+2} ions. This is because entrapment of Zn^{+2} ions into thick negatively charged peptidoglycan layers causes less toxicity than that of thinner peptidoglycan layered Gram-negative bacteria.³⁷ A thin layer of peptidoglycan in Gram negative bacteria showed less resistance for internalization of ZnO nanoparticles. Zang et al.⁸⁴ suggested that water chemistry has an essential role in the toxicity mechanism of ZnO in water. In this study, they used five different aqueous media which is: ultrapure water, 0.85% NaCl, phosphate buffer saline (PBS), minimal Davis (MD) and Luria bertani. In this media combined results of antibacterial activity showed toxicity, is because of free zinc ions and labile zinc complexes. The toxicity of ZnO in five media was like that of ultrapure>NaCl>MD>LB>PBS. These results highlight the role of aqueous media in the physico-chemical properties of nanoparticles and the physiological function of the organism. Release of the Zn^{+2} ions is strongly affected by the morphology of nanoparticles. Spherical nanoparticles release more Zn^{+2} ions than rod shaped ZnO, due to a smaller surface area and high equilibrium

Chapter 2: ZnO nanoparticles as an antibacterial and antibiofilm agent: Survey of development

solubility. Zn^{+2} ions cause conformational changes in enzymes leading to the distortion of active sites in enzymes resulting in competitive or non-competitive reversible inhibition. Zinc ions mainly interact with cysteine, aspartate and histidine side chains of proteins or enzymes and cause inhibition of enzymes like glyceraldehydes 3 phosphate dehydrogenase, aldehyde dehydrogenase, protein tyrosine phosphatases (PTPs). Zn^{+2} is a competitive inhibitor of aspartate and magnesium.⁴⁹ The number of Zn^{+2} ions increases by balancing pH less than or greater than 6 above because the solubility of ZnO increases at these pH values.³⁴

2.6.3 Other possible mechanisms:

Mainly negatively charged ROS cannot quickly enter the bacterial cell; however, positively charged H_2O_2 can easily interact with the bacterial cell. It is considered that, as soon as membrane disrupts by H_2O_2 or $\text{HO}\bullet$, negatively charged ROS can easily penetrate the cytoplasmic region, which enhances antibacterial activity.⁴² Released H_2O_2 strongly interacts with cysteine, thiol residues in intracellular space and deactivates enzyme glyceraldehydes-3 phosphodehydrogenase. Physical interaction of ZnO with the bacterial cell also causes antibacterial activity. It is reported that positively charged ZnO possesses zeta potential value of +24mV.⁸⁸ A bacterial cell has a negative electrostatic surface charge at physiological pH values. These opposite charges significantly enhance interaction between them. The size of nanoparticles is also an important factor for internalization with bacteria; smaller nanoparticles interact and accumulate on the outer surface and the plasma membrane leads to increased surface tension and membrane depolarization by neutralizing surface potential. This causes membrane permeability and results in cytoplasmic fluid leakage that leads to cell death. However, many reports state that this is not the only mechanism responsible.³⁴ It is also reported that the interaction between cells and nanoparticles increases cell permeability. Surface defects, surface charges, and the presence of numerous edges and corners of ZnO nanoparticles affect the intensity of antibacterial activity. Prasanna et al.⁸⁸ studied the antimicrobial activity of microparticle, nanoparticle and capped nano-ZnO in dark and light conditions, and concluded that ROS are mainly produced from an

Chapter 2: ZnO nanoparticles as an antibacterial and antibiofilm agent: Survey of development

aqueous suspension of ZnO in dark. Further, they also concluded that surface defects on ZnO played an important role in presence and absence of light. They observed the highest antimicrobial activity for nano-ZnO, and lowest for micro ZnO with capped ZnO that highlighted the important role of surface defects in ROS generation. ZnO NPs are excellent antibacterial agents because of their good antimicrobial property. However, the precise mechanism of ZnO is not fully understood. Studies should be focused on theoretical experiments and quantum chemistry calculations that will provide basic and routine toxicity experiments, such as simple assays for oxidative stress and measurement of metal ion release and ROS generation.

Chapter 2: ZnO nanoparticles as an antibacterial and antibiofilm agent: Survey of development

References

- 1 S. S. Kumar, P. Venkateswarlu, V. R. Rao and G. N. Rao, *Int. Nano Lett.*, 2013, **3**, 1–30.
- 2 M. Rai, A. Yadav and A. Gade, *Biotechnol. Adv.*, 2009, **27**, 76–83.
- 3 J. Sawai, *J. Microbiol. Methods*, 2003, **54**, 177–182.
- 4 M. Roselli, A. Finamore, I. Garaguso, M. S. Britti and E. Mengheri, *J. Nutr.*, 2018, **3**, 4077–4082.
- 5 Q. Chaudhry, M. Scotter, J. Blackburn, B. Ross, L. Castle, R. Aitken, R. Watkins and Chaudhry, *Food Addit. Contam.*, 2016, **49**, 241–258.
- 6 J. W. Rasmussen, E. Martinez, P. Louka and D. G. Wingett, *Drug Deliv.*, 2010, **7**, 1063–1077.
- 7 Z. Zhang and H. Xiong, *Materials (Basel)*, 2015, **8**, 3101–3127.
- 8 S. Kim, S. Y. Lee and H. Cho, *nanomaterials*, 2017, **7**, 1–13.
- 9 G. Yi, C. Wang and W. Il Park, *semicond.Sci.Technol*, 2005, **20**, S22–S34.
- 10 F. Demoisson, R. Piolet and F. Bernard, *Cryst. Growth Des.*, 2014, **14**, 5388–5396.
- 11 V. K. H. Bui, D. Park and Y. C. Lee, *Polymers (Basel)*, 2017, **9**, 1–24.
- 12 P. P. Mahamuni-Badiger, P. M. Patil, M. V. Badiger, P. R. Patel, B. S. Thorat-Gadgil, A. Pandit and R. A. Bohara, *Mater. Sci. Eng. C*, 2020, **108**, 1–74.
- 13 H. Mirzaei and M. Darroudi, *Ceram. Int.*, 2017, **43**, 907–914.
- 14 M. Vaseem, A. Umar and Y. Hahn, *ZnO Nanoparticles : Growth, Properties, and Applications*, 2010, vol. 5.
- 15 S. B. Bagherzadeh and M. Haghighi, *Energy Convers. Manag.*, 2017, **142**, 452–465.

Chapter 2: ZnO nanoparticles as an antibacterial and antibiofilm agent: Survey of development

- 16 E. Nosál and L. Reinprecht, *BioResources*, 2017, **12**, 7255–7267.
- 17 S. Shahid, S. A. Khan, W. Ahmad, U. Fatima and S. Knawal, *Indian J. Pharm. Sci.*, 2018, **80**, 173–180.
- 18 A. B. Djuri, X. Y. Chen and Y. H. Leung, *Recent Pat. Nanotechnol.*, 2012, **6**, 124–134.
- 19 P. P. Mahamuni, P. M. Patil, M. J. Dhanavade, M. V. Badiger, P. G. Shadija, A. C. Lokhande and R. A. Bohara, *Biochem. Biophys. Reports*, 2019, **17**, 71–80.
- 20 F. Iskandar, *Adv. Powder Technol.*, 2009, **20**, 283–292.
- 21 W. Ao, J. Li, H. Yang, X. Zeng and X. Ma, *Powder Technol.*, 2006, **168**, 148–151.
- 22 A. Kołodziejczak-radzimska, E. Markiewicz and T. Jesionowski, *J. Nanomater.*, 2012, **2012**, 1–9.
- 23 O. U. Native and M. Chitosans, *Materials (Basel).*, 2013, **6**, 4198–4212.
- 24 P. Rai, W. Kwak and Y. Yu, *Appl. Mater. Interfaces*, 2013, **5**, 3026–2023.
- 25 B. Bonthagarala, *Int. J. Pharm. Res. Bio-Science*, 2018, **6**, 170–177.
- 26 H. Agarwal, S. Venkat Kumar and S. Rajeshkumar, *Resour. Technol.*, 2017, **3**, 406–413.
- 27 N. Salah, S. S. Habib, Z. H. Khan, A. Memic, A. Azam, E. Alarfaj, N. Zahed and S. Al-Hamed, *Int. J. Nanomedicine*, 2011, **6**, 863–869.
- 28 Y. Qian, J. Yao, M. Russel, K. Chen and X. Wang, *Environ. Toxicol. Pharmacol.*, 2015, **39**, 736–746.
- 29 J. M. Yousef and E. N. Danial, *Int. J. Heal. Sci.*, 2012, **2**, 38–42.
- 30 X. W. Yiguang Qian, Jun Yao, Mohammad Russelc, Ke Chena, *Environ. Toxicol. Pharmacol.*, 2015, **39**, 736–746.

Chapter 2: ZnO nanoparticles as an antibacterial and antibiofilm agent: Survey of development

- 31 B. Woei and Y. Ying, *Mater. Lett.*, 2012, **73**, 78–82.
- 32 H. Dong, Y.-C. Chen and C. Feldmann, *Green Chem.*, 2015, **17**, 4107–4132.
- 33 J. Zhang, B. Zhao, Z. Pan, M. Gu and A. Punnoose, *Cryst. Growth Des.*, , DOI:10.1021/cg5017017.
- 34 M. Shimizu, *J. Ferment. bioengineering*, 1998, **86**, 521–522.
- 35 V. Sharma, D. Anderson and A. Dhawan, *Apoptosis*, 2012, **17**, 852–870.
- 36 P. Taylor, H. A. Jeng and J. Swanson, *J. Environ. Sci. Heal. Part A*, 2006, **41**, 2699–2711.
- 37 S. Pal, Y. K. Tak and J. M. Song, *Applied Environ. Microbiol.*, 2007, **73**, 1712–1720.
- 38 G. R. Li, T. Hu, G. L. Pan, T. Y. Yan, X. P. Gao and H. Y. Zhu, *J. Phys, Chem*, 2008, **112**, 11859–11864.
- 39 J. Ma, J. Liu, Y. Bao, Z. Zhu, X. Wang and J. Zhang, *Ceram. Int.*, 2013, **39**, 2803–2810.
- 40 D. Uskokovi, *Colloids Surf. B Biointerfaces*, 2013, **102**, 21–28.
- 41 N. Padmavathy and R. Vijayaraghavan, *Sci. Technol. Adv. Mater.*, 2008, **9**, 1–7.
- 42 L. Zhang, Y. Jiang, Y. Ding, M. Povey and D. York, *J. Nanoparticle Res.*, 2007, **9**, 479–489.
- 43 N. J. Rogers, S. C. Apte, G. E. Batley, G. E. Gadd and P. S. Casey, *Environ.sci. Technol*, 2007, **41**, 8484–8490.
- 44 O. Yamamoto, *Int. J. Inorg. Mater.*, 2001, **3**, 643–646.
- 45 S. Ahmed, G. Cheng, X. Chai, J. Cai, Y. Wu, F. Wang, Y. Gu, J. Li, C. Zhang and S. Xie, *Front. Pharmacol.*, 2017, **8**, 1–11.
- 46 J.-H. Lee, Y.-G. Kim, M. H. Cho and J. Lee, *Microbiol. Res.*, 2014, **169**, 888–896.

Chapter 2: ZnO nanoparticles as an antibacterial and antibiofilm agent: Survey of development

- 47 J. Bao, I. Shalish, Z. Su, R. Gurwitz, F. Capasso, X. Wang and Z. Ren, *Nanoscale Res. Lett.*, 2011, **6**, 1–7.
- 48 G. Zhou, Y. Li, W. Xiao, L. Zhang, Y. Zuo, J. Xue and J. A. Jansen, *J. Biomed. Mater. Res. - Part A*, 2007, **85A(4)**, 929–937.
- 49 R. Brayner, R. Ferrari-iliou, N. Brivois, S. Djediat, M. F. Benedetti, F. Fie, P. Cedex and L. De Ge, *Nano Lett.*, 2006, **6(4)**, 2–6.
- 50 P. K. Stoimenov, R. L. Klinger, G. L. Marchin and K. J. Klabunde, *Langmuir*, 2002, **18**, 6679–6686.
- 51 P. Lin, S. Lin, P. C. Wang and R. Sridhar, *Biotechnol. Adv.*, 2013, **32(4)**, 711–726.
- 52 V. Vijayakumar, S. K. Samal, S. Mohanty and S. K. Nayak, *Int. J. Biol. Macromol.*, 2018, #pagerange#.
- 53 B. Jamil, R. Abbasi, S. Abbasi, M. Imran, S. U. Khan, A. Ihsan, S. Javed, H. Bokhari and M. Imran, *Front. Microbiol.*, 2016, **7**, 1–10.
- 54 M. Ferrari, *Nanogeometry*, 2008, **3**, 1–2.
- 55 S. George, S. Lin, Z. Ji, C. R. Thomas, L. Li, M. Mecklenburg, H. Meng, X. Wang, H. Zhang, T. Xia, J. N. Hohman, S. Lin, J. I. Zink and G. E. T. Al, *ACS Nano*, 2012, **6**, 3745–3759.
- 56 P. C. Balaure, A. M. Holban, A. M. Grumezescu, G. D. Mogoşanu, T. A. Bălşeanu, M. S. Stan, A. Dinischiotu, A. Volceanov and L. Mogoantă, *Int. J. Pharm.*, 2019, **557**, 199–207.
- 57 H. Yang, C. Liu, D. Yang, H. Zhang and Z. Xi, *J. Appl. Toxicol.*, 2009, **29**, 69–78.
- 58 A. Al-Kattan, V. P. Nirwan, E. Munnier, I. Chourpa, A. Fahmi and A. V. Kabashin, *RSC Adv.*, 2017, **7**, 31759–31766.
- 59 C. X. Yu Gao , Yiyuan Han , Mingyue Cui, Hong Liang Tey, Lianhui Wang, *J. Mater.*

Chapter 2: ZnO nanoparticles as an antibacterial and antibiofilm agent: Survey of development

- Chem. B*, 2017, **5(23)**, 4535–4541.
- 60 K. T. Shalumon, K. H. Anulekha, S. V Nair, S. V Nair, K. P. Chennazhi and R. Jayakumar, *Int. J. Biol. Macromol.*, 2011, **49**, 247–254.
- 61 Y. Chen, W. Lu, Y. Guo, Y. Zhu and Y. Song, *Nanomaterials*, 2019, **9**, 525–532.
- 62 K. Sudesh, H. Abe and Y. Doi, *Prog. Polym. Sci.*, 2000, **25**, 1503–1555.
- 63 P. Kuppan, K. S. Vasanthan, D. Sundaramurthi, U. M. Krishnan and S. Sethuraman, *Biomacromolecules*, 2011, **12**, 3156–3165.
- 64 N. Nagiah, L. Madhavi, R. Anitha, C. Anandan, N. Tirupattur and U. Tirichurapalli, *Mater. Sci. Eng. C*, 2013, **33**, 4444–4452.
- 65 S. M. Tan, J. Ismail, C. Kummerlöwe and H. W. Kammer, *J. Appl. Polym. Sci.*, 2006, **101**, 2776–2783.
- 66 S. H. Diermann, M. Lu, G. Edwards, M. Dargusch and H. Huang, *J. Biomed. Mater. Res. - Part A*, 2018, **107**, 1–9.
- 67 B. Veleirinho, D. S. Coelho, P. F. Dias, M. Maraschin, R. M. Ribeiro-do-valle and J. A. Lopes-da-silva, *Int. J. Biol. Macromol.*, 2012, **51**, 343–350.
- 68 S. Modi, K. Koelling and Y. Vodovotz, *Eur. Polym. J.*, 2015, **47**, 179–186.
- 69 P. P. Mahamuni-Badiger, P. M. Patil, P. R. Patel, M. J. Dhanavade, M. V. Badiger, Y. N. Marathe and R. A. Bohara, *New J. Chem.*, , DOI:10.1039/d0nj01384f.
- 70 S. E. M. Catoni, K. N. Trindade, C. A. T. Gomes, A. L. S. Schneider, A. P. T. Pezzin and V. Soldi, *Polimeros*, 2013, **23**, 320–325.
- 71 A. M. Behrens, B. J. Casey, M. J. Sikorski, K. L. Wu, W. Tutak, A. D. Sandler and P. Ko, *ACS Macro Lett.*, 2014, **3**, 249–254.

Chapter 2: ZnO nanoparticles as an antibacterial and antibiofilm agent: Survey of development

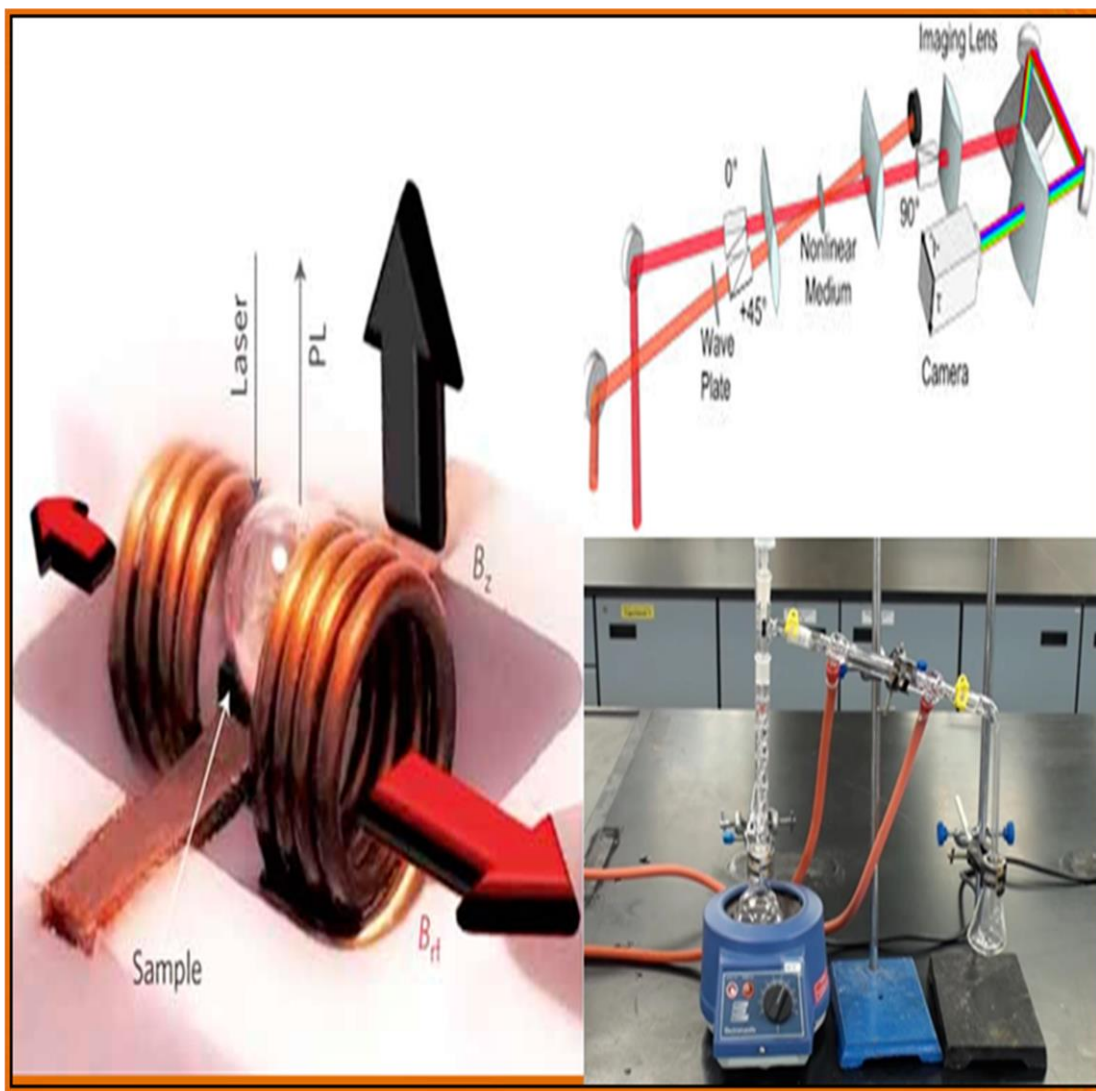
- 72 Y. Li, F. X. Zhao, X. X. Lian, Y. L. Zou, Q. Wang and Q. J. Zhou, *J. Electron. Mater.*, 2016, **45**, 3149–3156.
- 73 M. M. Mihai, M. B. Dima, B. Dima and A. M. Holban, *Materials (Basel)*., 2019, **12**, 1–16.
- 74 R. Thaya, B. Malaikozhundan, S. Vijayakumar, J. Sivakamavalli, R. Jeyasekar, S. Shanthi, B. Vaseeharan, P. Ramasamy and A. Sonawane, *Microb. Pathog.*, 2016, **100**, 124–132.
- 75 T. A. Ostomel, Q. Shi, P. K. Stoimenov and G. D. Stucky, *Langmuir*, 2007, **23**, 11233–11238.
- 76 M. Talebian, N., Amininezhad, S. M., & Doudi, *J. Photochem. Photobiol. B Biol.*, 2013, **120**, 66–73.
- 77 M. Jiang, J. Zhang, L. Qian, Y. Miao, W. Song, H. Liu and R. Li, *iScience*, 2018, **11**, 189–204.
- 78 H. Chen, C. Liu, D. Chen, K. Madrid, S. Peng, X. Dong, M. Zhang and Y. Gu, *Mol. Pharm.*, 2015, **12(7)**, 2505–2516.
- 79 R. Rodrigo, M. Libuy, F. Feliú and D. Hasson, *BioMed*, 2013, **2013**, 15.
- 80 A. Jain, R. Bhargava and P. Poddar, *Mater. Sci. Eng. C*, 2013, **33**, 1247–1253.
- 81 M. Fang, J. Chen, X. Xu, P. Yang and H. F. Hildebrand, *Int. J. Antimicrob. Agents*, 2006, **27**, 513–517.
- 82 L. S. Reddy, M. M. Nisha, M. Joice and P. N. Shilpa, *Pharm. Biol.*, 2014, **52**, 1388–1397.
- 83 K. R. Raghupathi, R. T. Koodali and A. C. Manna, *Langmuir*, 2011, **27**, 4020–4028.
- 84 X. Zhang, X. Zhou, H. Xi, J. Sun, X. Liang, J. Wei, X. Xiao, Z. Liu, S. Li, Z. Liang, Y. Chen and Z. Wu, *Colloids Surfaces B Biointerfaces*, 2019, **177**, 454–461.

Chapter 2: ZnO nanoparticles as an antibacterial and antibiofilm agent: Survey of development

- 85 R. Balasubramanian, S. S. Kim, J. Lee and J. Lee, *Int. J. Biol. Macromol.*, 2019, **123**, 1020–1027.
- 86 B. Ahmed, B. Solanki, A. Zaidi, M. S. Khan and J. Musarrat, *Toxicol. Res. (Camb)*., 2019, **8**, 246–261.
- 87 A. Kumar, A. K. Pandey, S. S. Singh, R. Shanker and A. Dhawan, *Chemosphere*, 2011, **83**, 1124–1132.
- 88 J. Lee, M. Ramasamy and J. Lee, *Biomed Res. Int.*, 2016, **2016**, 1–18.

CHAPTER 3

Experimental Techniques



“Outside their laboratories, the physicians and chemist are soldiers without arms on the field of battle.” - Louise Pasteur

3.1. Introduction

The selection of the method of synthesis carries a significant role in the morphology of ZnO nanoparticles, which in turn makes it potential material with desirable properties for biological applications. ZnO Nps are synthesized by chemical methods and their properties are improved with further functionalisation.

After synthesis, the primary step is the characterization of the material. The material characterization provides information by which one could decide its applicability for directed applications. The material needs characterization that depends upon its application. This led to the advancement of different techniques in the field of analytical science. The phase analysis, compositional analysis, surface characterization, structural analysis and activity of synthesized nanoparticles toward biofilm forming pathogenic microorganisms and mammalian cells were characterized by various techniques like UV-visible (UV-Vis) spectroscopy, X-ray diffraction (XRD), Scanning Electron Microscopy (SEM), Transmission Electron Microscopy (TEM), Energy dispersive microanalysis (EDX), Fourier Transform Infra-Red (FTIR) Spectroscopy, Thermogravimetric analysis (TGA), Differential Scanning Calorimetry (DSC), Swelling studies, Dynamic mechanical analysis (DMA) and toxicological studies: cytotoxicity studies, hemolysis studies. This chapter explains the principles and operations of mentioned analytical techniques used for characterization.

3.2 Synthesis of ZnO nanoparticles

In material science, zinc oxide is classified as a semiconductor in group II-VI, with band gap energy (3.37 eV), high bond energy (60 meV) and high thermal and mechanical stability.^{1,2} A variety of techniques are used to synthesize zinc oxide nanoparticles as chemical, physical and biological methods. The chemical method includes a liquid phase synthesis and gas phase synthesis. The liquid phase synthesis consists of hydrothermal synthesis, precipitation, polyol method, sol-gel process, colloidal method, precipitation method. The use of polyols in the synthesis process allows nanoparticles to be produced with high crystallinity by restricting agglomeration and controlled morphology as polyols possess unique properties like high boiling point, a high dielectric constant and solubility of metal salt precursors.³ Physical or mechanical

Chapter 3: Experimental techniques

methods of synthesis consist of high energy ball milling, physical vapor deposition, sputter deposition, melt mixing and ion implantation. These methods mostly preferred in industrial processes that yield ZnO with high production rates.⁴ The biological method or green synthesis method include the use of green routes that include use of micro-organisms like bacteria, fungi, algae and plants in the ZnO NPs synthesis. For the purpose of monodispersed and reduced size particles, chemical method is used for the synthesis of ZnO nanoparticles.⁵⁻¹¹ Benefits and drawbacks of synthesis methods are described in chapter 2.

3.2.1 Electrospinning technique

With the development in nanotechnology, the electrospinning technique has received much more attention because of its versatility and potential for applications in various fields. The remarkable applications include tissue engineering, biosensors, filtration, wound dressings, and drug delivery. The fine fibers are produced under the strong electric field on polymer solution. The electrospun fibers possess different properties like a high surface area to volume ratio, controlled porosity, and varieties of compositions in order to get desired properties. From a long time, more than 200 polymers have been used to design electrospun fibers for various applications. Furthermore, a DC voltage of kVs is important to generate the electrospinning. This process is carried out at room temperature. There are two standard setups of electrospinning, vertical and horizontal. A typical setup is shown in figure3.1. This system composed of three major components: a high voltage power supply, a spinneret, and a grounded collecting plate and uses a high voltage source to inject polymer solution or melt, which is collected towards a collector plate. Most of the polymers are dissolved in some solvents and added into the capillary tube for electrospinning. A polymer solution is subjected to an electric field and electric charge is generated on the liquid surface. When an applied electric field reaches a higher level, a charged jet of the solution is released from the tip of Taylor cone and gets collected on plate that leads to the evaporation of the solvent, leaving polymer behind. There are varieties of polymers used in the electrospinning process. Poly (3-hydroxybutyrate-co-3-hydroxyvalerate)(PHBV), is a member of polyhydroxyalkanoates (PHA), is bio-degradable, biocompatible, and nontoxic polyester produced from bacteria. Also, PHBV have good mechanical strength and its degradation product (R)-3-hydroxybutyric acid, which is a normal component of human blood.

Chapter 3: Experimental techniques

So, PHBV can be extensively used as biomaterials. However, its use is restricted due to high crystallinity, fragility and poor hydrophilicity. So to overcome the defects of PHBV, it can be blended with other polymers. Poly (ethylene oxide)(PEO) is a biocompatible, hydrophilic polymer which is easy to electrospin and possesses greater solubility not only in water but also in organic solvents.¹² Here in the present study we have blended hydrophobic PHBV with hydrophilic PEO and incorporated ZnO NPs and tested for their antibacterial and antibiofilm applications against pathogenic microorganisms.

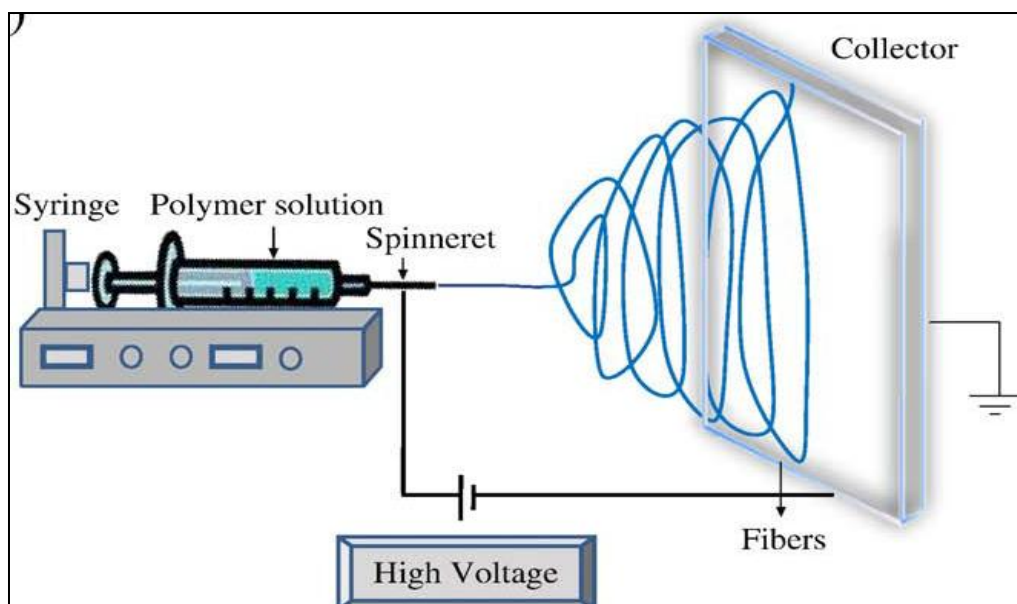


Figure 3.1: Schematic representation of electrospinning process.¹²

3.3 Characterization techniques

3.3.1. Structural and phase analysis

3.3.1.1. X-ray Diffraction (XRD)

The discovery of X-ray was done by Wilhelm Roentgen (1895) who suggested that any produced radiation could find out that travel to the opaque matter. X-ray Diffraction technique (XRD) is a non-destructive very important technique which is commonly used to characterize the material. X-ray diffraction provides useful information such as crystal structures, crystal defects, stresses, grain size and orientation, the composition of phases, film thickness and identification

Chapter 3: Experimental techniques

of unknown materials. In XRD, diffraction that ranges from 0.7 to 2\AA typically occurs when the wave motion's wavelength is of the same magnitude as the repeat distance between scatterings points. This diffraction by the crystalline phases in the specimen is given by Bragg's law and formulated by the mathematical expression which is represented in equation 3.1

$$2d \sin\theta = n\lambda \dots\dots\dots (3.1)$$

Where,

d = interplanar spacing

θ = diffraction angle

λ = wavelength of X-ray

n = order of diffraction

Generally, four types of diffraction techniques are considered as Laue photographic method, Bragg X-ray spectrometer method, Rotating crystal method, and the powder method.¹³ The extensively used X-ray diffraction technique is the powder technique. This method is used throughout the proposed work where the value of λ is constant and the value of θ is variable. This technique requires only a small quantity as 1 mg of sample for the study. Finely powder samples are kept in the monochromatic X-ray beam. Each particle randomly rotated with respect to the incident X-ray beam. In the powder method, rotation is not necessary, because the sample contains micro-crystals that move in all possible orientations. Figure 3.2 shows the X-ray diffractometer. A diffractometer is commonly constructed on the basis of Bragg-Brentano geometry. Mostly it consists of an X-ray source and detector for detection of diffracted X-rays and figure 3.2 (b) shows bench top X-ray instrument. In a crystallite, solid atoms undergo in the particular repeated pattern referred with its inter-atomic spacing comparable to wavelength of X-ray ($0.5\text{--}2.5 \text{\AA}$).¹⁴ The orientation of diffracted X-rays gives information of the atomic arrangements and phase formation and crystal structure can be ensured by X-ray diffraction studies.

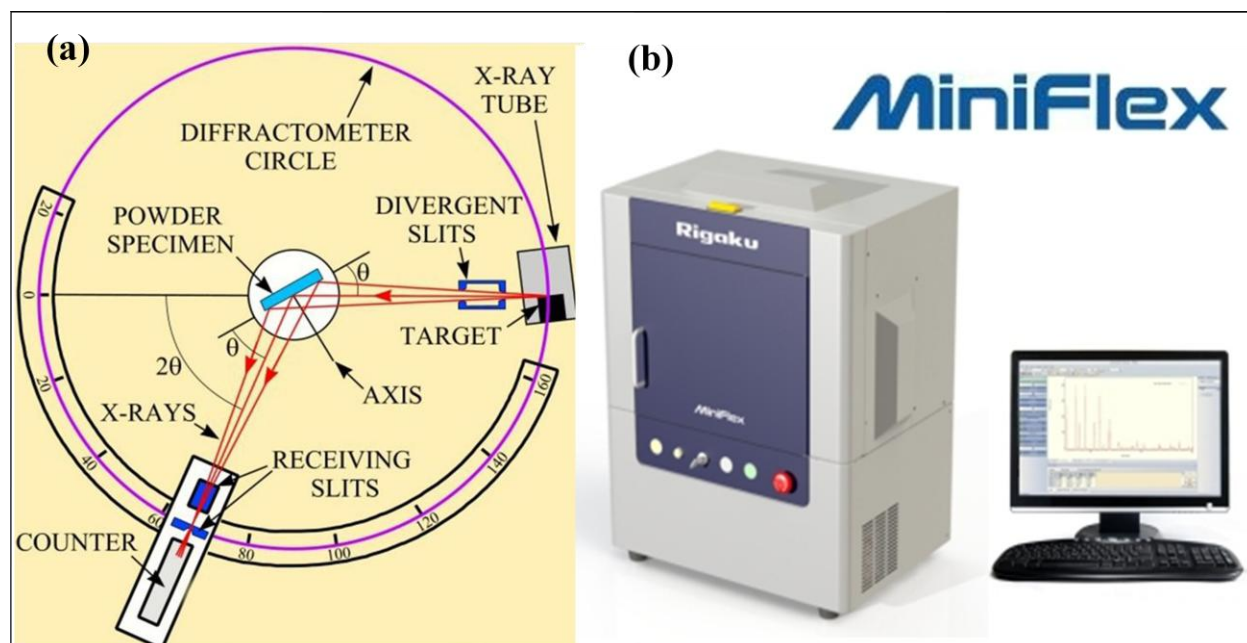


Figure 3.2: (a) Schematic representation of X-ray diffractometer technique¹⁵ (b) Image of X-ray diffraction instrument^{16,17}

Phase identification

Phases can be determined from the d-spacing, with the help of standard JCPDS powder diffraction file generated by the International Center for Diffraction Data (ICDD) and reflection is matched with Miller indices. If the average crystallite size is very tiny (below ~ 2000 Å diameter), there is an additional broadening of the diffracted X-ray beam. From this broadening of a peak, crystallite size can be determined by Scherrer equation 3.2

$$D = \frac{0.9\lambda}{\beta \cos \theta} \dots \dots \dots (3.2)$$

Where,

D = particle size,

θ = diffraction angle

λ = wavelength of X-rays

β = line broadening at Full Width at Half Maxima (FWHM).

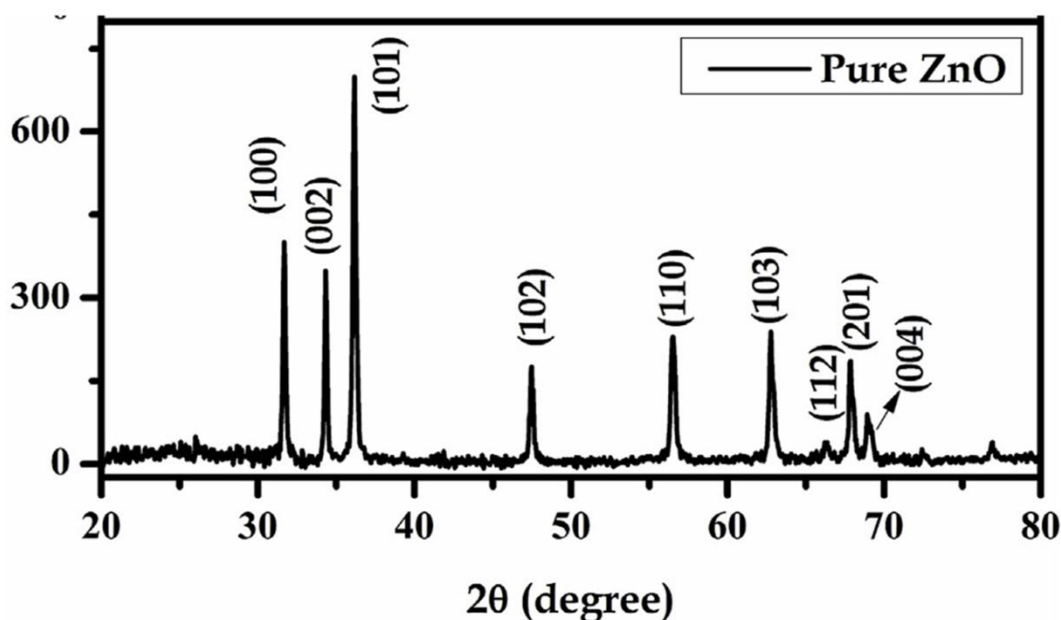


Figure 3.3: A typical XRD pattern of pure ZnO nanoparticles.¹⁷

The Specifications of the instrument Rigaku 600Miniflex X-ray diffraction instrument (XRD) with $\text{CuK}\alpha$ radiation ($\lambda = 1.5412 \text{ \AA}$) in the scanning range of 10° - 80° . Figure 3.3 represents typical XRD pattern of ZnO nanoparticles.

3.3.1.2 Fourier Transform Infrared Spectroscopy (FTIR)

FTIR is a powerful analytical technique that was developed in the 1970s to characterize organic and inorganic compounds by using infrared absorption of molecules. Its working is based upon the principle that particular molecules absorb light energy of a particular wavelength, termed as their resonance frequencies. The energy transfer is in different forms like bond vibrations, electron ring shifts, rotations, and translations. So, the confirmation of specific functional groups or chemical bonds is easily possible as each will show different patterns of absorption.^{18,19} Therefore, to confirm functionalisation of ZnO nanoparticles, we have used FTIR technique throughout the presented work. The basic components of the FTIR are shown in figure 3.4. Infrared radiations with broad band of different wavelength get emitted by the infrared source. It passed through an interferometer where infrared radiations get modulated. The interferometer activates an optical inverse Fourier transform as soon as IR radiation enters. The

Chapter 3: Experimental techniques

gas sample receives the altered IR beam where it gets absorbed to a various extent at different wavelengths by the different molecules present in a test sample. Finally, the detector which is a liquid-nitrogen cooled MCT (Mercury-Cadmium-Telluride) detector detects the intensity of the IR beam. Then the detected signal is digitized and Fourier transformed by the computer to obtain the IR spectrum of the sample gas. The main part of the spectrometer is the interferometer. Figure 3.4 (a) is showing a Michelson type plane mirror interferometer in which only one sliding mirror is present. The generated interferogram by this sliding get converted by a Fourier transformer. The wavelength of the absorption relies on the force constants of the bonds, geometry of atoms and the relative masses of the atoms. This result in vibrations of the chemical groups on the material surface and give rise to closed packed absorption bands that are expressed in terms of transmittance (T) or absorbance (A). The specification of the instrument that is used throughout the proposed work is JASCO INC 410, Japan, in a range of $400\text{--}4000\text{ cm}^{-1}$.

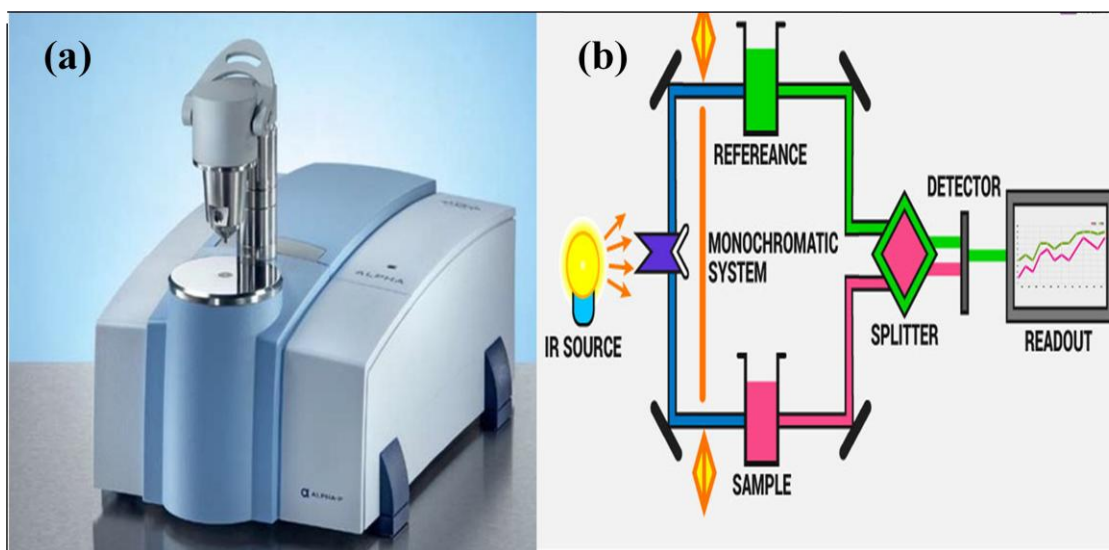


Figure 3.4: (a) A FTIR instrument and (b) Schematic representation of FTIR.^{20, 21}

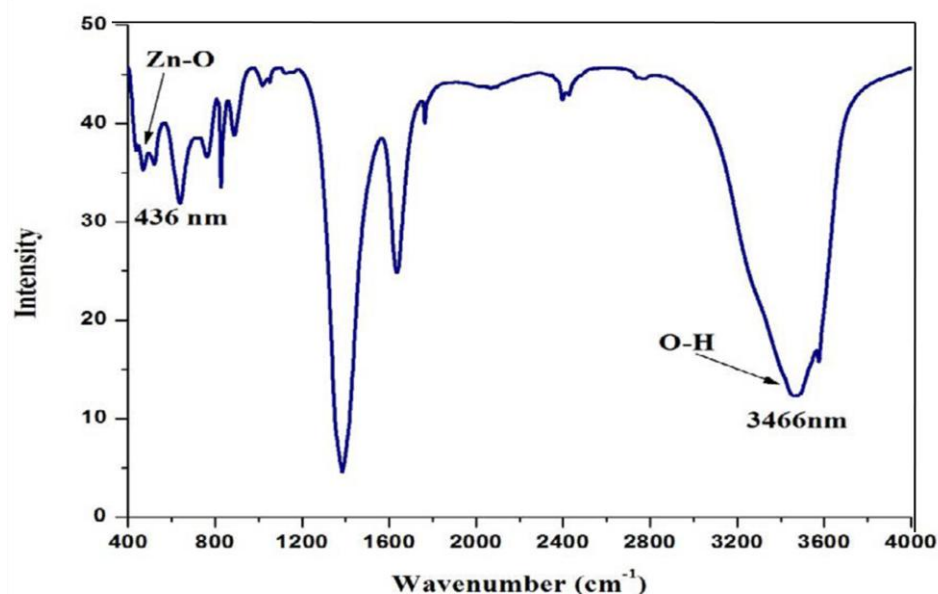


Figure 3.5: FTIR spectrum of pure ZnO nanoparticles.²²

Figure 3.5 represents a FTIR spectrum of zinc oxide nanoparticles with a characteristic peak at 436 nm.

3.3.1.3. Thermogravimetric Analysis (TGA)

Thermogravimetric analysis is the analytical technique in which the mass of a sample is monitored against time and temperature. The widely accepted definition of thermogravimetry is, “It is a technique whereby the weight of a substance, in an environment heated or cooled at a controlled rate, is recorded as a function of time or temperature.” This analysis is carried out for the following purposes:

- (i) To observe the weight loss, weight gains that occurs because of decomposition and oxidation of the sample.
- (ii) To get the thermal stability of the material at a higher temperature.
- (iii) To determine constituents of the material.

Generally, there are three types of thermogravimetric analysis, (a) Quasistatic Thermogravimetry, (b) Dynamic Thermogravimetry, and (c) Isothermal or Static Thermogravimetry. In quasistatic thermogravimetry, the sample is heated with a constant weight with gradual rise in temperature. In the dynamic thermogravimetry, heating is done with a constant rate. Lastly, in the isothermal or static thermogravimetry, weight of sample is observed

Chapter 3: Experimental techniques

with respect to time at a constant temperature.¹³ For TG analysis, the sample is placed in a small pan, connected to microbalance and heated for a specific time in a controlled manner. To avoid the oxidation of sample, an inert gas like nitrogen is released in the balance. The obtained results are presented in the form of graph plot of weight change vs. temperature or time. Thermogravimetric analysis of materials performed throughout the proposed work which is done on instrument PerkinElmer STA-5000 model of TA Instruments Inc., USA. Figure 3.6 (a) shows a typical thermogravimetric analyzer and figure 3.6 (b) shows a schematic representation of thermogravimetric analysis, while figure 3.7 shows a TGA curve of zinc oxide nanoparticles, in which horizontal pattern shows the absence of weight loss and curved region represents weight loss.

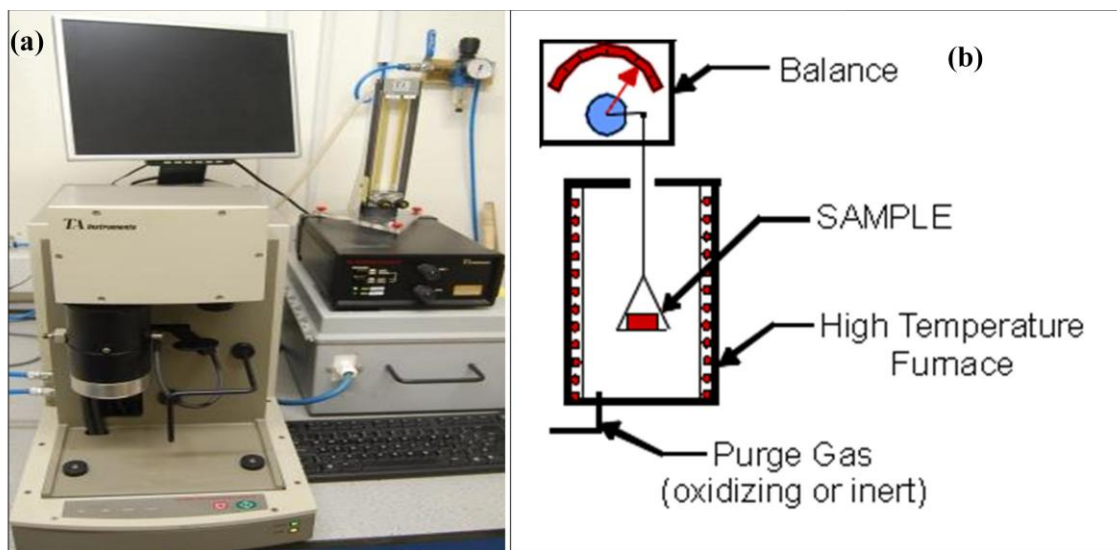


Figure 3.6: (a) Typical TG instrument and (b) Schematic representation of TGA.²³

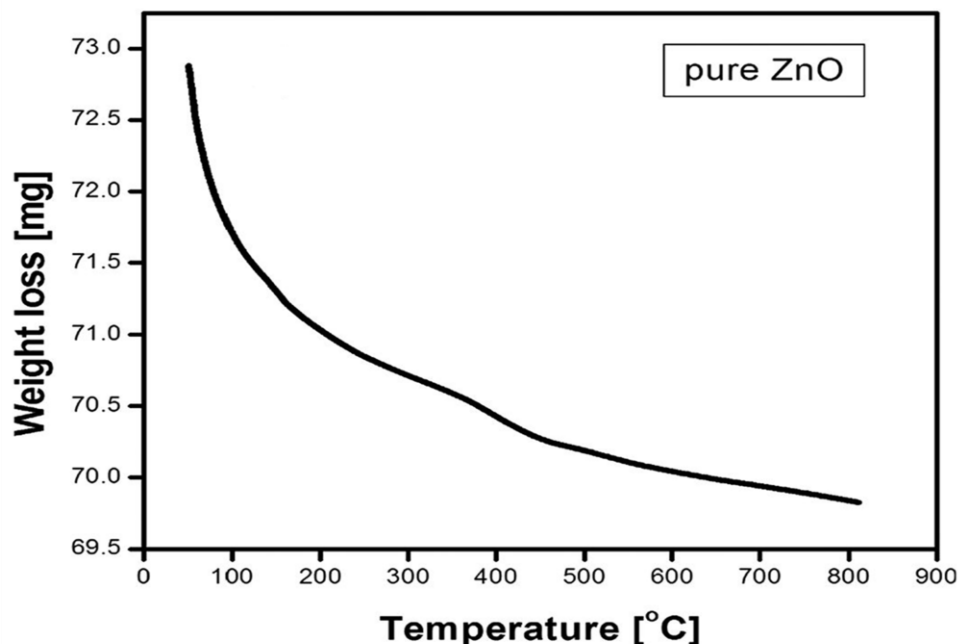


Figure 3.7: TGA curve of pure ZnO nanoparticle.²⁴

3.3.1.4. Differential Scanning Calorimetry (DSC)

Differential scanning calorimetry is a thermoanalytical analysis in which the difference in the quantity of heat needed to increase or decrease the temperature of a sample and reference is measured as a function of temperature. Sample and reference are kept at nearly the same temperature throughout the experiment. The calorimetry detects the changes in phase transitions. Different biochemical reactions can be studied by using DSC, where a single molecule gets transformed into another form. Thermal transition temperatures (T_t : melting points) of the samples can be also determined in solution, solid, or mixed phases such as suspensions. In DSC analysis, energy is supplied to a sample cell and reference cell. The temperature of both cells is increased simultaneously over time. The difference in the given energy needed to match the temperature of the sample to that of the reference sample will be the amount of excess heat absorbed or released by the molecule in the sample. Due to the presence of a test molecule, more amount of energy is needed to maintain the sample to the same temperature as the reference. So, the concept of heat excess displays into the picture. Factors that play a major role in the folding and stability of biomolecules can be investigated by DSC. Changes in the C_p reflect the disruption of the forces stabilizing the original protein structure.²⁵ The analysis of DSC is performed by the data curve of heat flux vs. temperature or time. The data curve detects the

Chapter 3: Experimental techniques

enthalpies of transitions. These calculations are done by combining the peak corresponding to the transition. The enthalpy of transition can be determined by the following equation,

$$\Delta H = KA \dots\dots\dots(3.3)$$

Where,

ΔH = enthalpy of transition

K = calorimetric constant

A = area under the curve

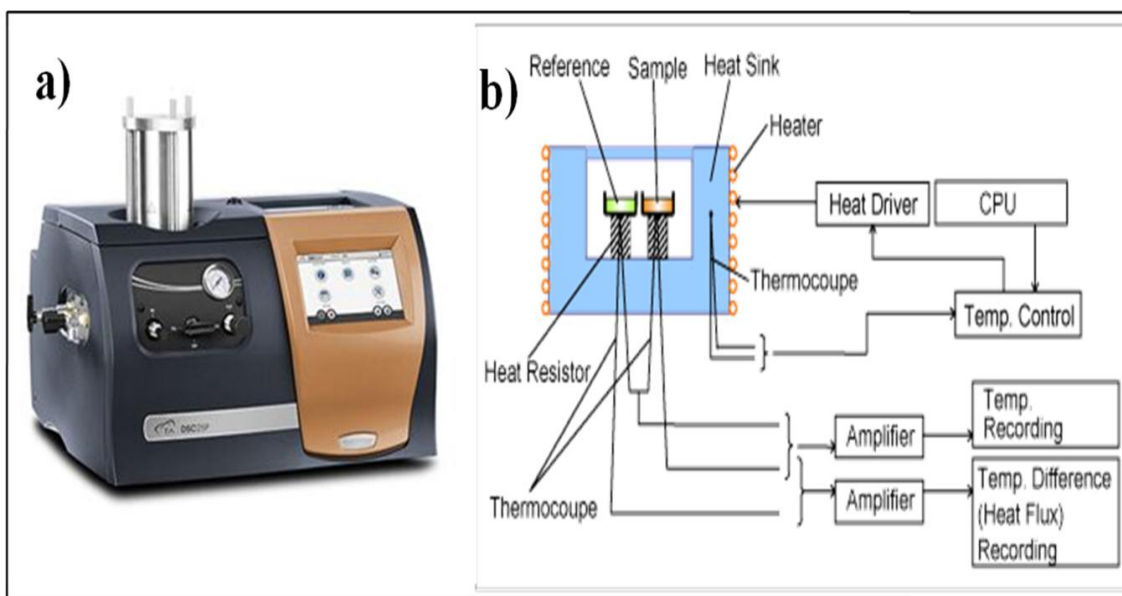


Figure 3.8: (a) A typical DSC instrument,²⁶(b) A block diagram of DSC working.²⁷

The specification of the DSC instrument used throughout the proposed work is Model Q10 DSC, TA Instruments, and New Castle, DE, USA. A typical DSC instrument and block diagram is represented in figure 3.8(b).

3.3.1.5. Ultra violet- Visible (UV-Vis) spectroscopy

UV-Vis spectroscopy is also termed as absorption spectroscopy or reflectance spectroscopy in the UV-Vis spectral region. UV-Vis spectroscopy is mainly used for the quantitative detection of different analytes in the field of analytical chemistry, such as highly conjugated organic compounds, transition metal ions, and biological macromolecules. Absorption spectroscopy uses electromagnetic radiations in a range of 190nm to 800nm and further divided into the ultraviolet (190-400nm) and visible (400-800nm) regions.

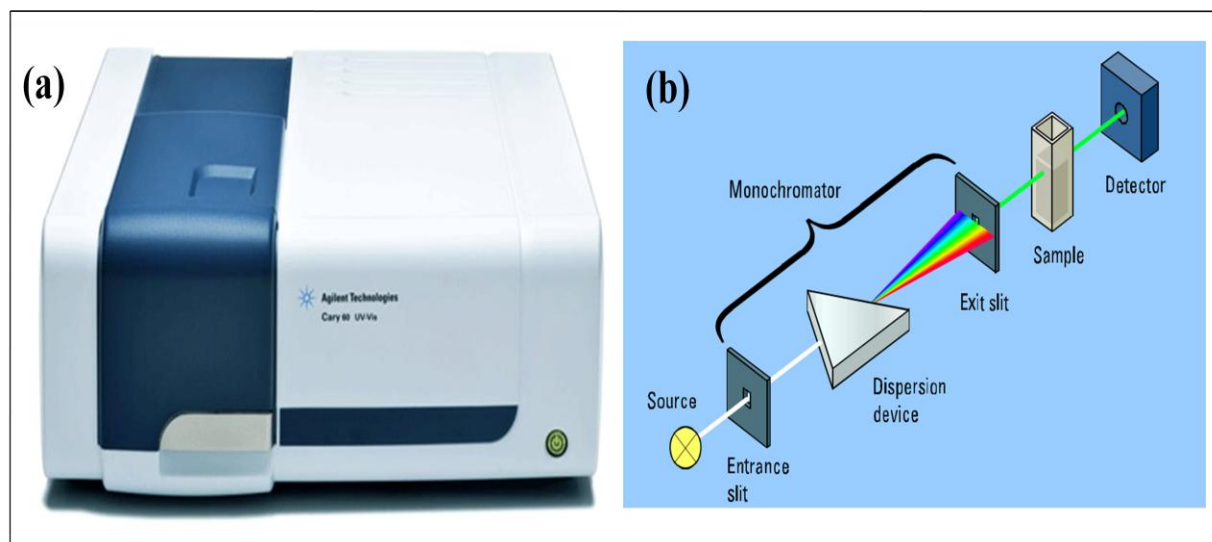


Figure 3.9: (a) A typical Ultra violet- Visible (UV-Vis) spectroscopy instrument, (b) Schematic representation of UV-Vis spectroscopy.²⁸

Light is a form of energy and when it is absorbed by the matter causes the energy of the molecule to rise. The potential energy of a molecule is given by equation 3.3.

$$E = h\nu, \nu = c/\lambda \dots \dots \dots (3.3)$$

Where,

E = energy of a photon, h = Planck's constant, ν = frequency (of associated wave), λ = wavelength, c = speed of light.

The internal energy of the molecule depends upon its electronic, Vibrational and rotational energies. The algebraic form of these statements follows,

$$\Delta E_{\text{total}} = \Delta E_{\text{elec}} + \Delta E_{\text{vib}} + \Delta E_{\text{rot}} \dots \dots \dots (3.4)$$

Where, ΔE_{elec} , ΔE_{vib} , and ΔE_{rot} are the changes in electronic, vibrational and rotational energy respectively. Photons of UV and visible light have enough energy that causes the transitions between the different electronic energy levels. The amount of energy required to move an electron from a lower energy level to a higher energy level is the wavelength of light absorbed. The basic principle of the UV-Vis spectroscopy is based upon Beer-Lambert law.

$$I = I_0 \times 10^{-\epsilon c l} \dots \dots \dots (3.5)$$

Where ϵ is the molar absorptivity or molar extinction coefficient, and l is the path length. Putting this equation together with that connecting absorbance and light intensity gives the expression equation 3.6:

$$A = c \times \epsilon \times l \dots\dots\dots (3.6)$$

where, A is measured absorbance and c is the concentration of the analytes.²⁹

The specification of UV-visible (UV-vis) spectroscopy instrument used throughout the proposed work is Agilent Technologies Cary 60 UV-vis with the wavelength range of 200-600nm. A typical UV spectrum of pure ZnO nanoparticles is shown in figure3.10. It shows the absorption peak in a range of 360-380nm.³⁰

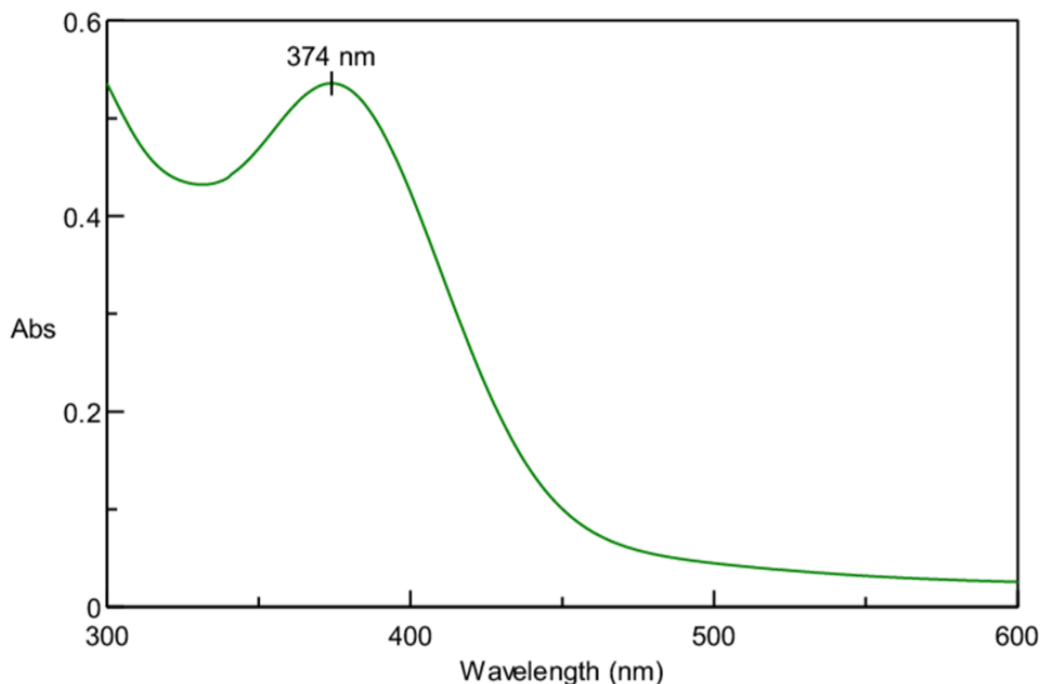


Figure 3.10: UV-Vis spectrum of pure ZnO nanoparticle.³⁰

3.3.2 Elemental analysis

3.3.2.1 Energy Dispersive X-ray spectroscopy (EDX)

Energy dispersive X-ray spectroscopy (EDX) is a standard method used to identify and quantify elemental compositions in a very small amount of sample material (even a few cubic micrometers). This method is employed with conjugation of a scanning electron microscope (SEM). In properly equipped SEM, the electron beam causes the excitation of the surface atoms that emits a specific wavelength of X-rays that are characteristic of the atomic structure of the elements. Appropriate elements are assigned, gives the composition of the atoms on the sample surface. Incident X-ray hits the detector. This results in the formation of a charge pulse that gets converted into a voltage which is quantified. The mechanism of EDX is represented in

figure 3.11(a) and the EDX spectrum of ZnO is shown in figure 3.11(b). The specification of the instrument used throughout the proposed work is JSM-6701F, JOEL, Japan.

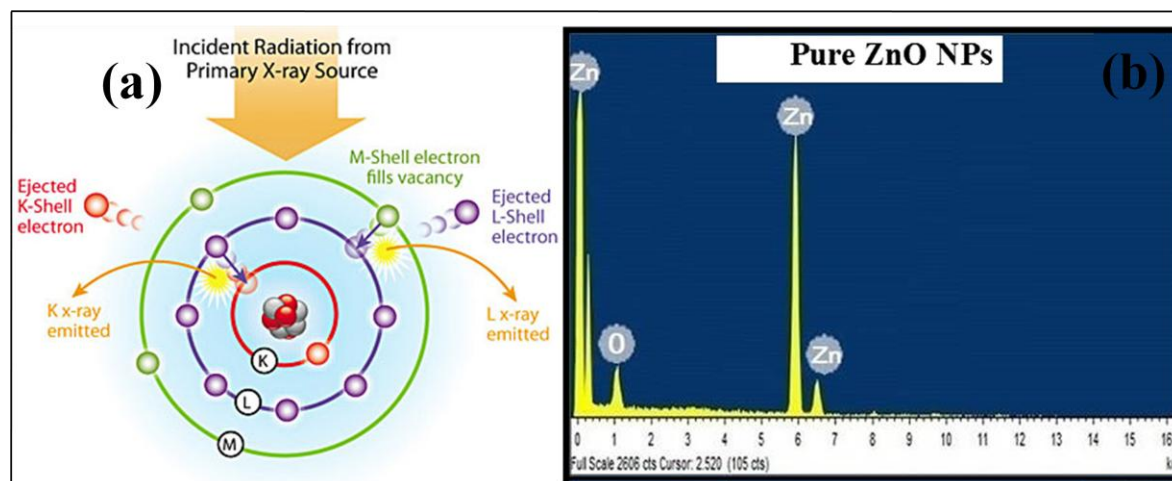


Figure 3.11:(a) Schematic representation of EDX,³⁰ (b) EDX spectra of pure ZnO nanoparticles.³¹

3.3.3 Morphological analysis

3.3.3.1 Scanning Electron Microscopy (SEM)

Scanning Electron Microscope is employed to study the surface which gives better resolution and depth of field. The interaction between the electron beam and atom present in the sample causes inelastic and elastic scattering. The elastic scattering emits high energy electrons known as back scattered electrons while those emitted by elastic scattering are termed as secondary electrons. When the beam scans the sample's surface, the interaction between the sample and electron beam generates variety of electron signals at or near the specimen surface. These signals get collected, processed, and translated in the form of pixels on a monitor and produce a three-dimensional image of the specimen's surface topography. Excitation of secondary electrons with low-energy on the sample's surface is the most common signal detected. The lower surface of specimen emits high-energy backscattered electrons and X-rays that provide information of specimen composition.³² The schematic representation of SEM is shown in figure 3.12 (a) and figures 3.12 (b) display SEM of ZnO nanoparticles. The details of the instrument in the present work are Micro Analysis System and Model Phoenix, Cambridge, England, U.K.

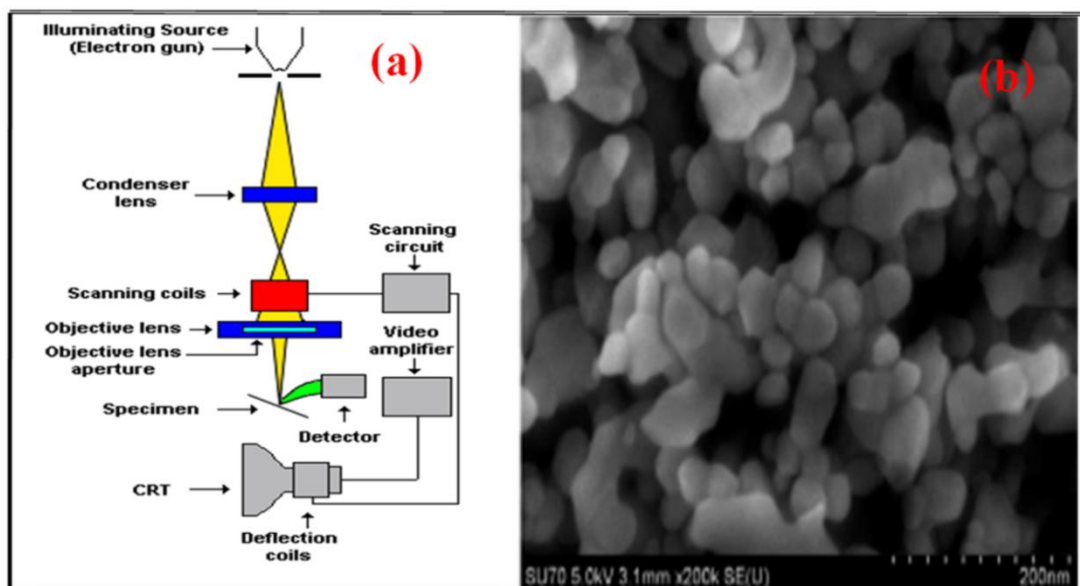


Figure 3.12: (a) Ray diagram of SEM³² (b) SEM image of ZnO nanoparticles.³³

3.3.3.2. Transmission Electron Microscopy (TEM)

Transmission Electron Microscopy (TEM) is a very powerful technique of characterization mostly used for measuring particle size, shape, size distribution, and morphology of the compound. The real space image of atomic distribution in nanostructures can be obtained. TEM analysis provides detailed information at atomic resolution and lattice images at a spatial resolution of 1 nm or less. It consists of an imaging system of the objective lens and one or more projector lens. Objective lenses provide detailed information at different degrees of resolution. The initial image of the illuminated part of the specimen in a plane is formed by the objective lens which is further enlarged by the projector lenses. The projector lens projects the final magnified image on the screen. In TEM, electrons of high power have used that pass from the object. Initially the electron beam enters through the electromagnetic condenser lens and beam gets concentrated on the sample. Some amount of electrons pass through object while other hit molecules in sample and get scattered. This beam then passes through an objective lens, projector lens and on fluorescent screen where final image get displayed. The image provides interior view of the object as electron beam passes entirely through the object. The ray diagram of TEM instrument is represented in figure 3.13 (a). For the analysis purpose, the sample should

Chapter 3: Experimental techniques

not be extremely thick and should be in the range of 0.1 to 1.0 μm . Preparation of the sample is the key step in the analysis. The standard procedure for the preparation of sample includes spreading of specimen in the solvents like water to form a colloidal solution. From this solution only one drop is kept on a conducting copper or silver grid (sq. size is $\sim 1\mu\text{m}$) and allowed to dry. This dried grid is used for the analysis of the specimen. The typical TEM image of ZnO NPs is shown in figure 3.13 (b).

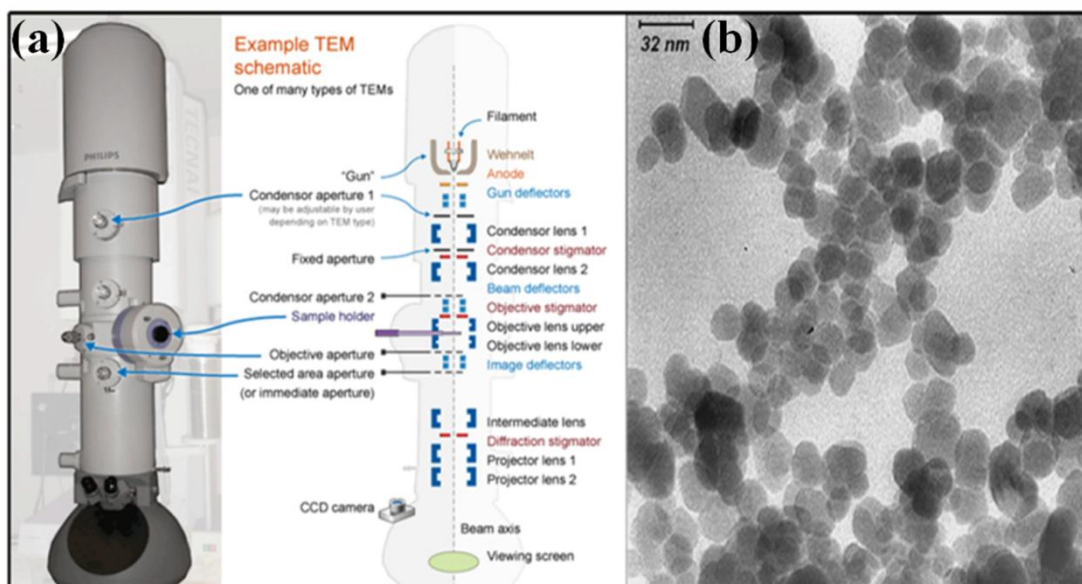


Figure 3.13: (a) Ray diagram of TEM³⁴ and (b) TEM image of ZnO nanoparticles.³⁵

3.3.4 Mechanical Properties

Forces exerted on the fibers may cause in the permanent change in structure or failure. Therefore there is need to detect the mechanical properties of single nanofibers. Universal testing machine (UTM) is used to study the physical characteristics of materials like polymers or metallic films deposited onto polymeric substrates. The mechanical testing systems are available commercially to analyze smaller (10 μm in diameter) fibers. In the working principle, UTM works by the hydraulic transmission of load from the test sample to a separately housed load indicator. This setup is convenient as it avoids transmission of load through knife edges, which are easy to wear and damage because of shock on rupture of test samples. The load is put into ram which is hydrostatically lubricated and main cylinder pressure is transmitted to cylinder of

Chapter 3: Experimental techniques

pendulum dynamometer system housed in the control panel. The cylinder is self-lubricating design. Proper gripping and proper alignment of specimen is important. Because of small size of specimen conventional mechanical grips are not convenient for gripping the two ends of the fiber. Young's modulus or modulus of elasticity quantifies the stiffness of material. The dynamic mechanical analyzer is shown in figure 3.14. In the present thesis, mechanical properties are tested on dynamic mechanical analyzer (RSA3, TA Instruments, USA).



Figure 3.14: Dynamic mechanical analyzer.³⁶

3.3.5. Biological Characterization

3.3.5.1. Biocompatibility

In this study, the compatibility of the material with the biological system is tested. This study provides information about the interaction of materials with the human body and their harmful physiological effects.³⁷ In the detailed study of nanocomposites to test biocompatibility is an important area of research. In the present thesis, this is carried out by studying hemocompatibility and cytocompatibility or cytotoxicity.

3.3.5.1.1. Cytocompatibility study

Chapter 3: Experimental techniques

Cytotoxicity is one of the most important indicators for biological evaluation in vitro studies. The development of nanotechnology has led to increased research on the toxic effects of nanomaterials on human health and the environment. In this regard, the detailed investigation of nanoparticles toxicity has become an important aspect of research. Among commercially available nanoparticles, ZnO is the most used, mainly due to their antibacterial activity. For safe in vivo application of ZnO NPs, the biocompatibility study is crucial. The use of appropriate assay for investigation of biocompatibility is important because nanoparticles can become redox active by adsorbing dyes. If results indicate only minimal or neutral effects in the used concentrations, then samples are further tested in vivo on animals that are closely related to the human model. If that is safe, then the product can be considered for FDA approval and for first human trials. Different assays are used to investigate biocompatibility. Different *in-vitro* toxicity assays are used for toxicity studies on mammalian cell lines and explained briefly in table 3.1. The use of suitable assay is important for the assessment of nanomaterials toxicity. In the proposed work, MTT assay was employed to determine the cytotoxicity of ZnO nanoparticles to mammalian cell lines (L929). In vitro assays are the earliest and simplest techniques designed for biocompatibility evaluation of the materials. In the MTT assay, the reduction of tetrazolium salts is considered to examine cell proliferation. The yellow 3-(4, 5-dimethylthiazolyl-2)-5-diphenyltetrazolium bromide (tetrazolium MTT) gets reduced by metabolically active cells by the dehydrogenase enzymes, to liberate NADH and NADPH. In this reduction process, intracellular purple formazan get formed which can be solubilized and quantified spectrophotometrically. The MTT assay measures the cell proliferation rate. In the absence of cells, the MTT doesn't produce high background absorbance values.³⁸ The cell viability can be determined by the using following equation,

$$\text{Cell viability} = A_{\text{treated}} / A_{\text{control}} \times 100 \dots \dots \dots (3.6)$$

Where, A_{treated} and A_{control} are the test sample and control sample respectively.

Chapter 3: Experimental techniques

Table 3.1: List of cytotoxicity assays commonly used to detect toxicity of ZnO NPs³⁹

Cytotoxicity assays based on different principles	Examples of assays
Proliferation assay (It measures cellular metabolism by assessing metabolically active cells)	MTT (3-(4,5-dimethylthiazol-2-yl)-2,5-diphenyltetrazolium bromide Assay
Apoptosis assay (It detects generated excessive free radicals due to cell apoptosis and DNA damage)	DNA Fragmentation Terminal deoxynucleotidyl Transferase dUTP Nick End-Labeling assay (TUNEL), Cytochrome c release assay
Necrosis assay (Necrosis is measured by the integrity of membrane and commonly used to determine the viability of the cells)	Neutral Red assay, Tryptan blue assay
Oxidative stress assay (measures ROS and RNS i.e. reactive nitrogen species)	lipid peroxidation C11-BIODIPY assay and TBA assay for malondialdehyde

3.3.5.1.2. Hemocompatibility

To understand the biocompatibility of nanoparticles, its exact interaction with the biological system should be revealed. Different factors such as size, shape, composition, and route of administration of nanoparticles confirm the fate of the nanoparticles. Also, their interference and unwanted effects on the host system decide their biocompatibility. Varieties of assays can be employed to investigate the hemocompatibility such as erythrocyte composition (hemolysis and hemagglutination), thrombogenicity, cytokine assays, complement activation, and phagocytosis. In proposed work, the percentage of hemolysis was calculated.⁴⁰

3.3.5.2. Swelling behavior

Swelling behavior of the material results in the increase of volume of material due to the absorption of a solvent, mostly in the case of polymers. It determines the water uptake capacity of the material. In this method, the prepared microfibers are dipped in phosphate buffer saline (PBS) solution at pH 7.4 at room temperature till saturation and swelling ratio of microfibers can be calculated by measuring the weight of swollen films divided by the weight of completely dried films. This water uptake capacity is important for wound dressing application, as this measures the absorption capacity of wound exudates. The swelling ratio can be calculated by using the formula given in equation (3.7),

$$\text{Degree of swelling} = [(W_t - W_d)/W_d] \times 100 \dots\dots\dots(3.7)$$

Where, W_s is the weight of the swollen microfiber sample, W_d is the dried weight of the sample dipped in the buffer medium, measured by drying microfiber in an oven at 40^0C for 10 min to obtain constant weight. ⁴¹

3.3.5.3 Antibacterial activity

In regard to the attractive antimicrobial properties of ZnO nanoparticles, it is important to discuss different techniques used to screen antibacterial activities. Varieties of methods are available to evaluate or screen the in vitro antimicrobial activity of antibacterial agents or other substances. These are listed below,

- Agar well diffusion method
- Agar disc diffusion method
- Shake flask method

3.3.5.3.1. Agar well diffusion method

In the agar well diffusion method, the agar plates are inoculated by a volume of bacterial inoculum over the whole plate. Then a hole of the diameter of about 6-8 mm is made by using a sterile cork borer or tip and about 80-100 μ l volume of ZnO nanocomposites are introduced into the well with the help of sterile micropipette. Then, agar plates are incubated in the incubator under suitable conditions as per test organisms. ZnO NPs diffuse in agar plate and inhibits the growth of microbial strain and the zone of inhibition is measured. Agar well diffusion method is

Chapter 3: Experimental techniques

presented in figure3.15. In the present work, we have used agar well diffusion method and discussed accordingly in detail in respective chapters.

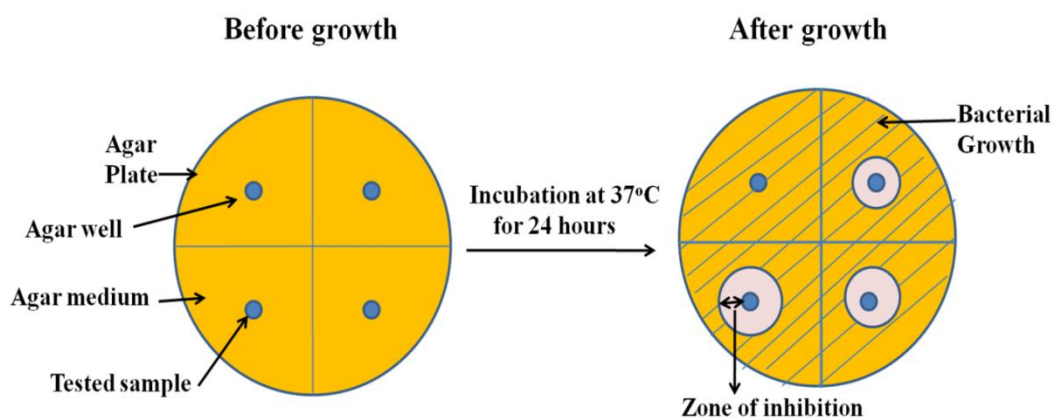


Figure 3.15: Schematic representation of agar well diffusion method

3.3.5.3.2. Agar disc diffusion method

The disc diffusion method is simple, easy, and widely used in the study of antibacterial activity. In this method, test organisms are spread over the surface of the nutrient agar medium and then the discs of antibacterial agents are placed on the surface of the sterile nutrient agar medium plate. Tested samples are kept in the refrigerator for 10 minutes.

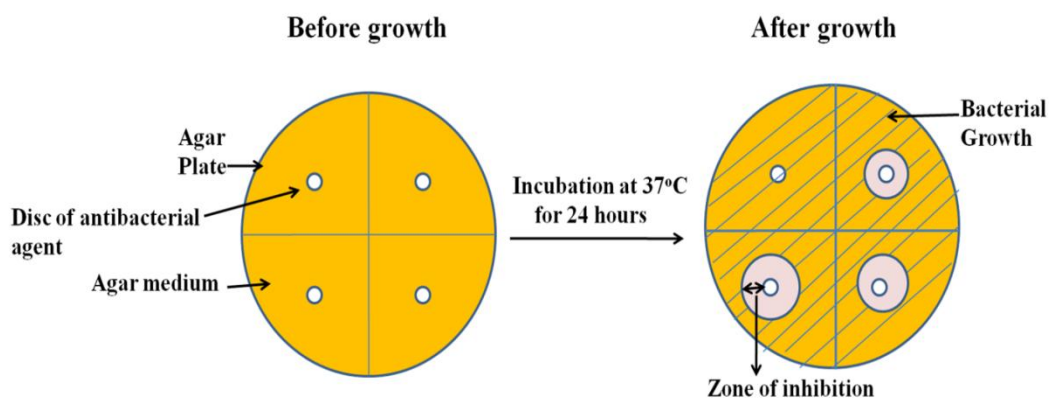


Figure 3.16: Schematic diagram of agar disc diffusion method.

Chapter 3: Experimental techniques

After incubation of plate at 37°C for 24 hours, the zones of inhibition around each disc are measured by using the millimeter scale. The schematic representation of this method is given in figure 3.16.

3.3.5.3.3. Minimum Inhibitory Concentration

Minimum inhibitory concentration (MIC) can be defined as the least concentration of antibacterial agents that inhibit the visible growth of the bacteria. The MIC of the antibacterial agents can be performed by the two different methods listed below,

- Agar dilution method
- Broth dilution method

In the agar dilution method, a known number of bacterial cell suspension is inoculated directly onto the nutrient agar plates with different concentrations of antibacterial agents. The method is mostly used for antibiotics available in ample amount. This method determines the large number of bacterial species at a time.

In the broth dilution method, the liquid medium is used for the determination of MIC. In this method, the liquid growth medium is containing increasing concentration of antibacterial agents. The microdilution is carried out in the microtiter plates by using < 500 µl per well. The appearance of the samples shows the growth of the organisms, after the incubation period. Both methods evaluate the least concentration of antibacterial agent that inhibits the growth of bacteria.⁴²

In the present work antibacterial activity is tested by agar well diffusion method. The MIC was done by the broth dilution method.

3.3.5.4. Antibiofilm activity

Different methods like tube method, Congo red agar method, microtiter plate assay, plate counting of biofilm-embedded bacteria, PCR, mass spectrometry, confocal laser scanning microscopy (CLSM) etc are available for the identification of biofilm by microorganisms and antibiofilm activity of compounds. Investigation of antimicrobial activity of agents against biofilm production is most commonly performed by microtiter plate assay. The standard protocol for this assay is described as follows: Bacteria are inoculated in the sterile tryptic soy broth and incubated for 24 h at 37°C. 200µl of medium with the sample is inoculated with 10µl of bacterial

Chapter 3: Experimental techniques

suspension and incubated for 24 h at 37°C. After incubation, the wells are drained, washed with phosphate buffer saline, fixed with cold methanol and then stained with 1% crystal violet for 30 min. Biofilm formed in the well is resuspended in 30% of acetic acid. The intensity of suspension is measured at 570 nm by microtiter plate reader and the percentage of biofilm inhibition is calculated by using the equation (3.8) given below.

$$\text{Percentage of biofilm inhibition} = \frac{\text{OD of control} - \text{OD of test}}{\text{OD of control}} \times 100 \dots (3.8)^{43}$$

In the present thesis, 96 well microtiter plate assay is used with slight modifications and discussed in detail in respective chapters.

References

- 1 E. Bacaksiz, M. Parlak, M. Tomakin, A. Özçelik, M. Karakiz and M. Altunbaş, *J. Alloys Compd.*, 2008, **466**, 447–450.
- 2 J. Wang, J. Cao, B. Fang, P. Lu, S. Deng and H. Wang, *Mater. Lett.*, 2005, **59**, 1405–1408.
- 3 A. Anžlovar, K. Kogej, Z. Crnjak Orel and M. Žigon, *Express Polym. Lett.*, 2011, **5**, 604–619.
- 4 N. Salah, S. S. Habib, Z. H. Khan, A. Memic, A. Azam, E. Alarfaj, N. Zahed and S. Al-Hamedi, *Int. J. Nanomedicine*, 2011, **6**, 863–869.
- 5 N. Z.- A, T. Antibacterial and X. Wang, *Environ. Toxicol. Pharmacol.*, , DOI:10.1016/j.etap.2015.01.015.
- 6 W. Ao, J. Li, H. Yang, X. Zeng and X. Ma, *Powder Technol.*, 2006, **168**, 148–151.
- 7 A. Kołodziejczak-radzimska, E. Markiewicz and T. Jesionowski, , DOI:10.1155/2012/656353.
- 8 O. U. Native and M. Chitosans, *Materials (Basel)*, 2013, **6**, 4198–4212.
- 9 P. Rai, W. Kwak and Y. Yu, *Appl. Mater. Interfaces*, 2013, **5**, 3026–2023.
- 10 B. Bonthagarala, *Int. J. Pharm. Res. Bio-Science*, 2018, **6**, 170–177.
- 11 H. Agarwal, S. Venkat Kumar and S. Rajeshkumar, *Resour. Technol.*, 2017, **3**, 406–413.
- 12 N. Bhardwaj and S. C. Kundu, *Biotechnol. Adv.*, 2010, **28**, 325–347.
- 13 H.Kaur, *Instrumental method for chemical analysis*, Pragati publications, 2009.
- 14 A. A. Bunaciu, E. gabriela Udriștioiu and H. Y. Aboul-Enein, *Crit. Rev. Anal. Chem.*, 2015, **45**, 289–299.
- 15 <https://pubs.usgs.gov/of/2001/of01-041/html/docs/xrpd.htm>, .

- 16 [Http://www.rigaku.com](http://www.rigaku.com), .
- 17 C. Abinaya, M. Marikkannan, M. Manikandan, J. Mayandi, P. Suresh, V. Shanmugaiah, C. Ekstrum and J. M. Pearce, *Mater. Chem. Phys.*, 2016, **184**, 172–182.
- 18 Z. Bacsik, J. Mink and G. Keresztury, *Appl. Spectrosc. Rev.*, 2004, **39**, 295–363.
- 19 H. S. Kim, S. J. Lee, N. H. Kim, J. K. Yoon, H. K. Park and K. Kim, *Langmuir*, 2003, **19**, 6701–6710.
- 20 U. . Cullity, B. D, *Elements of X-ray diffractions, Third Edition*, 2001.
- 21 H. bruker. [com/products/infrarednear-infrared-and-raman-spectroscopy/ft-ir-routinespectrometers](http://www.bruker.com/products/infrarednear-infrared-and-raman-spectroscopy/ft-ir-routinespectrometers). [Alpha/overview.html](http://www.bruker.com/products/infrarednear-infrared-and-raman-spectroscopy/ft-ir-routinespectrometers), .
- 22 S. H. Khan, R. Suriyaprabha, B. Pathak and M. H. Fulekar, *Front. Nanosci. Nanotechnol.*, , DOI:10.15761/FNN.1000105.
- 23 .
https://www.lpdlabservices.co.uk/analytical_techniques/chemical_analysis/thermal_gravimetric_analysis.php, .
- 24 P. J. Lee, E. Saion, N. M. Al-hada and N. Soltani, *Metals (Basel)*, 2015, **5**, 2383–2392.
- 25 P. Gill, T. T. Moghadam and B. Ranjbar, *J. Biomol. Tech.*, 2010, **21**, 167–193.
- 26 <https://www.tainstruments.com/dsc-250/>, .
- 27 <https://www.hitachi-hightech.com/global/products/science/tech/ana/thermal/descriptions/dsc.html>, .
- 28 <https://www.agilent.com/en/products/uv-vis-uv-vis-nir/uv-vis-uv-vis-nir-systems/cary-60-uv-vis>, .
- 29 J. Q. Brown, K. Vishwanath, G. M. Palmer and N. Ramanujam, *Curr. Opin. Biotechnol.*, 2009, **20**, 119–131.

Chapter 3: Experimental techniques

- 30 B. N. Patil and T. C. Taranath, *Int. J. Mycobacteriology*, 2016, **5**, 197–204.
- 31 K. Pradeev raj, K. Sadaiyandi, A. Kennedy, S. Sagadevan, Z. Z. Chowdhury, M. R. Bin Johan, F. A. Aziz, R. F. Rafique, R. Thamiz Selvi and R. Rathina bala, *Nanoscale Res. Lett.*, , DOI:10.1186/s11671-018-2643-x.
- 32 D. B. W. and C. B. C. . (2009. Transmission Electron Microscopy”, 2nd edition, Springer, New York, *No Title*, 1985.
- 33 A. Kmita, E. Olejnik and T. Tokarski, , DOI:10.2478/amm-2013-0023.
- 34 [Http://www.ammrf.org.au/myscope/tem/introduction](http://www.ammrf.org.au/myscope/tem/introduction), .
- 35 R. Jalal, E. K. Goharshadi, M. Abareshi and M. Moosavi, *Mater. Chem. Phys.*, 2013, **121**, 198–201.
- 36 E. P. S. Tan and C. T. Lim, *Compos. Sci. Technol.* 66, 2006, **66**, 1102–1111.
- 37 B. Swetha, S. Mathew, B. V. S. Murthy, N. Shruthi and S. H. Bhandi, *Int. Dent. Med. J. Adv. Res. - Vol. 2015*, 2015, **1**, 1–6.
- 38 Ö. S. Aslantürk and S. Aslantürk, *Genotoxicity- A Predict. Risk to Our Actual World*, 1–18.
- 39 M. Omid, A. Fatehinya, M. Farahani, Z. Akbari, S. Shahmoradi, F. Yazdian, M. Tahriri, K. Moharamzadeh, L. Tayebi and D. Vashae, *7. Characterization of biomaterials*, Elsevier Ltd, 2017.
- 40 S. Agrawal, P. R. Patel and R. V. N. Gundloori, *ACS Omega*, 2019, **4**, 6301–6310.
- 41 Z. Xu, J. Li, H. Zhou, X. Jiang, C. Yang and F. Wang, *RSC Adv.*, 2016, **6**, 43626–43633.
- 42 A. J. O’Neill, I. Chopra, *Exp. Opin. invest. Drugs*, 2004, **13**, 1045–63.
- 43 P. P. Mahamuni, P. M. Patil, M. J. Dhanavade, M. V. Badiger, P. G. Shadija, A. C. Lokhande and R. A. Bohara, *Biochem. Biophys. Reports*, 2019, **17**, 71–80.

CHAPTER 4

Synthesis and characterization of zinc oxide nanoparticles by using polyol chemistry

SCI journal

Biochemistry and Biophysics Reports 17 (2019) 71–80



Contents lists available at ScienceDirect

Biochemistry and Biophysics Reports

journal homepage: www.elsevier.com/locate/bbrep



Synthesis and characterization of zinc oxide nanoparticles by using polyol chemistry for their antimicrobial and antibiofilm activity



Pranjali P. Mahamuni^a, Pooja M. Patil^a, Maruti J. Dhanavade^b, Manohar V. Badiger^c, Prem G. Shadija^a, Abhishek C. Lokhande^d, Raghvendra A. Bohara^{a,e,*}

^a Centre for Interdisciplinary Research, D.Y. Patil University, Kolhapur, India

^b Department of Microbiology, Shivaji University, Kolhapur, India

^c CSIR, National Chemical Laboratory, Pune, India

^d Department of Materials Science and Engineering, Chonnam National University, Gwangju, Republic of Korea

^e CURAM, Center for Research in Medical Devices, National University of Ireland Galway, Ireland

“Nanotechnology is manufacturing with atoms”

- William Powell

Chapter 4: Synthesis and characterization of zinc oxide nanoparticles by using polyol chemistry

4.1 Introduction

Nanomaterials exhibit unique properties like variations in size, shape and high surface area to volume ratio that plays a key role in antibacterial and antibiofilm applications due to improved physical, chemical, biological properties and functionality. Therefore, to synthesize nanomaterials with controlled morphology and their processing are involved in the first step in nanotechnology.¹ The use of simple, easy and effective methods for the synthesis of nanomaterials has become more important to control the size, shape and morphology of nanomaterials. The use of the chemical method for the synthesis allows the easy tailoring of synthesis parameters throughout the whole reaction process that results in the production of particles with defined size, dimension, composition and structure.²

The present chapter focuses on the facile polyol mediated synthesis and characterization studies of ZnO NPs. The ZnO NPs are synthesized by applying the following approaches, (i) regular synthesis in polyols, (ii) in the presence of sodium acetate and (iii) increasing reaction time. The synthesis method involves the reflux of zinc acetate dihydrate precursor in diethylene glycol (DEG) and triethylene glycol (TEG) in presence and absence of weak base sodium acetate for varied time reaction time. Further, these are characterized by X-ray diffraction (XRD), UV-visible spectroscopy (UV), thermogravimetric analysis (TGA), Fourier transform infrared spectroscopy (FTIR), field emission scanning electron microscopy (FESEM), transmission electron microscopy (TEM) and energy dispersive X-ray spectroscopy (EDX) technique.

4.2. Experimental

All chemicals used were of analytical grade and used without further purification. Zinc acetate dehydrate (CH_3CO_2)₂. 2H₂O, diethylene glycol (DEG) and triethylene glycol (TEG) from Loba fine chemicals, Mumbai, India. Double distilled water was used throughout the experiments.

4.2.1. Synthesis of ZnO NPs by using diethylene glycol and triethylene glycol

Chapter 4: Synthesis and characterization of zinc oxide nanoparticles by using polyol chemistry

ZnO NPs were synthesized by the reflux method.^{3,4} In brief, the precursor 0.1M $\text{CH}_3(\text{COO})_2 \cdot 2\text{H}_2\text{O}$ is added to diethylene glycol (DEG)/triethylene glycol (TEG) in a flat bottom flask and kept for reflux action at $180^\circ\text{C}/220^\circ\text{C}$ in the presence and absence of weak base sodium acetate(0.01M). DEG/TEG was used to assist the hydrolysis of zinc acetate. The reaction time was varied from 2 hours to 3 hours. Before the refluxing process, the solution was kept on the magnetic stirrer at 80°C for 1h. After completion of the reaction, white colloidal solution formed at the bottom of the flask. The samples were centrifuged at 8000 rpm for 15 minutes and washed with distilled water and ethanol for three times. Further it was dried at 80°C for overnight. Fig.4.1 shows the schematic representation of the synthesis of ZnO NPs by using different approaches by using a reflux instrument.

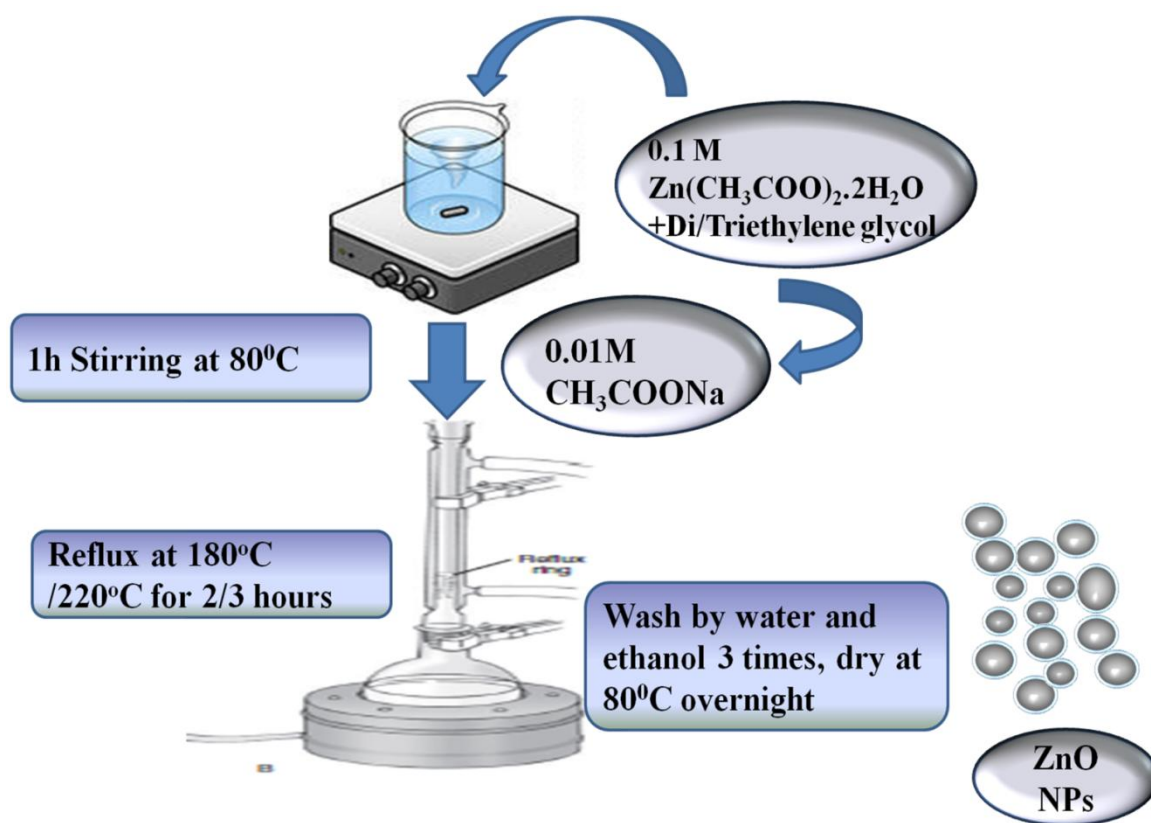
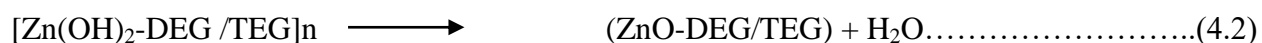


Figure 4.1: Schematic representation of DEG and TEG mediated synthesis of ZnO NPs.

Reaction mechanism of ZnO NPs:

Chapter 4: Synthesis and characterization of zinc oxide nanoparticles by using polyol chemistry

In this study, the reflux method was employed to synthesize ZnO NPs as mentioned above. The mechanism of the ZnO NPs formation can be proposed as follow,



Formation of ZnO NPs takes place in two steps, (i) hydrolysis reaction and, (ii) condensation reaction. The hydrolysis reaction requires water molecules in the reaction. The absence of water in the reaction leads into failure of next step that is condensation reaction. Firstly, the reaction between zinc acetate dehydrate and DEG/TEG leads to the formation of $\text{Zn}(\text{OH})_2$. Further its dehydration results into formation of ZnO NPs.⁵

Table4.1: Reaction conditions used for the synthesis of ZnO NPs.

Polyol used	$\text{Zn}(\text{CH}_3\text{COO})_2 \cdot 2\text{H}_2\text{O}$	CH_3COONa		Reaction time and temperature
DEG	0.1M	0.01M	All 8 samples were kept on the magnetic stirrer at 80°C for 1 h.	Refluxed for 2h at 180°C
		Not used		
		0.01M		Refluxed for 3h at 180°C
		Not used		
TEG	0.1M	0.01M		Refluxed for 2h at 220°C
		Not used		
		0.01M		Refluxed for 3h at 220°C
		Not used		

Chapter 4: Synthesis and characterization of zinc oxide nanoparticles by using polyol chemistry

The basic approach of use of sodium acetate is the addition of excess acetate ions that gives different morphology than particles synthesized in absence of sodium acetate. Further the prepared solutions are washed with distilled water and then ethanol three times. Then samples are dried overnight at 80⁰C (Table 4.1).

4.2.2. Characterization Studies

4.2.2.1. Structural analysis

The synthesized all ZnO NPs were characterized using X-ray diffraction (XRD) (Rigaku 600 Miniflex X-ray diffraction instrument) in the scanning range of 10⁰ -80⁰.

4.2.2.2. Spectroscopic analysis

The UV-visible absorption spectra of all synthesized ZnO NPs were recorded in the wavelength range of 200 nm to 600 nm using Agilent Technologies Cary 60 UV-Vis. For the detection of functional groups on the surface of the ZnO, Fourier transform infrared (FTIR) spectra of all prepared ZnO NPs were observed by using JASCO INC 410, Japan, in the range of 400-4000 cm⁻¹.

4.2.2.3. Morphological analysis

The surface morphology of all synthesized ZnO NPs was studied by field emission scanning electron microscopy (FESEM) and transmission electron microscopy (TEM).

4.2.2.4. Elemental analysis

Elemental analysis was performed by energy-dispersive X-ray (EDX) spectroscopy by using JSM-6701F, JOEL, Japan).

4.2.2.5. Thermal analysis

Thermal gravimetric analysis (TGA) was carried out to observe the thermal stability of all ZnO samples on the instrument PerkinElmer STA-5000. All samples were heated from 50-900⁰C at the rate of 10⁰C/min.

4.3. Results and Discussion

4.3.1. Structural analysis

4.3.1.1. X-ray diffraction

Figure 4.2 represents the XRD data of ZnO NPs. The ZnO NPs are used for the analysis of XRD. The XRD of all samples having 2 θ values are showing diffraction peaks at 31.72⁰ (100),

Chapter 4: Synthesis and characterization of zinc oxide nanoparticles by using polyol chemistry

34.39° (002), 36.23° (101) and 47.44° (102) correspond to JCPDS card No. 36-1451. These all diffraction peaks fit well with the hexagonal wurtzite structure of ZnO which proves the preparation of ZnO NPs. The absence of any other peaks of other phases shows that single phase wurtzite zinc oxide nanoparticles have been obtained. The intensity of peaks is sharp and narrow, confirming of high quality of the sample with good crystallinity and fine grain size. The crystallite sizes of ZnO NPs are calculated from FWHM of the most intense peak (reflection plane used for calculation is 101) by using the Debey Scherrer formula (equation 3.2).⁶ The crystallite size of ZnO NPs is in the range of 15-23nm. ZnO NPs prepared by refluxing DEG for 3 h showed the least crystallite size (~15nm) as compared with other ZnO NPs. The calculated crystallite size of ZnO NPs is given in table 4.2.

Table 4.2: Calculated crystallite size of ZnO NPs

ZnO samples	Crystallite size from XRD in nm
DEG 2h	~ 22 nm
DEG 2h with sodium acetate	~23nm
DEG 3 h	~15nm
DEG 3h without sodium acetate	~18nm
TEG 2h	~20nm
TEG 2h with sodium acetate	~21nm
TEG 3h	~18nm
TEG 3h without sodium acetate	~18nm

The crystallite sizes of ZnO NPs are calculated are consistent with the size calculated by FESEM and TEM analysis. The crystallite size of ZnO NPs synthesized in DEG and TEG increased with increase in the chain length of polyols. Also, the presence of weak base sodium acetate affected the crystallite size of the particle.⁷

Chapter 4: Synthesis and characterization of zinc oxide nanoparticles by using polyol chemistry

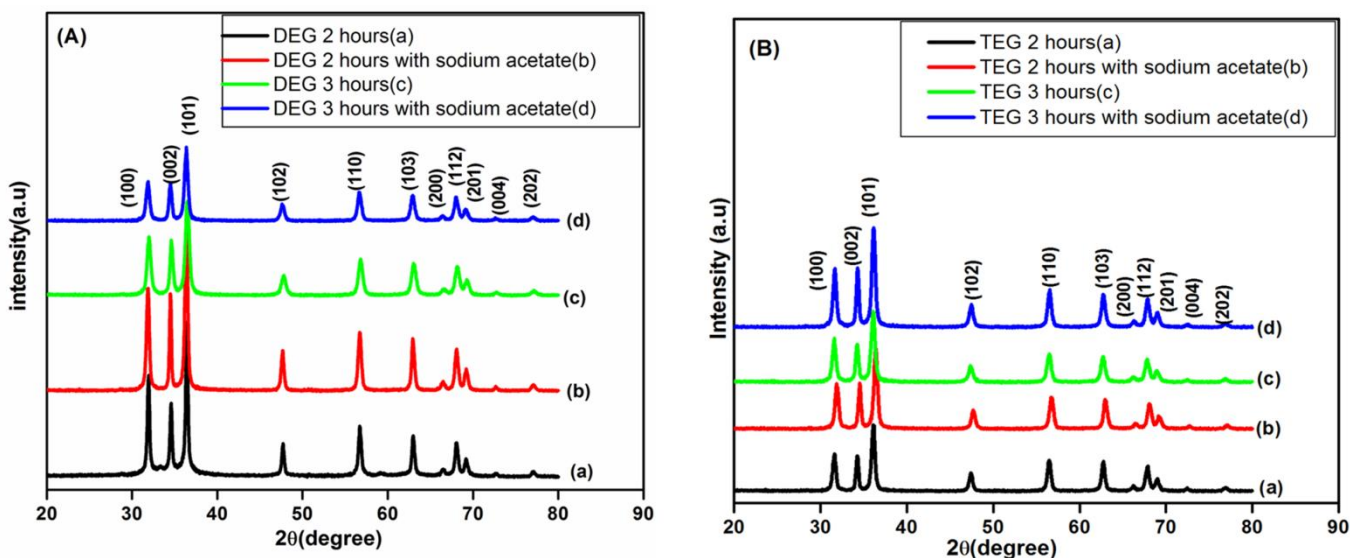


Figure 4.2: (A) XRDs of ZnO NPs synthesized in DEG 2h (a), DEG 2h with sodium acetate (b), DEG 3h (c), DEG 3h with sodium acetate (d), (B) TEG 2h (a), TEG 2h with sodium acetate (b), TEG 3h (c), TEG 3h with sodium acetate (d).

4.3.2. Spectroscopic analysis

4.3.2.1. UV-visible spectroscopy

The UV-vis spectroscopy study of all synthesized ZnO NPs is represented in figure 4.3. The absorption peaks are recorded in each spectrum in the range of 360-380 nm which is a characteristic band of pure ZnO. The absence of any other peak confirms the successful production of pure ZnO NPs.⁸ It is revealed that the intensity of absorption peak in the UV-visible spectrum depends upon the particle size of nanoparticles. With a decrease in particle size, the absorption peak shifts towards the lower range. Briefly, in the DEG and TEG mediated synthesis of ZnO NPs, DEG 2h sample showed an absorption peak at 366 nm while, DEG 2h sample with sodium acetate shows an absorption peak at 368 nm. In the same way, all other samples showed blue shift with decrease in particle size from which it can be concluded that the intensity of an absorbance peak shows a slight blue shift with a decrease in particle size. It can be suggested that, the results obtained by UV-Vis spectroscopy are in good agreement with the XRD results of all ZnO NPs particle size detection. Different factors like, type of polyols used, temperature and reaction time affect on the absorption peak.⁷

Chapter 4: Synthesis and characterization of zinc oxide nanoparticles by using polyol chemistry

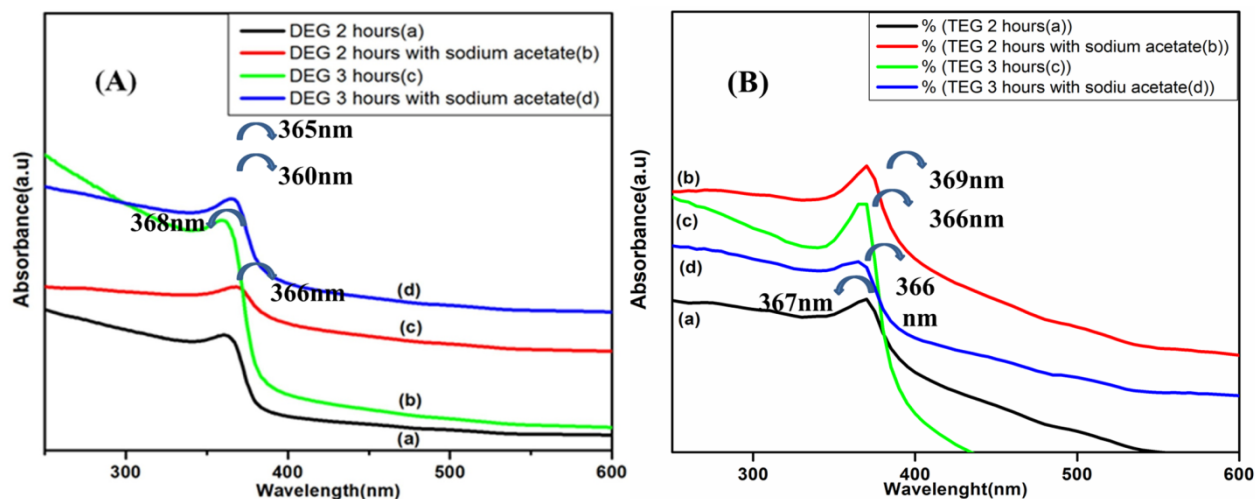
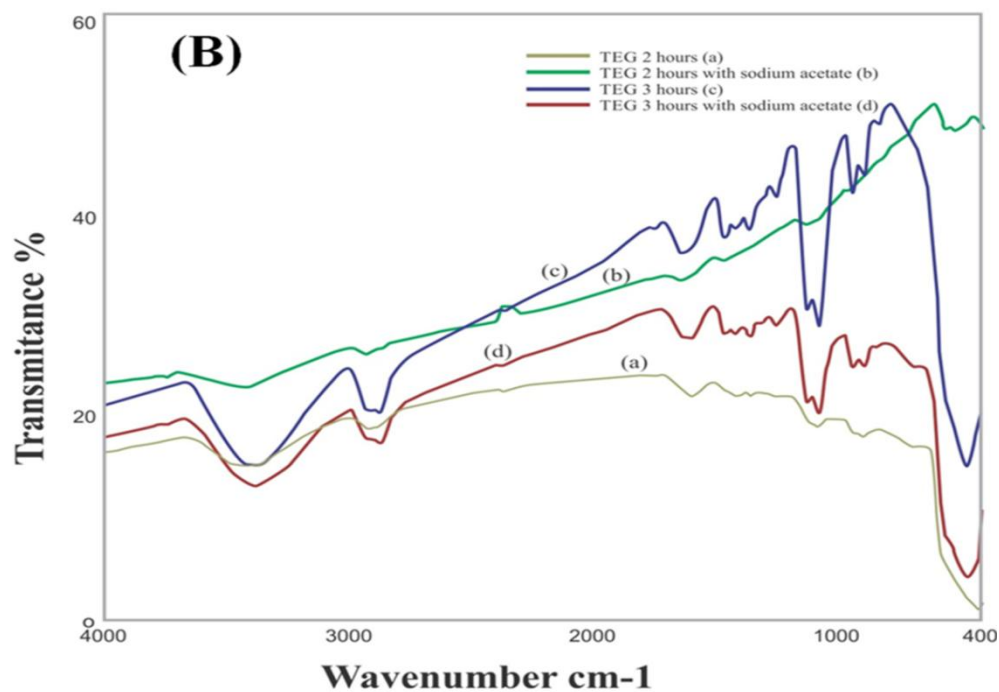
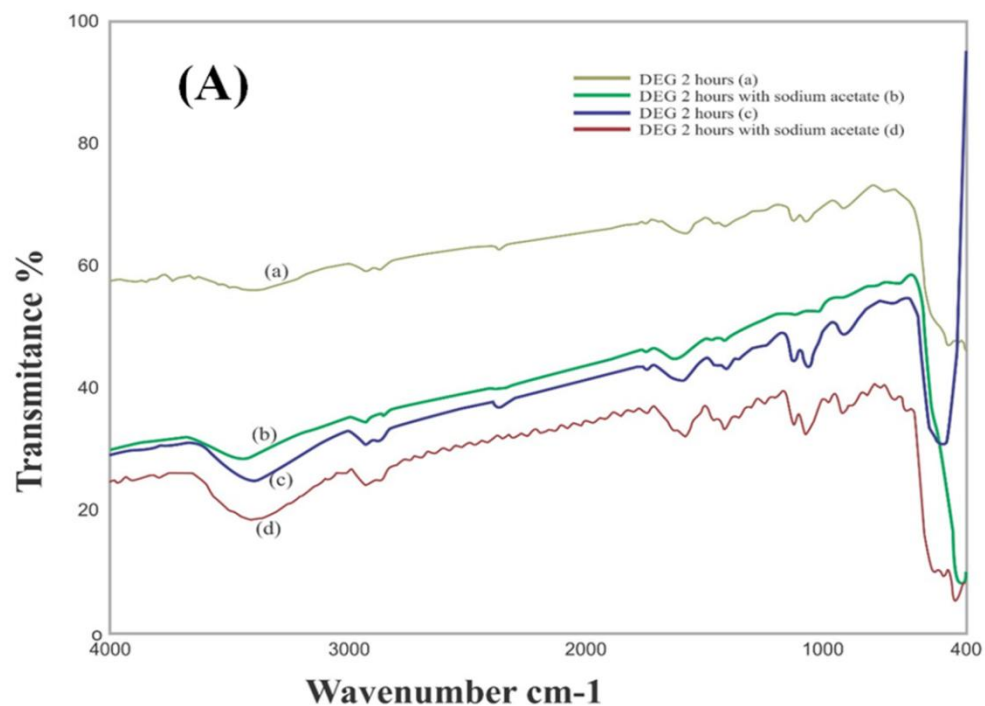


Figure 4.3: UV-visible spectroscopy of ZnO NPs synthesized in, (A) DEG 2h (a), DEG 2h with sodium acetate (b), DEG 3h (c), and DEG 3h with sodium acetate (d), and (B) TEG 2h (a), TEG 2h with sodium acetate (b), TEG 3h (c), and TEG 3h with sodium acetate (d).

4.3.2.2. Fourier Transform Infrared Spectroscopy

The FTIR analysis is done to confirm the functional groups present on the surface of ZnO NPs. Figure 4.4 (A) and (B) represents the FTIR spectra of DEG and TEG mediated synthesized ZnO NPs. The peak appearing at $\sim 3433\text{cm}^{-1}$ is assigned to stretching vibration of hydroxyl groups^{3,9} and peaks at $\sim 2922\text{cm}^{-1}$ are attributed to $-\text{CH}$ stretching showing the presence of $-\text{CH}_2$, $-\text{CH}_3$ groups.¹⁰ The peaks at around $\sim 1586\text{cm}^{-1}$ and 1412cm^{-1} are directed to symmetric and asymmetric $\text{C}=\text{O}$ stretching.¹¹ The peak at 1125cm^{-1} is attributed to $-\text{CH}$ deformation confirming $-\text{CH}_2$, $-\text{CH}_3$ bending. Because of interatomic vibrations, metal oxides generally show the absorption bands in the fingerprint region below 1000cm^{-1} .¹² In the infrared region, the peaks at around $415\text{--}480\text{cm}^{-1}$ corresponds to ZnO that shows the stretching vibration of Zn-O .¹³ This study indicated that, DEG or TEG molecules get adsorbed on the synthesized ZnO NPs. The difference in the particle size may lead to different wave numbers and frequencies are consistent to the reported literature.¹⁴ The results of the FTIR analysis are in good agreement with the results obtained from TGA analysis.

Chapter 4: Synthesis and characterization of zinc oxide nanoparticles by using polyol chemistry



Chapter 4: Synthesis and characterization of zinc oxide nanoparticles by using polyol chemistry

Figure 4.4: FTIR of ZnO NPs synthesized in, (A) DEG 2h (a), DEG 2h with sodium acetate (b), DEG 3h (c), DEG 3h with sodium acetate (d), (B) TEG 2h (a), TEG 2h with sodium acetate (b), TEG 3h (c), TEG 3h with sodium acetate (d).

Frequency Range (cm^{-1})	Functional groups
3433	-OH vibration
2922	Stretching of $-\text{CH}_2$, CH_3 groups
1586, 1412	Symmetric and asymmetric stretching of $\text{C}=\text{O}$
1125	-CH deformation
415-480	Stretching vibration of Zn-O

Table 4.3: FTIR analysis of ZnO NPs

4.3.3. Morphological analysis

4.3.3.1. Field Emission Scanning Electron Microscopy (FESEM) and Transmission Electron Microscopy (TEM)

Field emission scanning electron microscopy is used to study the surface morphology of the synthesized ZnO NPs. Surface morphology of all ZnO NPs are presented in figure 4.5. It is observed that the ZnO NPs obtained by refluxing diethylene glycol and triethylene glycol for 2h and 3h in the presence and absence of sodium acetate have uniform shape and size with different morphology. An images depict addition of sodium acetate, use of different polyol and change in the reflux time from 2h to 3h result in difference in morphology from oval to rod shape with average particle size of ~15-100 nm. FESEM and TEM analysis reports DEG refluxed for 3h in the absence of sodium acetate showed the least particle size of ~15 nm.

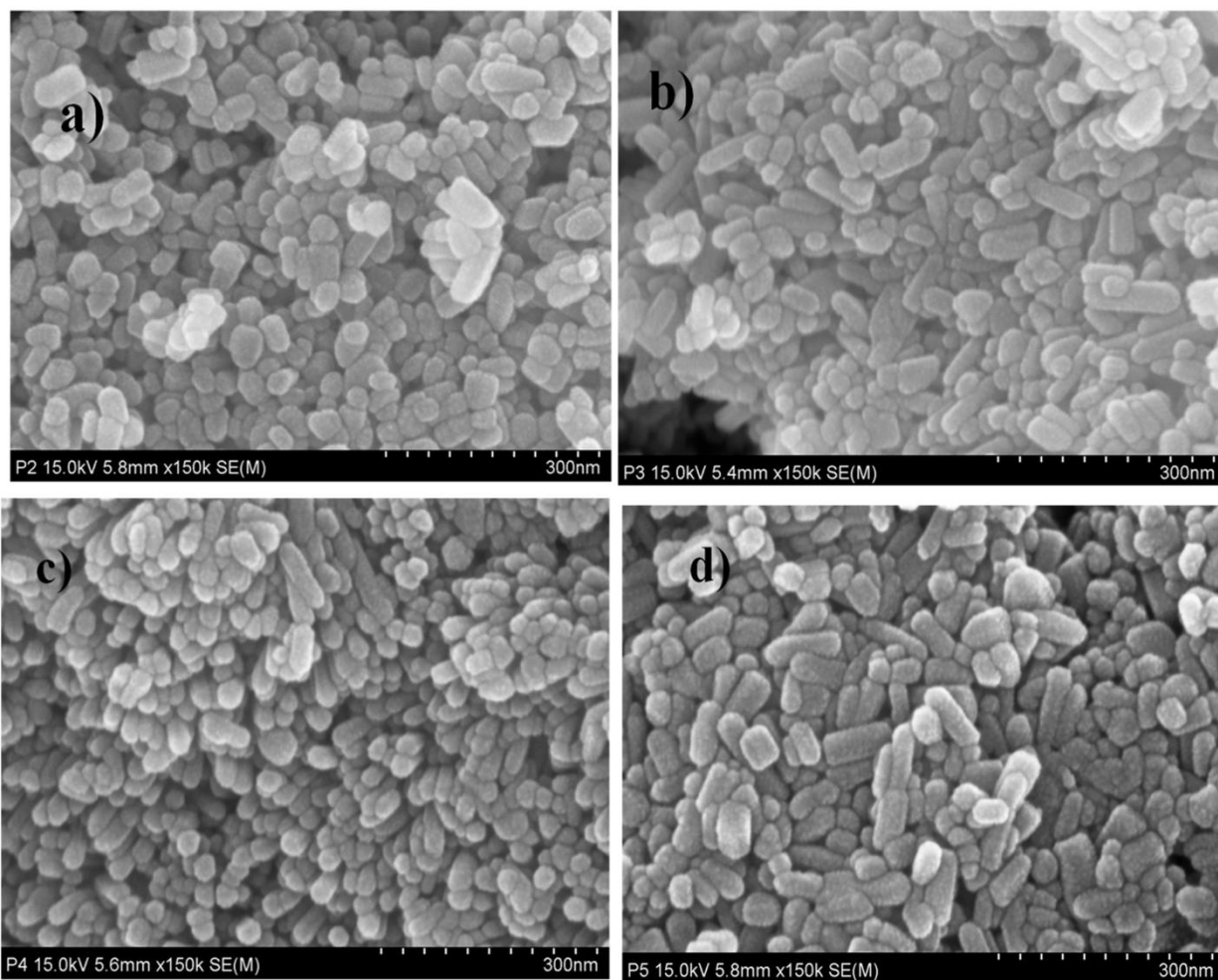
Transmission Electron Microscopy (TEM) is very important technique used for the measurement of particle size and to determine morphology of the sample. The TEM analysis is performed to measure the size of synthesized ZnO NPs. Figure 4.6 represents the TEM analysis of ZnO NPs. Herein, we are reporting the TEM images of only DEG 3h, DEG 3h with sodium

Chapter 4: Synthesis and characterization of zinc oxide nanoparticles by using polyol chemistry

acetate, TEG 3h and TEG with sodium acetate as these ZnO NPs possess comparatively smaller size than other ZnO NPs which is calculated from the XRD result.

From the figures 4.5 and 4.6, it is observed that the difference found in the morphology of the ZnO NPs depends upon the release rate of OH^- ions. The average particle size observed is consistent with XRD data. FESEM and TEM analysis reports DEG refluxed for 3h in the absence of sodium acetate showed the least particle size of ~15 nm. The size gained from the TEM images are consistent with the crystallite size calculated from XRD patterns of ZnO NPs. In the presence of sodium acetate the release rate of OH^- ions become slow due to its weak hydrolyzing ability of acetate ions, which affects on the condensation and nucleation process, so particles show elongated rod-shaped morphology.^{15,16} Also, from FESEM images it is observed that the effect of the addition of sodium acetate on the morphology is more pronounced in case of samples prepared in TEG than in DEG. This is because, in the case of DEG, the glycol is forming an ester bond with the acetate ions from the zinc acetate dehydrate. However, since when using the sodium acetate as a source of hydroxyl ions (as it is alkaline), it is also forming esters with the glycol of DEG which is more easily available from zinc acetate. Therefore, maybe there is no conclusive change observed in FESEM images of ZnO synthesized in DEG. While, in case of TEG, there are more glycol functional groups to trap the acetate ions from zinc acetate as well as sodium acetate and that is why we got a better results as a larger part of added zinc acetate is getting converted to zinc hydroxide ions in presence of sodium acetate.¹⁷

Chapter 4: Synthesis and characterization of zinc oxide nanoparticles by using polyol chemistry



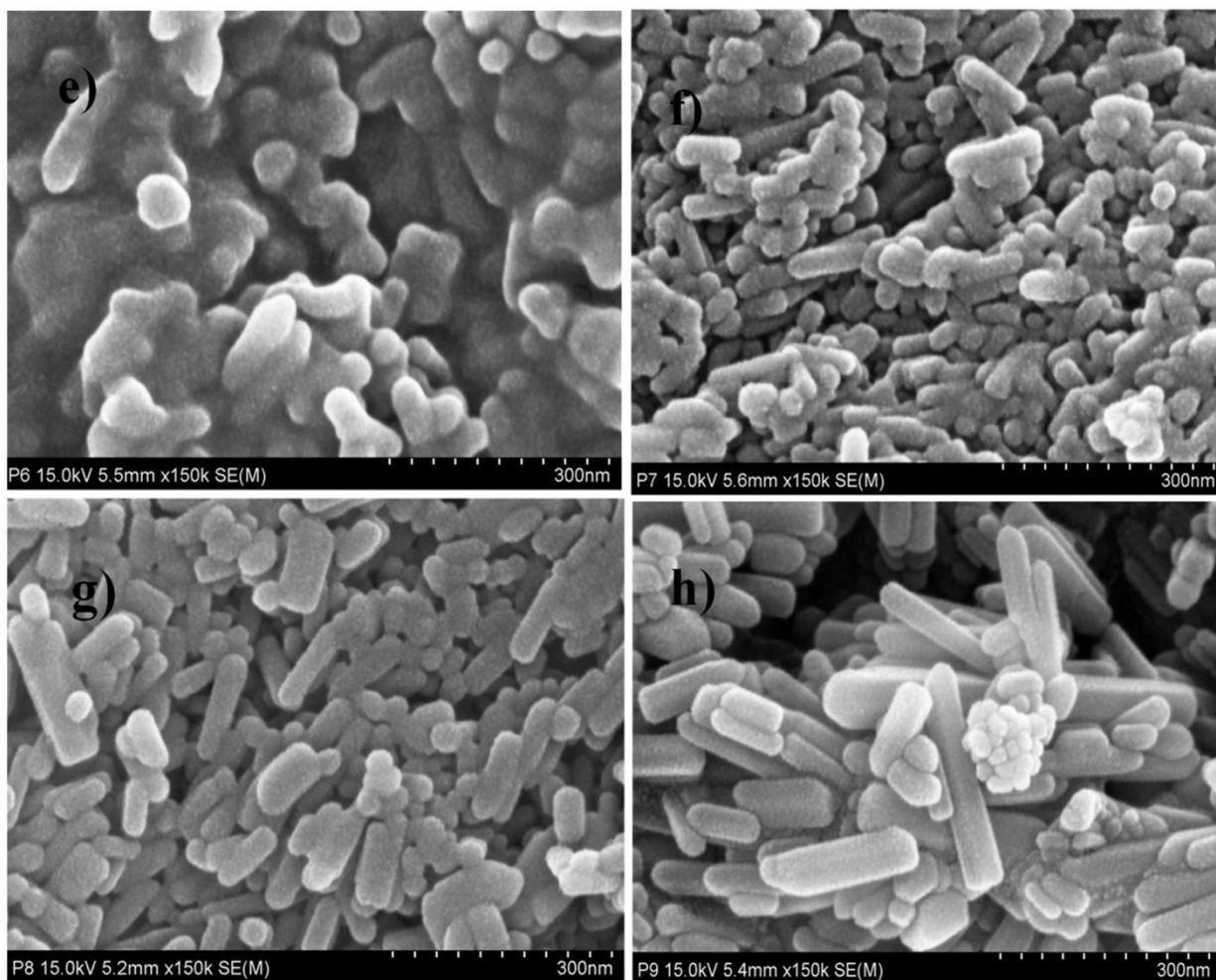


Figure 4.5: FESEM images of ZnO NPs synthesized in, DEG 2h (a), DEG 2h with sodium acetate (b), DEG 3h (c), DEG 3h with sodium acetate (d), TEG 2h (e), TEG 2h with sodium acetate (f), TEG 3h (g), TEG 3h with sodium acetate (h).

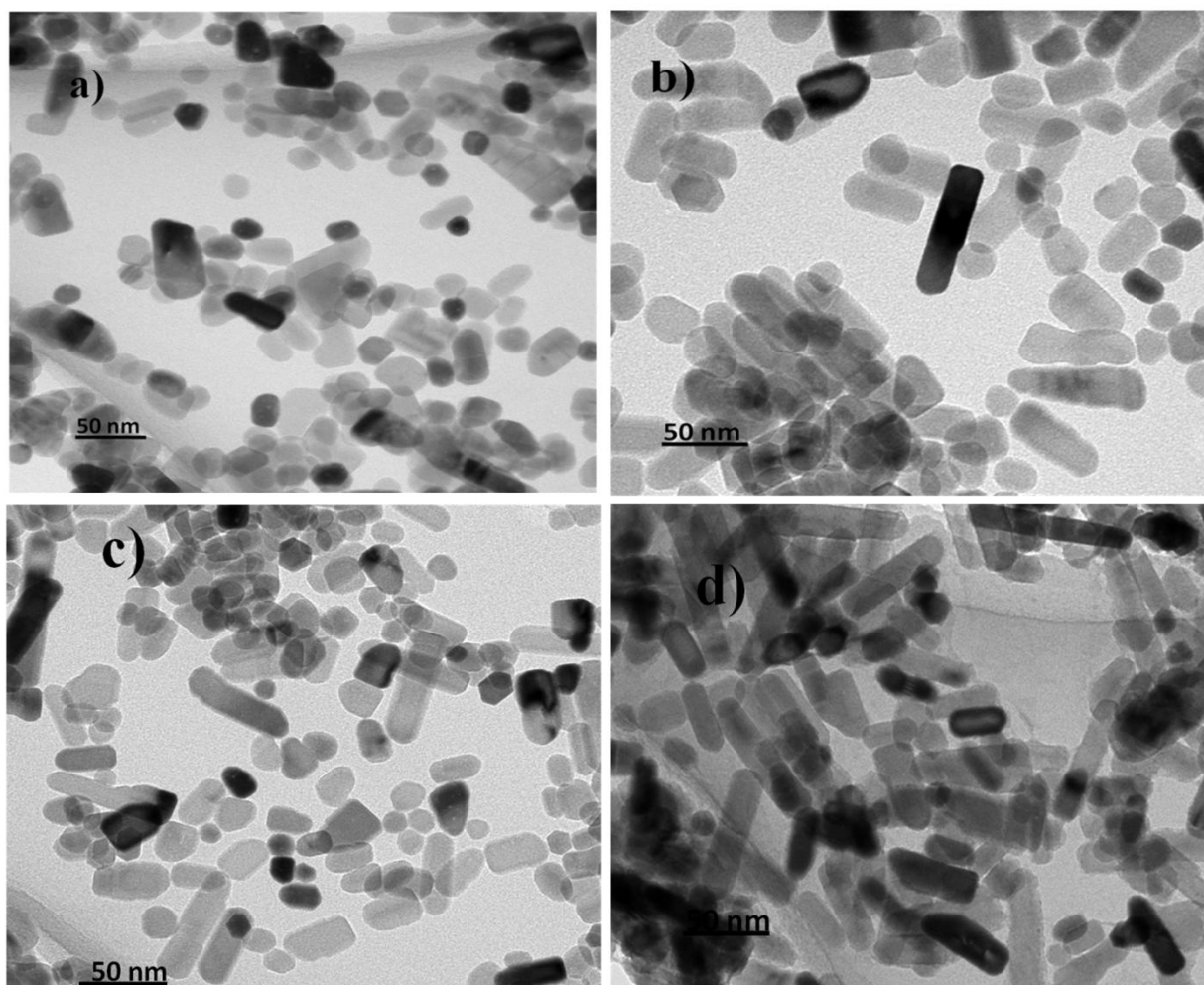


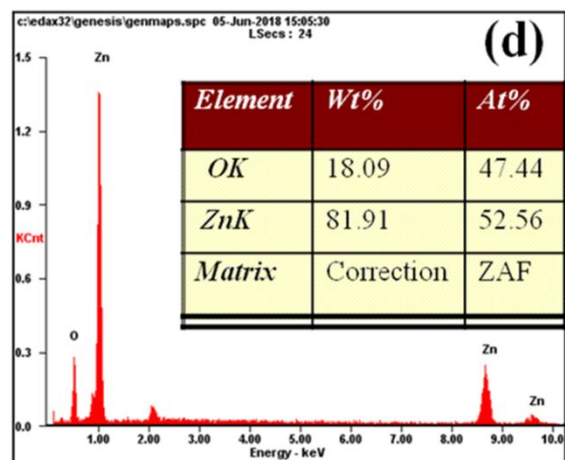
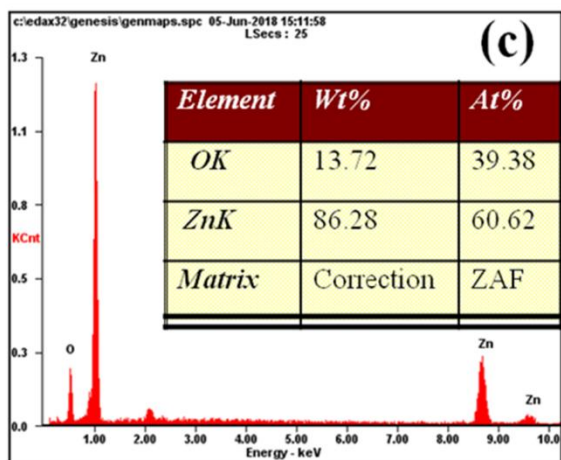
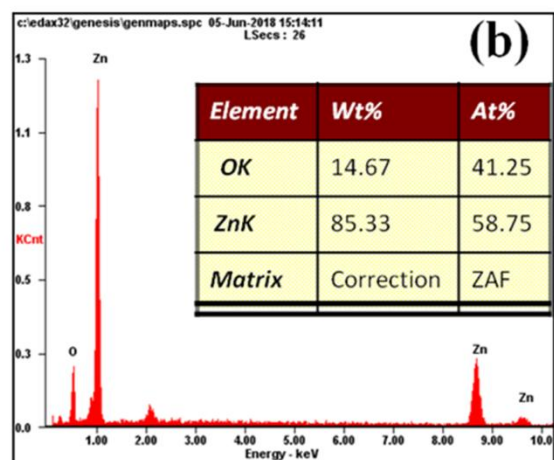
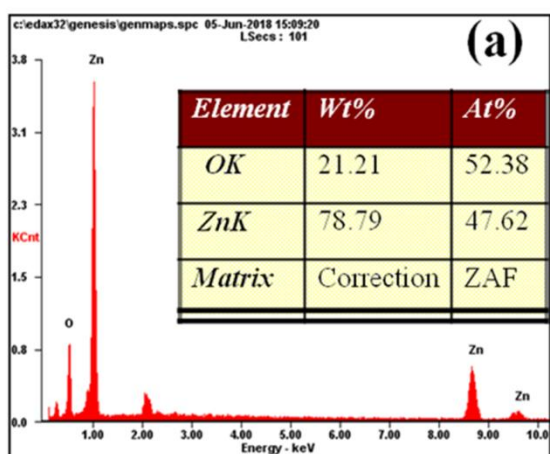
Figure 4.6: TEM images of ZnO NPs synthesized in DEG 3h (a), DEG 3h with sodium acetate (b), (B) TEG 3h (c), TEG 3h with sodium acetate (d).

4.3.4. Elemental analysis

4.3.4.1. Energy Dispersive X-ray

The elemental analysis of all ZnO NPs is carried out by EDX spectroscopy. Figure 4.7 shows the EDX of all ZnO NPs. It is revealed the presence of Zn and O indicates the synthesis of impurity-free ZnO nanoparticles.¹⁸ The absence of any other peaks confirmed the formation of impurity-free ZnO NPs.

Chapter 4: Synthesis and characterization of zinc oxide nanoparticles by using polyol chemistry



Chapter 4: Synthesis and characterization of zinc oxide nanoparticles by using polyol chemistry

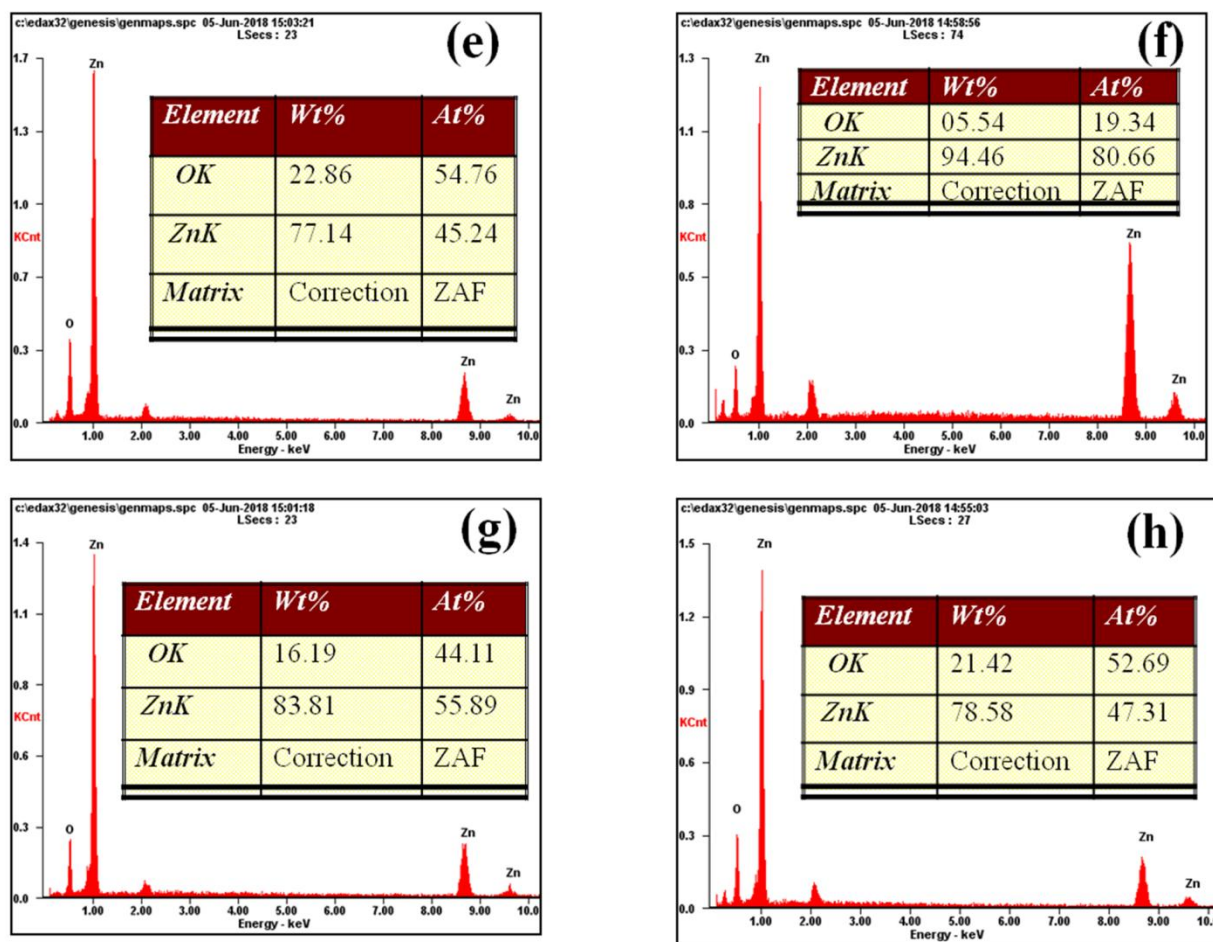


Figure 4.7: EDX studies of ZnO Nps synthesized in DEG 2h (a), DEG 2h with sodium acetate (b), DEG 3h (c), DEG 3h with sodium acetate (d), TEG 2h (e), TEG 2h with sodium acetate (f), TEG 3h (g), TEG 3h with sodium acetate (h).

4.3.5. Thermal analysis

4.3.5.1. Thermogravimetric analysis

The thermal decomposition behavior of all synthesized ZnO NPs is analyzed by TGA. All samples are heated from 50°C-900°C at the rate of 10°C/minute. Figure 4.8 (A) and (B) shows the thermal decomposition of DEG and TEG mediated synthesized ZnO NPs respectively. The two successive decompositions are observed in all samples. The initial weight loss observed is observed in the range of 145°C-257°C and further 2nd stage of decomposition is observed in the range of 452°C-490°C.

Chapter 4: Synthesis and characterization of zinc oxide nanoparticles by using polyol chemistry

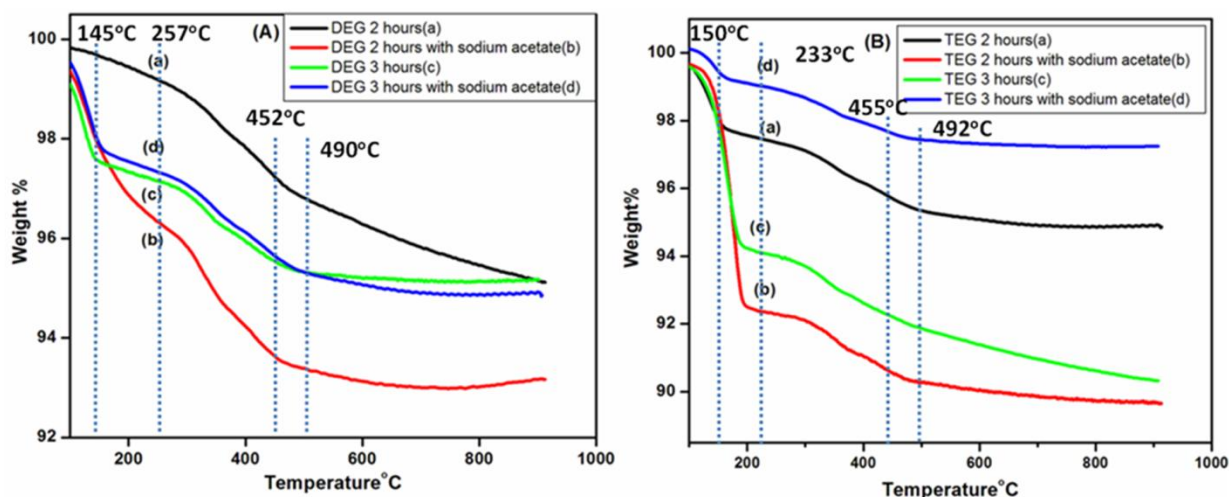


Figure 4.8: TGA of ZnO NPs synthesized in, (A) DEG 2h (a), DEG 2h with sodium acetate (b), DEG 3h (c), and DEG 3h with sodium acetate (d) and, (B) TEG 2h (a), TEG 2h with sodium acetate (b), TEG 3h (c), and TEG 3h with sodium acetate (d).

The initial weight loss is observed in the range of 145°C-257°C because of the evaporation of surface adsorbed water and moisture¹⁹ and further 2nd stage of decomposition is observed in the range of 452-492°C due to loss of the adsorbed DEG/TEG molecules in all samples and which is consistent with the results of FTIR. The thermal stability supports the presence of surface adsorbed molecules.²⁰

4.5. Conclusions

In the present investigation, we have synthesized ZnO NPs by applying different approaches, (i) regular synthesis in polyols, (ii) In presence of sodium acetate, and (iii) increasing reaction time. It has been suggested that it is possible to control the shape and size of nanoparticles through these approaches. XRD analysis revealed the phase purity. The synthesized nanoparticles have crystallite nature having hexagonal wurtzite structure. UV spectroscopy showed that the absorption edges are shifted to lower wavelength showing blue shift due to decrease in crystal size. FTIR and TGA analysis showed that DEG and TEG molecules are adsorbed on ZnO nanoparticles. The most interesting observation found in present study is that all synthesized nanoparticles exhibited nicely organized oval and rod-shaped morphology with different size. In case of nanoparticles synthesized by using polyol DEG, it is

Chapter 4: Synthesis and characterization of zinc oxide nanoparticles by using polyol chemistry

observed that, addition of sodium acetate and increase in reflux time from 2h to 3h changes morphology of nanoparticles from oval to rod shape, while in case of nanoparticles synthesized by using polyol TEG all particles showed rod shaped morphology and increase in size with addition of sodium acetate and increase in reflux time from 2h to 3h which highlights the role of sodium acetate in change of morphology. Out of all ZnO NPs, ZnO NP synthesized by refluxing zinc acetate precursor in DEG for 3h in absence of sodium acetate exhibited the least particle size of ~15nm. All these data obtained revealed that the use of different approaches in the synthesis of ZnO NPs could yield the differences in the morphology.

Chapter 4: Synthesis and characterization of zinc oxide nanoparticles by using polyol chemistry

Reference:

- 1 S. Li, S. Dong, W. Xu, S. Tu, L. Yan, C. Zhao, J. Ding and X. Chen, *Adv. Sci.*, 2018, **5**, 1–17.
- 2 R. M. Patil, N. D. Thorat, P. B. Shete and P. A. Bedge, *Biochem. Biophys. Reports*, 2018, **13**, 63–72.
- 3 J. V. Meshram, V. B. Koli, M. R. Phadatare and S. H. Pawar, *Mater. Sci. Eng. C*, 2017, **73**, 257–266.
- 4 L. Li, Y. Zhang, L. Li and Y. Zhang, *J. Appl. Phys.*, 2017, **121**, 1–4.
- 5 P. P. Mahamuni, P. M. Patil, M. J. Dhanavade, M. V. Badiger, P. G. Shadija, A. C. Lokhande and R. A. Bohara, *Biochem. Biophys. Reports*, 2019, **17**, 71–80.
- 6 A. Król, P. Pomastowski, K. Rafińska, V. Railean-Plugaru and B. Buszewski, *Adv. Colloid Interface Sci.*, 2017, **249**, 37–52.
- 7 B. Woei and Y. Ying, *Mater. Lett.*, 2012, **73**, 78–82.
- 8 G. S. Dhillon, S. Kaur and S. K. Brar, *Int. Nano Lett.*, 2014, **4**, 1–11.
- 9 N. L. Gavade, A. N. Kadam, Y. B. Gaikwad, M. J. Dhanavade and K. M. Garadkar, *J. Mater. Sci. Mater. Electron.*, 2016, **27**, 11080–11091.
- 10 M. K. Johnson, D. B. Powell and R. D. Cannon, *Spectrochim. Acta - Part A Mol. Biomol. Spectrosc.*, 1981, **37**, 899–904.
- 11 M. A. S. Dinesh and N. K. K. Balamurugan, *J. Mater. Sci. Mater. Electron.*, 2016, **27(12)**, 12517–12526.
- 12 Z. C. Orel, K. Kogej and M. Zigon, *J. Nanomater.*, 2012, **2012**, 1–9.
- 13 M. J. Chithra and M. S. K. Pushpanathan, *Acta Met. Sin.*, 2015, **98 (3)**, 394–404.
- 14 A. C. Janaki, E. Sailatha and S. Gunasekaran, *Spectrochim. ACTA PART A Mol. Biomol. Spectrosc.*, 2015, **144**, 17–22.
- 15 M. Guo, P. Diao and S. Cai, *J. Solid State Chem.*, 2005, **178**, 1864–1873.
- 16 J. Yang, T. C. Deivaraj, H. Too and J. Y. Lee, *Langmuir*, 2004, **20**, 4241–4245.
- 17 E. H. Sa, C. Frandsen, F. J. La, C. J. Serna, S. Veintemillas-verdaguer and M. P. Morales, 2017, 7172–7184.
- 18 S. Agarwal, L. K. Jangir, K. S. Rathore, M. Kumar and K. Awasthi, *Appl. Phys. A*, 2019,

Chapter 4: Synthesis and characterization of zinc oxide nanoparticles by using polyol chemistry

125, 553–557.

- 19 V. R. V. Gopal and S. Kamila, *Appl. Nanosci.*, 2017, **7**, 75–82.
- 20 S. Kazan, R. Topkaya, A. Baykal and B. Aktas, *Arab. J. Chem.*, 2016, **9**, 1131–1137.

CHAPTER 5

Comparative study of antibacterial and antibiofilm activity of ZnO nanoparticles synthesized by using polyols

SCI journal

Biochemistry and Biophysics Reports 17 (2019) 71–80



Contents lists available at ScienceDirect

Biochemistry and Biophysics Reports

journal homepage: www.elsevier.com/locate/bbrep



Synthesis and characterization of zinc oxide nanoparticles by using polyol chemistry for their antimicrobial and antibiofilm activity



Pranjali P. Mahamuni^a, Pooja M. Patil^a, Maruti J. Dhanavade^b, Manohar V. Badiger^c, Prem G. Shadija^a, Abhishek C. Lokhande^d, Raghvendra A. Bohara^{a,e,*}

^a Centre for Interdisciplinary Research, D.Y. Patil University, Kolhapur, India

^b Department of Microbiology, Shivaji University, Kolhapur, India

^c CSIR, National Chemical Laboratory, Pune, India

^d Department of Materials Science and Engineering, Chonnam National University, Gwangju, Republic of Korea

^e CURAM, Center for Research in Medical Devices, National University of Ireland Galway, Ireland

"I feel that the greatest reward for doing is the opportunity to do more."

-Jonas Salk

Chapter 5: Comparative study of antibacterial and antibiofilm activity of ZnO NPs synthesized by using polyols

5.1. Introduction

Biofilm are the communities of varieties of micro-organisms that remain attached to any biological or non-biological surface that remains enclosed in self-produced hydrated polymeric matrix. Microorganisms in biofilm transcribe different genes than the genes present in planktonic bacteria.¹ It has been reported that the maximum number of bacterial infections treated in hospitals is associated with bacterial biofilm.² The microorganisms in biofilm get escaped from phagocytosis and, develop high resistance to antibiotics that make them difficult to treat. Their resistance to antibiotics is a slow but serious threat to public and domestic health. Both Gram-positive and Gram-negative bacteria can cause chronic infections. In this regard, *Staphylococcus aureus* and *Proteus vulgaris* are biofilm-forming pathogens that produce severe biofilm associated infections such as urinary tract infection, musculoskeletal infection and respiratory tract infection.³ As reported earlier, *S. aureus* and *P. vulgaris* are drug-resistant bacteria that are critical to treat and indeed untreatable with conventional antibiotics like ampicillin, amoxicillin, methicillin, oxacillin and 1st generation of cephalosporin. So there is an urgent need to search an alternative approach to treat bacterial infections caused by drug-resistant microorganisms.^{4,5}

Until now, zinc oxide nanoparticles are widely reported for their antimicrobial and antibiofilm activities against a broad spectrum of microbes with low toxicity to human cells. It has been reported that the intensity of antibacterial activity is inversely proportional to the size of the ZnO nanoparticles. Smaller sized ZnO NPs indeed possess high antibacterial and antibiofilm activity than larger particles.

In the present chapter, the comparative study of antibacterial, antibiofilm activity, biocompatibility and hemocompatibility of ZnO NPs prepared by using different approaches like by refluxing diethylene glycol (DEG) for 2h and 3h in the absence and presence of sodium acetate and by refluxing triethylene glycol (TEG) for 2h and 3h in the absence and in presence of sodium acetate has been studied in detail, from which the better one can be used as a potential candidate for the incorporation in the polymer to prepare microfibers for further wound dressing applications.

5.2. Experimental

Chapter 5: Comparative study of antibacterial and antibiofilm activity of ZnO NPs synthesized by using polyols

5.2.1. Reagents and Materials

All glassware used was cleaned with distilled water and sterilized in an autoclave at 121°C for 20 min before use. The microorganisms *S. aureus* (NCIM 2654) and *P. vulgaris* (NCIM 2613) were collected from the National Collection of Industrial Microorganisms (NCIM), Pune, India. The media were purchased from HiMedia Laboratory. A blood sample used was obtained from the slaughter house and it doesn't have any ethical issues for human and animal rights in the ethical statement section. The present work does not involve the use of human and animal subjects. All the reagents used were supplied by analytical grade (AR grade) and used as it is without further purification. Double distilled water was used throughout the experiments.

5.2.2. Bacterial sample preparation

The bacterial cultures were maintained at 4°C in the nutrient agar medium. The composition of nutrient agar media used for the growth of bacteria is given below. The cultures were allowed to grow at 37°C on the rotary shaker maintained at the speed of 150 rpm for 16 h. The bacterial concentration was maintained to the desired level by recording optical density at 600nm (OD 600nm). For safety, all bacterial cultures were autoclaved at 121°C for 20 minutes to destroy bacteria before disposal and all glassware used were autoclaved before and after experiments.

Composition of Nutrient broth

- Peptone (1%)
- Beef extract (1%)
- Sodium chloride (0.5%)
- pH after sterilization 7.3

The OD of bacterial cultures was adjusted to the concentration of approximately 1×10^7 CFU/ml.

6

5.2.3. Determination of Antibacterial activity by Agar Well Diffusion assay

Antibacterial study of all synthesized ZnO NPs was carried out by the agar well diffusion method. The comparative antibacterial activity of these samples is studied against both Gram-positive *S. aureus* (NCIM 2654) and Gram-negative *P. vulgaris* (NCIM 2613) bacteria. In this

Chapter 5: Comparative study of antibacterial and antibiofilm activity of ZnO NPs synthesized by using polyols

assay, in each well 1mg/ml concentration of all ZnO NPs was inoculated on nutrient agar plates which were previously seeded by 100µl of 24h old bacterial inocula. ZnO samples were sonicated for 15 min. in distilled water before inoculation. Then the plates were kept for incubation at 37°C for 24h for the growth of microorganisms. Antimicrobial activity was observed by measuring the inhibition zone diameter (mm).

5.2.5. Determination of Minimum Inhibitory Concentration (MIC)

Minimum inhibitory concentration is the lowest concentration that can inhibit visible bacterial growth. Micro dilutions and agar dilutions are the quantitative methods used to determine MIC values. In the present study, the determination of MIC was performed in the sterile Muller-Hinton broth at the concentration of ZnO NPs in the range of 10mg to 50mg/ml. This assay was carried out in 96 well plates by using a tryptic soy broth medium. For this, 200 µl volume of tryptic soy medium was added in each well and inoculated with 24h old 10µl of bacterial inocula. One well was maintained without the addition of nanoparticles, used as a control. The microplates were kept for incubation at 37°C for 24h. After incubation OD was recorded at 600nm. From the graph, the minimum inhibitory concentration and the percentage of each concentration were determined. The MIC concentrations values help in diagnostic laboratories to confirm the resistance of microorganisms to antimicrobial materials. Also, the antibacterial activity of new antimicrobial agents can be monitored. This method is clinically used to detect the concentration of antibiotic/test samples that will be effective in the patient and the type of antibiotic to be utilized.⁷

5.2.6. Determination of Growth curves of bacteria

Growth curves were determined by bacterial cells without exposure to ZnO NPs used as a control and with exposure to ZnO NPs at the concentration of 20µg/ml in nutrient broth. The bacterial cell concentration was maintained at 10⁷ CFU/ml. Culture flasks were kept for incubation in a shaking incubator at 150 rpm at 37°C. The bacterial cell growth pattern was examined for every 2h at 600 nm wavelength.⁸

5.2.7. Antibiofilm activity

The antibiofilm activity was tested by using a microtiter plate method. In this assay, the test organisms were inoculated in sterile tryptic soy broth and incubated for 24h at 37°C. Then

Chapter 5: Comparative study of antibacterial and antibiofilm activity of ZnO NPs synthesized by using polyols

the samples were centrifuged at 5000rpm and the pellet was suspended in phosphate buffer (pH 7.0). 1mg/ml stock of all ZnO samples was prepared. In a brief, 200µl medium with known concentrations of ZnO was inoculated with 10 µl of bacterial sample and incubated for 24h at 37°C. After incubation, the wells were drained, washed with phosphate buffer saline (PBS), fixed with cold methanol, and then stained with 1% of crystal violet for 30 min. Biofilm formed in the wells was resuspended in 30% of acetic acid. The intensity of the suspension was measured at 570nm and the percentage of biofilm inhibition was calculated by using the equation 3.8 given in chapter 3.⁹

5.2.8. Hemocompatibility

Goat blood was collected from a slaughterhouse and stabilized in EDTA. The density gradient centrifugation was used for the separation of RBCs from the collected blood. 5ml of whole blood was gently poured on the top of 5ml of PBS solution and then allowed for centrifugation at 2000rpm for 30 min. The supernatant was removed, and red blood cells were collected. Later, RBCs were rinsed with phosphate buffer saline (pH 7.4) and allowed for centrifugation at 2000rpm for 30 min. A stock solution of RBCs was prepared without serum at 2% (v/v) using phosphate buffer (pH 7.4). After that, 2ml of the diluted RBC solution was added to 2ml Eppendorf tubes containing all ZnO NPs. The negative and positive blood samples were prepared in the same way without NPs and deionized water, respectively. All Eppendorf tubes were kept for incubation for 2h at 37°C. At an interval of 30 min, tubes were gently shaken and were allowed for centrifugation at 1500g for 10 min at room temperature. The supernatant of PBS was transferred to another 96 well microtiter plate and hemoglobin (Hb) release was observed on a spectrophotometer (OD 550nm) at 541 nm with the microtiter plate reader (Tecan). The hemolysis percentage can be calculated by the considering that 100% RBC lysis takes place in mixing blood with distilled water at 1:1 (v/v) ratio. The hemolytic percentage was calculated by using the following equation:

$$HP\% = (D_t - D_{nc}) / (D_{pc} - D_{nc}) \times 100 \dots\dots\dots (5.1)$$

Where D_t is the absorbance of the test samples and D_{pc} and D_{nc} are the absorbances of positive and negative control respectively.¹⁰

Chapter 5: Comparative study of antibacterial and antibiofilm activity of ZnO NPs synthesized by using polyols

Schematic representation of hemolytic assay is given in fig. 5.1.

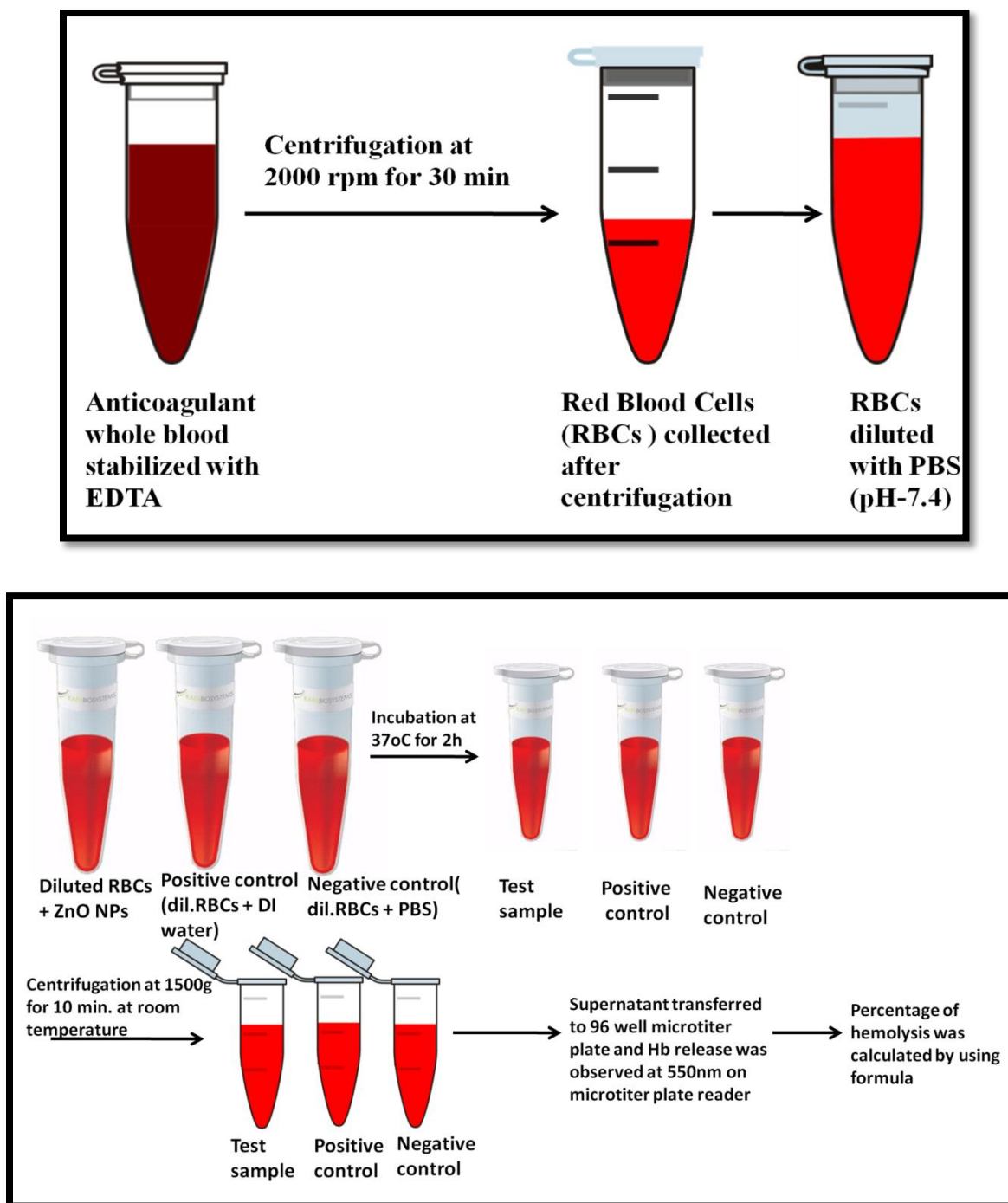


Figure 5.1: A schematic representation of the hemolysis assay.

Chapter 5: Comparative study of antibacterial and antibiofilm activity of ZnO NPs synthesized by using polyols

5.2.9. Cell viability study of ZnO NPs

The cell viability of synthesized ZnO NPs samples was investigated by MTT assay with the help of mammalian fibroblast L929 cell lines.¹¹ Dulbecco's minimal essential medium (DMEM) supplemented with 10% fetal bovine serum (FBS) and 1% antibiotic penicillin (1000U/mL penicillin G), and 100 µg/mL streptomycin was used for culturing of the cells. Then cells with the density of 1×10^4 cells/well with DMEM containing serum were transferred into 96 well plates and incubated overnight in a humidified incubator. The NPs were added at a concentration of 1mg/ml in serum-containing media and kept for incubation for 24h, 48h, and 72 h at 37°C. Blank that is well without ZnO NPs was used as a control. After incubation, the media was discarded. Cells were rinsed with phosphate buffer saline (pH 7.2) and 100 µL of MTT (0.5mg/mL) prepared in serum-free medium was added to each well and kept for incubation for 4h. Then the medium was decanted and dimethyl sulphoxide (DMSO) was poured to each well for solubilization of formazan crystals. The concentration of formazan was investigated by a multiwell plate reader at 570nm absorbance. The cell viability was calculated by using equation 3.6 given in chapter 3.

5.3 Results and discussion

5.3.1 Antimicrobial activity of ZnO NPs

5.3.1.1 Determination of the antibacterial activity of all synthesized ZnO NPs

Antibacterial activity of synthesized all ZnO NPs is carried out by agar well diffusion assay, as shown in fig.5.2. Gram-positive *S. aureus* (NCIM 2654) and Gram-negative *P. vulgaris* (NCIM 2613) bacteria are used as test organisms.

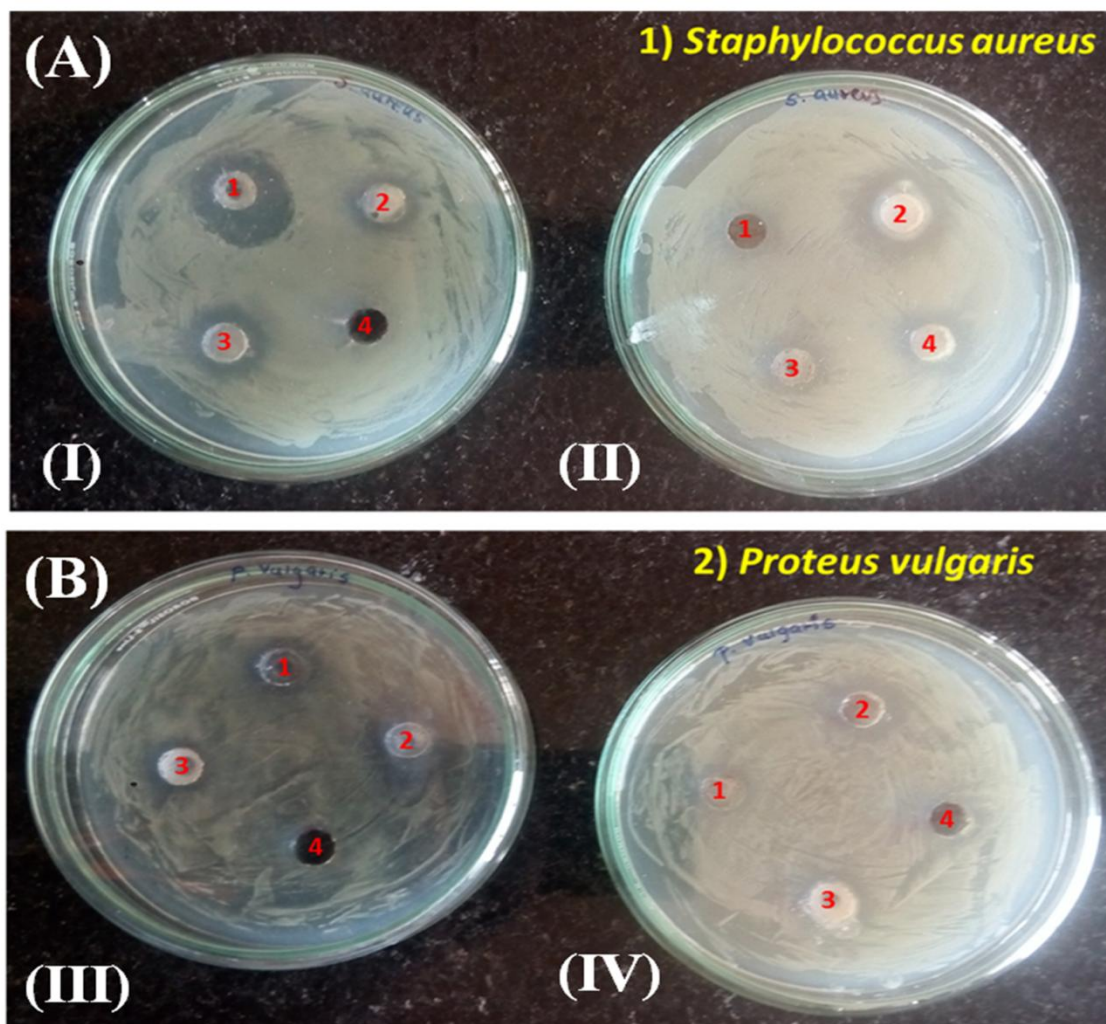


Figure 5.2: Antibacterial activity of DEG and TEG mediated synthesized ZnO NPs (1mg/ml) against Gram-positive *S. aureus* (NCIM 2654) (A) and Gram-negative *P. vulgaris* (NCIM 2613) (B), In the plate (I) and (III) samples inoculated are (1) DEG 3h, (2) DEG 3h with sodium acetate, (3) DEG 2h, and (4) DEG 2h with sodium acetate and in plate (II) and (IV) samples inoculated are (1) TEG 2h with sodium acetate, (2) TEG 3h, (3) TEG 3h with sodium acetate, and (4) TEG 2h.

From figure 5.2 and data indicated in table 5.1, it is observed that among all synthesized ZnO NPs the smallest ZnO NPs synthesized in DEG for 3h showed significant zone of inhibition (14mm) against Gram-positive *S. aureus* (NCIM 2654) and Gram-negative *P. vulgaris* (NCIM 2613). The intensity of antibacterial activity is size-dependent that is it is inversely proportional

Chapter 5: Comparative study of antibacterial and antibiofilm activity of ZnO NPs synthesized by using polyols

to the size of ZnO nanoparticles. It's small size and high surface area to volume ratio may help for more interaction with bacterial cells, than other ZnO NPs with comparatively greater size.¹²

Table 5.1: Diameter of zone of inhibition by ZnO against *S. aureus* (NCIM 2654) (A) and *P. vulgaris* (NCIM 2613)

Sample	Zone of inhibition diameter(in mm)	
	<i>S. aureus</i>	<i>P. vulgaris</i>
DEG 3 hours	14	6
DEG 3 hours with sodium acetate	6	4
DEG 2 hours	6	2
DEG 2hours with sodium acetate	1	1
TEG 2 hours with sodium acetate	1	1
TEG 3 hours	7	4
TEG 3 hours with sodium acetate	4	3
TEG 2 hours	4	1

5.3.1.2 Determination of minimum inhibitory concentration of all synthesized ZnO NPs

The minimum inhibitory concentration of synthesized ZnO NPs for *S. aureus* (NCIM 2654) and *P. vulgaris* (NCIM 2613) is determined by the serial dilution method. From the results evaluated in fig 5.3, it is concluded that the minimum inhibitory concentration for all samples is in the range of 10-20µg/ml concentration of ZnO NPs. It is revealed that among all samples DEG 3h sample showed significant % of inhibition for *S. aureus* it is 32.67% and for *P. vulgaris* it is 22.38% at 50µg/ml concentration respectively.

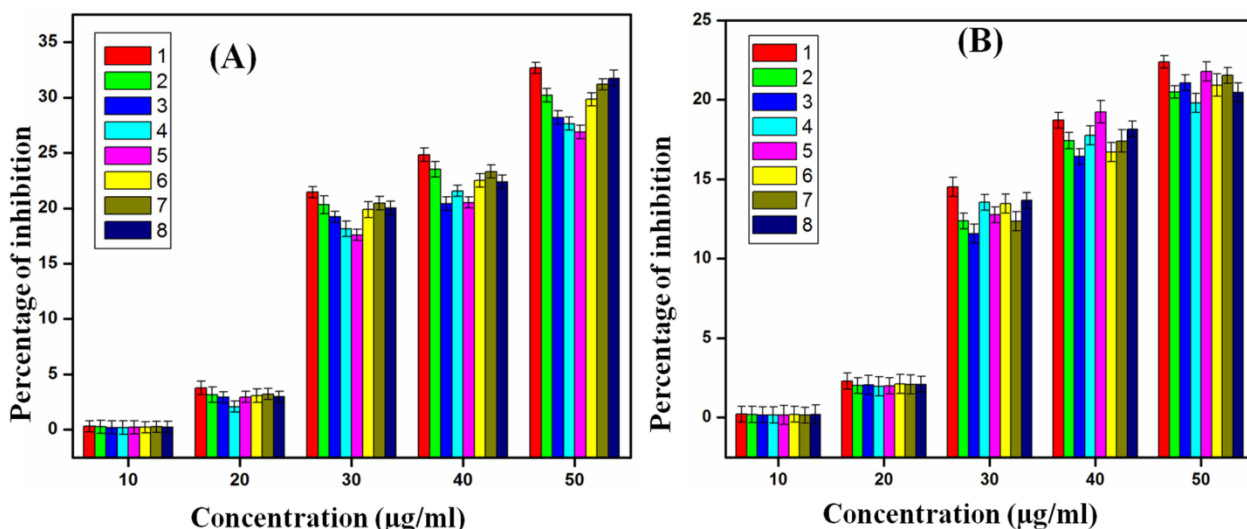


Figure 5.3: Percentage of inhibition of all ZnO NPs at different concentrations of all ZnO NPs against *S. aureus* (NCIM 2654) (A) and *P. vulgaris* (NCIM 2613) (B), (1) DEG 3h, (2) DEG 3h with sodium acetate, (3) TEG 3h, (4) TEG 3h with sodium acetate, (5) TEG 2h, (6) TEG 2h with sodium acetate, (7) DEG 2h, and (8) DEG 2h with sodium acetate.

5.3.1.3 Determination of growth curve of bacterial cells

Figure 5.4 (A) and (B) denote the growth curve of all synthesized ZnO NPs for *S. aureus* (NCIM 2654) and *P. vulgaris* (NCIM 2613). The results indicated that the exposure of ZnO NPs to bacterial cells decreased cell growth as compared to control. The absorbance of the sample increases with the increase in bacterial cell growth. In this experiment, ZnO NPs have slightly more activity against *S. aureus* than *P. vulgaris* at a concentration of 20 µg/ml. Since the Gram-positive bacteria are more susceptible towards the metal nanoparticles as previously reported.¹³

Chapter 5: Comparative study of antibacterial and antibiofilm activity of ZnO NPs synthesized by using polyols

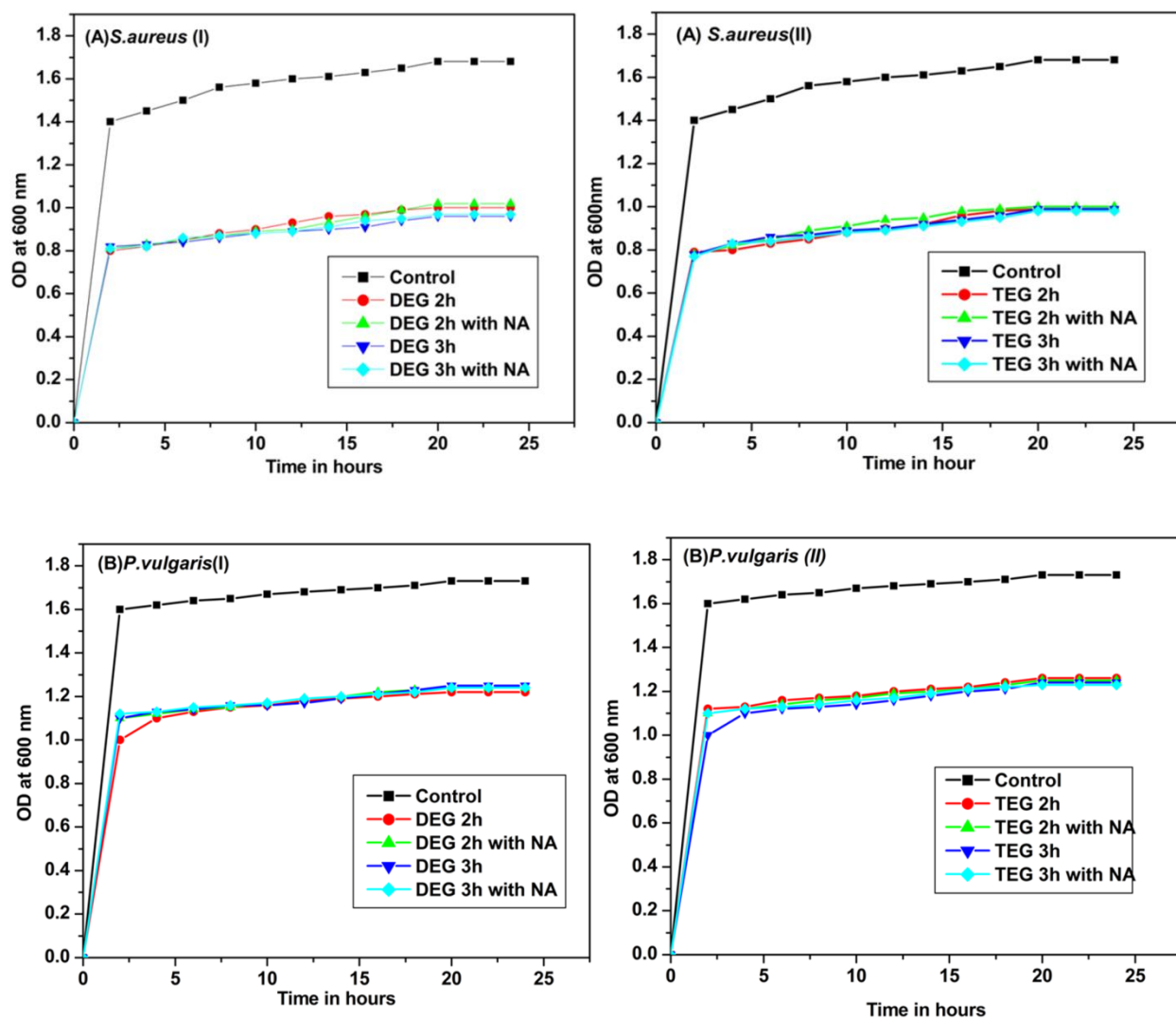


Figure 5.4: Growth curves of ZnO NPs samples against (A) *S. aureus* and, and (B) *P. vulgaris*.

5.3.1.4 Determination of antibiofilm activity

Effect of all synthesized ZnO NPs on biofilm formation on *S. aureus* (NCIM 2654) (A) and *P. vulgaris* (NCIM 2613) (B) is shown in fig 5.5A and B. From these graphs it can be predicted that all ZnO NPs synthesized by using DEG and TEG, inhibited the activity of biofilm formation. Out of all synthesized ZnO NPs, ZnO synthesized by refluxing DEG for 3h without sodium acetate showed a significant percentage of inhibition in *S. aureus* as compared to *P. vulgaris* at each concentration. All ZnO samples showed an increased percentage of inhibition with an increase in concentration. At 250 μ g/ml concentration of ZnO synthesized by DEG for 3h

Chapter 5: Comparative study of antibacterial and antibiofilm activity of ZnO NPs synthesized by using polyols

exhibited a maximum of 67.3 and 58.18% biofilm inhibition against *S. aureus* and *P. vulgaris* respectively.

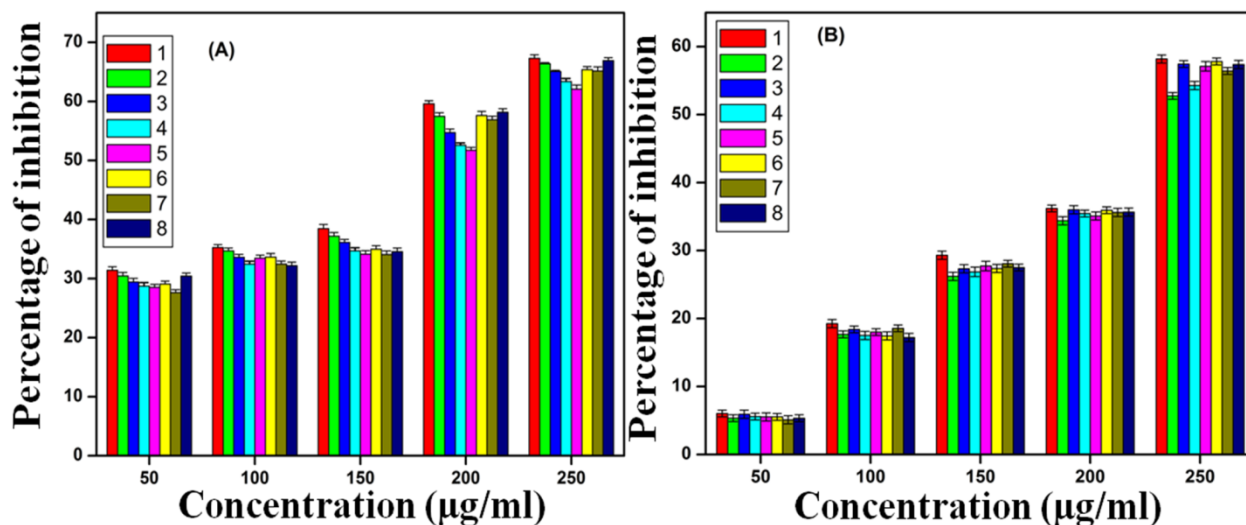


Figure 5.5:Percentage of biofilm inhibition of ZnO samples at different concentrations of ZnO NPs against *S. aureus* (NCIM 2654) (A) and *P. vulgaris* (NCIM 2613) (B), (1) DEG 3h, (2) DEG 3h with sodium acetate, (3) TEG 3h, (4) TEG 3h with sodium acetate, (5) TEG 2h, (6) TEG 2h with sodium acetate, (7) DEG 2h, and (8) DEG 2h with sodium acetate.

• Mechanism of antibacterial activity of ZnO NPs

The most widely reported and accepted mechanism for the antibacterial activity of ZnO NPs is the release of reactive oxygen species (ROS). The mechanism of antibacterial and antibiofilm activity of ZnO NPs is represented in figure 5.6. ROS includes highly reactive ionic species, free radicals such as $O^{\bullet-}$, $HO\bullet_2$, H_2O_2 , and $HO\bullet$ that destroy cells by induction of oxidative stress. The imbalance between generated ROS and their reducing equivalents is termed as oxidative stress.¹⁴ It destroys cellular biomolecules such as DNA, lipids, and proteins. All these factors trigger the apoptosis pathway and ultimately kill the bacterial cell. Another important mechanism of the antibacterial activity of ZnO Nps is the release of zinc ions in an aqueous media that contain ZnO NPs and bacteria. Zn^{+2} ions mainly cause the conformational changes in enzymes that result in distortion of active sites in enzymes resulting in competitive or non-competitive reversible inhibition.¹⁵ Zinc ions mainly interact with cystein, aspartate and histidine

Chapter 5: Comparative study of antibacterial and antibiofilm activity of ZnO NPs synthesized by using polyols

side chains of proteins or enzymes and cause inhibition of enzymes like glyceraldehydes 3 phosphate dehydrogenase, aldehyde dehydrogenase, protein tyrosine phosphatase (PTPs).¹⁶

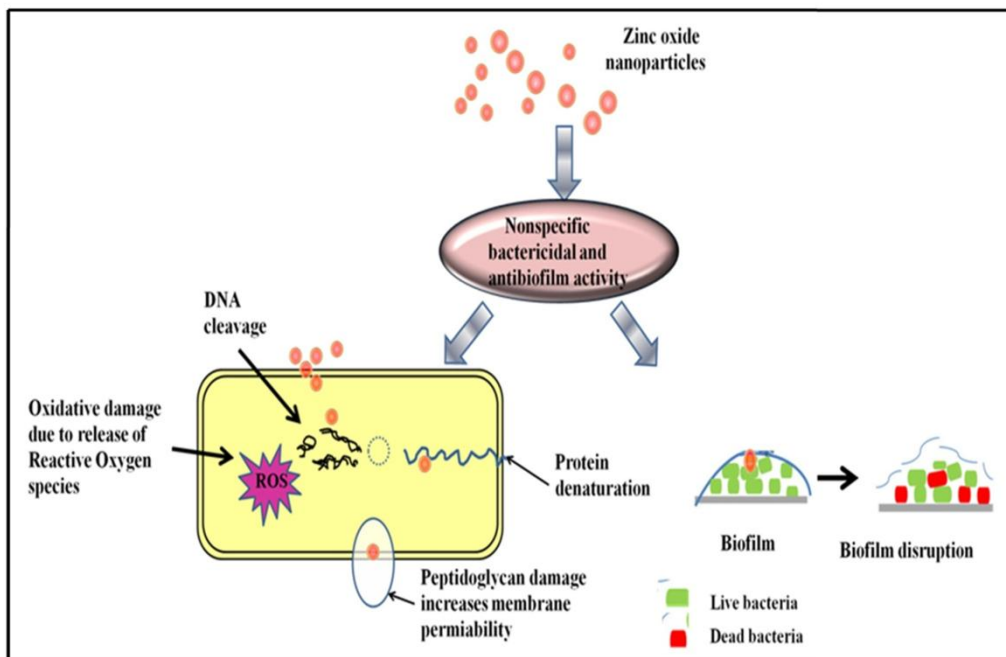


Figure 5.6: Schematic representation of the antibacterial and antibiofilm activity of ZnO NPs.¹⁷

- **Different factors affecting the antibacterial and antibiofilm activity of ZnO NPs**

Various factors affect the antibacterial and antibiofilm activity of ZnO NPS such as size, shape, concentration, and surface area to volume ratio. ZnO NPs with greater antibacterial activity could be a potential candidate in the various research areas and different fields like pharmaceuticals, food packaging, cosmetics, and wound dressing applications. The size of ZnO NPs is the most important factor that determines the degree of antibacterial activity because it affects on the internalization of NPs inside the cell. Smaller nanoparticles interact and get accumulated on the outer surface and plasma membrane that increases the surface tension and membrane depolarization by neutralizing surface potential. This results in increased membrane permeability and results in cytoplasmic leakage that leads to cell death. As the bacterial cell ranges from 0.2-10 micron, the smaller material can get readily penetrated the biofilm matrix and then into the cell.¹⁸ In the reported study, it is observed that the ZnO Nps with comparatively least particle size (~15nm) showed maximum antibacterial and antibiofilm activity against *S. aureus* and *P. vulgaris*. It is also reported that the interaction between cells and nanoparticles

Chapter 5: Comparative study of antibacterial and antibiofilm activity of ZnO NPs synthesized by using polyols

increases cell permeability. Surface defects, surface charges, and the presence of numerous edges and corners of ZnO NPs have a great impact on the intensity of antibacterial activity. Another important factor affecting antibacterial activity is the shape of the nanoparticles. The presence of sharp edges, spikes, pillars or protrusions on the surface of ZnO NPs pierce and rupture the bacterial cell due to high local stress.¹⁹

Also, the antibacterial and antibiofilm activity of ZnO NPs depends upon the concentration of NPs. It is reported that the more the concentration and larger surface area of NPs maximum antibacterial and antibiofilm activity. The intensity of antibacterial activity can be increased with an increase in concentration and surface area. Also, the synthesis process employed for ZnO NPs production has an impact on the antibacterial activity. The synthesis methods include the chemical precipitation method, hydrothermal, sol-gel, simple thermal, combustion, polymerized complex method, vapor-liquid-solid techniques and biological methods. Out of these techniques, chemical methods are widely used as they can control the size of NPs by controlling reaction parameters. Other factors like types of solvent used, precursor, temperature, pH also affect the antibacterial and antibiofilm activity of ZnO Nps.^{20,21}

5.3.2 Biocompatibility study of ZnO NPs

5.3.2.1 Hemocompatibility of all synthesized ZnO NPs

Hemocompatibility is a very important method to prove the in vitro biocompatibility of compounds by using RBCs isolated from blood. As per ASTM F-756-08, the hemolytic percentage below 2% is considered as non-hemolytic, 2-5% is slightly hemolytic and more than 5% is considered as hemolytic. Figure 5.6 (A) and (B) show the percentage of hemolysis of DEG and TEG mediated synthesized ZnO NPs at concentration of 1mg/ml. It is reported that the smaller NPs exhibit higher hemolytic activity than larger once.²² From the obtained results it can be concluded that all ZnO NPs showed below 2% hemolysis, so these NPs can be used as a promising agent in biomedical fields.

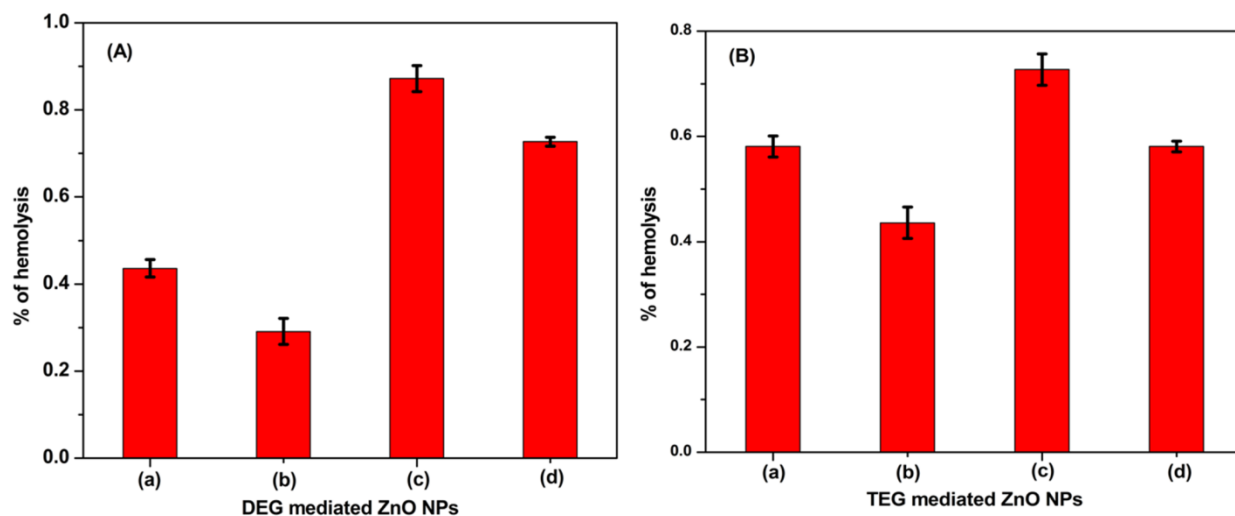


Figure 5.6: Hemocompatibility of DEG mediated ZnO NPs (A), (a) DEG 2h, (b)DEG 2h with NA, (c)DEG 3h, (d) DEG 3h with NA and TEG mediated ZnO NPs (B), (a) TEG 2h, (b) TEG 2h with NA, (c) TEG 3h and, (d) TEG 3h with NA.

5.3.6 Cell viability study of all synthesized ZnO NPs

The cell viability studies of all synthesized ZnO NPs are investigated by using MTT assay and represented in figure 5.7 (A) and (B).

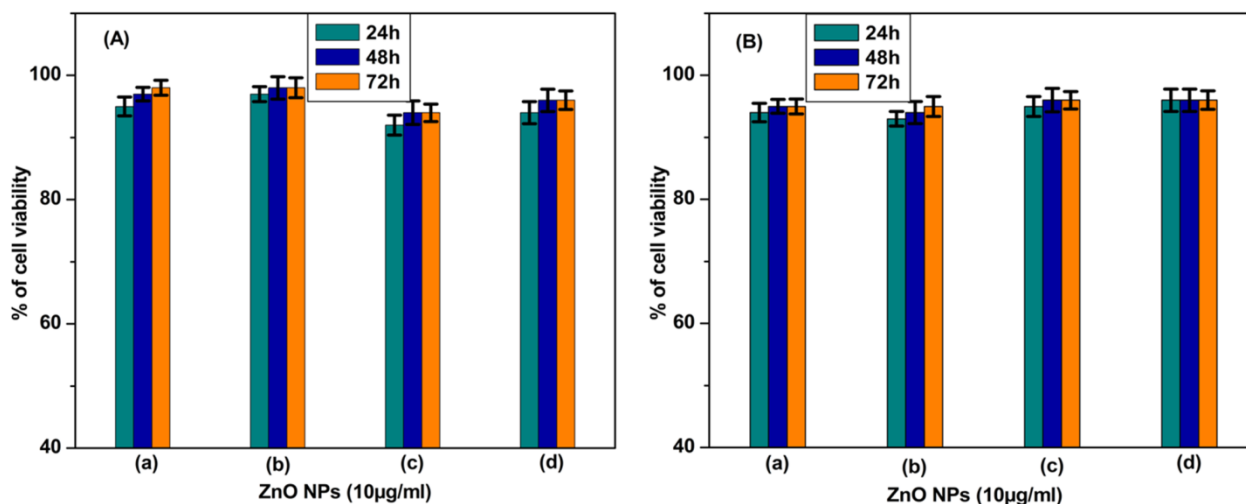


Figure 5.7:Percentage of cell viability of ZnO NPs synthesized in (A) (a) DEG 2h, (b) DEG 2h with NA, (c) DEG 3h,and (d) DEG 3h with NA, and (B) (a) TEG 2h, (b) TEG 2h with NA, (c) TEG 3h,and (d) TEG 3h with NA.

Chapter 5: Comparative study of antibacterial and antibiofilm activity of ZnO NPs synthesized by using polyols

This assay is carried out by using L929 fibroblast cells. The well without ZnO NPs is used as a control. It is observed that the cell viability is slightly increased after 24h for 48 and 72h. As previously reported, it can be suggested that the intensity of cytotoxicity is inversely proportional to the size of NPs. From these results, we can say that ZnO NPs with the least size had maximum cytotoxicity and less percentage of cell viability.

5.4 Conclusions

The present study evaluated the comparative study of the antibacterial and antibiofilm activity of ZnO NPs synthesized by using different approaches. Also, their hemocompatibility and biocompatibility were studied. It was observed that all synthesized ZnO NPs possess antibacterial and antibiofilm activity against *S. aureus* and *P. vulgaris*. However, the ZnO NPs synthesized in diethylene glycol for 3hours in the absence of sodium acetate with comparatively least particle size (~15nm) showed maximum antibacterial and antibiofilm activity. This study revealed the size dependent efficacy of ZnO NPs. These ZnO NPs showed antibacterial activity against both Gram positive and Gram negative bacteria. Additionally, it exhibited a higher zone of inhibition against *S. aureus* as compared with *P. vulgaris* at 1mg/ml concentration. ZnO synthesized by using diethylene glycol for 3h showed maximum zone of inhibition against *S. aureus* as compared with *P. vulgaris* than other ZnO NPs synthesized. The obtained results depicted that the zone of inhibition increased with a decrease in particle size. Similarly, in case of antibiofilm activity, ZnO NPs synthesized in DEG 3h showed maximum percentage of inhibition 67.3% and 58.18% against *S. aureus* and *P. vulgaris*, respectively at 250µg/ml concentration. The minimum inhibitory concentration of all ZnO NPs is in range of 10-20 µg/ml. We also observed the growth patterns of *S. aureus* and *P. vulgaris* at 20 µg/ml concentration which showed all ZnO NPs affected the growth of these bacteria. All ZnO NPs exhibited percentage of hemolysis below 2%. According to ASTM F-756-08, the hemolytic percentage less than 2% is considered as non-hemolytic. The ZnO NPs with the least particle size showed a maximum percentage of hemolysis. However, it is suitable for further biomedical applications. Also cell viability study showed that all ZnO NPs are biocompatible. Based on these results we have concluded that the ZnO NPs with the least particle size (~15nm) is a potential antibacterial candidate that can be further incorporated in the polymers for the wound dressing applications.

Chapter 5: Comparative study of antibacterial and antibiofilm activity of ZnO NPs synthesized by using polyols

References

- 1 J. Lellouche, E. Kahana, S. Elias, A. Gedanken and E. Banin, *Biomaterials*, 2009, **30**, 5969–5978.
- 2 F. Martinez-Gutierrez, L. Boegli, A. Agostinho, E. M. S?nchez, H. Bach, F. Ruiz and G. James, *Biofouling*, 2013, **29**, 651–660.
- 3 A. Sirelkhatim, S. Mahmud, A. Seenii, N. H. M. Kaus, L. C. Ann, S. K. M. Bakhori, H. Hasan and D. Mohamad, *Nano-Micro Lett.*, 2015, **7**, 219–242.
- 4 V. Van Giau, S. S. A. An and J. Hulme, *Drug Des. Devel. Ther.*, 2019, **13**, 327–343.
- 5 R. Vasudevan, *J. Microbiol. Exp.*, 2014, **1**, 1–16.
- 6 W. Diao, L. Zhang, S. Feng and A. N. D. J. Xu, *J. Food Prot.*, 2014, **77**, 1740–1746.
- 7 M. Elshikh, S. Ahmed, M. McGaw, R. Marchant, S. Funston, P. Dunlop and I. M. Banat, *Biotechnol. Lett.*, 2016, **38**, 1015–1019.
- 8 G. R. Navale, C. S. Rout, K. N. Gohil, M. S. Dharne, D. J. Late and S. S. Shinde, *RSC Adv.*, 2015, **5**, 74726–74733.
- 9 C. Ashajyothi, K. H. Harish, N. Dubey and R. K. Chandrakanth, *J. Nanostructure Chem.*, 2016, **6**, 329–341.
- 10 S. Agrawal, P. R. Patel and R. V. N. Gundloori, *ACS Omega*, 2019, **4**, 6301–6310.
- 11 K. Sudesh, H. Abe and Y. Doi, *Prog. Polym. Sci.*, 2000, **25**, 1503–1555.
- 12 O. Yamamoto, *Int. J. Inorg. Mater.*, 2001, **3**, 643–646.
- 13 Z. Huang, X. Zheng, D. Yan, G. Yin, X. Liao, Y. Kang, Y. Yao, D. Huang and B. Hao, 2008, 4140–4144.
- 14 M. Jiang, J. Zhang, L. Qian, Y. Miao, W. Song, H. Liu and R. Li, *iScience*, 2018, **11**, 189–204.
- 15 H. Chen, C. Liu, D. Chen, K. Madrid, S. Peng, X. Dong, M. Zhang and Y. Gu, *Mol. Pharm.*, 2015, **12(7)**, 2505–2516.
- 16 R. Rodrigo, M. Libuy, F. Feliú and D. Hasson, *BioMed*, 2013, **2013**, 15.
- 17 P. P. Mahamuni, P. M. Patil, M. J. Dhanavade and M. V Badiger, *Biochem. Biophys. Reports*, 2019, **17**, 71–80.
- 18 M. J. Hajipour, K. M. Fromm, A. Akbar Ashkarran, D. Jimenez de Aberasturi, I. R. de

Chapter 5: Comparative study of antibacterial and antibiofilm activity of ZnO NPs synthesized by using polyols

- Larramendi, T. Rojo, V. Serpooshan, W. J. Parak and M. Mahmoudi, *Trends Biotechnol.*, 2012, **30**, 499–511.
- 19 D. J. Hickey, M. Andersson, M. Stolzoff, T. J. Webster and J. Penders, *Int. J. Nanomedicine*, 2017, **12**, 2457–2468.
- 20 K. E. Jones, N. G. Patel, M. A. Levy, A. Storeygard, D. Balk, J. L. Gittleman and P. Daszak, *Nature*, 2008, **451**, 990–993.
- 21 P. P. Mahamuni-Badiger, P. M. Patil, M. V. Badiger, P. R. Patel, B. S. Thorat-Gadgil, A. Pandit and R. A. Bohara, *Mater. Sci. Eng. C*, 2020, **108**, 1–74.
- 22 N. Interactions, K. M. De Harpe, P. P. D. Kondiah, Y. E. Choonara, T. Marimuthu, L. C. Toit and V. Pillay, *Cells*, 2019, **8**, 1–25.

CHAPTER 6

Synthesis and characterization of hybrid PHBV-PEO-ZnO prepared by using the electrospinning technique



IF 3.2

rsc.li/njc

1 of 35

New Journal of Chemistry

View Article Online
DOI: 10.1039/D0NJ01384F

Electrospun poly (3-hydroxybutyrate-co-3-hydroxyvalerate)/Polyethylene oxide (PEO) microfibers reinforced with ZnO nanocrystals for antibacterial and antibiofilm wound dressing applications

Pranjali P. Mahamuni-Badiger¹, Pooja M. Patil¹, Pratiksh Kumar R. Patel², Maruti J. Dhanavade³,
Manohar V. Badiger², Yogesh N. Marathe², Raghvendra A. Bohara^{1,4*}

"It is not the possession of truth, but the success which attends the seeking after it, that enriches the seeker and brings happiness to him." -Max Planck

Chapter 6: Synthesis and characterization of hybrid PHBV-PEO-ZnO microfibers prepared by using the electrospinning technique

6.1 Introduction

In recent years, researchers have extensively focused on the development of newer and advanced technology for biomedical applications. For the prevention of initial colonization of biofilm forming bacteria, varieties of techniques have emerged for the synthesis of bio-friendly nanofibers with antibacterial and antibiofilm properties. There are various techniques developed for the synthesis of polymer nanofibers such as drawing, template synthesis, phase separation, self-assembly and electrospinning. But, as compared with other methods, electrospinning possesses the superiority for the preparation of one-by-one continuous fibers from few micrometers to nanometer range in simple, cheap and versatile way.¹ It also gives the high surface area and ability of various surface modifications. In this method, the nanoparticles with antibacterial properties can be reinforced into the matrix of polymers. These polymers can be used in biomedical applications.^{2,3}

Nowadays, the preparation of wound dressings with antibacterial and antibiofilm properties based on ZnO NPs blended into polymeric matrix has become an important topic in the research field.⁴ Reinforcement of ZnO NPs in polymers is suitable because of its good tissue adhesive property and antibacterial properties. Also, it provides the flexibility to enhance the biocompatibility and hemocompatibility.^{5,6}

The present chapter highlights the synthesis and characterization of electrospun poly (3-hydroxybutyrate-co-3-hydroxyvalerate) (PHBV) / Polyethylene oxide (PEO) microfibers reinforced with previously reported ZnO NPs. Poly (3-hydroxybutyrate-co-3-hydroxyvalerate) (PHBV) is biocompatible, thermoplastic, biodegradable and non-toxic polyester produced by bacteria that makes it a promising agent in the biomedical field. But due to their poor mechanical performance, high crystallinity, inherent rigidity, and hydrophobicity this material should blend with other polymer.⁷⁻⁹ Polyethylene oxide (PEO) is certified by the FDA and highly preferred because of its properties like biocompatibility, hydrophilicity, non-antigenicity, non-immunogenicity, non-toxicity, and low adsorption of surface properties.¹⁰ The present study is aimed to report the physical–chemical properties of microfibers. The reinforcement of ZnO NPs is performed in such a way that it will be suitable for end application of wound dressing. Also, their morphology, thermal stability, mechanical properties were evaluated.

Chapter 6: Synthesis and characterization of hybrid PHBV-PEO-ZnO microfibers prepared by using the electrospinning technique

6.2 Experimental

Poly (3-hydroxybutyrate-co-3-hydroxyvalerate) (PHBV) with (MW12, 00,000) and, poly (ethylene oxide) (PEO) with (MW 300,000) powder were purchased from alfa aesar) and chloroform (CHL) (CHCl_3 , 99.94%) was supplied by Merk, Mumbai, India. All reagents and solvents were of analytical grade and used as purchased without any further purification. Double distilled water was used throughout the experiments.

6.2.1 Electrospinning technique

Electrospinning is a highly flexible method that can process solutions or melts, mainly of polymers, into continuous fibers with a diameter of few micrometers to nanometers. It is mainly based upon the electrostatic forces on the droplets of liquid polymer or polymer solution. The polymers to be used in the electrospinning process can be modified chemically and their properties can be tailored with the additives. Electrospinning is an intricate process that depends upon a multitude of molecular process and technical parameters used throughout the electrospinning process. This process requires a high voltage power supply, syringe with small diameter needle and conductive collector.^{11,12}

6.2.2 Importance of incorporation of ZnO NPs in polymers

Nanomaterials have a wide range of applications in biomedical fields. Recently many researchers have suggested the design and development of nanoparticles, mainly inorganic metal oxide, ZnO NPs as potential agent for application in pathological conditions, including wound healing. As per reports, various nano-therapies have been used to treat different stages of wound healing. Two approaches can be used in wound healing; (i) NPs play a role of drugs that act intrinsically in wound healing, (ii) nanomaterials behave as vehicle or carrier to deliver therapeutic agents for wound healing.¹³ As per reports, ZnO NPs possess strong antibacterial and antibiofilm activity. So they can act intrinsically in the wound healing process. However, these NPs can have toxic effects as therapy in humans. Optimization of ZnO NPs concentration to nonhazardous levels without changing their functional properties would diminish the cytotoxic effect of this system. This issue can be achieved by their incorporation into a polymeric matrix for their wound dressing application. Nanofibers have been received great attention as a scaffold

Chapter 6: Synthesis and characterization of hybrid PHBV-PEO-ZnO microfibers prepared by using the electrospinning technique

in tissue engineering because of structural resemblance to the extracellular matrix and high surface area to volume ratio. Among all methods for the synthesis of nanofibers, electrospinning technique is a simple, cheap and versatile method. So it is widely used to design nanofibers for different applications. Zinc is an essential trace element that found as a cofactor in many enzymes. Nanoform zinc such as ZnO NPs has been widely studied for applications in wound healing. The production of ROS species, cell migration and adhesion ability help in the wound healing process by activating growth factor mediated pathways.¹²⁻¹⁴

6.2.3 Synthesis procedure

6.2.3.1 Preparation of PHBV-PEO-ZnO electrospinning solution

The 10% of the polymer solution containing PHBV and PEO (8:2) was prepared and kept on magnetic stirrer overnight.¹⁵ This solution was mixed with previously prepared ZnO NPs¹⁶ with different concentrations of (0, 1, 3, and 5wt %) in chloroform solutions and kept for sonication for 1 hour. The final solutions were kept for stirring for 12 hours before the electrospinning process.

6.2.3.2 Electrospinning process

The PHBV-PEO-ZnO microfibers were prepared by the electrospinning process with slight modifications.¹⁷ The conditions used as: the applied voltage as 10 kV, the feeding rate as 0.3ml/h, and tip-collector distance as 14 cm. The solution was filled in a 10ml syringe equipped with a metallic needle (0.70×38mm) and rectangular steel plate covered with aluminum foil paper was used as a collector. The schematic representation of electrospinning process is given in figure 6.1.

Chapter 6: Synthesis and characterization of hybrid PHBV-PEO-ZnO microfibers prepared by using the electrospinning technique

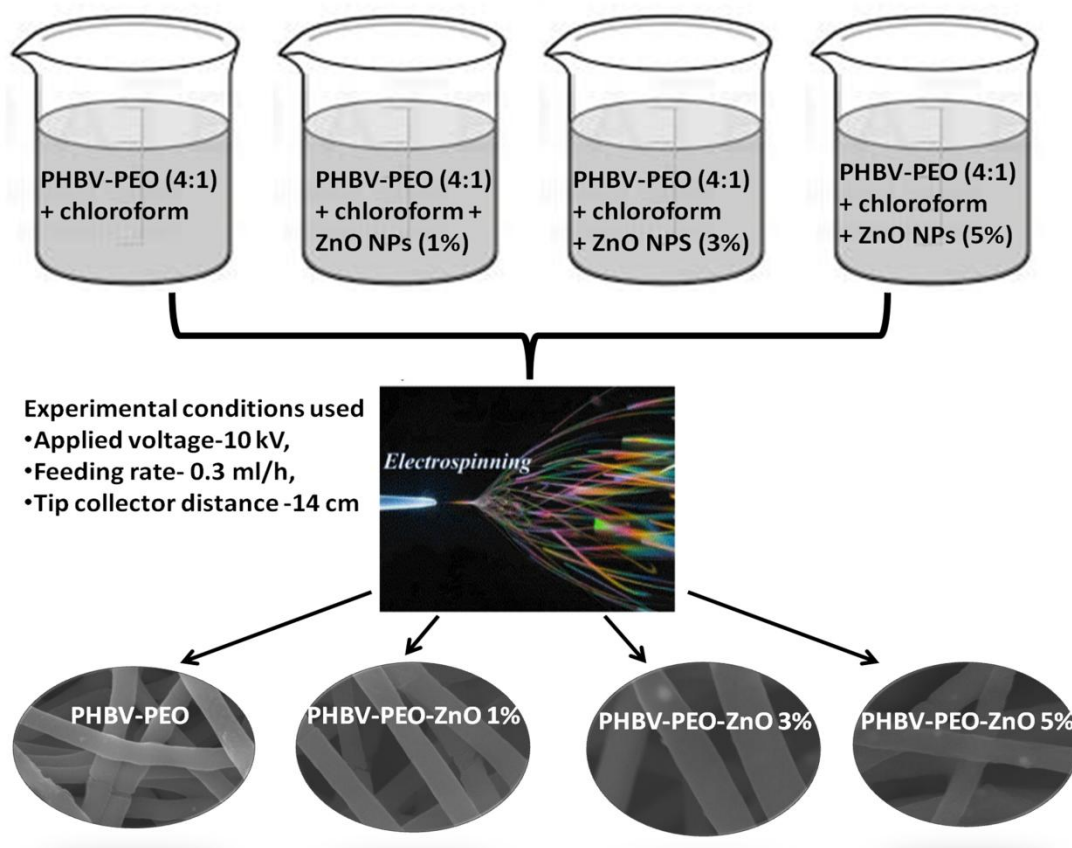


Figure 6.1: Schematic representation for preparation of PHBV-PEO-ZnO nanofibers through the electrospinning process (Polymer ratio PHBV:PEO, 4:1 is kept constant and ZnO NPs concentration is varied as 1, 3 and 5 by wt% , Conditions used for electrospinning process are, applied voltage 10kV, feeding rate 0.3ml/h, tip-collector distance 14cm).

6.2.3.3 Characterization of prepared microfibers

6.2.3.3.1 Spectroscopic analysis

The functional groups present on synthesized microfibers were examined by using Fourier transform infrared spectroscopy (FTIR). FTIR spectra were observed on [PerkinElmer, Spectrometer I, FTIR diffused reflectance (DRIFT) mode, USA] in the range of $4000\text{--}400\text{cm}^{-1}$.

6.2.3.3.2 Morphological analysis

The morphology of the electrospun microfibers was studied by SEM (scanning electron microscopy), model (Micro Analysis System and Model Phoenix, Cambridge, England, U.K.).

6.2.3.3.3 Elemental analysis

Chapter 6: Synthesis and characterization of hybrid PHBV-PEO-ZnO microfibers prepared by using the electrospinning technique

Elemental investigation of the microfibers was performed by the EDX which was connected to the scanning electron microscope.

6.2.3.3.4 Thermal analysis

The thermal properties were studied by TGA (thermogravimetric analysis), model SDT model Q600 of TA Instruments Inc., USA, under the continuous flux of nitrogen at 100 mL/min. Differential scanning calorimetry (DSC) was investigated by using model Q10 DSC, TA Instruments, New Castle, DE, USA. The measurements were performed at a heating rate of 10°C/min in 25-600°C.

6.2.3.3.5 Mechanical Properties

The mechanical properties of prepared microfibers were studied by the dynamic mechanical analyzer (RSA3, TA Instruments, USA) at ambient temperature. Electrospun mats were cut into $20 \times 0.5 \text{ cm}^2$ wide shape. The tensile strength, Young's modulus, and elongation at break were determined.

6.2.3.3.6 Swelling studies

The swelling studies of PHBV-PEO-ZnO microfibers were carried out by a previously reported method.¹⁸ It was analyzed by placing a known weight of nanofiber mat in phosphate buffer saline (pH 7.4) at 37°C. These mats are removed from the medium after 24 hours. The percentage of the degree of swelling was calculated by using equation 3.7 given in chapter 3.

6.3 Results and discussion

6.3.1 Spectroscopic analysis

The functional groups present on PHBV-PEO-ZnO microfibers are analyzed by FTIR. ATR-FTIR spectra of PHBV/PEO electrospun fibers with different concentration of ZnO NPs is given in figure 6.2 (I) and (II). As per literature reports, for all PHBV/PEO electrospun fibers, the peak at 1722 cm^{-1} depicts the stretching band of ester group $\text{C}=\text{O}$.¹⁰ The spectrum of ZnO shows a broad peak at the center of 3450 cm^{-1} is attributed to the stretching of hydrogen bonded $-\text{OH}$ groups on the nanoparticle surface. The peak becomes more intense than that of PHBV/PEO which is in agreement with increasing concentration of ZnO nanoparticles.¹⁹

Chapter 6: Synthesis and characterization of hybrid PHBV-PEO-ZnO microfibers prepared by using the electrospinning technique

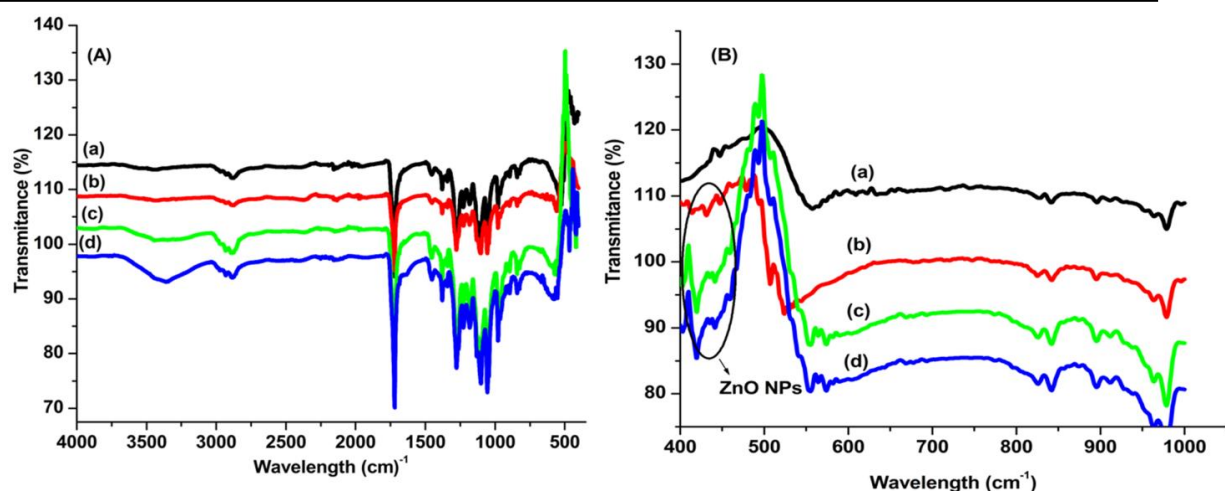


Figure 6.2: (A) FTIR spectra of PHBV/PEO electrospun fiber with different concentration of ZnO nanoparticles in 400-4000 cm^{-1} range, (B) FTIR spectra of PHBV/PEO electrospun fiber with different concentration of ZnO nanoparticles in 400-1000 cm^{-1} range (a) PHBV-PEO, (b) PHBV-PEO-ZnO (1 Wt %), (c) PHBV-PEO-ZnO (3 Wt %), (d) PHBV-PEO-ZnO (5Wt%)

The spectrum of ZnO shows a broad peak at the center of $\sim 3450\text{cm}^{-1}$ which is attributed to hydrogen-bonded $-\text{OH}$ groups stretching that become more intense with the increased percentage of ZnO NPs in PHBV-PEO microfibers. The sharp peak appears at $\sim 440\text{cm}^{-1}$ attributed to the stretching of the Zn-O bond that is increased with an increase in the percentage of ZnO NPs.²⁰ The peaks at around 2930cm^{-1} correspond to asymmetric and symmetric stretching of $-\text{CH}_2$ and intense peak at 1731cm^{-1} assigned to $\text{C}=\text{O}$ stretching of ester group;¹⁹ the peaks at 1280cm^{-1} and 1262cm^{-1} are attributed to asymmetric and symmetric stretching of $\text{C}-\text{O}-\text{C}$; peaks at 1133cm^{-1} and 1100cm^{-1} are assigned to asymmetric and symmetric stretching of $\text{C}-\text{O}$; peak at 1232cm^{-1} thought to be $-\text{CH}_3$ vibration; peak at 1187cm^{-1} depicts $\text{C}-\text{O}-\text{C}$ stretching and peak at 1055cm^{-1} is assigned to $\text{C}-\text{O}$ stretching and CH_2 rocking.^{21,22} The frequency range and related functional groups are given in table 6.1.

Chapter 6: Synthesis and characterization of hybrid PHBV-PEO-ZnO microfibers prepared by using the electrospinning technique

Table 6.1: FTIR analysis of PHBV-PEO and PHBV-PEO-ZnO microfibers (1,3 and 5 wt% of ZnO NPs)

Frequency Range (cm^{-1})	Functional groups
3450	-OH stretching
2890-2980	Symmetric and asymmetric stretching of $-\text{CH}_2$ group
1722, 1731	Stretching of ester group $\text{C}=\text{O}$
1262, 1280	Symmetric and asymmetric stretching of $\text{C}-\text{O}-\text{C}$
1232	$-\text{CH}_3$ vibration
1187	$\text{C}-\text{O}-\text{C}$ stretching
1100, 1133	Symmetric and asymmetric stretching of $\text{C}-\text{O}$
1055	Stretching vibration of $\text{C}-\text{O}$
440	Stretching of $\text{Zn}-\text{O}$

6.3.2 Morphological analysis

Typical morphologies of PHBV-PEO (4:1) and PHBV-PEO reinforced with various concentrations of ZnO are shown in figure 6.3. It is observed that as compared to PHBV-PEO microfibers, ZnO reinforced microfibers possess a slightly higher diameter. PHBV-PEO hybrid microfibers obtained have diameter of 2.04-2.2 μm , whereas all other microfibers with different ZnO concentrations showed diameter of 2.2-3.1 μm .

Chapter 6: Synthesis and characterization of hybrid PHBV-PEO-ZnO microfibers prepared by using the electrospinning technique

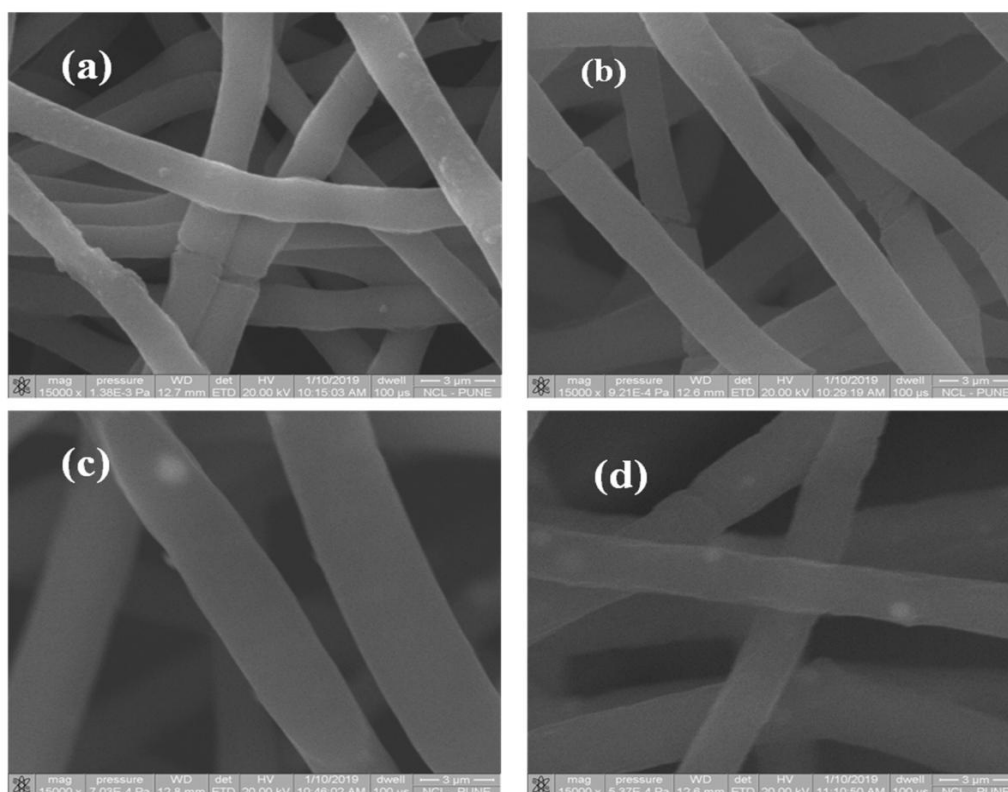


Figure 6.3: SEM images of PHBV-PEO (a) and microfibers reinforced with ZnO of 1 wt% (b), 3% (c), and 5% (d)

It is noted that the diameter distribution of microfibers become wider upon the addition of ZnO nanoparticles with uniform morphology. It is also revealed that with an increase in ZnO contents, the fiber diameter increased from to 3% concentration of ZnO nanoparticles and reduced for 5% concentration of ZnO NPs. This reduction in diameter of microfibers may be due to increased electric field because of increased charge density, the conductivity of electrospinning solution during the electrospinning process.²³

6.3.3 Elemental analysis

The elemental analysis of PHBV-PEO and ZnO reinforced PHBV-PEO microfibers are performed by Energy Dispersive X-ray (EDX).

Chapter 6: Synthesis and characterization of hybrid PHBV-PEO-ZnO microfibers prepared by using the electrospinning technique

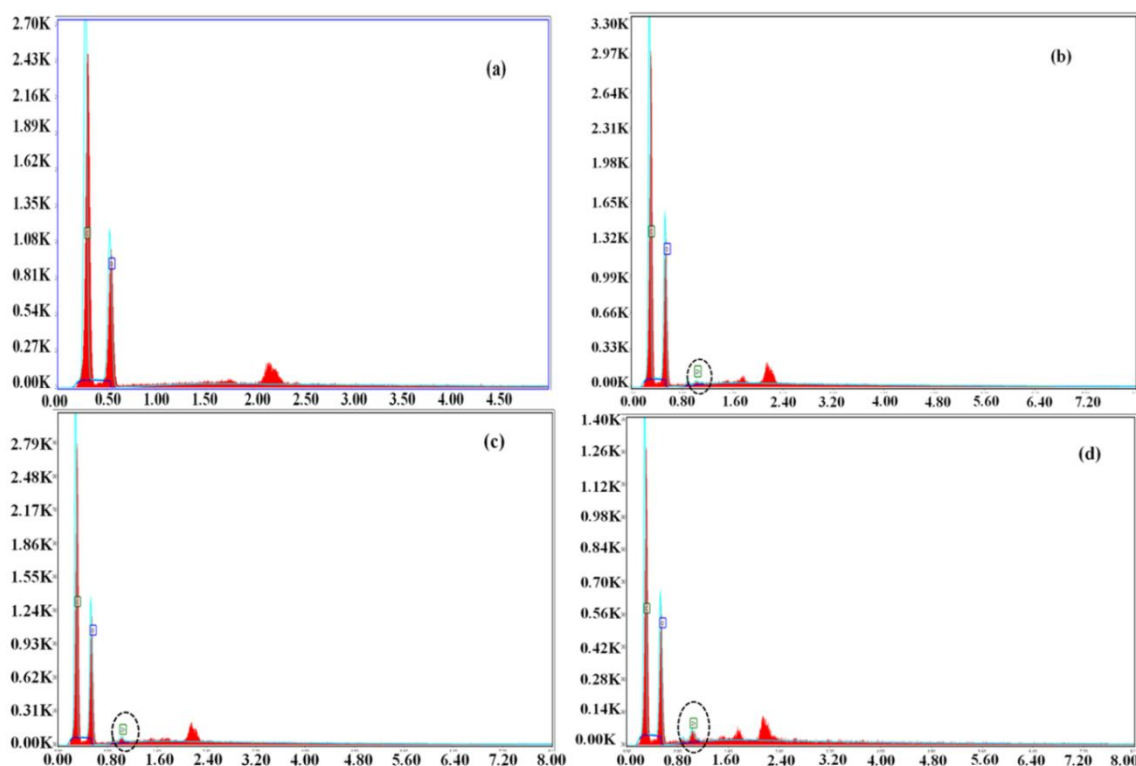


Figure 6.4: EDX spectra of PHBV-PEO (a), PHBV-PEO-ZnO 1wt% (b), PHBV-PEO-ZnO 3wt% (c) and PHBV-PEO-ZnO 5wt% (d)

It is revealed that Zinc and oxygen are present. EDX results confirmed the successful incorporation of ZnO NPs in PHBV-PEO microfibers. Also, it can be revealed that the percentage of ZnO NPs is increased from PHBV-PEO to 5 wt % of PHBV-PEO-ZnO microfibers. The increasing peaks of Zn from 1wt% to 5wt% of PHBV-PEO-ZnO microfibers confirms the successful incorporation of ZnO NPs in increasing amount from 1wt% to 5wt% in PHBV-PEO microfibers. The EDX spectra for respective microfibers are shown in figure 6.4.

6.3.4 Thermal analysis

Thermal analysis is performed by using thermogravimetric analysis (TGA). Figure 6.5 shows two distinguishable thermal decomposition peaks correspond to PHBV-PEO-ZnO components. The analysis is done at a heating rate of 10°C/min in 25-600°C. It is observed that PHBV-PEO-ZnO fibers showed two weight losses. Two successive decompositions are observed in all samples. The first decomposition weight loss is in range of 215-310°C and second weight

Chapter 6: Synthesis and characterization of hybrid PHBV-PEO-ZnO microfibers prepared by using the electrospinning technique

loss is in range of 345-417°C. The temperature of the maximum weight loss is 220-262°C and 373-410°C respectively. PHBV-PEO displayed approximately 86% of initial mass loss and it is attributed to the degradation of polymer themolecule.¹⁵ No significant weight loss is observed at 100°C which shows the absence of water molecules in fiber composition. Functionalisation of fibers with ZnO NPs with ZnO showed ~ 80%, ~83% and ~ 89% of weight loss for 1%, 3% and 5% ZnO NPs respectively. As the percentage of ZnO NPs increases, the degradation temperature of microfibers also increases. The shifting of the curve of PHBV-PEO microfibers to the high temperature suggests better thermal stability, which may be due to the crystalline structure of NPs.^{24,25}

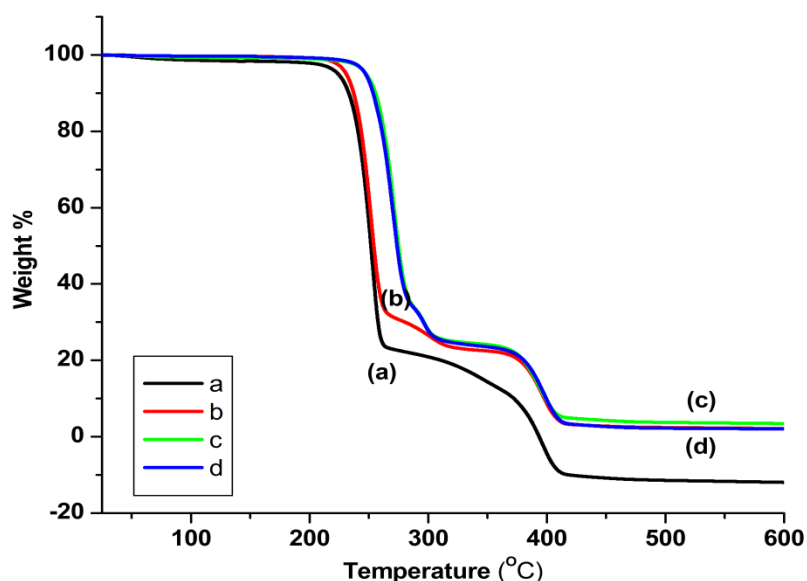


Figure6.5: TGA curves of (a) PHBV-PEO, (b) PHBV-PEO-ZnO (1 Wt %) , (c) PHBV-PEO-ZnO (3 Wt %), and (d) PHBV-PEO-ZnO (5%).²⁶

It is very important to study the crystallization and melting behavior of polymer nanocomposite as it affects on the crystalline structure, morphology and macroscopic properties of the materials. Non-isothermal melt crystallization of PHBV-PEO and their nanocomposites is studied by DSC analysis, and their cooling and heating thermograms are shown in figure 6.6(A), (B) respectively. The thermal parameters obtained from DSC curves are collected in table 6.2. In DSC thermograms, ZnO crystallization peak is not detectable due to the low amount in the blend.²⁷ With the increase in ZnO content new melt crystallization temperature is slowly

Chapter 6: Synthesis and characterization of hybrid PHBV-PEO-ZnO microfibers prepared by using the electrospinning technique

decreases which shows the addition of ZnO decreases crystallization rate of PHBV-PEO.²⁸ Appearance of 1st melting peak is around 40°C and 2nd melting peak around 95°C for all samples suggests that addition of ZnO does not affect main crystal structure and lamellar size. The intensity of the 2nd melting peak is decreased as compared with PHBV-PEO due to decreased mobility of polymer chains. With an increase in the ZnO content, T_{m2} for PHBV and PEO is slightly shifted towards a lower degree. The PHBV-PEO and PHBV-PEO-ZnO composites exhibit similar cooling scans decreasing crystallization enthalpy (ΔH_c) and T_c with ZnO addition, suggesting decreasing degree of crystallization of PHBV-PEO.²⁹ In the first heating process of DSC, it is observed that T_m does not affect significantly before and after the incorporation of ZnO NPs.

Table6.2: Melting temperature (T_m), crystallization temperature (T_c), melting enthalpy (ΔH_m), crystallization enthalpy (ΔH_c), and crystallinity degree (χ) of PHBV-PEO and PHBV-PEO-ZnO microfibers.

Sample	First Heating						First Cooling				Second heating		
	T _{m1} (^o C)		ΔH m(J/g)		X ₁ (%)		T _c 1 (^o C)		ΔH _{c1} (J/g)		T _{m2} (^o C)		
	PEO	PHB V	PEO	PHB V	PEO	PH B V	PE O	PHB V	PEO	PHB V	PEO	PH BV	
												m21	m22
PHBV-PEO	61	60	6	9	3	5	9	5	7	8	1	49	57
PHBV-PEO- ZnO (1%)	2	61	7	0	3	6	1	6	4	0	0	46	56
PHBV-PEO- ZnO (3%)	2	59	0	3	0	0	6	5	2	2	0	46	57
PHBV-PEO- ZnO (5%)	3	60	9	0		7	4	6	1	9	1	46	58

From these results, it is observed that the addition of ZnO NPs does not affect the basic crystalline structure of microfibers. The relative crystallinity lowers after the addition of ZnO

Chapter 6: Synthesis and characterization of hybrid PHBV-PEO-ZnO microfibers prepared by using the electrospinning technique

NPs confirming that they behave as a retarding agent for the crystallization in the electrospun microfibers.

Many studies reported that the crystallinity of the polymer matrix increases with addition of nanomaterials which acts as a nucleating agent. Here in this study, the crystallinity of the electrospun microfibers does not increase after the addition of ZnO NPs but it decreases. Yu et al.²⁷ suggested the retarding effect of the addition of ZnO particles on the crystallization of PHBV-nanofibers and showed null effect on T_m value. This observation is attributed to the hydrogen bonds formation between ZnO and PHBV, disturbing PHBV chains mobility and decreasing crystallinity.

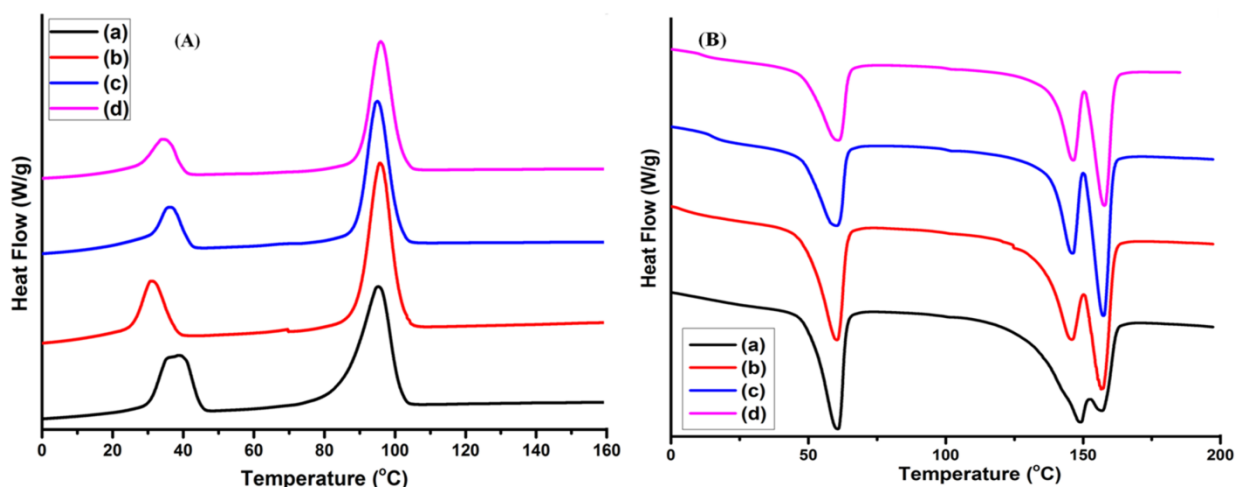


Figure 6.6: DSC thermogram of (a) PHBV/PEO, (b) PHBV/PEO/ZnO (1 Wt %), (c) PHBV/PEO/ZnO (3 Wt %), (d) PHBV/PEO/ZnO (5%) (A) heating scan, (B) cooling scan.

6.3.5 Mechanical properties

The room temperature static mechanical properties of PHBV-PEO-ZnO microfibers are evaluated and represented in figure 6.7. Their values of the tensile strength (σ_y), Young's modulus (E) and elongation at break (ϵ_b) are plotted as a function of ZnO concentration in figure 6.7 A-C. From these results, it can be concluded that mechanical properties are mainly affected by the presence of ZnO NPs. ZnO NPs might have a role in effective stress transfer through the polymer matrix as tensile strength is observed to increase with ZnO addition into PHBV-PEO matrix. Young's modulus values are reduced slightly with increased addition of ZnO NPs. The

Chapter 6: Synthesis and characterization of hybrid PHBV-PEO-ZnO microfibers prepared by using the electrospinning technique

addition of ZnO into the PHBV-PEO matrix remarkable increased elongation break. These results are in good agreement with the DSC findings since lower crystallinity is related to higher ductility. In general, mechanical properties of fibers are affected by factors such as the interaction between ZnO and PHBV-PEO, fiber diameter and porosity.³⁰

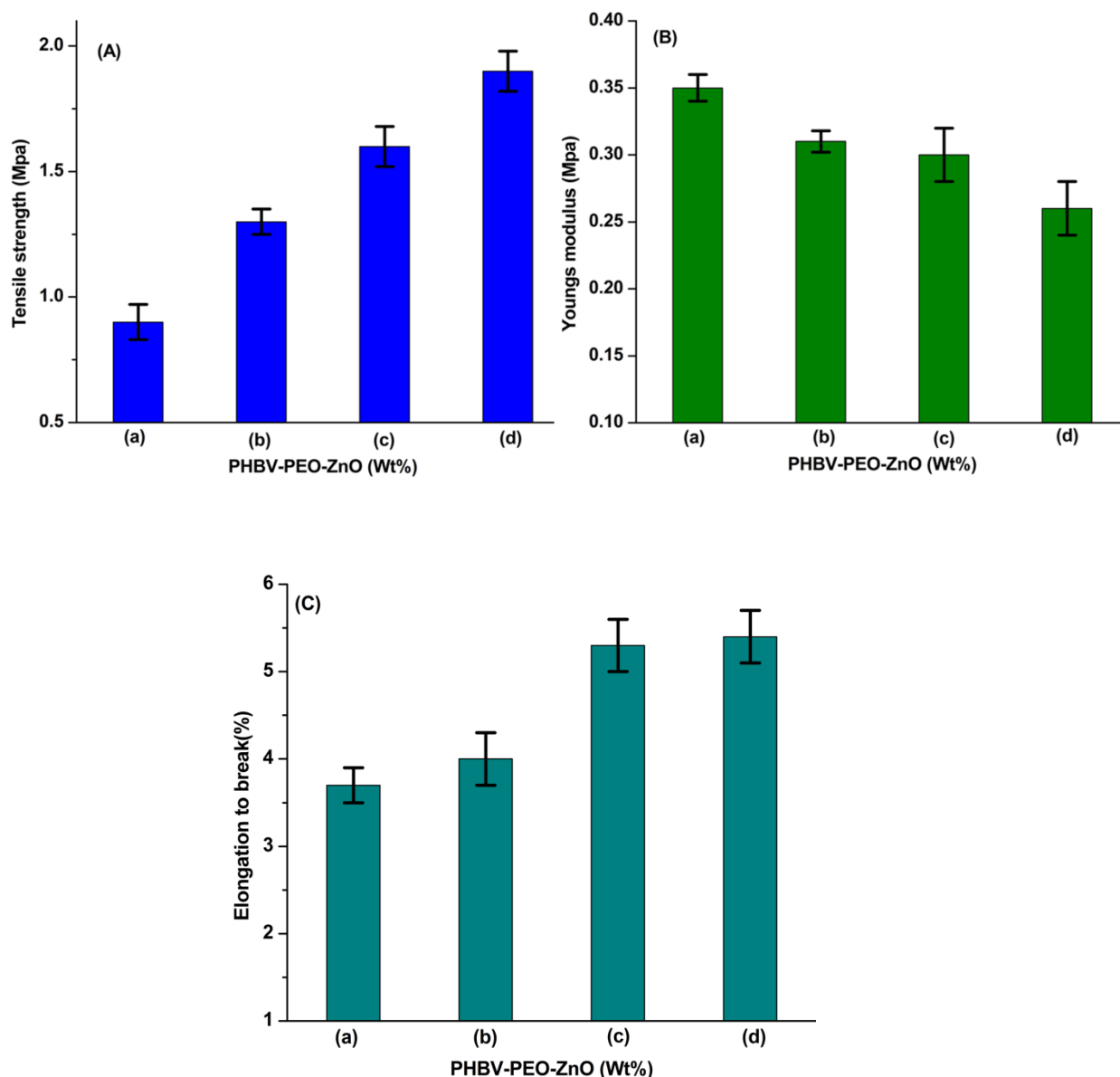


Figure 6.7 : Mechanical properties of (a) PHBV-PEO, (b) PHBV-PEO-ZnO (1 wt %), (c) PHBV-PEO-ZnO (3 wt %), and (d) PHBV-PEO-ZnO microfibers (5 wt %). (A) tensile strength, (B) Young's modulus, and (C) elongation to break

Chapter 6: Synthesis and characterization of hybrid PHBV-PEO-ZnO microfibers prepared by using the electrospinning technique

6.3.6 Swelling behavior

Figure 6.8 shows the percentage of weight gain of PHBV-PEO MFs, 1% ZnO-PHBV-PEO MFs, 3% ZnO-PHBV-PEO MFs and 5% ZnO-PHBV-PEO MFs. PHBV-PEO microfibers showed higher percentage of weight gain than PHBV-PEO-ZnO microfibers. The addition of ZnO NPs slightly reduces the percentage of weight gain as microfibers with ZnO had lower porosity than PHBV-PEO microfibers. This can be attributed to the fiber diameter. The fibers with the finest diameter showed maximum swelling and fibers with thicker diameter showed relatively poor swelling.²⁰

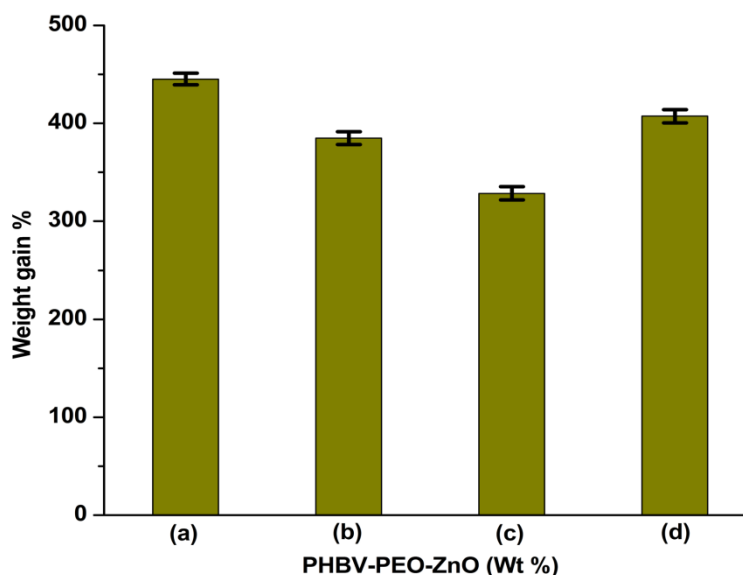


Figure 6.8: Percentage of weight gain of (a) PHBV-PEO, (b) PHBV-PEO-ZnO (1 wt %), (c) PHBV-PEO-ZnO (3 wt %), (d) PHBV-PEO-ZnO microfibers(5 wt %)

The results concluded that 1 and 5wt% NFs have good uptake capacity than other 3% of ZnO microfibers.³¹

6.4 Effect of reinforcement of ZnO NPs in PHBV-PEO microfibers

For the electrospinning process, the solution of PHBV-PEO and ZnO at different concentrations i.e. 1, 3, and 5% are taken in chloroform solution. The ratio of PHBV-PEO (4:1) for all samples is kept constant. The FTIR spectra of all samples show that the functional groups

Chapter 6: Synthesis and characterization of hybrid PHBV-PEO-ZnO microfibers prepared by using the electrospinning technique

are present in microfibers. The morphological analysis reveals that with the addition of ZnO NPs, the diameter is increased upto 3% of ZnO, while for 5% of ZnO NPs it is slightly reduced. This reduction in diameter of microfibers may be due to excess addition of ZnO NPs that increased charge density and the conductivity of electrospinning solution. The addition of ZnO NPs affected the mechanical properties of PHBV-PEO microfibers. It may have a role in effective stress transfer across the polymer matrix since the tensile strength is increased. It also increases the percentage of elongation break. However, Young's modulus is decreased with increased concentration of ZnO NPs. These results are with correspondence with DSC findings. The effect of ZnO on swelling behavior is that the addition of ZnO increased the fiber diameter. So, the swelling ratio is lowered with an increase in ZnO NPs concentration.

6.5 Conclusions

The high surface area of ZnO reinforced PHBV-PEO microfibers provide potential dressing material for antibacterial wound dressing. The ZnO NPs which were previously prepared with least particle size and maximum antibacterial activity is incorporated into PHBV-PEO microfibers. In FTIR analysis the increased order in the intensity of peaks at $\sim 440\text{ cm}^{-1}$ assigned to the stretching of Zn-O bond confirms the successful addition of ZnO NPs in increasing order in PHBV-PEO microfibers. Other peaks were also in agreement with the presence of functional groups of ZnO, PHBV and PEO showing the proper blending of PHBV-PEO-ZnO in microfibers. The SEM analysis showed that ZnO reinforced microfibers exhibit slightly higher diameter (2.2-3.1 μm). The change in fiber diameter confirms the successful reinforcement of ZnO NPs into PHBV-PEO microfibers. The elemental analysis was carried out by EDX spectroscopy which shows that synthesized microfibers are impurity-free, suggesting incorporation of ZnO NPs into PHBV-PEO matrix. Absence of any other peak showed the purity of microfibers. The TGA analysis showed the better thermal stability of PHBV-PEO-ZnO microfibers as compared with PHBV-PEO microfibers highlighting the role of ZnO NPs for thermal stability. The DSC analysis showed the retarding effect of ZnO NPs on the crystallization behavior of PHBV-PEO polymers. The mechanical properties i.e. tensile strength and percentage of elongation break increased and Young's modulus decreased with increased concentration of ZnO NPs. The swelling ratio slightly decreased with an increase in the

Chapter 6: Synthesis and characterization of hybrid PHBV-PEO-ZnO microfibers prepared by using the electrospinning technique

concentration of ZnO NPs. The fibers with finest diameter showed the maximum swelling and fibers with thicker diameter showed relatively poor swelling. From this analysis it can be concluded that the microfiber and microfibers with 1 and 5% of ZnO NPs will have good uptake capacity of exudates as compared with 3 wt% of PHBV-PEO microfibers. The obtained results promote the use of ZnO-PHBV-PEO microfibers for further wound dressing applications.

Chapter 6: Synthesis and characterization of hybrid PHBV-PEO-ZnO microfibers prepared by using the electrospinning technique

References

- 1 Y. Xu, L. Zou, H. Lu, Y. Wei, J. Hua and S. Chen, *J. Mater. Sci.*, 2016, **51**, 5695–5711.
- 2 Y. M. Lvov, P. Pattekari, X. Zhang and V. Torchilin, *Langmuir*, 2011, **27**, 1212–1217.
- 3 A. Kumar and M. Gupta, *Biomaterials*, 2005, **26**, 3995–4021.
- 4 N. Padmavathy and R. Vijayaraghavan, *Sci. Technol. Adv. Mater.*, 2008, **9**, 1–7.
- 5 A. Khalid, R. Khan, M. Ul-islam, T. Khan and F. Wahid, *Carbohydr. Polym.*, 2017, **164**, 214–221.
- 6 C. H. Li, C. C. Shen, Y. W. Cheng, S. H. Huang, C. C. Wu, C. C. Kao, J. W. Liao and J. J. Kang, *Nanotoxicology*, 2012, **6**, 746–756.
- 7 P. Kuppan, S. Sethuraman and U. M. Krishnan, *J. Biomater. Sci. Polym. Ed.*, 2014, **25**, 574–593.
- 8 A. M. Díez-pascual and A. L. Díez-vicente, 2014, 10950–10973.
- 9 N. Nagiah, L. Madhavi, R. Anitha, C. Anandan, N. T. Srinivasan and U. T. Sivagnanam, *Mater. Sci. Eng. C*, 2013, **33**, 4444–4452.
- 10 Y. Xu, L. Zou, H. Lu and T. Kang, *RSC Adv.*, 2017, **7**, 4000–4010.
- 11 A. Greiner and J. H. Wendorff, *Angew. Chemie - Int. Ed.*, 2007, **46**, 5670–5703.
- 12 P. R. Kumar, N. Khan, S. Vivekanandhan, N. Satyanarayana, A. K. Mohanty and M. Misra, *J. Nanosci. Nanotechnol.*, 2012, **12**, 1–25.
- 13 S. K. Nethi, S. Das, C. R. Patra and S. Mukherjee, *Biomater. Sci.*, 2019, **7**, 2652–2674.
- 14 R. Naphade and J. Jog, *Fibers Polym.*, 2012, **13**, 692–697.
- 15 A. Bianco, M. Calderone and I. Cacciotti, *Mater. Sci. Eng. C*, 2013, **33**, 1067–1077.
- 16 P. P. Mahamuni, P. M. Patil, M. J. Dhanavade and M. V Badiger, *Biochem. Biophys. Reports*, 2019, **17**, 71–80.
- 17 A. L. Rivera-Briso and Á. Serrano-Aroca, *Polymers (Basel)*, 2018, **10**, 1–28.
- 18 N. Killi, A. T. Pawar and R. V. N. Gundloori, *ACS Appl. Bio Mater.*, 2019, **2**, 3341–3351.
- 19 X. Hu, S. Liu, G. Zhou, Y. Huang, Z. Xie and X. Jing, *J. Control. Release*, 2014, **185**, 12–21.
- 20 M. J. Fabra, A. M. Pourrahimi, R. T. Olsson and J. M. Lagaron, *Food Bioprod. Process.*, 2016, **101**, 32–44.
- 21 G. Kim, G. H. Michler, S. Henning, H. Radusch and A. Wutzler, *J. Appl. Polym. Sci.*,

Chapter 6: Synthesis and characterization of hybrid PHBV-PEO-ZnO microfibers prepared by using the electrospinning technique

- 2006, **103**, 1860–1867.
- 22 Y. Ding, J. A. Roether, A. R. Boccaccini and D. W. Schubert, *Eur. Polym. J.*, 2014, **55**, 222–234.
- 23 H. Joo and M. Otto, *Chem. Biol.*, 2012, **19**, 1503–1513.
- 24 A. V. Kabashin and M. Meunier, *J. Appl. Phys.*, 2003, **94**, 7941–7943.
- 25 P. Blandin, K. A. Maximova, M. B. Gongalsky, J. F. Sanchez-Royo, V. S. Chirvony, M. Sentis, V. Y. Timoshenko and A. V. Kabashin, *J. Mater. Chem. B*, 2013, **1**, 2489–2495.
- 26 P. P. Mahamuni-Badiger, P. M. Patil, P. R. Patel, M. J. Dhanavade, M. V. Badiger, Y. N. Marathe and R. A. Bohara, *New J. Chem.*, , DOI:10.1039/d0nj01384f.
- 27 W. Yu, C. Lan, S. Wang, P. Fang and Y. Sun, *Polymer (Guildf)*., 2010, **51**, 2403–2409.
- 28 A. M. Díez-Pascual and A. L. Díez-Vicente, *Int. J. Mol. Sci.*, 2014, **15**, 10950–10973.
- 29 M. Öner, A. A. Çöl, C. Pochat-Bohatier and M. Bechelany, *RSC Adv.*, 2016, **6**, 90973–90981.
- 30 T. Bekat and M. Oner, *Pure Appl. Chem.*, 2017, **89**, 89–96.
- 31 S. H. Pawar, P. P. Patil, R. A. Bohara, S. G. Nanaware and J. V. Meshram, *Int. J. Biol. Macromol.*, 2018, **122**, 1305–1312.

CHAPTER 7

Antibacterial, antibiofilm and biocompatibility studies of PHBV-PEO-ZnO microfibers



ROYAL SOCIETY
OF CHEMISTRY

IF 3.2

rsc.li/njc

1 of 35

New Journal of Chemistry

View Article Online
DOI: 10.1039/D0NJ01384F

Electrospun poly (3-hydroxybutyrate-co-3-hydroxyvalerate)/Polyethylene oxide (PEO) microfibers reinforced with ZnO nanocrystals for antibacterial and antibiofilm wound dressing applications

Pranjali P. Mahamuni-Badiger¹, Pooja M. Patil¹, Pratiksh Kumar R. Patel², Maruti J. Dhanavade³,
Manohar V. Badiger², Yogesh N. Marathe², Raghvendra A. Bohara^{1,4*}

"It is not the possession of truth, but the success which attends the seeking after it, that enriches the seeker and brings happiness to him." -Max Planck

Chapter 7: Antibacterial, antibiofilm and biocompatibility studies of PHBV-PEO-ZnO microfibers

7.1 Introduction

Skin is the largest organ in the human body that works as a protective barrier from the harmful physical and chemical environments and adhesion of bacteria. Skin and soft tissue infections (SSTIs) are a very commonly occurring infections.¹ It is reported that about 14 million people every year get affected by SSTIs in the United States. Gram-positive cocci such as *S. aureus*, *S. epidermis*, *Streptococcus* and Gram-negative bacilli like *E. coli*, *P. aeruginosa*, *K. pneumonia* and *Proteus* species are most common pathogens isolated from the wounds.^{2,3} As previously reported, *S. aureus* is most common wound- infecting Gram positive multiple drug resistant bacteria causing hospital-acquired and community-acquired infections.⁴ Another common Gram negative bacteria *P. aeruginosa* that occur in wound infections has been detected to be resistant to the variety of antibiotics.⁵ In a normal human being, the infection can be cured by the immune system by diminishing invaded pathogens. However, if the immune system is weak and unable to clear pathogens then infection persists and results in physiological damage like damage of granulation tissues, growth factors, and extracellular components that interfere in the general process of wound healing process.⁶ Therefore, it is crucial to develop wound dressing material that can prevent bacterial adhesion or inhibit bacterial growth.⁷

Inorganic metal oxide nanoparticles have attracted significant attention due to their significant antibacterial activity. Until now, ZnO NPs have been widely used as an antibacterial agent.⁸ However, the intensity of antibacterial activity is size dependent. It is inversely proportional to the size of the nanoparticle.⁹ For their application in wound healing ZnO NPs must be incorporated into an appropriate polymer. The electrospun fibers are extensively used in different medical applications like tissue engineering, drug release, wound healing, and fabrication of antimicrobial agents that contain biopolymer nanofibers.^{10,11}

In the present chapter, we have studied PHBV-PEO and PHBV-PEO-ZnO (1, 3, and 5 wt% of ZnO NPs) microfibers for their antibacterial, antibiofilm and biocompatible properties.

7.2 Experimental

7.2.1 Reagents and materials

Chapter 7: Antibacterial, antibiofilm and biocompatibility studies of PHBV-PEO-ZnO microfibers

All glasswares were rinsed by using distilled water and sterilized in an autoclave at 121⁰C for 20 minutes before use. The two bacteria Gram-positive *S. aureus* and Gram-negative *P. aeruginosa* were used as test organisms for antibacterial and antibiofilm activity. All media used in this experiment were purchased from Himedia laboratories.

7.2.2 Determination of Antibacterial activity

The disc diffusion method was used to evaluate the antibacterial activities of synthesized microfibers against pathogenic bacteria Gram positive *Staphylococcus aureus* (NCIM 2654) and Gram negative *Pseudomonas aeruginosa* (NCIM 5032). In this method, bacterial cultures were used which was obtained by growing bacteria on nutrient agar medium for overnight. 100 µl of cell suspension of culture was poured on the agar plates with the help of the sterile glass spreader. The discs of microfibers were kept under UV light for half an hour for the sterilization purpose. Then, discs were placed on the surface of agar plates with the help of sterile forceps. Then the plates were kept for incubation at 37⁰C for 24 hours. After 24 hours incubation, the zones of inhibition were observed on the plates and measured in mm.¹²

7.2.3 Determination of antibiofilm activity

Determination of antibiofilm activity of PHBV-PEO-ZnO microfibers against Gram-positive bacteria (*Staphylococcus aureus*) (NCIM 2654) and Gram-negative bacteria (*Pseudomonas aeruginosa*) (NCIM 5032) was performed by previously reported method with slight modifications.⁹ These bacteria were inoculated in the sterile tryptic soy broth and incubated for 24h at 37⁰C. Synthesized membranes were sterilized with the help of 99% ethanol. Then membranes were allowed to dry inside laminar airflow aseptically and transferred to sterile 24 well plates that contain 1.5ml of sterile nutrient broth. 150 µl of bacterial suspension from the log phase was added to the wells containing sterile tryptic soy broth. The microtiter plate was incubated at 37⁰C for successive three days for the biofilm formation. Membrane without ZnO NPs was used as a control. Membranes deeped in sterile media without any bacterial growth were also used as a control. Once biofilm is grown on the membranes, the membranes were carefully transferred to new 24 well plates that contain media and incubated at 37⁰ C. After incubation quantification is performed by crystal violet assay. The biofilm formed on the

Chapter 7: Antibacterial, antibiofilm and biocompatibility studies of PHBV-PEO-ZnO microfibers

membrane was washed three times with sterile PBS buffer (pH 7.4). Then biofilm was stained by 500 μ l of 0.4% crystal violet dye for 15 minutes. Unattached dye was discarded with PBS buffer wash for 3 times. Crystal violet retained by biofilm was solubilized in 500 μ l of 33 % acetic acid and absorption was determined at 620 nm by microtiter plate reader.^{13,14} Percentage of biofilm inhibition was calculated by using equation 3.8 given in chapter 3.

7.2.4 Biocompatibility

7.2.4.1 Hemocompatibility study of synthesized microfibers

A blood sample was collected from goat in a slaughter house and was added in EDTA for stabilization. Density gradient centrifugation was used to separate the RBCs from whole blood. 5ml of whole blood was gently added on the top of 5ml of PBS solution and then allowed for centrifugation at 2000 rpm for 30 min. The supernatant was decanted, and red blood cells were collected. After that, RBCs were rinsed with phosphate buffer saline (pH 7.4) and kept for centrifugation at 2000 rpm for 30 min. A stock solution of RBCs was prepared without serum at 2% (v/v) using phosphate buffer (pH 7.4). After that, 2ml of the diluted RBC solution was added to 2ml eppendorf tubes containing PHBV-PEO and PHBV-PEO-ZnO microfibers (1%, 3%, and 5%). The negative and positive blood samples were prepared in the same way without microfibers and deionized water, respectively. All eppendorf tubes were kept for incubation for 2h at 37°C. After the interval of 30 min, tubes were gently shaken and allowed centrifugation at 1500g for 10 min at room temperature. The PBS supernatant was transferred to another 96 well microtiter plate and hemoglobin (Hb) release was observed spectrophotometrically (OD 550nm) at 541 nm with microtiter plate reader (Tecan). The percentage of hemolysis can be calculated by the considering that 100% RBC lysis takes place in mixing blood with distilled water at 1:1 (v/v) ratio.¹⁵ Hemolytic percentage was calculated by using the equation 5.1 given in chapter 5

7.2.4.2 Cell viability study of Microfibers

The cell viability of all synthesized microfibers was investigated by MTT assay by using mammalian fibroblast L929 cell lines.¹⁶ Microfibers were sterilized under UV light for overnight. Dulbecco's minimal essential medium (DMEM) supplemented with 10% fetal bovine serum (FBS) and 1% antibiotic penicillin (1000U/mL penicillin G), and 100 μ g/mL streptomycin

Chapter 7: Antibacterial, antibiofilm and biocompatibility studies of PHBV-PEO-ZnO microfibers

was used for the culturing of the cells. Then cells with a density of 1×10^4 cells/well with DMEM containing serum were transferred into 96 well plates and incubated overnight in a humidified incubator. The sterilized microfiber mats were transferred in serum-containing media and kept for incubation for 24h, 48h, and 72 h at 37°C. PHBV-PEO microfibers were used as a control. After incubation, the media was discarded. Cells were rinsed with phosphate buffer saline (pH 7.2) and 100 μ L of MTT (0.5mg/mL) prepared in serum-free medium was added to each well and incubated for 4h. Then the medium was discarded and dimethyl sulphoxide (DMSO) was added to each well for solubilization of formazan crystals. The concentration of formazan was investigated by multiwell plate reader at 570 nm absorbance. The cell viability was calculated by using the equation 3.6 given in chapter 3.

7.3 Results and Discussion

7.3.1 Determination of the antibacterial activity of synthesized PHBV-PEO-ZnO microfibers

The application of antibacterial agents is mainly to treat infections and for wound healing. The incorporation of nanoparticles into the polymeric matrix makes them effective biomaterial from toxicological and biocompatibility point of view. The antimicrobial activity of nanoparticles or fibers is because of the high surface/volume ratio.¹⁷ Therefore, in this study ZnO NPs are incorporated into the PHBV-PEO matrix for preparing antibacterial membrane by electrospinning technique. The antibacterial activity of the control sample (PHBV-PEO) and microfibrinous composite membranes with different ZnO NPs concentration are observed by measuring the zones of inhibition of *S.aureus* and *P. aeruginosa* as shown in figure 7.2.

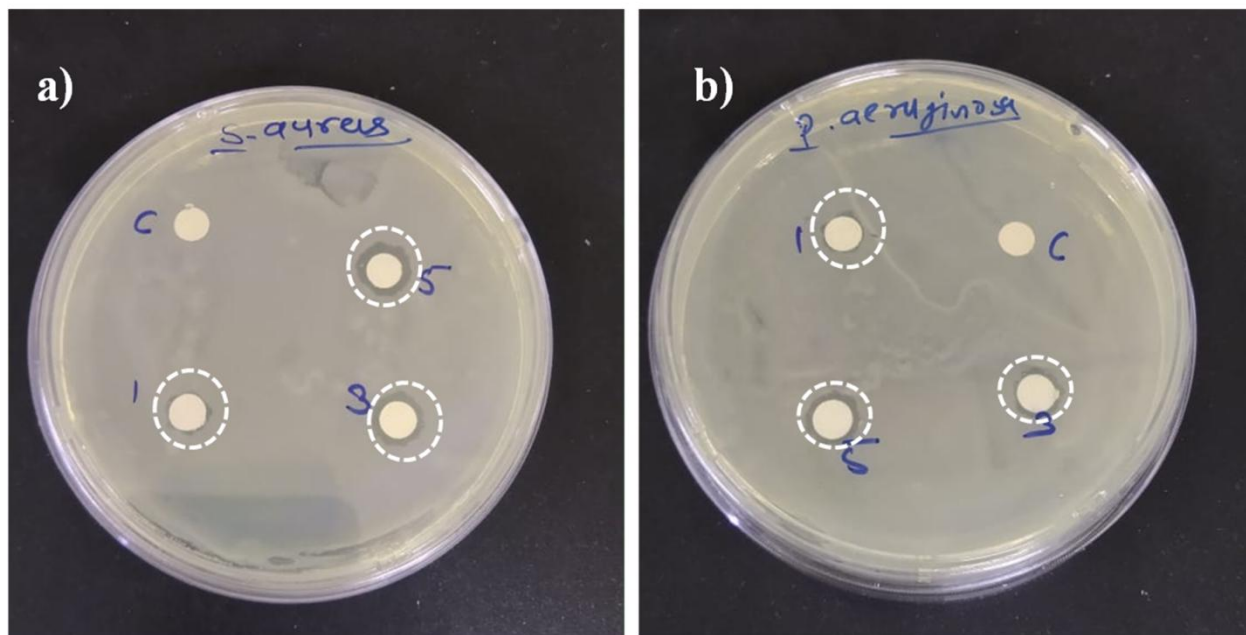


Figure 7.2: Antibacterial activity of (C) PHBV-PEO, PHBV-PEO-ZnO (1%), PHBV-PEO-ZnO (3%), PHBV-PEO-ZnO (5%) microfibers against (A) *S. aureus* (NCIM 2654) and (B) *P. aeruginosa* (NCIM 5032).

The zones of inhibition are given in table 7.1. It can be clearly observed that PHBV-PEO microfiber which is used as a control showed no zone of inhibition, while composite microfibers with 1, 3 and 5% of ZnO NPs showed zone of inhibition against *S. aureus* and *P. aeruginosa* are (1, 3 and 4mm) and (1, 2 and 3mm) respectively. The antimicrobial activity of ZnO NPs has been widely reported in the literature.¹⁸ The mechanism of ZnO Nps antibacterial action in the PHBV-PEO matrix involves the slight contact with the cell wall rather than the penetration that alters the microenvironment, enhancing the solubilization of metal or ROS species that destroy the cell membrane.¹⁹ The maximum antibacterial activity is observed for the samples with 5wt % ZnO.

Chapter 7: Antibacterial, antibiofilm and biocompatibility studies of PHBV-PEO-ZnO microfibers

Table 7.1: Diameters of zone of inhibitions of PHBV-PEO and PHBV-PEO-ZnO (1, 3 and 5wt% of ZnO Nps) against *S. aureus* and *P. aeruginosa*

Sample	Zones of inhibition (in mm)	
	<i>S. aureus</i>	<i>P. aeruginosa</i>
PHBV-PEO	0	0
PHBV-PEO-ZnO (1%)	1	1
PHBV-PEO-ZnO (3%)	3	2
PHBV-PEO-ZnO (5%)	4	3

7.3.2 Determination of antibiofilm activity

Effect of all synthesized PHBV-PEO-ZnO microfibers on biofilm formation of *Staphylococcus aureus* (NCIM 2654) and *Pseudomonas aeruginosa* (NCIM 5032) is shown in figure 7.3. This graph indicated that ZnO incorporated PHBV-PEO microfibers inhibited biofilm formation. Among all 5% PHBV-PEO-ZnO microfibers showed maximum % of inhibition against *S. aureus* (28.17%) as compared with *P.aeruginosa* (24.51%), while PHBV-PEO-ZnO (1%) and PHBV-PEO-ZnO (3%) microfibers showed 10.17% and 19.18% of inhibition against *S. aureus* and 18.28% and 24.51% against *P.aeruginosa* respectively. *S.aureus* and *P.aeruginosa* are opportunistic pathogens that have the ability to form biofilm on medical implants and in wounds. The wound infections are difficult to eradicate due to antibiotic resistant nature of biofilm.⁸ This result shows that the antibiofilm activity is dependent on ZnO NPs concentration in the PHBV-PEO matrix. ZnO NPs are well reported for their antibacterial and antibifilm activity.²⁰ Therefore, the incorporation of ZnO NPs in the development of the antimicrobial surface is a promising way for developing biofilm resistant surfaces. The results obtained from this study demonstrated that microfibers incorporated with ZnO NPs exhibited remarkable antibiofilm activity.

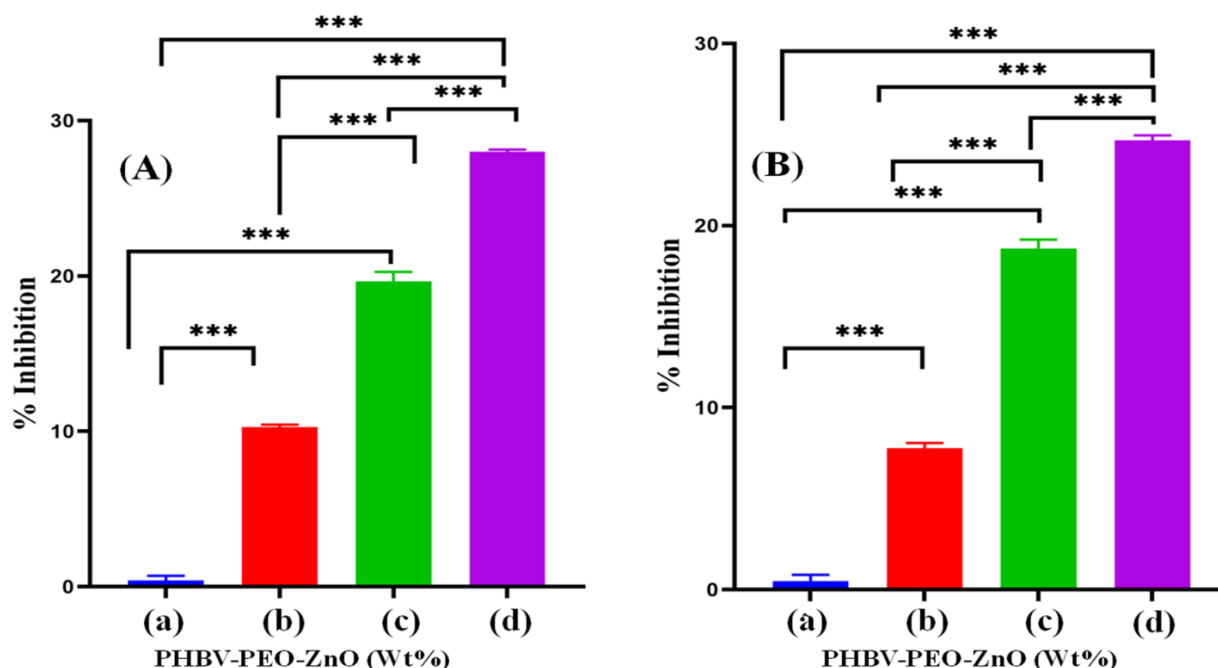


Figure 7.3: Antibiofilm activity of PHBV-PEO microfiers (0%) and PHBV-PEO microfibers with 1, 3 and 5 Wt% ZnO NPs against *S.aureus* (NCIM 2654) and *P.aeruginosa* (NCIM 5032)

7.3.3 Mechanism of antibacterial and antibiofilm activity of PHBV-PEO-ZnO microfibers

The antimicrobial activity of ZnO NPs or composite nanofibers mainly depend upon their high volume/surface area.²¹ In the present study, ZnO NPs are incorporated in different concentrations into the PHBV-PEO matrix as a wound dressing material through the electrospinning technique. The intensity of antibacterial and antibiofilm activity is different against *S.aureus* and *P.aeruginosa*. This can be related to the difference in the cell wall structure. Gram-positive bacteria have single cytoplasmic membrane and thick wall composed of multilayers of peptidoglycan, while Gram-negative bacteria have a more complex cell wall structure with outer membrane of lipopolysaccharide, middle thin layer of peptidoglycan and cytoplasmic membrane. The mechanism of ZnO NPs in the PHBV-PEO microfibers may involve the slight contact with the cell wall rather than penetration. *S. aureus* has a smaller negative charge as compared with *P.aeruginosa*. This would allow the maximum level of penetration of negatively charged free radicals from ZnO such as superoxide radicals anions and peroxide ions

Chapter 7: Antibacterial, antibiofilm and biocompatibility studies of PHBV-PEO-ZnO microfibers

that caused destruction and cell death to *S.aureus* at a comparatively less concentration than required to damage *P.aeruginosa*. In both bacteria damage of cell membrane that leads to leakage of cell content and cell death.^{22,23}

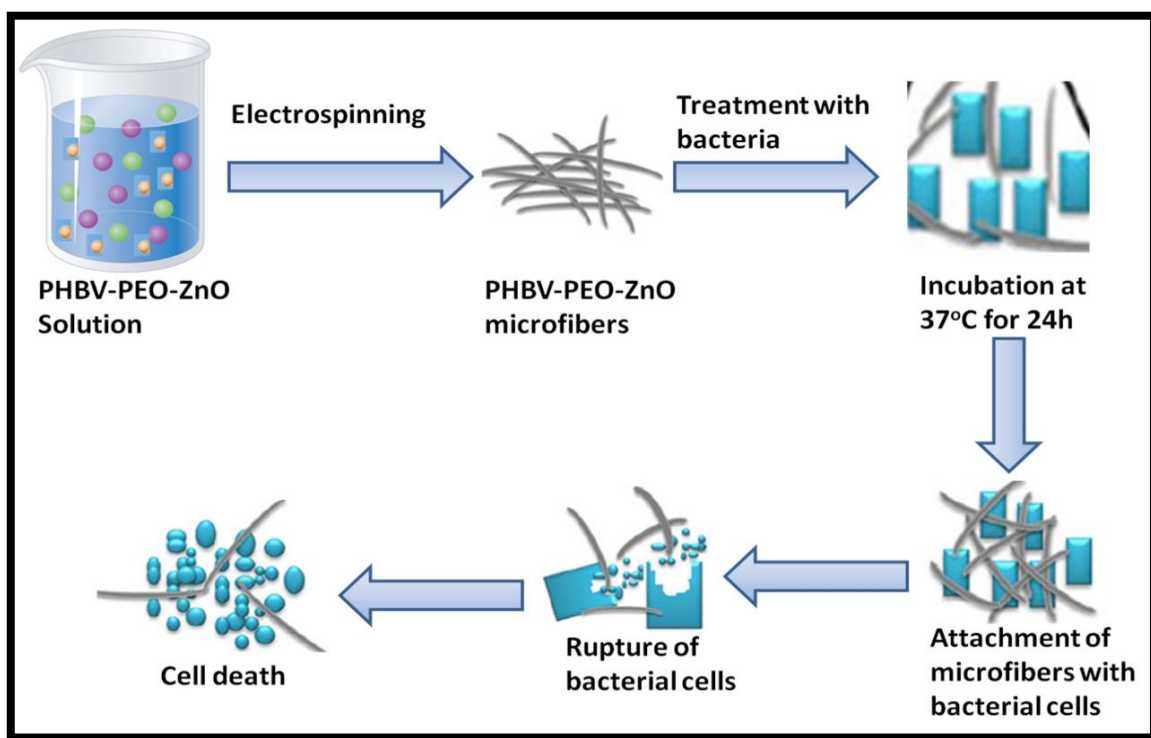


Figure 7.4: Schematic representation of antibacterial action of PHBV-PEO-ZnO microfibers.

7.3.4 Biocompatibility

7.3.4.1 Determination of hemocompatibility

Hemocompatibility is one of the most important methods to prove the in vitro biocompatibility of polymeric materials that uses RBCs isolated from blood. As per ASTM F-756-08, the hemolytic percentage below 2% is considered as non-hemolytic, 2-5% is slightly hemolytic and more than 5% is considered as hemolytic.¹⁶ Figure 7.5 shows the percentage of hemolysis of PHBV-PEO and PHBV-PEO-ZnO microfibers. The results show that the percentage of hemolysis of PHBV-PEO-ZnO microfibers is higher than that of PHBV-PEO

Chapter 7: Antibacterial, antibiofilm and biocompatibility studies of PHBV-PEO-ZnO microfibers

microfibers. The hemolysis percentage is 0.8%, 1.1%, 1.8% and 1.9% for PHBV-PEO, PHBV-PEO-ZnO (1%), 3% and 5 % respectively.

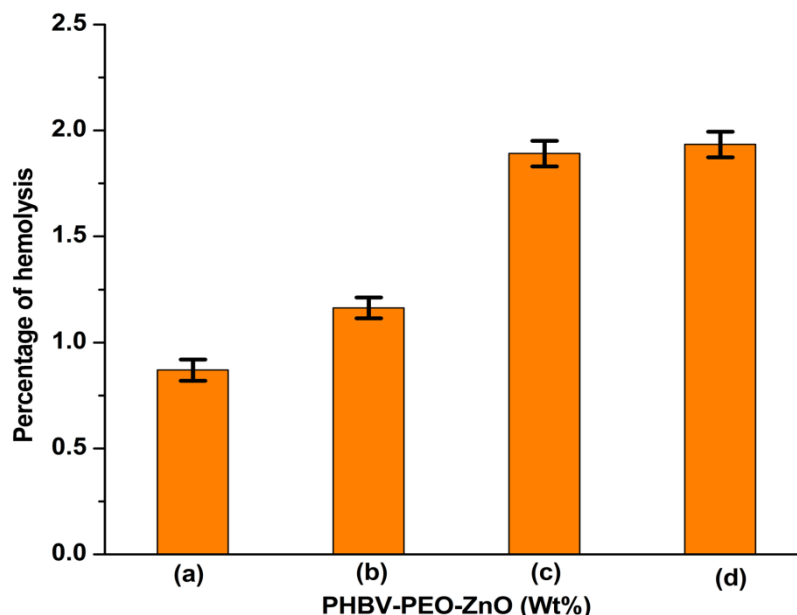


Figure 7.5: Hemocompatibility of PHBV-PEO-ZnO microfibers showing hemolysis below 2%. The percentage of hemolysis is increased with increase in ZnO NPs concentration indicating concentration dependant hemolytic activity. The percentage of hemolysis observed is below 2% indicating non-hemolytic nature of all microfibers.²⁴

The hemolysis percentage of all microfibers is below 2% indicating that microfibers are non-hemolytic in nature. The observed results demonstrates that the hemolysis percentage is increased with increasing concentration of ZnO NPs. ZnO NPs are responsible for hemolysis when they come in contact with blood in a concentration dependent manner.²⁴ The results show that these microfibers can be used for wound dressing applications.

7.3.4.2 Cell viability study

7.3.4.2.1 Selection of cell line

The toxicity of nanomaterials depends upon the organ and type of cell lines because of differences in cell physiology, the proliferation of the cell, membrane characteristics and

Chapter 7: Antibacterial, antibiofilm and biocompatibility studies of PHBV-PEO-ZnO microfibers

phagocytic properties. The important aspect in the determination of cytotoxicity assay is to select appropriate cell types, optimizing the number and condition of the cells.²⁵ To evaluate the exact effect of nanomaterials on the cells of interest, the cells must be chosen in a way that will represent the exposure route and organs targeted by the nanomaterials. Among the commonly used cell lines, fibroblast cells are suitable for the trial. In addition, cancer cells are also suitable than normal cells as they possess enhanced growth rate, metabolic activity and easy to handle.²⁶ In the present chapter, L929 mouse fibroblast cell lines have used for the study of biocompatibility of prepared PHBV-PEO-ZnO microfibers. These cell lines are commonly used to evaluate the biocompatibility of materials.

7.3.4.2.2 Selection of Cytotoxicity assay

Selecting appropriate cytotoxicity assay is an important aspect of the assessment of nanomaterials toxicity. As compared with animal studies, cellular assay is less ethically ambiguous, easy to control, reproducible, and cost-effective. For the selection of cytotoxicity assay, it is also important to observe that whether NPs can adsorb dyes and be redox active. Common methods used for evaluation of cytotoxicity are observation of cell morphology (structure) before and after exposure to sample, assay to evaluate the degree of DNA damage. Each assay varies in terms of time required and suitability. Different types of assays are represented in fig. 7.6. Among all assays MTT assay is most commonly used and easy to handle. Therefore, in the present study, the cytotoxicity assay has been determined by using MTT assay to minimize the errors and to get accurate data. The assay is cost-effective and easy to handle. 3-(4,5-Dimethylthiazol-2-yl)-2,5-Diphenyltetrazolium bromide (MTT) get reduced in the metabolically active cells and measures the cell proliferation.

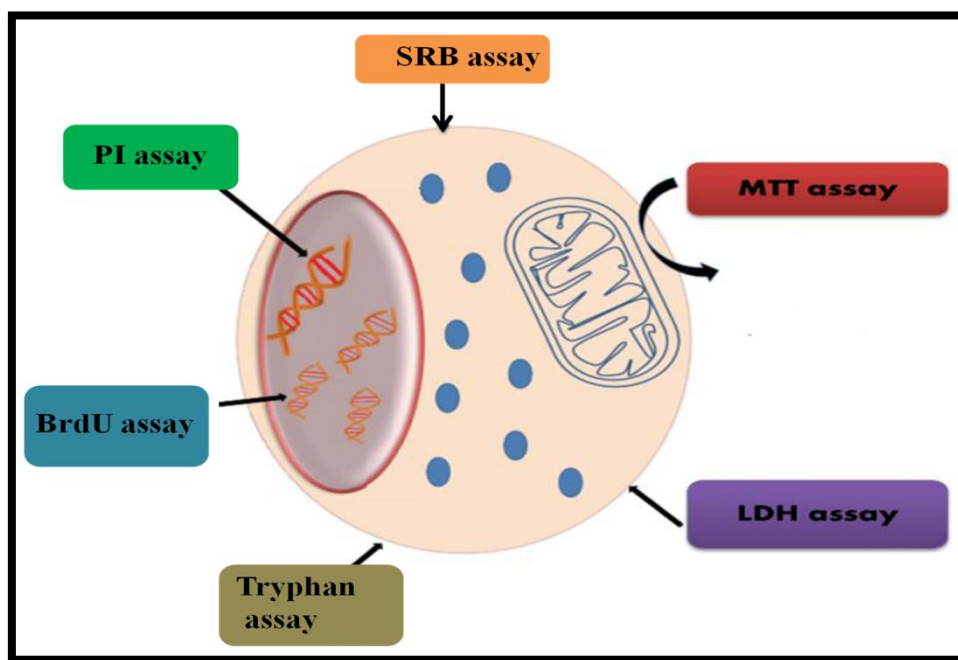


Figure 7.6: Overview of different cytotoxicity assays.²⁷

7.3.4.2.3 MTT assay of synthesized PHBV-PEO-ZnO microfibers

The cell viability studies of PHBV-PEO and PHBV-PEO-ZnO (1%, 3%, and 5%) microfibers are evaluated and represented in fig. 7.7. Material to be used for a wound dressing purpose should be non-toxic and biocompatible. This study is performed by using L929 fibroblast cells by using MTT assay. PHBV-PEO mats are used as a control. It is revealed that the cell viability is decreased for 24h, 48h, and 72h as the concentration of ZnO NPs are increased. It is also investigated that the cell viability of PHBV-PEO-ZnO microfibers slightly increased after 48h and 72h of incubation than 24h incubation for PHBV-PEO-ZnO microfibers.

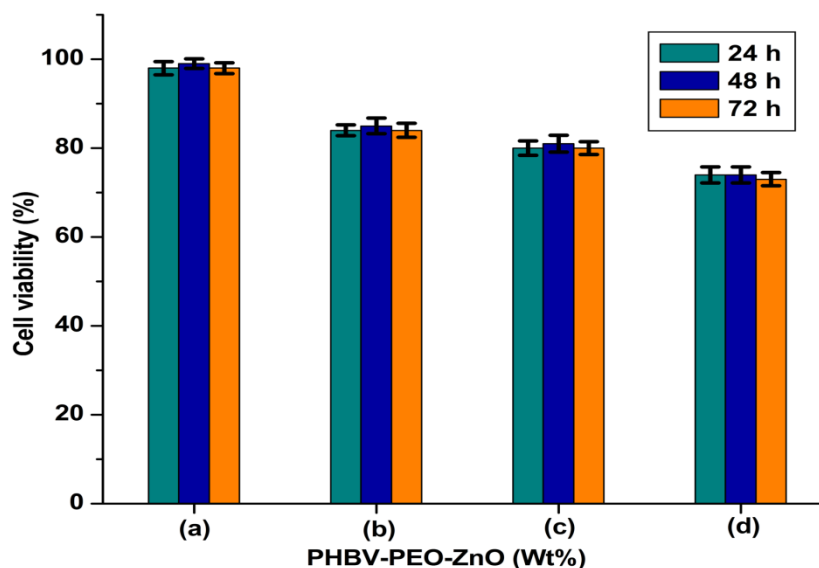


Figure7.7: Cytotoxicity of PHBV-PEO and PHBV-PEO-ZnO (1, 3, and 5%) microfibers in L929 fibroblast cells by MTT assay.

Cell viability of PHBV-PEO microfibers is 98% for 24h and 99% for 48h and 72h of incubation. However, the cell viability is 84% after 24h incubation and 85% after 48h and 72 h incubation for 1% of ZnO content in PHBV-PEO microfiber, 80% after 24h incubation and 81% after 48h and 82% after 72 h incubation for 3% of ZnO and 73% after 24h incubation and 75% after 48h and 72 h incubation for 5% of ZnO content in PHBV-PEO microfibers. From this investigation, it can be concluded that these microfibers are non-toxic to cells.²⁸

7.3.4.2.4 Mechanism of cytotoxicity of synthesized microfibers

The properties of metal oxide nanomaterials make them suitable for wound-dressing applications. Along with their use, it also leads to nanosized related toxicity. In microfibers, nanoparticles are embedded therefore it is important to evaluate their potential toxic effects of nanoparticles. Nowadays the toxic effects of nanoparticles on the environment and humans are the hot research topic that received much more attention. ZnO NPs show toxicity by different mechanisms mentioned below,

- ZnO NPs release corresponding toxic ions.

Chapter 7: Antibacterial, antibiofilm and biocompatibility studies of PHBV-PEO-ZnO microfibers

- ZnO NPs generate excess reactive oxygen species.
- Their toxicity mainly affected by the size, shape, surface charge, chemical stability.

The mechanism of ZnO NPs toxicity in cell lines occurs in different ways. ZnO NPs get dissolved in the extracellular region and increase the intracellular level of Zn^{+2} ions. Increased level of Zn^{+2} ions increases acidic condition that damages the cytoskeleton of the cell and also reduces the activity of Zn-dependent enzymes and transcription factors. Reactive oxygen species (ROS) that involve superoxide anion (O_2^-), hydrogen peroxide (H_2O_2), hydrogen radical ($\text{HO}\bullet$) released by ZnO NPs result in major cell damage by inducing genotoxicity, inflammation, and destruction of biomolecules like DNA, protein and lipids. This process leads to cell apoptosis and damage to cells.²⁹ In another mechanism, ZnO NPs enter inside the cell and disrupt Zn-dependent enzymes and transcription factors. The intensity of toxicity also depends upon size, shape and surface charge of nanoparticles. The minimum size of NPs permits it to enter inside the cell easily.²⁶ The spherical NPs are faster and easier for endocytosis than rod shaped NPs. The total charge on the surface of NPs enhances the adsorption of ions and biomolecules. As compared with anionic particles, cationic particles are stable and show maximum cytotoxicity effects. Toxicity of ZnO NPs can be minimized by combining the ZnO NPs with other biocompatible and biodegradable materials.^{30,31,32} Therefore in the previous work we have incorporated ZnO NPs into PHBV-PEO microfibers.

7.4 Conclusions

This chapter presents the study of antibacterial, antibiofilm and biocompatibility study of synthesized PHBV-PEO-ZnO microfibers prepared by electrospinning technique. The antibacterial study of PHBV-PEO-ZnO microfibers showed the maximum zone of inhibition at 5 wt% concentration of ZnO NPs against *S. aureus* as compared with *P. aeruginosa*. The antibiofilm activity of PHBV-PEO-ZnO (5 wt %) was maximum as compared with other microfibers of PHBV-PEO-ZnO (1 and 3 wt %) against *S. aureus* as compared with *P. aeruginosa*. Biocompatibility study was done by hemocompatibility, and cytocompatibility assay. The percentage of hemolysis of all microfibers was below 2% indicating non-hemolytic nature of all microfibers. Cytocompatibility study showed PHBV-PEO-ZnO microfibers with 5

Chapter 7: Antibacterial, antibiofilm and biocompatibility studies of PHBV-PEO-ZnO microfibers

wt% of ZnO NPs showed minimum cell viability (73-75%) after 24h, 48h and 72h of incubation as compared with other microfibers indicating non-toxic nature of microfibers. All these data revealed that the prepared PHBV-PEO-ZnO microfibers are biocompatible and can be used as antibacterial and antibiofilm candidate in the wound dressing applications.

Chapter 7: Antibacterial, antibiofilm and biocompatibility studies of PHBV-PEO-ZnO microfibers

References

- 1 N. Black and J. W. Schrock, *Emerg. Med. Int.*, 2018, **2018**, 1–7.
- 2 N. M. Atef, S. M. Shanab, S. I. Negm and Y. A. Abbas, *Bull. Natl. Res. Cent.*
- 3 N. A. Kassam, D. J. Damian, D. Kajeguka, B. Nyombi and G. S. Kibiki, *BMC Res. Notes*, 2017, 19–21.
- 4 Koulenti, Xu, Mok, Song, Karageorgopoulos, Armaganidis, Lipman and SotiriosTsiodras, *Microorganisms*, 2019, **7**, 1–24.
- 5 S. I. Ahmad, *Med. Hypotheses*, 2002, **58**, 327–331.
- 6 K. Rahim, S. Saleha, X. Zhu, L. Huo and A. Basit, *Microb. Ecol.*, 2016, **73(3)**, 710–721.
- 7 P. Vonaesch, M. Anderson and P. J. Sansonetti, *FEMS Microbiol. Lett.*, 2018, **42**, 243–292.
- 8 M. Kanitkar, V. P. Kale, A. Jaiswal, J. R. Bellare, R. Deshpande and H. Chhabra, *RSC Adv.*, 2015, **6**, 1428–1439.
- 9 K. R. Raghupathi, R. T. Koodali and A. C. Manna, *Langmuir*, 2011, **27**, 4020–4028.
- 10 W. Zhang, S. Ronca and E. Mele, *Nanomaterials*, 2017, **7**, 1–17.
- 11 S. M. Tan, J. Ismail, C. Kummerlöwe and H. W. Kammer, *J. Appl. Polym. Sci.*, 2006, **101**, 2776–2783.
- 12 S. H. Pawar, P. P. Patil, R. A. Bohara, S. G. Nanaware and J. V. Meshram, *Int. J. Biol. Macromol.*, 2018, **122**, 1305–1312.
- 13 G. S. Dhillon, S. Kaur and S. K. Brar, *Int. Nano Lett.*, 2014, **4**, 1–11.
- 14 C. Ashajyothi, K. H. Harish, N. Dubey and R. K. Chandrakanth, *J. Nanostructure Chem.*, 2016, **6**, 329–341.

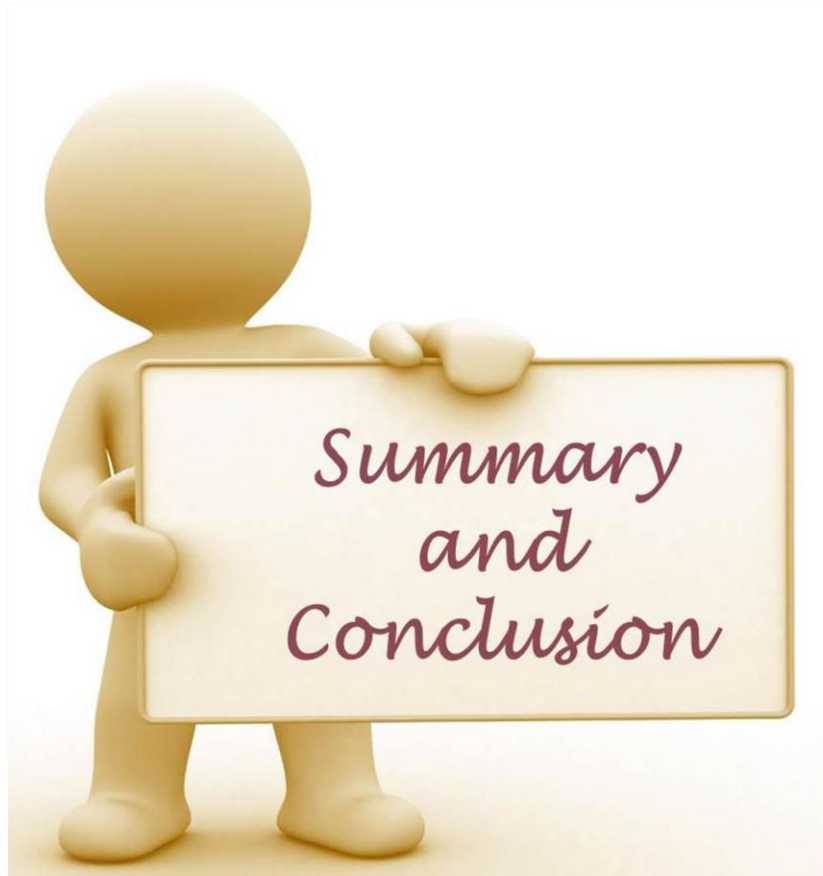
Chapter 7: Antibacterial, antibiofilm and biocompatibility studies of PHBV-PEO-ZnO microfibers

- 15 S. Agrawal, P. R. Patel and R. V. N. Gundloori, *ACS Omega*, 2019, **4**, 6301–6310.
- 16 R. A. Bohara and S. H. Pawar, *Appl Biochem Biotechnol*, 2015, **176**(4), 1044–1058.
- 17 J. S. Boateng, K. H. Matthews, H. N. E. Stevens and G. M. Eccleston, *J. Pharm. Sci.*, 2008, **97**, 2892–2923.
- 18 P. P. Mahamuni-Badiger, P. M. Patil, M. V. Badiger, P. R. Patel, B. S. Thorat-Gadgil, A. Pandit and R. A. Bohara, *Mater. Sci. Eng. C*, 2020, **108**, 1–74.
- 19 A. Emamifar, M. Kadivar, M. Shahedi and S. Soleimanian-Zad, *Innov. Food Sci. Emerg. Technol.*, 2010, **11**, 742–748.
- 20 K. T. Shalumon, K. H. Anulekha, S. V Nair, S. V Nair, K. P. Chennazhi and R. Jayakumar, *Int. J. Biol. Macromol.*, 2011, **49**, 247–254.
- 21 S. Y. H. Abdalkarim, H. Y. Yu, D. Wang and J. Yao, *Cellulose*, 2017, **24**, 2925–2938.
- 22 T. Amna and M. S. Hassan, 2012, 743–751.
- 23 L. Chuo, S. Mahmud, S. Khadijah, M. Bakhori, A. Sirelkhatim, D. Mohamad, H. Hasan, A. Seeni and R. Abdul, *Ceram. Int.*, 2014, **40**, 2993–3001.
- 24 Z. J. Deng, N. J. Butcher, G. M. Mortimer, Z. Jia, M. J. Monteiro, D. J. Martin and R. F. Minchin, *Drug Metab. Dispos.*, 2014, **42**, 377–383.
- 25 A. Z. Mohajeri, M. Leila, R. Farzad, B. Aziz, M. S. Mojtaba, H. S. Alireza and S. Marjan, *Drug Metab. Rev.*, 2019, **0**, 1–28.
- 26 C. Riebeling, J. Piret, B. Trouiller, C. Saout, O. Toussaint and A. Haase, *NANOIMPACT*, 2017, **10**, 1–10.
- 27 H. Markides, M. Rotherham and A. J. El Haj, *J. Nanomater.*, 2012, **11**, 13–15.
- 28 S. Malmir, L. Barral, R. Bouza, M. Esperanza, M. Seoane, S. Feijoo-Bandín and F. Lago, *Cellulose*, 2019, **26**, 2333–2348.

Chapter 7: Antibacterial, antibiofilm and biocompatibility studies of PHBV-PEO-ZnO microfibers

- 29 R. Cai, H. Wang, M. Cao, L. Hao, L. Zhai, S. Jiang and X. Li, *Mater. Des.*, 2015, **87**, 17–24.
- 30 S. Malmir, L. Barral, R. Bouza, M. Esperanza, F. Lago and M. S. S. Feijoo-bandı, , DOI:10.1007/s10570-018-2216-2.
- 31 Ü. Özgür, Y. I. Alivov, C. Liu, A. Teke, M. A. Reshchikov, S. Doğan, V. Avrutin, S. J. Cho and H. Morkoç, *J. Appl. Phys.*, 2005, **98**, 1–103.
- 32 M. D. Ana and L. D. Angel, *Int. J. mo*, 2014, **15**, 10950–10973.

CHAPTER 8



Observe, record, tabulate, communicate. Use your five senses. Learn to see, learn to feel, learn to smell, and know that by practice alone you can become expert.

-William Osler



8.1 Introduction

Wound infection causes microbes to settle down at the infection site, where they can sustain antibiotic treatment, so developing antibiotic resistance. It is widely reported that specific strains of microbes have started to develop antibiotic resistance. The World Health Organization (WHO) recently ranked microbes that should be seriously considered for the development of new antibiotics. Drug resistance in planktonic microorganisms is attributed to the mutation or exchange of antibiotic-resistant genes. They gain susceptibility to antibiotics when they disperse from the biofilm; Bacteria in the biofilm are more effectively protected from the host immune system than from the planktonic bacteria. Antibiotic resistance increases with the maturation of the biofilm. Multidrug resistance behavior in Gram-positive and Gram-negative bacteria is critical to treat and indeed untreatable with conventional antibiotics that can delay the wound-healing process. Wound infections mostly caused by indigenous microflora or an environment that grows in the wounded area. To treat infection by drug-resistant bacteria there is an urgent need to use a new antibacterial agent rather than conventional antibiotics.

Hence, the present thesis is focused on the synthesis of novel microfibers incorporated with ZnO NPs for wound dressing applications. PHBV, PEO, and ZnO NPs are used for the synthesis of novel microfibers. PHBV is a natural biopolymer that possesses excellent properties like biocompatibility, biodegradability, non-toxicity and thermo plasticity. However, due to its poor mechanical performance, high crystallinity, inherent rigidity, and hydrophobicity this material can blend with other hydrophilic polymers. Among those polymers, PEO, which is certified by the FDA, is highly preferred because of its excellent properties like biocompatibility, hydrophilicity, and malleability. It is non-immunogenic, non-antigenic, non-toxic, and low adsorption capacity of surface proteins. Furthermore, from PEO it is very easy to obtain fibers by electrospinning technique than other polymers because of its high solubility in water as well as in different types of organic solvents. The blends of PHBV-PEO has been prepared earlier, but not used for the further antibacterial applications. To make their potential use as an antibacterial wound dressing the addition of inorganic materials such as metal oxide nanoparticles is needed. Among different metal oxide nanoparticles, ZnO NPs are widely reported for their antibacterial and antibiofilm activities against a wide range of Gram-positive and Gram-negative bacteria with low toxicity to human cells at the appropriate concentration. Therefore, in these studies, firstly

Chapter 8: Summary and conclusions

ZnO NPs are synthesized by using different approaches like; (i) regular synthesis in polyols, (ii) in presence of sodium acetate, (iii) increasing reaction time, polyols used are diethylene glycol and triethylene glycols, by using the reflux method and to study their morphological, thermal, spectroscopic and elemental properties. Secondly, these all prepared ZnO NPs are studied for their antibacterial, antibiofilm activities, and hemocompatibility and cell viability studies. Thirdly, among these ZnO NPs, the ZnO NPs with good antibacterial and antibiofilm activity with different concentrations are incorporated into the unique blend of PHBV-PEO polymers. The prepared microfibers are subjected for the mechanical study, thermal stability, morphological study, swelling, biocompatibility, hemocompatibility, antibacterial and antibiofilm study. Finally, these microfibers are evaluated for the potential wound dressing applications.

8.2 Competent component of the thesis

The principle aim of this thesis is to develop antibacterial and antibiofilm microfibers based on the PHBV-PEO polymers and ZnO NPs for wound dressing application.

The antibacterial properties of the materials are a prime important factor in the field of wound management. From the last few decades, the properties of wound dressings based on the ZnO NPs with polymers have become hot area of research. ZnO NPs have gained much more significance due to their good antibacterial, antibiofilm properties, tissue adhesive property, and biocompatibility. Also, these nanoparticles reduce microbial adhesion, proliferation, and biofilm growth. ZnO NPs damage bacterial cells by the formation of ROS that is $O^{\cdot-}$, HO_2^{\cdot} , H_2O_2 , HO^{\cdot} , and Zn^{2+} ions. However, their intensity of antibacterial and antibiofilm activity gets affected by the varieties of factors like size, shape, concentration, UV illumination, surface modification, and surface defects. The size and shape can be controlled by selecting an appropriate synthesis method.

The modified reflux method is used for the synthesis of ZnO NPs. In this method, different approaches were used like, (i) in the presence of sodium acetate, (ii) by using two different polyols (diethylene glycol and triethylene glycol), (iii) change in the reaction time. The main benefit of this method is the size of synthesized ZnO NPs is smaller. Also, the use of the above different approaches affected the size and morphology of ZnO NPs. The synthesis method is simple, easy, gives high purity and homogeneity at the molecular level. All synthesized 8 ZnO

Chapter 8: Summary and conclusions

NPs were characterized by different analyses. The structural and spectroscopic characterization of the synthesized ZnO NPs is performed by XRD, UV-vis spectroscopy and FTIR techniques. The size and morphology of synthesized ZnO NPs were characterized by FESEM and TEM analysis. These analyses offered different morphology from oval to rod shape with an average size of ~15-100nm. The ZnO NPs obtained by refluxing DEG for 3hours in the absence of sodium acetate exhibited the least particle size of ~15 nm. The UV vis-spectrum showed the intensity peaks which are related to the particle size of NPs. As the particle size decreased, the absorption peak shifted towards the lower range that is a blue shift. Also, the type of polyols used, temperature and reaction time affect on the absorption peak. The phase identification and crystallite size of all synthesized ZnO NPs were examined by the XRD analysis. All the diffraction peaks fit well with the hexagonal wurtzite structure of ZnO. The average crystallite size of all nanoparticles is in the range of ~15-23nm. The ZnO NPs synthesized in DEG in absence of sodium acetate for 3hours showed the least size of ~15nm. The molecular structure of ZnO NPs is revealed by FTIR spectroscopy. The thermal analysis is performed by the TGA, which showed two successive decompositions. ***All the XRD, UV, FTIR, and TGA results suggested that ZnO NPs synthesized by using different approaches showed the varieties in properties.*** The surface morphology of ZnO NPs is examined by FESEM and TEM. ***The results indicated that the addition of sodium acetate, use of different polyols, and change in the reflux time from 2h to 3h gave a difference in the morphology from oval to rod shape with an average particle size ~15-100nm.*** The ZnO NPs refluxed in DEG for 3h in the absence of sodium acetate exhibited the least particle size.

The biological characterization study is done by using antibacterial activity, antibiofilm activity, minimum inhibitory concentration (MIC), in-vitro cytotoxicity, and hemocompatibility. Antibacterial study of all synthesized ZnO NPs is carried out by agar well diffusion method against pathogens like Gram-positive *Staphylococcus aureus* and Gram-negative *Proteus vulgaris*. The results concluded that the degree of antibacterial activity is size-dependent. It is inversely proportional to the size of nanoparticles. Out of all synthesized ZnO NPs, ZnO NPs prepared by using DEG for 3hours in absence of sodium acetate with the least particle size ~15nm exhibited remarkable antibacterial activity against both pathogens. Also, it is revealed that the antibacterial activity is the maximum against *S. aureus* as compared with *P. vulgaris*

Chapter 8: Summary and conclusions

because of differences in cell wall compositions in Gram-positive and Gram-negative bacteria. ***MIC of all ZnO NPs is in the range of 10-20µg/ml. ZnO NPs with the least size showed a significant percentage of inhibition against S. aureus than P. vulgaris, which is 32.67% and 22.38% respectively at 50µg/ml of concentration. Also, these ZnO NPs showed the highest zone of inhibition as compared with other ZnO NPs against S. aureus (14mm) than P. vulgaris (6mm).***

Antibiofilm activity of all ZnO NPs is tested against *S. aureus* and *P. vulgaris* by using 96 well-plate microtiter plates. All ZnO samples showed an increased percentage of inhibition with an increase in concentration. ***ZnO NPs with the least size exhibited maximum percentage of biofilm inhibition that is 67.3% and 58.18% against S. aureus and P. vulgaris respectively at the concentration of 250µg/ml.***

Hemocompatibility is a very important method to prove the in-vitro biocompatibility of materials by using RBCs isolated from blood. It is reported that smaller nanoparticles exhibit higher hemolytic activity than larger once. ***All ZnO NPs showed hemolysis below 2%, which showed that these nanoparticles can be used as a promising agent in the biomedical field.***

The cell viability of all ZnO NPs is investigated by using MTT assay in L929 fibroblasts cells. Results concluded that the intensity of cytotoxicity is inversely proportional to the size of nanoparticles. ***It is revealed that ZnO NPs with the least size had maximum cytotoxicity and less percentage of cell viability.*** The cell viability of ZnO NPs with the least size showed 92% after 24h, 94% after 48h, and 72 h. The cell viability is slightly increased after 24h for 48h and 72h. ***The results suggested that among all synthesized ZnO NPs with the least size showed good hemocompatibility and biocompatibility which can be further used in wound dressing applications.***

The next part of the thesis is the addition of ZnO NPs into the unique blend of PHBV-PEO polymers (4:1) for wound dressing applications. To make previously prepared ZnO NPs with comparatively good antibacterial and antibiofilm activity compatible for further wound dressing applications, these ZnO NPs are reinforced into the blend of PHBV-PEO polymers by using the electrospinning technique.

Chapter 8: Summary and conclusions

There is well-reported literature on the addition of ZnO NPs into the PHBV matrix for antibacterial applications. Also the preparation, characterization of PHBV-PEO blends in the different ratios, the influence of PEO on the properties of PHBV, the effect of ZnO addition on the crystallization behavior of PHBV is reported. However, no study is reported on the addition of ZnO NPs into blends of the PHBV-PEO matrix for their antibacterial and antibiofilm applications.

The incorporation of ZnO NPs in the PHBV-PEO blends is done by using the electrospinning technique. Of all available strategies for the synthesis of one-dimensional nanofiber, electrospinning is one of the most adopted and widely advanced techniques. The advantage of this method is that it can yield continuous nanoscale fibers with diameters in the sub-micrometer to nanometer range by using high voltage power supply. Also, they possess outstanding properties like high porosity, small diameter, and high surface to volume ratio.

The role of incorporated ZnO NPs on the structural and morphological characteristics is studied. ZnO NPs are incorporated into PHBV-PEO blends at different concentrations like 1%, 3%, and 5%. The ratio of the PHBV-PEO blend used is 4:1. During the process of synthesis of PHBV-PEO blends the ZnO NPs concentration is varied.

The surface morphology is determined by FESEM analysis. *The FESEM analysis observed, as compared with PHBV-PEO microfibers, ZnO reinforced microfibers exhibited slightly higher diameter. The average diameter of PHBV-PEO microfibers is 2.04-2.2 μ m, whereas microfibers with different ZnO concentration showed an average diameter of 2.2-3.1 μ m.*

The spectroscopic analysis of prepared microfibers is done by the ATR-FTIR analysis. The elemental analysis is done by the EDX analysis. The results suggested the successful addition of ZnO NPs in the increasing order. The EDX results also confirmed the successful incorporation of ZnO into PHBV-PEO microfibers.

Thermal analysis is done by DSC and TGA analysis. TGA analysis showed that PHBV-PEO microfibers possess better thermal stability due to the crystalline nature of ZnO NPs. DSC analysis showed that the incorporation of ZnO NPs doesn't have any effect on the crystalline

Chapter 8: Summary and conclusions

nature of PHBV-PEO microfibers. The relative decrease in crystallinity due to the addition of ZnO NPs, confirmed that they act as a retarding agent for the crystallization in the microfibers.

The next characterization study of microfibers is swelling behavior. It is observed that PHBV-PEO microfibers showed a higher percentage of weight gain than PHBV-PEO-ZnO microfibers. The incorporation of ZnO NPs slightly reduced the percentage of weight gain as microfibers with ZnO had lower porosity than PHBV-PEO microfibers.

The mechanical properties are mainly influenced by the presence of ZnO NPs. Tensile strength is increased with the addition into PHBV matrix. Young's modulus values are reduced slightly with increased addition of ZnO NPs, while the incorporation of ZnO into the PHBV-PEO matrix significantly increased elongation break. ***It is concluded that the obtained results of mechanical properties were sufficient for wound during application as compared with PHBV-PEO microfibers.***

The successful dressing application of microfibers is possible after confirming their biological study. The biological characterization study is done by using antibacterial activity, antibiofilm activity in-vitro cytotoxicity, and hemocompatibility and cell adhesion study.

The antibacterial study of PHBV-PEO and microfibers with different ZnO concentrations is done by the disc diffusion method. It is observed by measuring the zones of inhibition against wound infection-causing pathogens, Gram-positive *S. aureus* and Gram-negative *P. aeruginosa*. It is clearly observed that PHBV-PEO microfibers showed no zone of inhibition, while composite microfibers with 1, 3, and 5% of ZnO NPs showed zone of inhibition against *S.aureus* and *P. aeruginosa* are (1mm, 3mm, 4mm) and (1mm, 2mm, 3mm) respectively. ***It is observed that the intensity of the antibacterial activity is increased as the ZnO Nps concentration increased.***

The antibiofilm activity of PHBV-PEO and PHBV-PEO-ZnO microfibers are studied against *S. aureus* and *P. aeruginosa*. It is observed that among all 5% PHBV-PEO-ZnO microfibers showed the maximum percentage of inhibition against *S.aureus* (28.17%) as compared with *P. aeruginosa* (24.51%), while 1% and 3% microfibers showed 10.17% and

Chapter 8: Summary and conclusions

19.18% against *S. aureus* and 18.28% and 24.51% against *P. aeruginosa*. ***The results concluded that the intensity of antibiofilm activity is increased as ZnO NPs concentration increased.***

For wound dressing application, hemocompatibility and cell viability study are important that can decide the ability of the material to be used for the in-vitro application. Hemocompatibility study showed that the percentage of hemolysis of PHBV-PEO-ZnO microfibers is higher than PHBV-PEO microfibers. It is 0.8%, 1.1%, 1.8% and 1.9% for PHBV-PEO and PHBV-PEO-ZnO (1, 3, and 5%) respectively. ***These results concluded that these microfibers are non-hemolytic as the hemolysis percentage of all microfibers is below 2%.***

The cell viability study of microfibers is performed by using the L929 fibroblast cell line with MTT assay for 24h, 48h, and 72h incubation. It is observed that the cell viability decreased for 24h, 48h, and 72h as the ZnO concentration increased. It is also investigated that the cell viability of microfibers slightly increased after 48h and 72h of incubation than 24h of incubation. Cell viability of PHBV-PEO microfibers is 98% for 24h and 99% for 48h and 72h incubation. The cell viability is 84% after 24h, 85% after 48h and 72h incubation for 1% ZnO content, 80% after 24h, and 81% after 48h, 82% after 72h incubation for 3% of ZnO content, 73% after 24h, 75% after 48h and 72h of incubation for 5% of ZnO content in PHBV-PEO microfibers. ***From this investigation, it is concluded that these microfibers are non-toxic to cells. From all the above observations, it is concluded that ZnO incorporated PHBV-PEO microfibers can be used as a potential candidate in the wound dressing application.***

9.3 Summary of thesis

Chapter 1 introduces all the necessary part in brief like biofilm-related information, biofilm formation, drug resistance, different approaches to control biofilm and planktonic cells, properties of the antibacterial and antibiofilm agent, ZnO NPs properties and biomedical application, wound dressings, wound healing process, properties of ideal wound dressings, biomaterials used for wound dressing, use of PHBV and PEO for wound dressings.

Chapter 2 introduces the theoretical background regarding ZnO NPs and their use in wound dressing applications. ZnO NPs are well reported for their antibacterial and antibiofilm applications. For the application of ZnO NPs in the wound dressing, application their

Chapter 8: Summary and conclusions

incorporation in polymers is an important factor. Different polymers can be used for the incorporation of ZnO NPs for wound dressing applications. PHBV-PEO hybrid microfibers have gained a lot of interest in the development as a wound dressing material. However, to use them as a wound dressing material antibacterial agents like ZnO NPs can be incorporated in it.

Chapter 3 focuses on characterization techniques for wound dressing materials. This chapter discusses characterization techniques that are used to determine physical, chemical, mechanical, swelling capacity, and biological properties.

Chapter 4 deals with the synthesis of pure ZnO NPs in polyols by using a modified reflux method with the application of different approaches. It also covers the physical, chemical studies of pure ZnO NPs.

Chapter 5 deals with the comparative study of the antibacterial and antibiofilm activity of all ZnO NPs synthesized by using polyols. This chapter covers the brief comparative study of these synthesized ZnO NPs for antibacterial and antibiofilm activity against pathogens. Besides, it includes a comparative study of hemocompatibility, cytotoxicity study by using the L929 fibroblast cell line.

Chapter 6 focuses on the synthesis of hybrid PHBV-PEO-ZnO microfibers by using the electrospinning technique. This chapter covers a brief study on the hybrid PHBV-PEO-ZnO microfibers. It includes spectroscopic, morphological, mechanical, elemental, thermal, and swelling studies.

Chapter 7 focuses on the antibacterial and antibiofilm study of the synthesized PHBV-PEO-ZnO microfibers. ZnO NPs were incorporated in different concentrations. All antibacterial study is performed against wound infection associated micro-organisms such as Gram-positive *S. aureus* and Gram-negative *P. aeruginosa*. This chapter also covers the hemocompatibility, cytotoxicity study in L929 fibroblast cells and cell adhesion and proliferation study.

Chapter 8 deals with the summary and conclusions of the thesis.

9.4 Major conclusions

Chapter 8: Summary and conclusions

The ZnO NPs are successfully synthesized by the modified reflux method by using different approaches like (i) in presence of sodium acetate, (ii) by using different polyols like DEG and TEG, and (iii) change in the reaction time. Out of these approaches ZnO NPs synthesized by using DEG in the absence of sodium acetate refluxed for 3h exhibited the least crystallite size of ~ 15nm.

The physicochemical characterization of all synthesized ZnO NPs investigated by employing structural and spectroscopic analysis confirmed the proper synthesis of pure ZnO NPs. Besides, it provided basic information on materials such as size, shape, structure, chemical bonding etc.

The phase identification is confirmed by XRD analysis as the hexagonal wurtzite structure of ZnO. The average crystallite size of all ZnO NPs is in the range of ~15-23nm.

The UV-visible spectroscopy showed that the absorption peaks in 360-380nm which is a characteristic peak for ZnO NPs. Also it is observed that the absorption peaks shifted towards a slightly shorter wavelength with a decrease in crystalline size that is blue shift.

FTIR analysis showed all the peaks that correspond to the molecular structure of ZnO. This analysis also revealed the adsorption of DEG/TEG molecules on the surface of ZnO NPs.

FESEM and TEM analysis revealed the morphology of synthesized ZnO NPs. These analyses confirmed the differences in the morphology from oval to rod shape with an average particle size of ~15-100nm. The size obtained from the FESEM and TEM images is consistent with the crystallite size calculated from the XRD patterns of ZnO NPs.

The thermal analysis showed two successive decompositions. The first decomposition occurred in the range of 145-257°C which is due to evaporation of surface adsorbed water and moisture, while the second decomposition occurred in the range of 452-490°C which is due to the loss of adsorbed DEG/TEG molecules in all samples. This investigation is consistent with FTIR results that confirmed the adsorption of DEG/TEG molecules on the ZnO NPs.

The antibacterial study of all synthesized ZnO NPs showed the size-dependent antibacterial activity. It is concluded that the intensity of antibacterial activity is inversely

Chapter 8: Summary and conclusions

proportional to the size of nanoparticles. Out of all synthesized ZnO NPs the ZnO NPs with the least particle size (~15nm) showed maximum antibacterial activity against *S. aureus* as compared with *P. vulgaris*.

The minimum inhibitory concentration of synthesized ZnO NPs is in the range of 10-20 μ g/ml. It is concluded that among all samples ZnO NPs with least size exhibited maximum percentage of inhibition for *S. aureus* (32.67%) than *P. vulgaris* (22.38%) at a concentration of 50 μ g/ml.

The growth curve pattern of *S. aureus* and *P. vulgaris* in the presence of all ZnO NPs indicated decreased bacterial cell growth. From these results it can be concluded that the ZnO NPs show slightly more activity against *S. aureus* than *P. vulgaris*.

ZnO NPs with the least size exhibited maximum percentage of biofilm inhibition as compared with other synthesized ZnO NPs against *S. aureus* and *P. vulgaris* that is 67.3% and 58.18% respectively at the concentration of 250 μ g/ml.

The hemocompatibility study of all ZnO NPs showed below 2% hemolysis. Smaller NPs showed higher hemolytic activity than larger once. From the obtained results it can be concluded that all ZnO NPs can be used as a promising agent in biomedical fields.

The in vitro cytotoxicity studies of all synthesized ZnO NPs showed the nontoxic nature of all nanoparticles carried out by using the fibroblast L929cell line by using MTT assay. From these results, it is concluded that these nanoparticles are biocompatible and can be further used for wound dressing application.

Novel PHBV-PEO microfibers reinforced with uniformly dispersed ZnO NPs are successfully prepared by using the electrospinning technique. The physical, chemical and morphological characteristics are studied by using different spectroscopic techniques.

The FTIR analysis showed peaks that suggest the successful incorporation of ZnO NPs in different concentrations like 1, 3, and 5% in PHBV-PEO microfibers.

Chapter 8: Summary and conclusions

The FESEM analysis observed that as compared with PHBV-PEO microfibers, ZnO incorporated microfibers exhibited a slightly higher diameter. The average diameter of PHBV-PEO microfibers is 2.04-2.2 μ m, whereas microfibers with different ZnO concentration showed an average diameter of 2.2-3.1 μ m showing the successful incorporation of ZnO NPs.

EDX analysis confirmed the successful incorporation of ZnO NPs in different concentrations like 1,3 and 5% in PHBV-PEO microfibers.

Thermal analysis is performed by TGA and DSC analysis. TGA study showed that PHBV-PEO microfibers possess better thermal stability due to the crystalline nature of ZnO NPs. It can be concluded that the addition of ZnO NPs into PHBV-PEO microfibers increased thermal stability. DSC analysis showed that the incorporation of ZnO NPs doesn't have any effect on the crystalline nature of PHBV-PEO microfibers showing the retarding action of ZnO NPs for the crystallization in electrospinning microfibers.

The mechanical study of these microfibers suggested that, ZnO incorporated PHBV-PEO microfibers possess sufficient mechanical properties as compared with PHBV-PEO microfibers.

The swelling study suggested that the fibers with finest diameter showed maximum swelling and fibers with the thicker diameter showed relatively poor swelling. It also showed that ZnO incorporated microfibers have better uptake capacity of exudates.

The in vitro antibacterial study showed that PHBV-PEO-ZnO (5%) exhibited a maximum diameter of zone of inhibition against *S. aureus* (4mm) as compared with *P. aeruginosa* (3mm). It can be concluded that the degree of antibacterial activity is increased with an increased concentration of ZnO NPs.

The results of the antibiofilm study revealed that the intensity of antibiofilm activity is increased with an increase in the concentration of ZnO NPs in PHBV-PEO microfibers.

Hemocompatibility study suggested that these microfibers are non-hemolytic, as a hemolytic percentage of all microfibers were below 2%.

The in vitro cell viability study by using L929 fibroblast cell line showed that all microfibers have 73-99% cell viability, showing that these microfibers are non-toxic.

Chapter 8: Summary and conclusions

The biocompatibility, non-toxicity, hemocompatibility, swelling property, better thermal and mechanical properties suggested that it can be employed as a potential antibacterial candidate in wound dressing applications.

9.5 Future scope of the thesis

❖ Zinc oxide nanoparticles: Alternative to drug-resistant microorganisms

The synthesized all ZnO nanoparticles have good antibacterial and antibiofilm activity. Additionally, they are biocompatible. To treat different infections caused by drug-resistant bacteria, ZnO NPs can be used as a potential antibacterial candidate rather than the use of conventional antibiotic therapy to treat infections.

❖ Reinforcement of ZnO NPs in PHBV-PEO microfibers: Can be significantly utilized in the wound dressing applications

The prepared PHBV-PEO-ZnO microfibers possess better antibacterial and antibiofilm activity. Also they show a biocompatible nature. These microfibers can be significantly utilized for industrial and commercial purposes by carrying in-vivo experiments on animals.

Abbreviations

A:

Ag: Silver

AHL: Acyl homoserine lactones

ABPs: Antimicrobial peptides

ATP: Adenosine triphosphate

ATR: Attenuated Total Reflection

B:

bFGF: Basic fibroblast growth factor

C:

CFR: Code of federal regulation

Cs: Chitosan

D:

DABCO-dium: 1, 4-diazabicyclo [2.2.2] octane-1, 4-dium

DMA: Dynamic Mechanical Analysis

DNA: Deoxyribonucleic acid

DNases I: Deoxyribonuclease I

DSC: Differential Scanning Calorimetry

E:

ECM: Extracellular matrix

EDX: Energy Dispersive X-ray spectroscopy

E.coli: Escherichia coli

EG: Ethylene glycol

EGF: Epidermal growth factor

EPS: Extracellular polymeric substance

F:

FESEM: Field Emission Scanning Electron Microscopy

FDA: Food and Drug Administration

FTIR: Fourier Transform Infra-red Spectroscopy

FWHM: Full Width at Half Maxima

G:

GRAS: Generally Recognized As Safe

H:

H₂O₂: Hydrogen peroxide

I:

ICCD: International Center for Diffraction Data

IgE: Immunoglobulin E

Im: Imidazolium

I (IL-1) β : Interleukin

IR: Infra-red

L:

lcl: Long Chain Length

M:

MCT: Mercury-Cadmium-Telluride

MD: Minimal Davis

MTT: (3-(4,5-dimethylthiazol-2-yl)- 2,5-diphenyltetrazolium bromide sAssay

N:

NaCl: Sodium chloride

NaOH: Sodium hydroxide

NCIM: National collection centre for Industrial Microorganisms

NCs: Nanocomposites

NPs: Nanoparticles

O:

1-D: One dimensional

P:

PBS: Phosphate buffer saline

PEG: Polyethylene glycol

PDGF: Platelet-derived growth factor

PHA: Polyhydroxyalkanoates

PHB: Poly (3-hydroxybutyrate)

PHBV: Poly (3-hydroxybutyrate-co-3-hydroxyvalerate)

PHHp: Polyhydroxyheptanoate

PHN: Polyhydroxynanoate

PHO: Polyhydroxyoctanoate

PHV: Poly (3-hydroxyvalerate)

PHHx: Polyhydroxyhexanoate

PLA: Poly (lactic acid)

P. vulgaris: Proteus vulgaris

P. aeruginosa: Pseudomonas aeruginosa

PTPs: Protein tyrosine phosphatases

PHAs: Polyhydroxyalkanoates

PU: Polyurethane

Q:

QS: Quorum sensing

R:

ROS: Reactive oxygen species

RNA: Ribose nucleic acid

S:

SEM: Scanning Electron Microscopy

S. aureus: Staphylococcus aureus

S. pyogens: Streptococcus pyogens

T:

2-D: Two dimensional

TEG: Tetra ethylene glycol

TEM: Transmission Electron Microscopy

TGA: Thermogravimetric Analysis

TGF: Transforming growth factor

3-D: Three dimensional

TNF: Tumor necrosis factor

t-RNA: Transfer ribonucleic acid

TrEg: Triethylene glycol

U:

UTM: Universal Testing Machine

UV-Vis: Ultra-violet visible spectroscopy

X:

XRD: X-ray Diffraction

List of publications

1. Synthesis and characterization of zinc oxide nanoparticles by using polyols chemistry for their antimicrobial and antibiofilm activity, **Pranjali P. Mahamuni**, Pooja M. Patil, Maruti J. Dhanavade, Manohar V. Badiger, Prem G. Shadija, Abhishek C. Lokhande, Raghvendra A. Bohara, *Biochemistry and Biophysics Reports* 17 (2019) 71-80. (SCI Journal)
2. Electrospun poly (3-hydroxybutyrate-co-3-hydroxyvalerate)/Polyethylene oxide (PEO) microfibers reinforced with ZnO nanocrystals for antibacterial and antibiofilm wound dressing applications, **Pranjali P. Mahamuni-Badiger**, Pooja M. Patil¹., Pratikshkumar R. Patel., Maruti J. Dhanavade., Manohar V. Badiger., Yogesh N. Marathe, Raghvendra A. Bohara, Page 1 of 35 *New Journal of Chemistry*, DOI: 10.1039/D0NJ01384F (IF: 3.2)
3. Biofilm formation to inhibition: Role of zinc oxide-based nanoparticles, **Pranjali P. Mahamuni-Badiger**, Pooja M. Patil, Manohar V. Badiger, Pratiksh R Patel, Bhagyashi S. Thorat- Gadgil, Abhay Pandit, Raghvendra A. Bohara, *Materials Science & Engineering C*, <https://doi.org/10.1016/j.msec.2019.110319>. (IF: 5.8)
4. Conversion of organic biomedical waste into potential fertilizer using isolated organisms from cow dung for a cleaner environment, Pooja M. Patil¹ & **Pranjali P. Mahamuni**¹ & Mohamed M. Abdel-Daim & Lotfi Aleya⁴ & Roma A. Chougule⁵ & Prem G. Shadija & Raghvendra A. Bohara, *Environmental Science and Pollution Research*, doi.org/10.1007/s11356-019-05795-7 (IF: 3.0)
5. Conversion of organic biomedical waste into value added product using green approach, Pooja M. Patil & **Pranjali P. Mahamuni** & Prem G. Shadija & Raghvendra A. Bohara, *Environmental Science and Pollution Research* (2019) 26:6696–6705, doi.org/10.1007/s11356-018-4001-z (IF: 3.0)
6. Zinc Oxide-Based Nanomaterials for Anti-Biofilm Applications, **Pranjali P. Mahamuni-Badiger** and Raghvendra A. Bohara, *Progress and Prospects in Nanoscience Today*, 2020.



“In my end is my beginning”

.....T.S.Eliot

Miss. Pranjali Prabhakar Mahamuni.

Research Scholar

Centre for Interdisciplinary Research

D.Y. Patil Education Society,

Kolhapur-416 006 (M.S) India.

E-mail: pranjalisamsung@gmail.com

Date of birth: 3rd may 1989,

Permanent address: Anant Prestige, New shahupuri,

Kolhapur, 416006

Contact number: 7030361271

ACADEMIC PROFILE

Ph. D. in microbiology (Expected)

Submitted thesis in July 2020

Centre for Interdisciplinary Research

D.Y. Patil Education Society,

Kolhapur-416 006 (M.S) India.

M. Sc in Microbiology, 2011

(Specialization- Microbiology)



Shivaji University, Kolhapur,

Maharashtra- 416003, India.

B. Sc in Microbiology, 2009

(Specialization- Microbiology)

Kasturbai Walchand College, Sangli,

Maharashtra- 416 416, India.

TITLE OF THESIS

**“SYNTHESIS OF ZINC OXIDE NANOPARTICLES AND THEIR
APPLICATION FOR INHIBITION OF BIOFILM FORMATION IN DRUG
RESISTANT MICROORGANISMS”**

Date of Registration:

D.Y. Patil Education Society,

Kolhapur.

Pre-Ph. D exam appeared: July 2017

Seat No. 3814

Obtained percentage: 63.67%, Grade: A

RESEARCH EXPERIENCE:

1: Ph. D. Thesis entitled **“SYNTHESIS OF ZINC OXIDE NANOPARTICLES
AND THEIR APPLICATION FOR INHIBITION OF BIOFILM
FORMATION IN DRUG RESISTANT MICROORGANISMS”** under the

guidance of **Prof. Dr. P.G. Shadija**, Centre for interdisciplinary Research, D. Y. Patil Education Society, Kolhapur and co-guidance of **Dr. R.A. Bohara**, Irish Research council Postdoctoral Fellow, CÚRAM, Centre for Research in Medical Devices, National University of Ireland, Galway, Ireland.

2: Successfully completed the project entitled “**Proteolytic and lipolytic properties of endotoxins (enterotoxins) produced by *Salmonella typhi* NCIM 5255, *Salmonella typhimurium* NCIM 2501 and *Shigella flexneri* NCIM 5265**” for the partial completion of degree of M.Sc. in microbiology under the supervision of **Prof. (Dr.) Jay Ghosh, Shivaji University, Kolhapur.**

TEACHING EXPERIENCE:

- ❖ Worked as a microbiologist in Q. C. department in Symbiosis Co. Op. Pharmaceuticals Ltd. Sangli. (2011-2012)
- ❖ Worked as a lecturer in Tatyasaheb Ghatage Charitable Trust Vocational College Sangli and in R. R. Patil Nursing College, Sangli (2013-2015)
- ❖ Worked as a lecturer in Modern College, Kolhapur (2015-2016)
- ❖ Worked as a lecturer in M. Tech. Department, Shivaji University, Kolhapur. (2015-2016)

LIST OF PUBLICATIONS

1. Synthesis and characterization of zinc oxide nanoparticles by using polyol chemistry for their antimicrobial and antibiofilm activity, **Pranjali P. Mahamuni**, Pooja M. Patil, Maruti J. Dhanavade, Manohar V. Badiger, Prem G. Shadija, Abhishek C. Lokhande, Raghvendra A. Bohara, **Biochemistry and Biophysics Reports** **17** (2019) 71-80.

2. Electrospun poly (3-hydroxybutyrate-co-3-hydroxyvalerate)/Polyethylene oxide (PEO) microfibers reinforced with ZnO nanocrystals for antibacterial and antibiofilm wound dressing applications, **Pranjali P.Mahamuni-Badiger**, .Pooja M. Patil., Pratikshkumar R. Patel., Maruti J. Dhanavade., Manohar V. Badiger., Yogesh N. Marathe, Raghvendra A. Bohara, 1-35, **New Journal of Chemistry**, DOI: 10.1039/D0NJ01384F

3. Biofilm formation to inhibition: Role of zinc oxide-based nanoparticles, **Pranjali P. Mahamuni-Badiger**, Pooja M. Patil, Manohar V. Badiger, Pratiksh R Patel, Bhagyashi S. Thorat- Gadgil, Abhay Pandit, Raghvendra A. Bohara, *Materials Science & Engineering C*, <https://doi.org/10.1016/j.msec.2019.110319>.

4. Conversion of organic biomedical waste into potential fertilizer using isolated organisms from cow dung for a cleaner environment, Pooja M. Patil & **Pranjali P. Mahamuni** & Mohamed M. Abdel-Daim & Lotfi Aleya & Roma A. Chougule & Prem G. Shadija & Raghvendra A. Bohara, **Environmental Science and Pollution Research**, doi.org/10.1007/s11356-019-05795-7

5. Conversion of organic biomedical waste into value added product using green approach, Pooja M. Patil¹ & **Pranjali P. Mahamuni**¹ & Prem G. Shadija² & Raghvendra A. Bohara, **Environmental Science and Pollution Research** (2019) 26:6696–6705, doi.org/10.1007/s11356-018-4001-z

6. Zinc Oxide-Based Nanomaterials for Anti-Biofilm Applications, *Pranjali P. Mahamuni-Badiger and Raghvendra A. Bohara*, **Progress and Prospects in Nanoscience Today**, 2020.

7. Studies on mosquitocidal activity of metabolites from *Pseudomonas* species, Studies on mosquitocidal activity of metabolite from *pseudomonas* species, **Pranjali P. Mahamuni**, Reshma S. Shete and Hemlata V. Sonawane, **RJLBPCS** 2016
8. Isolation and characterization of endotoxin from *Salmonella typhimurium*, *S. typhi*, *Shigella* species, **Mahamuni, P.P**, Patil, A.R and *Ghosh, J.S, **International Food Research Journal** 24(6): 2685-2688 (December 2017).

Conferences/Workshops:

1. “**National Conference on Emerging Trend In Nanomaterials & Their Applications**” (ETNA), on 2, 3rd June, 2017, in D. Y. Patil Education Society, Kolhapur,.
2. Poster presented in International Conference On **Nanotechnology Addressing The Convergence Of Materials Science, Biotechnology and Medical Science, (IC-NACMBM)-2017 on 9-11th November** at D. Y. Patil Education Society, Kolhapur.
3. Work presented in **Anveshan-2017** on 17th November 2017, in D. Y. Patil Education Society, Kolhapur.

Hereby I declare that the information given above is true to the best of my knowledge.

Place: Kolhapur

Date:

Miss. Pranjali Prabhakar Mahamuni.

